UNIVERSITY OF SALERNO

DEPARTMENT OF CIVIL ENGINEERING

PHD PROGRAMME IN: "RISK AND SUSTAINABILITY IN CIVIL, ARCHITECTURAL AND ENVIRONMENTAL ENGINEERING SYSTEMS"

CURRICULUM: "ADVANCED TECHNOLOGIES, INFRASTRUCTURES AND LAND PROTECTION FOR SUSTAINABLE DEVELOPMENT"

XXXI CYCLE – NEW SERIES (2016-2018)

MONITORING STRATEGIES AND WARNING MODELS FOR WEATHER-INDUCED LANDSLIDES

(STRATEGIE DI MONITORAGGIO E MODELLI DI ALLERTA PER FRANE METEO-INDOTTE)

PhD candidate: GAETANO PECORARO

Supervisor:
PROF. MICHELE CALVELLO

Coordinator:
PROF. FERNANDO FRATERNALI

In copertina: Chiura Obata: Landslide, 1941

MONITORING STRATEGIES AND WARNING MODELS FOR WEATHER-INDUCED LANDSLIDES

Finito di stampare il 29/03/2019

TO MY FAMILY

INDEX

INDEX OF FIGURES

INDEX OF TABLES

ABSTRACT

Weather-induced landslides cause a large number of casualties as well as severe economic losses worldwide every year. Such a diffuse risk cannot be mitigated only by means of structural works, typically characterized by significant economic and environmental impacts. Therefore, landslide early warning systems (LEWS) are being increasingly applied as non-structural mitigation measures aiming at reducing the loss-of-life probability and other adverse consequences from landslide events by prompting people to act appropriately and in sufficient time to reduce the possibility of harm or loss. The systems can be distinguished, as a function of the scale of design and operation, in two different categories. Territorial systems (Te-LEWS), deal with multiple landslides over wide areas at regional scale, i.e. typically a basin, a municipality or a region; local systems (Lo-LEWS) address single landslides at slope scale.

In a preliminary phase of this study, a detailed review of Lo-LEWS operational worldwide is provided. The information has been retrieved from peer-reviewed articles published in scientific journals and proceedings of technical conferences, books, reports, and institutional web pages. The main characteristics of these systems have been summarized and described according to a scheme based on a clear distinction between three modules: landslide model, warning model and warning system. The monitoring strategies implemented therein have been presented and discussed, focusing on the monitored parameters and the monitoring instruments for each type of landslide. Subsequently, warning models developed within Te-LEWS for weather-induced landslides have been analyzed, pointing out that: their outputs are strongly dependent from the accurateness and reliability of the information on landslide occurrences; and only meteorological variables are considered in most of the cases, thus leading to an unavoidable uncertainty in the empirically defined thresholds. To overcome these issues, original procedures for defining warning models are herein proposed and tested on case studies in Campania and Emilia-Romagna regions (Italy) and in Norway. In Italy, a probabilistic approach has been developed to determine landslide conditional probabilities related to rainfall of specific intensity and

duration. The adopted Bayesian methodology allows to consider the uncertainty of the data and to provide a quantitative assessment of the reliability of the results. Data on landslide occurrences have been derived from a new landslide inventory, named "FraneItalia", wherein data are retrieved from online journalistic news; the correlations between landslides and rainfall have been assessed by analyzing satellite-rainfall records within weather alert zones. On the other hand, the methodology proposed for Norway aims at integrating the hydro-meteorological variables employed within the regional model used by the national early warning system (i.e. combinations of relative water supply and relative soil water saturation degree) with monitoring data collected at local scale, specifically pore water pressure observations acquired by the Norwegian Geotechnical Institute for a variety of projects. The analyses are carried out on a number of hydrological basins (test areas) defined at national scale and selected considering the occurrence of landslides in loose soils from 2013 to 2017 and the availability of a significant number of pore water pressure measurements. For each basin, the alerts issued by the regional model are assessed by means of a 2-step analysis employing indicators derived from simple moving averages of the pore water pressure measurements.

The warning models developed herein were successfully applied to selected case studies. Therefore, the proposed methodologies can be considered valuable frameworks considering aspects that are crucial for improving the efficiency of the models, such as: the potential of non-conventional landslide inventories and remote sensing monitoring instruments to complement the traditional sources of data, the use of probabilistic techniques for defining more objective rainfall thresholds, and the additional contribution of the information derived from the local observations of pore water pressures.

SOMMARIO

Le frane meteo-indotte causano un numero elevato di vittime oltre a ingenti perdite economiche in tutto il mondo ogni anno. Un rischio tanto diffuso non può essere mitigato solamente attraverso opere strutturali, tipicamente contraddistinte da considerevoli impatti economici e ambientali. Di conseguenza, i sistemi di allerta da frana (LEWS) vengono sempre più applicati come misure di mitigazione di tipo non strutturale con lo scopo di ridurre la probabilità di perdita della vita e altre conseguenze avverse derivanti da eventi franosi inducendo le persone ad agire responsabilmente e in tempo utile per ridurre la possibilità di danno o perdita. Tali sistemi possono essere classificati in due differenti categorie, in funzione della scala a cui vengono progettati e applicati. I sistemi territoriali (Te-LEWS), si occupano di numerose frane su vaste aree a scala regionale, tipicamente un bacino idrografico, un comune o una regione; i sistemi locali (Lo-LEWS) operano su singole frane alla scala di pendio.
In una fase preliminare di questo studio, è presentata una rassegna dettagliata dei sistemi di allerta locali operanti in tutto il mondo. Le informazioni sono state ricavate sia da articoli specializzati pubblicati in riviste, sia da atti di conferenze tecniche, libri, report e pagine web istituzionali. Le principali caratteristiche di questi sistemi sono state sintetizzate e descritte secondo uno schema basato su una chiara distinzione tra tre moduli: modello di franosità, modello di allerta e sistema di allerta. Le strategie di monitoraggio ivi implementate sono state presentate e discusse, concentrandosi particolarmente sui parametri monitorati e sugli strumenti di monitoraggio adottati per ciascun tipo di frana. Successivamente, sono stati analizzati i modelli di allerta sviluppati all'interno dei sistemi di allerta territoriali, rilevando che i loro rendimenti dipendono fortemente dall'accuratezza e dall'affidabilità delle informazioni sull'occorrenza delle frane e nella maggior parte dei casi sono considerate soltanto variabili meteorologiche, portando dunque a un'ineluttabile incertezza nelle soglie definite in via empirica. Al fine di risolvere queste problematiche, delle procedure originali per definire dei modelli di allerta sono proposte in questo lavoro e testate in casi di studio in Emilia-Romagna e Campania (Italia) e in Norvegia. In Italia, un

approccio probabilistico è stato sviluppato per determinare le probabilità condizionate relative a frane di specifica durata e intensità. La metodologia bayesiana adottata permette di considerare l'incertezza dei dati e di garantire una stima quantitativa dell'affidabilità dei risultati. Le informazioni sull'occorrenza delle frane sono state derivate da un nuovo inventario di frane, chiamato "FraneItalia", i cui dati sono ricavati da articoli di stampa online; le correlazioni tra frane e piogge sono state valutate analizzando dati satellitari di pioggia all'interno di zone di allerta meteo. Invece, la metodologia proposta per la Norvegia mira ad integrare le variabili meteorologiche impiegate nel modello regionale utilizzato dal sistema nazionale di allerta (combinazioni di apporto idrico e grado di saturazione del suolo relativi) con dati di monitoraggio raccolti a scala locale, nello specifico misure di pressioni interstiziali acquisite dal Norwegian Geotechnical Institute per diversi progetti. Le analisi sono eseguite su una serie di bacini idrografici (aree di studio) definiti a scala nazionale e selezionati considerando l'occorrenza di frane in sedimenti sciolti dal 2013 al 2107 e la disponibilità di un numero significativo di misure di pressioni interstiziali. Per ogni bacino le allerte emanate dal modello regionale sono valutate attraverso un'analisi in due passi che impiega indicatori derivati da medie mobili semplici delle misure di pressioni interstiziali.

I modelli di allerta sviluppati in questo studio sono stati applicati con successo ai casi di studio selezionati. Di conseguenza, le metodologie proposte possono essere considerate degli utili schemi che tengono conto di aspetti cruciali per migliorare l'efficienza dei modelli di allerta, fra cui: il potenziale di inventari di frana non convenzionali e strumenti in telerilevamento nell'integrare le tradizionali fonti di dati, l'utilizzo di tecniche probabilistiche per definire soglie pluviometriche più obiettive e il contributo addizionale delle informazioni derivate da osservazioni locali di pressioni.

ACKNOWLEDGEMENTS

Giunto alla fine di questo percorso, sento il dovere di ringraziare le persone con le quali ho lavorato e interagito durante questi anni.

In primo luogo, un enorme ringraziamento lo devo a *Michele,* per essere stato un punto di riferimento sempre presente, per il costante supporto e per tutte le possibilità di crescita che mi hai offerto durante questi anni. Svolgere questo dottorato sotto la tua supervisione è stato per me un onore.

Ringrazio poi tutti i componenti del Laboratorio di Geotecnica *"Giuseppe Sorbino"* per la loro professionalità, disponibilità e simpatia: a partire dal *Prof. Leonardo Cascini,* il *Prof. Ferlisi, Dario* e *Sabatino* e senza dimenticare i tecnici: il sempre disponibile *Vito* e il "colonnello" *Mauro.*

Ringrazio tutto il gruppo del Norwegian Geotechnical Institute di Oslo, in particolare *José,* per avermi concesso l'opportunità di vivere un'indimenticabile esperienza di vita e di ricerca.

Un ringraziamento speciale va a tutti gli assegnisti e i dottorandi che hanno condiviso con me negli anni questa esperienza, partendo ovviamente da *Pooyan,* con il quale ho iniziato questo percorso tre anni fa tra lamenti, arrabbiature, discorsi incomprensibili in un mix di inglese, italiano e persiano ma anche tra risate, divertimento e soprattutto con sincera e profonda amicizia. Conserverò sempre un ricordo felice di questi anni trascorsi insieme, "fratello".
Saluto e ringrazio per i consigli ricevuti nei primi mesi di questo percorso *Ilaria, Luca* e *Vittoria,* che stanno vivendo nuove ed entusiasmanti esperienze.
Un ringraziamento particolare va ai ragazzi che hanno dovuto sopportarmi nei travagliati mesi trascorsi a scrivere questa Tesi:
Gianfranco e *Mariagiovanna,* per i preziosi consigli e suggerimenti che solo chi ha già vissuto questa esperienza può dare e per le distrazioni dalla scrittura della Tesi durante le pause caffè.
Antonio, per le tante perle di saggezza che hai dispensato in questi anni e soprattutto per le tante risate che ci siamo fatti durante le pause pranzo (e

non solo) che mi hanno permesso di vivere con più leggerezza questo percorso.
Maria Grazia e *Maria Rosaria,* per l'allegria, la spensieratezza e la spontaneità che avete portato nel laboratorio e che compensano in parte il "pessimismo cosmico" di qualcun altro.
Maria "Lella" per l'esuberanza e l'ottimismo che ti contraddistinguono, per il tuo stile unico e inimitabile (per fortuna…) e per le tante volte in cui ti sei offerta (più o meno volontariamente) di ospitarmi per il pranzo sulla tua scrivania.
Angela, per la capacità di sintesi nei discorsi e per aver portato un po' di originalità nella stanza dottorandi tra tutte queste Marie.
A voi tutti, amici prima che colleghi auguro le migliori soddisfazioni sia personali che professionali.

Last but not least, desidero ringraziare la mia Famiglia, mio padre *Egidio,* mia madre *Rosa* e i miei fratelli *Fausto* e *Daniele.* A voi dedico questo elaborato finale con infinito affetto e con immensa gratitudine.

Un grazie a tutti, di cuore.

Gaetano

ABOUT THE AUTHOR

Gaetano Pecoraro graduated with 110/110 cum laude in Environmental and Territorial Engineering at the University of Salerno, Italy in December 2013 with a thesis on the definition and use of a landslide inventory for susceptibility and hazard analyses at regional scale. In 2015 he won a PhD scholarship at the same University to deal with the study of landslide early warning systems for weather-induced landslides. As a part of his PhD, he had the opportunity to spend a research period at the Norwegian Geotechnical Institute (NGI) in Oslo, Norway, where he collected widespread monitoring data and local observations to be employed for analyses on early warning scenarios. During his PhD, he developed innovative methodologies for the definition of warning models for weather-induced landslides. Some of the results obtained in this PhD thesis have been presented in National and International conferences and published in international scientific journals.

Gaetano Pecoraro si è laureato con 110/110 e lode in Ingegneria Civile per l'Ambiente ed il Territorio presso l'Università degli Studi di Salerno, Italia nel Dicembre 2013 con una tesi sulla definizione e l'utilizzo di un inventario di fenomeni franosi per analisi di suscettibilità e pericolosità a scala regionale. Nel 2015 ha vinto una borsa di dottorato presso la stessa Università finalizzata allo studio di sistemi di allerta per frane meteo-indotte. Nell'ambito del Dottorato di Ricerca, ha avuto l'opportunità di svolgere un periodo di ricerca presso il Norwegian Geotechnical Institute (NGI) ad Oslo in Norvegia, dove ha raccolto dati da monitoraggio diffuso e osservazioni locali per analisi su scenari di allerta. Nel corso del Dottorato di ricerca, ha sviluppato metodologie innovative per la definizione di modelli di allerta per frane meteo-indotte. Alcuni dei risultati ottenuti in questa Tesi di dottorato sono stati presentati in conferenze nazionali e internazionali e pubblicati in riviste scientifiche internazionali.

1 INTRODUCTION

Problem statement

Weather-induced landslides are widespread and destructive natural phenomena occurring all around the world that may cause severe human and economic losses. The continuous urbanization process in landslide prone areas and the increasing number of extreme atmospheric phenomena have drastically raised, worldwide, the exposure of people affected by weather-induced landslides. Landslide risk can be reduced by adopting different mitigation methods, such as: active measures reducing the probability of occurrence of landslides, engineering works decreasing the vulnerability of the elements at risk, and non-structural actions. Among the latter, landslide early warning systems (LEWS) certainly constitute a significant option available to the authorities in charge of risk management and governance. LEWS aim at reducing the loss-of-life probability and other adverse consequences from landslide events by informing individuals, communities, and organizations threatened by landslides to prepare and to act appropriately and in sufficient time to reduce the possibility of harm or loss (UNISDR 2006). LEWS have been recognized as important tools for landslide risk reduction and community resilience in many recent international initiatives (e.g., Sendai Framework for Disaster Risk Reduction 2015-2030, UN Agenda 2030 for sustainable development, European Climate Adaptation Platform). Therefore, in recent years scientists, governmental agencies and NGOs have shown an increasing interest in LEWS.

LEWS can be designed and employed at two different reference scales (e.g., Thiebes et al. 2012; Calvello 2017). Systems addressing single landslides at slope scale can be referred to as local systems (Lo-LEWS). Systems dealing with multiple landslides over wide areas at regional scale can be referred to as territorial systems (Te-LEWS), i.e., they can be employed over a basin, a municipality, a region, or a nation (Piciullo et al. 2018).

Many literature contributions describe LEWS operational at both local and regional scale dealing with weather-induced landslides. Yet, standard

requirements for the definition of an efficient LEWS still do not exist, thus crucial aspects may be neglected by systems developers and managers. The efficiency of LEWS strongly depends on the monitoring strategies adopted and the method developed for the definition of the warning model. Indeed, monitoring strategies play a central role, both in the design and in the operational phase of a LEWS, as suitable parameters to monitor must be identified and the most appropriate monitoring instruments need to be selected according to a set of criteria, such as simplicity, robustness, reliability, and cost. Another crucial issue is the definition of an appropriate warning methodology that considers the quantity and the quality of the input data and the expected outputs of the model.

Objectives

This PhD thesis aims at defining and testing original methodologies for improving the performance of warning models employed within LEWS for weather-induced landslides.

In the following, the main research questions and the respective objectives are summarized.

How to improve quantity and quality of landslide data?

- Definition and population of a landslide inventory from online news
- Analyses on landslide occurrences at regional scale

How to best incorporate remote sensing data into current land-based monitoring networks?

- Collection of meteorological monitoring data from satellite observations
- Analysis of remote sensing data at regional scale
- Integration between widespread meteorological monitoring data and local observations

How to define rainfall thresholds in an objective and reproducible way?

- Definition of probabilistic thresholds for landslide occurrence
- Development and implementation of a probabilistic warning model

How can local observations be profitably used within warning models implemented at regional scale?

- Identification of the most appropriate parameters to be monitored at local scale in relation to the types of landslide under surveillance

- Development and implementation of a multi-scalar warning model

Thesis Outline

Chapter 2 presents the main characteristics of the landslide phenomena addressed herein, their possible consequences in terms of human and economic losses, and the mitigation measures available for landslide risk management. Regarding non-structural options, LEWS are introduced by describing their structure and by summarizing the findings of literature contributions on Lo-LEWS and Te-LEWS operational all around the world. Concerning Lo-LEWS, the information refers to 29 systems for which the main characteristics are analyzed considering three main modules: landslide model, warning model, and warning system (Pecoraro et al. 2018). Information on Te-LEWS are derived from three recent literature reviews reporting 24 Te-LEWS operational worldwide for rainfall-induced landslides (Piciullo et al. 2018), 21 regional LEWS operational in Italy (Pecoraro and Calvello 2016), and rainfall thresholds employed within 45 Te-LEWS operational worldwide (Segoni et al. 2018a).

In Chapter 3 the monitoring strategies adopted within the reviewed Lo-LEWS and the Te-LEWS are discussed and analyzed in terms of monitored parameters and monitoring instruments. Moreover, the main characteristics of the warning models employed within the Te-LEWS are also reported. These analyses allow highlighting some relevant aspects that need to be taken into account in order to improve the efficiency of LEWS: the definition of objective and reproducible warning models; the availability of reliable landslide records and monitoring data; the integration of local geotechnical observations within warning models.

Chapter 4 introduces a framework highlighting the steps necessary for the definition of a warning model for weather-induced landslides: collection of the input data; delimitation of the warning zones; identification of the landslide events; selection of the warning parameters; spatial-temporal correlation between landslide events and weather events; calibration and validation of the warning model. Following this framework, two original methodologies are proposed for the definition of warning models for weather-induced landslides: a probabilistic warning model, developed by applying a Bayesian approach to determine the conditional probability of landslide occurrence; and a multi-scalar warning model, integrating

widespread meteorological monitoring data and geotechnical observations collected at local scale.
In Chapter 5 the probabilistic warning model is tested in two Italian regions, Emilia-Romagna and Campania, adopting as territorial units the weather warning zones defined by the two regional civil protection agencies. Data on landslide occurrences are derived from the "FraneItalia" catalog, a landslide inventory based on information retrieved from online Italian news (Calvello and Pecoraro 2018). Rainfall measurements are derived from the satellite-based NASA Global Precipitation Measurement (GPM) database, and are elaborated through Google Earth Engine, a cloud-platform for planetary-scale environmental data analysis. Triggering and non-triggering rainfall events are differentiated considering the spatial-temporal distribution of landslide events within each territorial unit. A Bayesian framework is applied to determine the probability of landslide occurrence associated to each combination of rainfall parameters and to define the warning levels within the model. The two probabilistic models are validated using two different validation procedures.
In Chapter 6, the multi-scalar warning model is applied considering 30 Norwegian hydrogeological basins starting from the nationwide Te-LEWS currently operational in Norway. These territorial units have been identified considering information available at national scale according to two selection criteria. The warning events issued by the national system, which only takes into account gridded monitoring data (i.e., rainfall and normalized values of water supply and soil water content), are assessed considering trends of local pore water pressure observations. The warning model is defined looking at the results of parametric analyses so as to identify the best-performing parameters to be employed. The multi-scalar warning model is finally validated employing statistical performance indicators.
Finally, in Chapter 7 the results achieved are discussed and analyzed in order to evaluate the potential of the proposed methodologies in improving the performance of warning models for weather-induced landslides.

2 EWS FOR WEATHER-INDUCED LANDSLIDES

Weather-induced landslides are widespread phenomena, representing a significant risk for people, structures and infrastructures in many parts of the world. Such a diffuse risk cannot be mitigated only by means of structural measures, thus landslide early warning systems (LEWS) are being increasingly applied as non-structural risk mitigation measures.
Section 2.1 introduces the main features and the possible consequences of the weather-induced landslides, also reporting the structural and non-structural risk mitigation measures. Section 2.2 focuses on landslides early warning systems, presenting their main structure and differentiating between local systems (Lo-LEWS) and territorial systems (Te-LEWS). Section 2.3 presents a literature review on Lo-LEWS and an analysis of their main characteristics considering three main modules: landslide model, warning model, and warning system. Finally, Section 2.4 summarizes information on Te-LEWS gathered from three recent literature contributions: Piciullo et al. (2018) described and analysed the main characteristics of territorial LEWS operational worldwide; Pecoraro and Calvello (2016) presented a review on regional LEWS for weather-induced landslides in Italy; Segoni et al. (2018a) investigated the procedures for defining rainfall thresholds for landslide occurrence.

2.1 WEATHER-INDUCED LANDSLIDES

2.1.1 Types of landslides and possible consequences

According to Cruden (1991), a landslide can be defined as *"a movement of a mass of rock, debris or earth down a slope"* activated or triggered by causes that can be either external or internal. However, the generic term "landslide" includes a variety of different phenomena, which are not perfectly repeatable, thus it is not possible to develop a taxonomic classification.

Therefore, since the early decades of the last century several classification schemes considering several discriminating factors have been proposed (e.g., Skempton 1953; Varnes 1958; Blong 1973; Varnes 1978; Hutchinson 1988: Cruden and Varnes 1996; Leroueil et al. 1996; Hungr et al. 2001: and Hungr et al. 2014). For instance, the classification proposed by Varnes (1978) distinguishes among three types of materials (i.e., rock, debris, and earth) and five types of movements (i.e., fall, topple, slide, lateral spread, and flow). An additional class (i.e., the complex movements) is introduced by the author in order to define any combination of more than one movement. Cruden and Varnes (1996) allows differentiating between slow- and fast-moving landslides on the basis of seven velocity classes, each of them associated to a probable destructive significance. Hungr et al. (2014) state that simple term assigned to a landslide type (or a specific case) should reflect the particular focus of the researcher. Following this approach, Calvello (2017) proposes that for early warning purposes a landslide should be classified on the basis of its propagation phase and taking into account four main characteristics: i) type of movement and material, ii) activity phase, iii) velocity, and iv) volume (Figure 2.1).

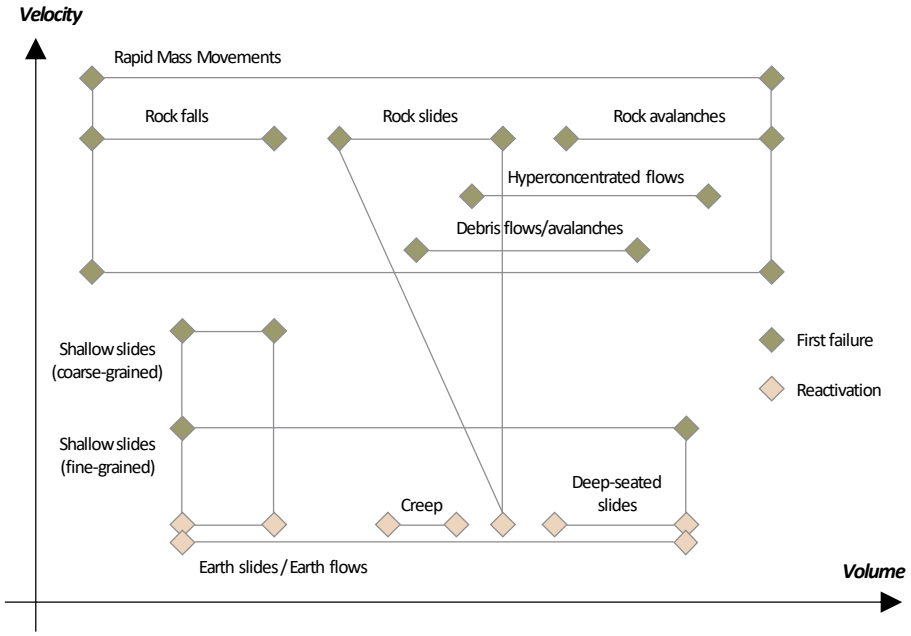

Figure 2.1 Example of landslide classification scheme for early warning purposes proposed by *Calvello (2017)*

This thesis addresses weather-induced landslides occurring in shallow soil layers as first failure phenomena. They comprise a wide range of slope movements of limited size that mainly develop in soil layers up to a maximum of a few meters, such as shallow slides, debris slides, debris flows, debris avalanches, and hyperconcentrated flows. The main triggering mechanism for these landslides typically consists of rain or snow infiltration in shallow soil layers, resulting in an increase of the pore water pressure and a decrease of the soil shear strength (Caine 1980), as well as in the loss of the apparent cohesion in partially saturated soils (Fredlund 1987). The triggering process is characterized by a nearly totally absence of warning signs. Although the triggering volume is often limited, the landslide mass may incorporate the soil material lying along the slope in the propagation phase, increasing significantly the volume. Moreover, in steep channels shallow slides may evolve into debris flows, destructive phenomena characterized by extremely high velocities (Hungr et al. 2014). Shallow weather-induced landslides can occur frequently and often simultaneously over large areas, thus they represent a widespread risk for local communities, structures, and infrastructures in many parts of the world (Calvello 2017). Recently, several different global databases (e.g., the EM-DAT International Disaster Database, the NASA Global Landslide Catalogue, and the Global Fatal Landslide Database) provided data on the societal impact of these landslides. However, information is generally related to all type of landslides and global databases generally underestimate the landslides impact on society, as landslide events are often incorporated in other major climate-related natural disasters (Petley 2012; Kirschbaum et al. 2015). Nevertheless, their analysis allows some general considerations on human and economic losses of weather-induced landslides, their spatial distribution and possible future trends. For instance, the EM-DAT database suggested that weather-induced landslides account for 5.2% of natural climate-related disaster events, resulting in 18,418 deaths and about 8 billion EUR of economic losses (Guha-Sapir et al. 2018). Moreover, Froude and Petley (2018) demonstrated that the majority of the 4862 fatal landslide events reported in the Global Fatal Landslide Database between 2004 and 2016 were triggered by rainfall or snowmelt (79%) and were mainly concentrated in: Central America, the Caribbean islands, Andes mountains, East Africa, the Himalayan Arc, China, and the European Alps. Finally, Haque et al. (2016) reported that 1.3 to 3.6 million Europeans live in landslide prone areas and 8000 to 20,000 km of roads and railways are highly exposed to landslides.

2.1.2 Structural and non-structural risk mitigation measures

The awareness of the possible catastrophic consequences of landslides, in terms of victims and social-economic impacts, led the technical and scientific community to the adoption of a rigorous approach aimed at an efficient and effective prevention, mitigation and control of landslide risk. To this aim, Fell et al. (2005) proposed an integrated logical framework for landslide risk management, including three phases: risk analysis, risk assessment, and risk management (Figure 2.2).

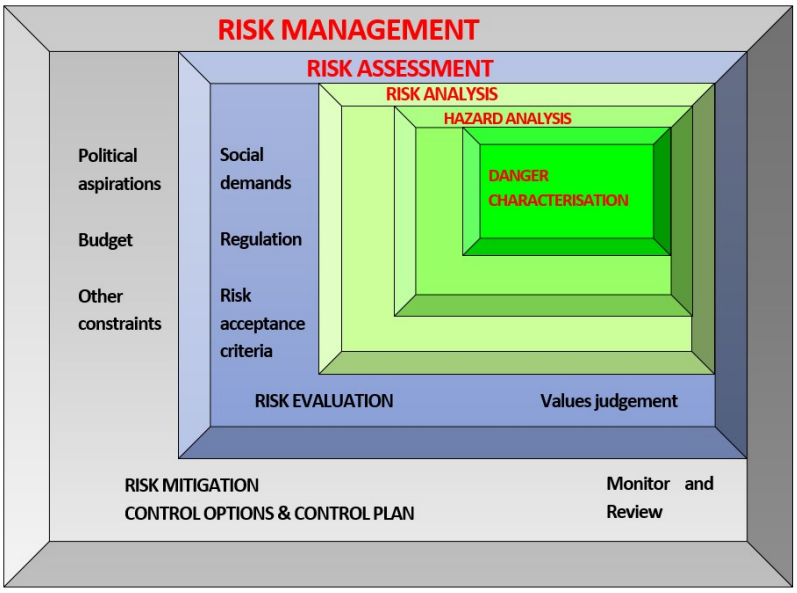

Figure 2.2 Schematic representation of the integrated risk management process proposed by *Fell et al. (2005)*

Within this framework, risk analysis represents the basic level of risk management process and it is essentially aimed at the estimation of the current or potential level of risk in a specific area affected by a given landslide phenomenon. Risk analysis generally contains the following steps: definition of scope, danger (threat) identification, estimation of probability of occurrence to estimate hazard, evaluation of the vulnerability of the element(s) at risk, consequence identification, and risk estimation.

In general terms, landslide risk *(R)* can be expressed through the widely accepted formula of Varnes (1984):

$$R = H \times E_R \times V \qquad (2.1)$$

where: *H* (hazard) is the probability that a particular landslide phenomenon occurs within a certain area in a given period of time; E_R (elements at risk) are people, building, engineering works, infrastructures, environmental features and economic activities in the area affected by a landslide; *V* (vulnerability) is the degree of loss to a given element or a set of elements within the area affected by a landslide, expressed on a scale from 0 (no loss) to 1 (total loss).

Risk assessment is the process of making a decision or recommendation on whether existing risks are tolerable and present risk control measures are adequate, and if not, whether alternative risk control measures are justified or will be implemented. To this aim, the outputs from the risk analysis are compared against values judgements and risk tolerance criteria determined taking account of political, legal, environmental, regulatory and societal factors.

Finally, risk management represents the systematic application of management policies, procedures and practices in order to identify, analyze, assess, and in case mitigate and monitor landslide risk. The risk management process is iterative, requiring consideration of the risk mitigation options and the results of the implementation of the mitigation measures and of the monitoring.

According to UNISDR (2006), mitigation measures can be classified into two main groups: structural measures (i.e., any physical construction to reduce or avoid possible impacts of landslides, or the application of engineering techniques or technology to achieve landslide resistance and resilience in structures or systems) and non-structural measures (i.e., mitigation strategies not involving physical construction which use knowledge, practice or agreement to reduce disaster risks and impacts, in particular through policies and laws, public awareness raising, training and education).

Following equation *(2.1),* structural measures mainly address either hazard (e.g., reduction of the general slope angle, modification of geometry and/or mass distribution, surface drains) or vulnerability (e.g., diversion channels, re-modelling of the slope, planting and vegetation of the slope, catch trenches). Conversely, non-structural measures usually address

elements at risk (e.g., land-use planning, early warning, public preparedness).
Within these frameworks, landslide early warning systems (LEWS) may be considered a non-structural passive mitigation option to be employed in areas where risk, occasionally, rises above defined acceptability levels (Calvello 2017).

2.2 LANDSLIDE EARLY WARNING SYSTEMS

2.2.1 Structure and main modules

LEWS are being increasingly applied worldwide, mainly because of: their lower economic costs and environmental impact compared to structural measures (e.g., Intrieri et al. 2012; Thiebes and Glade 2016); the continuous development of new technologies for landslide monitoring (e.g., Chae et al. 2017; Crosta et al. 2017); and increasing availability of reliable databases to calibrate the warning models (e.g., Haque et al. 2016; Calvello and Pecoraro 2018). LEWS aim at reducing the loss-of-life probability and other adverse consequences from landslide events by informing individuals, communities, and organizations threatened by landslides to prepare and to act appropriately and in sufficient time to reduce the possibility of harm or loss (UNISDR 2006).
The types of landslides and the mechanisms responsible of their occurrence or reactivation, as well as the early warning conditions that might be detected before a paroxysmal phase of movements, vary widely depending on the geo-environmental context. Therefore, it is necessary for managers of LEWS to adapt the design of the systems to the particular conditions at the locations where these systems will be operational. To this aim a certain degree of flexibility is required during the implementation, while at the same time universal standards should be defined so that uniformity in the development of such systems and improvement of community resilience in landslide prone areas can be obtained.
In 2006 UNISDR defined a simple list of the main elements and actions that national governments or community organizations can refer to when developing or evaluating people-oriented early warning systems for natural hazards. The checklist is structured around four key components: i) risk

knowledge, i.e., systematic assessment of hazards and vulnerabilities; ii) monitoring and warning service, i.e., accurate and timely forecasting of hazards using reliable, scientific methods and technologies; iii) dissemination and communication, i.e., clear and timely distribution of warnings to all those at risk; iv) response capability, i.e., national and local capacities and knowledge to act correctly when warnings are communicated. Di Biagio and Kjekstad (2007) focus on EWS for landslides and introduce a block diagram describing the four main activities that should be implemented in: monitoring, analysis of data and forecasting, warning and response. The framework proposed by Sassa et al. (2009) in the context of the project "Early Warning of Landslide" is divided into three main flows. The central flow contains the monitoring of triggering factors and the development of landslide risk maps and early warning technologies. The left flow represents an aspect of technology for site and time prediction of landslides. Finally, the right flow refers to the social aspects, including the risk communication and the evacuation systems. Intrieri et al. (2013) point out that an EWS may suffer from the imbalance among their components; for instance, often some of them may lack in the social/communication aspects. The authors describe landslide EWS as the balanced combination of four main activities: design, monitoring, forecasting and education. Recently, the scheme proposed by Piciullo et al. (2018) identifies the main components necessary to design a territorial EWS for rainfall-induced landslides, highlighting the importance of both technical and social aspects. For this purpose, the conceptual model is organized as a jigsaw puzzle, based on four main modules of the warning system: i) setting, ii) correlation law, iii) decisional algorithm, and iv) warning management.

Although the proposed schemes and the described elements correctly represent LEWS, a more detailed and representative conceptual model for LEWS is herein provided. For this purpose, Figure 2.3 introduces a scheme modified from a similar framework developed by Calvello (2017) for weather-induced landslides. The proposed layout clearly differentiates among three main modules: landslide model, warning model and warning system. Within this framework, a landslide model is one the components of a warning model and the latter is one of the components of an early warning system. A landslide model may be described as a functional relationship between landslide causes (e.g., weather, geomorphological, anthropic) and landslide events, taking into account the geological, geomorphological and hydrogeological features of the slope and the data

provided by monitoring instruments. A warning model includes the landslide model as well as warning criteria and warning levels. Warning criteria are represented by the decision-making procedures necessary for issuing the warnings and for establishing a connection between the outputs of the landslide model to a set of warning levels. Each warning level is associated to the state of activity of the landslide, to the possible consequences and, of course, to the expected actions from the actors involved (e.g., EW managers, politicians, scientist, stakeholders, citizens). The number of levels adopted by the model can vary from a minimum of two—i.e., warning, no warning—to five or more. Finally, a warning model is part of a warning system, whose other four components are: warning dissemination, communication and education, community involvement and an emergency plan. On this issue, it is important to stress the role of the community and the social aspects in general, at times neglected by technicians, but still essential, as well as other components, for LEWS to be effective.

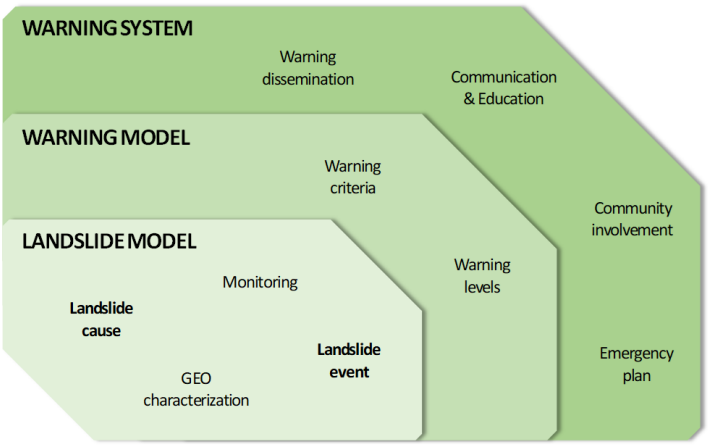

Figure 2.3 Framework identifying the main modules of landslide early warning systems (modified from *Calvello 2017)*

2.2.2 The scale of analysis

LEWS can be designed and employed at two different reference scales (e.g., Thiebes et al. 2012; Calvello and Piciullo 2016). Systems addressing single landslides at slope scale can be named as local (Lo-LEWS). Systems dealing with multiple landslides over wide areas at regional scale are

referred to as territorial systems (Te-LEWS), i.e., they can be employed over a basin, a municipality, a region, or a nation (Piciullo et al. 2018).

The main aim of Lo-LEWS is the temporary evacuation of people from areas where, at specific times, the risk level to which they are exposed is considered to be intolerably high. They typically implement a network of instruments to monitor the parameters most relevant for early warning purposes, considering predisposing and triggering factors. Their design and operation are strongly influenced by numerous constraints and factors, from time to time different, depending on the characteristics (e.g., size, possible precursors, potential velocity) of the landslide under surveillance.
On the other hand, Te-LEWS are used to provide generalized warnings to authorities, civil protection personnel and the population over appropriately-defined homogeneous warning zones of relevant extension. Typically, these systems address weather-induced landslides through the monitoring and prediction of meteorological parameters.
A key difference between local and territorial LEWS is represented by the definition of a "landslide event". Regarding local LEWS, a landslide event may be represented either by: a single active or dormant phenomenon; a potential slope instability, due to a first failure of a soil or rock mass. Differently, for territorial LEWS a landslide event may be defined as a series of landslides grouped on the basis of their characteristics, so as to implicitly evaluate the numerosity of a set of multiple phenomena occurring in a given area within a given time period.
The scale of analysis of a LEWS also inevitably influences the stakeholders involved as well as most of its operational characteristics, including: the model adopted to characterize a landslide event; the criteria to issue the warnings and their meaning; the lead time; the tools used to disseminate the warnings; the definition of the emergency plan.
Recently, Sättele et al. (2012) and Stähli et al. (2015) distinguished among three classes of EWS for natural hazards: i) alarm systems, detecting process parameters of a phenomena already in progress; ii) warning systems, monitoring triggering factors before the beginning of a landslide event; and iii) forecasting systems, predicting the level of danger of a landslide process. According to the authors, they can be differentiated considering: the area under surveillance, the lead time, the parameter monitored, the number of warning levels, and the degree of automation. Calvello (2017) presented a scheme combining the two categories of

LEWS defined on the basis of their scale of analysis with the classification proposed by Sättele et al. (2012) and Stähli et al. (2015). Local LEWS are indeed typically implemented as either alarm or warning systems; whereas territorial LEWSs are generally used as either warning or forecasting systems (Table 2.1).

Table 2.1 Local and territorial LEWS function of detection factors, lead time and warning characteristics *(Calvello 2017)*

Class (function of scale)	**Class *(Sättele et al. 2012)***	**Detection**	**Lead time**	**Warning**
Local	Alarm	Parameters of ongoing event	Short	Automatic
Local and territorial	Warning	Factors of susceptibility	Extended	Predefined thresholds
Territorial	Forecasting	Sensor data and forecasts	Regular intervals	Data interpretation

Many LEWS operational all around the world and reported in the scientific literature deal with weather-induced landslides. Comprehensive reviews of systems operational at both local and regional scale are presented in Sections 2.3 and 2.4, respectively.

2.3 REVIEW ON LOCAL LANDSLIDE EARLY WARNING SYSTEMS

(based on Pecoraro et al. 2018)

2.3.1 Location, period, and state of activity

Figure 2.4 presents a summary of the location and the period of activity of 29 Lo-LEWS operational all around the world. The majority of them (22) are currently active both as prototypes (4) and as operational systems (18). On the other hand, in five cases prototype systems were designed at operating for relatively limited periods of time: Nojiri River basin, Japan

(AS_1991_P); Moscardo catchment, Italy (EU_1995_P); Wollongong, Australia (OC_2005_P); Banjarnegara, Indonesia (AS_2007_P); and Swabian Alb, Germany (EU_2007c_P). Only two of the operational systems described herein are no longer active: Xintan Town, China (AS_1977_N) and North Vancouver, Canada (NA_2009_N). Among the 29 Lo-LEWS reported herein, only few applications have been gathered before the 2000s.

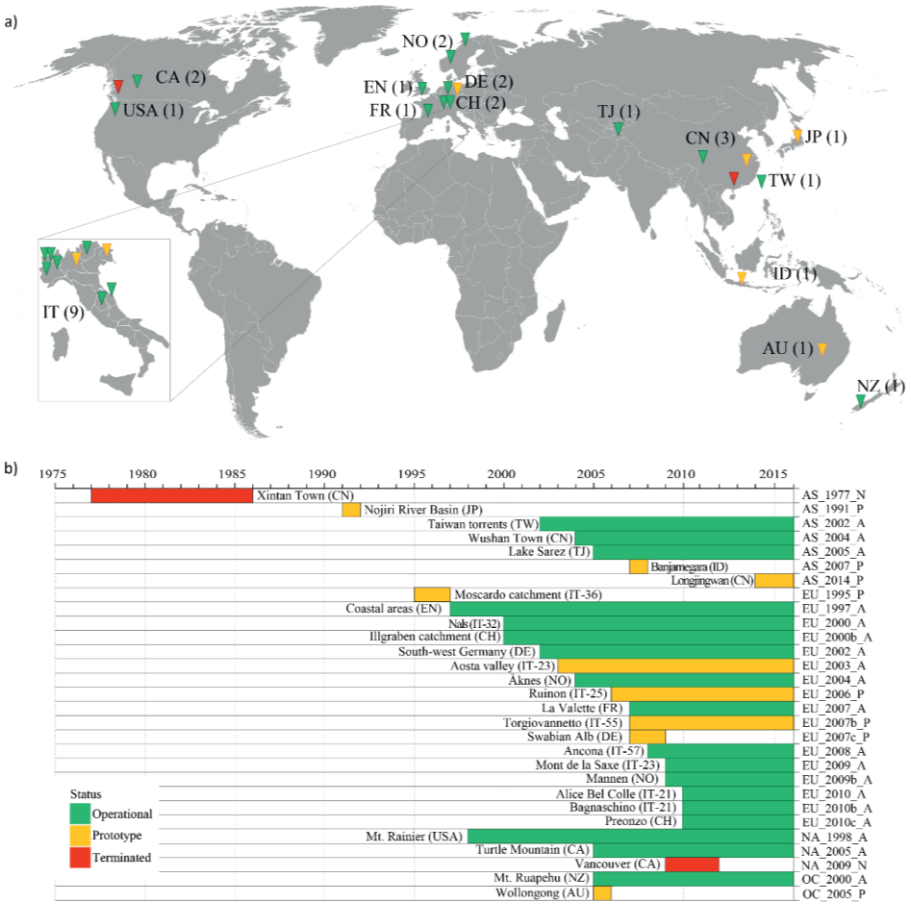

Figure 2.4 Local landslide early warning systems: a) national distribution; b) location and period of activity *(Pecoraro et al. 2018)*

The oldest system was designed in Xintan Town, China (AS_1977_N) in 1977 for addressing a large rock avalanche on the northern bank of the

Yangtze River. On 12 May 1985 the upper part of the hillside collapsed destroying the historical town located in front of the slope. However, the system successfully predicted the catastrophic collapse and all the 1371 inhabitants of the surrounding area were warned and evacuated in time (Wang 2009). In 1991, a prototype system was employed in the Nojiri River basin, Japan (AS_1991_P) for detecting the possible occurrence of debris flows on the flanks of Mt. Sakurajima volcano through embedded acoustic sensors (Takeshi 2011). In the early 1990s, USGS developed an automated lahar warning system comprising a network of geophones, a ground-based radio telemetry system and a warning-dissemination component. After a first application at Mt. Rainier, USA (NA_1998_A) in 1997, the system was installed in many other lahars-threatened areas situated in USA, Indonesia, the Philippines, Ecuador, Mexico, and Japan (Pierson et al. 2014). The first two systems operational in Europe were carried out in the Moscardo catchment, Italy (EU_1995_P) and in the south-eastern coastal areas of England (EU_1997_A). In the first case, seismic detectors were placed along debris flows prone channels in the summers 1995 and 1996 for assessing their capability to detect phenomena while in progress (Arattano 1999). In the second case, a series of dramatic landslide events led to the establishment of a number of real-time Lo-LEWS to safeguard people exposed at risk from future potential landslip and cliff-top recession (Clark et al. 1996). Furthermore, the large majority of the systems—24 out of 29—have been developed in the last 20 years, especially in Europe. Among them, the system operational in the Sorfjord region, Norway (EU_2004_A) since 2004 is particularly well-known and well-described in the scientific literature. Indeed, the Åknes rockslide under surveillance represents a significant threat to the local communities for the potential to trigger a tsunami as a consequence of the fall of the sliding mass into the fjord. For this reason, the landslide is investigated year-round by a variety of monitoring instruments, including nine corner reflectors, GPS, laser, radar and seismic sensors. However, it should be noted that the successful operation of this system relies more on social aspects, i.e. the trust between the experts making the observations and the residents of the area threatened by the tsunami, rather than on technical aspects (Blikra et al. 2013). Other relevant examples of local LEWS deployed in Europe are addressing the following: a complex slope movement in the Southern French Alps known as La Valette landslide since 2007 (EU_2007_A); a large and deep colluvial landslide affecting the municipality of Ancona, Italy since 2008 (EU_2008_A); and a complex

phenomenon composed of retrogressive rockslides and rock avalanches threatening the village of Preonzo in the Swiss Alps since 2010 (EU_2010c_A). Besides, many other LEWS exist at local scale outside Europe. In Asia, local LEWS have been implemented both at prototype (AS_2007_P, AS_2014_P) and operational systems (AS_2002_A, AS_2004_A, AS_2005_A). Among the latter, the system employed in Wushan Town, China (AS_2004_A) has been operational since 2004 for monitoring the Yuhuangge landslide, the largest of the 27 phenomena affecting the area where hundreds of building and structures have been relocated after the impoundment of the Three Gorges Reservoir in 2003 (Yin et al. 2010). In North America, a relevant example is represented by the system deployed in 2005 at Turtle Mountain, Canada (NA_2005_A) dealing with the Frank Slide, which partially buried the city of Frank in 1903, killing over 70 people (Read et al. 2005). In Oceania, a system has been installed since 2000 at Mt. Ruapehu, New Zealand (OC_2000_A), where lahars are likely to occur either when the crater lake over flows or when the tephra dam collapses with or without a volcanic eruption (Massey et al. 2009).

Table 2.2 lists information on the location and the country where the system has been employed, the institution in charge of operating the system, the source of the data used for the analyses and the year of the last information available. In the large majority of the cases—27 out of 29—the systems are operated either by government institutions, often directly involved in landslide risk management, or by civil protection agencies operating at national or regional level. Only two prototype systems are designed and managed by university research groups: the Nojiri River basin, Japan (AS_1991_P) and Wollongong, Australia (OC_2005_P). The information on the period of activity and the main characteristics of the Lo-LEWS was retrieved on different sources: articles published in international journal, proceeding of international conferences, web pages, and grey literature. Systems for which recent up to date information on the state of activity is not available have been considered operational for the following years, unless information on their termination was found in literature. It is worth mentioning that, besides the 29 Lo-LEWS reported in Table 2.2, many other systems are operational at local scale around the world to deal with unstable slopes in various contexts, such as: road and railway embankments, pipelines and open pit mines. If they have not been included herein, it means that information on these systems is not available, it was not found or it is privately disclosed in internal reports.

Table 2.2 Location, country, managing institution, source of information, and year of most recent information of the Lo-LEWS reviewed by *Pecoraro et al. (2018)*

ID	Location	Institution	Source of information	Latest information
AS_1977_N	Xintan Town (CN)	No info	[29], [46]	2016
AS_1991_P	Nojiri River Basin (JP)	Kyoto University	[21], [41]	2004
AS_2002_A	Taiwan torrents (TW)	SWCB	[52]	2011
AS_2004_A	Wushan Town (CN)	MLR	[47], [51]	2010
AS_2005_A	Lake Sarez (TJ)	Ministry of Defense	[13]	2007
AS_2007_P	Banjarnegara (ID)	AIT	[18], [39]	2009
AS_2014_P	Longjingwan (CN)	SKLGP	[19], [23]	2015
EU_1995_P	Moscardo catchment (IT)	Forest Service of Friuli-Venezia Giulia Region	[1]	1996
EU_1997_A	Coastal areas (EN)	No info	[8], [40]	2015
EU_2000_A	Nals (IT)	Civil Defence	[40], [44]	2015
EU_2000b_A	Illgraben catchmrnt (CH)	Cantonal CCU	[2], [23]	2009
EU_2002_A	South-west (DE)	No info	[44]	2002
EU_2003_A	Aosta Valley (IT)	Aosta Control Centre	[5], [42], [43]	2010
EU_2004_A	Åknes (NO)	Åknes/Tafjord Early Warning Centre	[3], [4,] [26], [27]	2013
EU_2006_P	Ruinon (IT)	ARPA Lombardia Early Warning Centre	[3], [10]	2006
EU_2007_A	La Valette (FR)	RTM	[48]	2017
EU_2007b_P	Torgiovannetto (IT)	No info	[20]	2007
EU_2007c_P	Swabian Alb (DE)	BMBF	[44]	2008
EU_2008_A	Ancona (IT)	Ancona Monitoring Center	[3], [6], [7], [9]	2012
EU_2009_A	Mont de La Saxe (IT)	Regional Geological Survey	[11], [12], [32]	2015
EU_2009b_A	Mannen (NO)	Åknes/Tafjord EWC	[3], [4], [26]	2013
EU_2010_A	Alice Bel Colle (IT)	Alice Bel Colle municipality	[36]	2010
EU_2010b_A	Bagnaschino (IT)	Geological Bureau of the Province of Cuneo	[17]	2012
EU_2010c_A	Preonzo (CH)	Department of Territory - Canton of Ticino	[30], [31]	2016
NA_1998_A	Mt. Rainier (USA)	USGS and PCEM	[28], [37], [49], [50]	2018
NA_2005_A	Turtle Mountain (CA)	Alberta Geological Survey	[16], [35], [38]	2014
NA_2009_N	Vancouver (CA)	Ministry of Forests	[22]	2011
OC_2000_A	Mt. Ruapehu (NZ)	Department of Conservation	[24], [33]	2010
OC_2005_P	Wollongong (AU)	University of Wollongong	[14], [15]	2005

← Legend:
a) Institution: SWCB: Soil and Water Conservation Bureau; MLR: Ministry of Land and Resource; AIT: Asian Institute of Technology; SKLGP: State Key Laboratory of Geohazard Prevention and Geoenvironment Protection; CCU: Cantonal Crisis Unit; RTM: Restauration des Terrains en Montagne; BMBF: German Federal Ministry of Education and Research; EWC: Early Warning Centre; USGS: United States Geological Survey; PCEM: Pierce County Emergency Management
b) Source of information: [1]: Arattano (1999); [2]: Badoux et al. (2009); [3]: Baroň et al. (2012); [4]: Blikra et al. (2013); [5]: Broccolato (2010); [6]: Cardellini and Osimani (2011); [7]: Cardinaletti et al. (2011); [8]: Clark et al. (1996); [9]: Cotecchia (2006); [10]: Crosta and Agliardi (2003); [11]: Crosta et al. (2014); [12]: Crosta et al. (2015); [13]: Di Biagio and Kjekstad (2007); [14] Flentje and Chowdhury (2005); [15]: Flentje and Chowdhury (2006); [16]: Froese and Moreno (2014); [17]: Giuliani et al. (2010); [18]: Honda et al. (2008); [19] Huang et al. (2013); [20] Intrieri et al. (2012); [21] Itakura et al. (2000); [22] Jakob et al. (2012); [23] Ju et al. (2015); [24]: Keys and Green (2008); [25]: Kristensen and Blikra (2011); [26]: Kristensen et al. (2010); [27]: Lacasse and Nadim (2011); [28]: LaHusen (1998); [29]: Li et al. (2016); [30]: Loew et al. (2012); [31]: Loew et al. (2016); [32]: Manconi and Giordan (2015); [33]: Massey et al. (2010); [34]: McArdell et al. (2007); [35]: Moreno and Froese (2010); [36]: Olivieri et al. (2012); [37]: Pierson et al. (2014); [38]: Read et al. (2005); [39]: Sassa et al. (2009); [40]: Stähli et al. (2015); [41]: Takeshi (2011); [42]: Tamburini (2005); [43]: Tamburini and Martelli (2006); [44]: Thiebes (2011); [45]: Thiebes et al. (2014); [46]: Wang (2009); [47]: Wang et al. (2008); [48]: web page from OMIV (accessed: 23 October 2017); [49]: web page from USGS (accessed: 05 September 2018); [50]: web page from PCEM (accessed: 05 September 2018); [51]: Yin et al. (2010); [52]: Yin et al. (2011)

In the following sections, the 29 Lo-LEWS introduced herein are discussed and analyzed considering the three main modules introduced by Calvello (2017) and already described in Chapter 2: landslide model, warning model and warning system.

2.3.2 Landslide model

The landslide model is the first module needed to design a Lo-LEWS, according to the scheme proposed in Section 2.2.1. Table 2.3 summarizes the landslide models used in the systems reported herein in terms of: covered area, landslide cause(s), type(s) of landslide, and monitoring system.

Table 2.3 Information on landslide model developed within the Lo-LEWS reviewed by *Pecoraro et al. (2018)*

ID	Covered area	Type(s) of landslide	Landslide cause(s)	Monitoring system
AS_1977_N	0.75 km^2	Rock avalanche	Rainfall	The, Crack, WLM
AS_1991_P	10 km^2	Debris flows	Rainfall	Geoph
AS_2002_A	17 + 3 sites (35,980 km^2)	Debris flows	Rainfall	*17 on-site + 3 mobile stations:* RG, Cam, Geoph, Hyd, WS
AS_2004_A	0.75 km^2	Deep-seated colluvial	Rainfall and human activity	GPS, TDR, Inc, Piez, RG, OptF, WLM
AS_2005_A	1.5 km^2	No info	Rainfall	WLM, Acc, GPS, SprS, WS
AS_2007_P	1 km^2	No info	Rainfall	EExt, RG, Piez, Cam
AS_2014_P	0.008 km^2	Rainfall-induced	Rainfall	RG, Inc, Piez
EU_1995_P	4.1 km^2	Debris flows	Rainfall	Seis
EU_1997_A	6 sites (1 km^2)	Cliff top recession	Sea activity	Tilt, EExt, PS, GPS, Inc
EU_2000_A	App. 0.3 km^2	Debris flows	Rainfall	Geoph, Piez, RG, Cam
EU_2000b_A	9.5 km^2	Debris flow	Rainfall	Geoph, Sat, Cam, RG
EU_2002_A	0.035 km^2	No info	No info	GPS
EU_2003_A	4 * < 1 km^2	No info	Rainfall and snowmelt	EExt, GPS, WS, TotS, Piez, GbSAR
EU_2004_A	0.75 km^2	Rockslide	Rainfall and snowmelt	GPS, TotS, GbSAR, BExt, Crack, Tilt, Geoph, WS, DMS, PS
EU_2006_P	0.26 km^2	Rockslide	Rainfall	EExt, TotS, WS, GPS, InSAR
EU_2007_A	0.5 km^2	Mudslide	Rainfall	WS, Inc, Piez, BExt, GPS, Cam, LiDAR
EU_2007b_P	0.03 km^2	Rockslide	Rainfall	EExt, RG, Cam
EU_2007c_P	0.4 km^2	Rockfall	Rainfall	Inc, Tilt, TDR, Tens, WS, Piez
EU_2008_A	App. 3 km^2	No info	Rainfall	TotS, GPS, RG, DMS, PS
EU_2009_A	0.15 km^2	Rockslide	Rainfall and snowmelt	*Surface:* InSAR, GPS, TotS *Deep:* Inc, BExt, PS, DMS
EU_2009b_A	0.25 km^2	Rockslide	Rainfall and snowmelt	BExt, GPS, GbSAR, DMS, PS, WS
EU_2010_A	0.45 km^2	No info	Rainfall	DMS, Inc, PS
EU_2010b_A	0.15 km^2	Deep-seated roto-translational	Rainfall and snowmelt	DMS, PS, TotS, WS, Inc
EU_2010c_A	0.01 km^2	Rockslides and rock avalanches	Rainfall	EExt, RG, TotS, Crack, GbSAR
NA_1998_A	100 km^2	Lahars	Snowmelt and volcanic activity	Geoph
NA_2005_A	0.5 km^2	Rock avalanche	Rainfall	Tilt, BExt, Crack, WS, RG, TDR
NA_2009_N	160.76 km^2	Debris flows	Rainfall	RG
OC_2000_A	0.2 km^2	Lahars	Dam break	3 Geoph, WLM
OC_2005_P	2 sites	Rainfall-induced	Rainfall	Inc, Piez, RG

← Legend: The: Theodolite; TotS: Total station; Crack: Crackmeter; Mic: Microphone; RG: Rain gauge; Cam: Camera; Geoph: Geophone; WLM: Water level meter; WS: Weather station; Bar: Barometer; GPS: Global positioning system; TDR: Time domain reflectometer; Inc: Inclinometer; Hyd: Hydrometer; PT: Pressure transducer; OptF: Optic fiber; Acc: Accelerometer; TM: Turbidity mteter; EExt: Embedded Extensometer; BExt: Borehole Extensometer; Seis: Seismometer; Tilt: Tiltmeter; Sat: Satellite sensor; GbSAR: Ground-based synthetic aperture radar; DMS: "Differential monitoring of instability" column; InSAR: Interferometric synthetic aperture radar; LiDAR: Light detection and ranging; Tens: Tensiometer)

Covered area

The reviewed systems are mostly designed to operate at slope scale, dealing with a single landslide system over a limited portion of territory. Although they have been designed to operate at the same scale of operation, the area under surveillance varies by orders of magnitude, ranging from less than 1 km^2 to more than 100 km^2 (Figure 2.5).

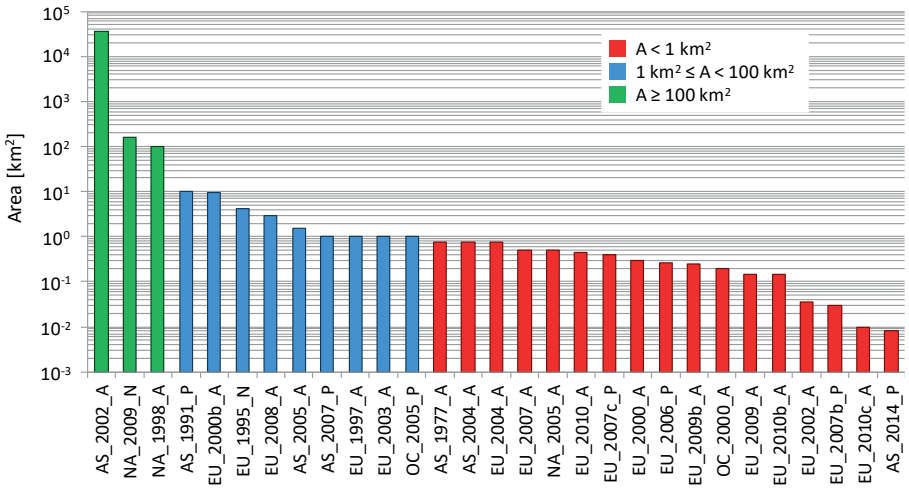

Figure 2.5 Lo-LEWS reported in the literature ordered by covered area

The smallest warning areas are covered by the systems operational in: Longjingwan, China (AS_2014_P); South-west Germany (EU_2002_A); Torgiovannetto, Italy (EU_2007b_P); and Preonzo, Switzerland (EU_2010c_A). The first one refers to a rather typical Lo-LEWS established in 2014 and aimed at monitoring the Longjingwan landslide, an unstable mass characterized by a length of 200 m and a width of 40 m (Figure 2.6). According to field surveys, the landslide was reactivated by an intense precipitation event on 24 June 1995. Despite the relatively small

sliding surface, the landslide represents a high potential risk for the inhabitants of the nearby Jinzhong Town (Ju et al. 2015).

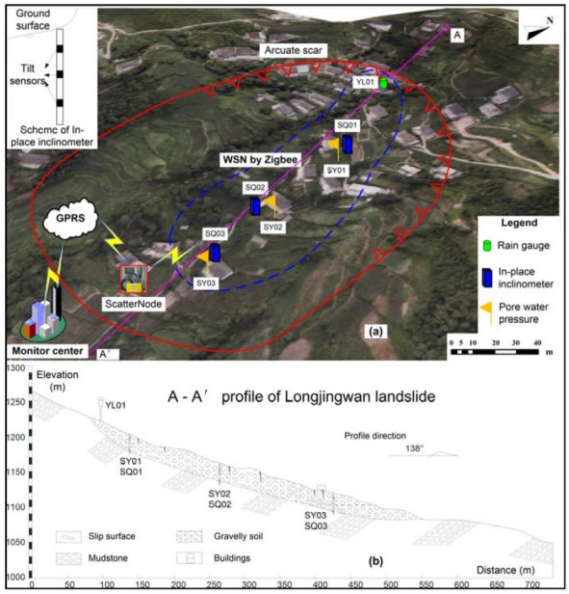

Figure 2.6 Schematic view (a) and cross section (b) of the Longjingwan landslide *(Ju et al. 2015)*

Conversely, larger areas are investigated by the following systems: Taiwan (AS_2002_A); Mount Rainier, USA (NA_1998_A); and North Vancouver, Canada (NA_2009_N). The former, established by the Taiwanese Council of Agriculture Soil and Water Conservation Bureau (SWCB) in 2002, is a peculiar Lo-LEWS, as it is formed by 17 on-site monitoring stations located in the proximity of potential debris flows torrents (Figure 2.7). However, the presence of 1,503 debris flows-prone channels around the island and the extreme variability of the rainfall regime in the monsoon season could lead to an ineffective warning. Therefore, in 2004 the system has been integrated by three more mobile monitoring stations, equipped with the same instruments of the on-site ones. This project is aimed both at increasing the capability of collecting field data and enhancing the probability of detecting debris flow events while already occurring (Yin et al. 2011).

Figure 2.7 Shenmu debris flow monitoring station, one of the 17 on-site monitoring station located around Taiwan island *(Yin et al. 2011)*

Landslide cause(s)

Figure 2.8 displays that twenty-six of the 28 Lo-LEWS for which the landslide cause is clearly specified deal with weather-induced landslides, i.e. triggered by rainfall, snowmelt or a combination of both. It should be stated that at Mt. Rainier, USA (NA_1998_A) the investigated lahars (volcanic debris flows) mainly form when water from snowmelt mixes with loose volcanic material. However, in some cases they can be directly associated with the effects of the volcanic activity when snow and glaciers are melted by lava and other pyroclastic surges produced by a volcanic eruption.

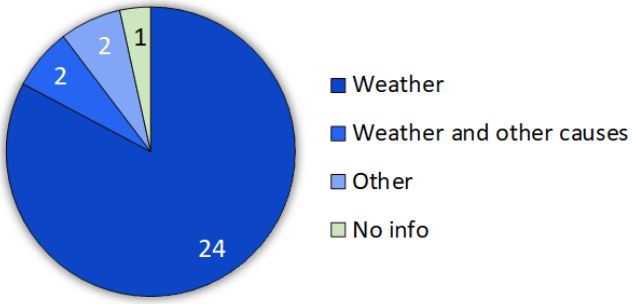

Figure 2.8 Causes of landslides addressed within the Lo-LEWS reviewed by *Pecoraro et al. (2018)*

In the two remaining cases, EU_1997_A and OC_2000_A, the landslides under surveillance are not triggered by weather conditions. The former has been designed to cope with cliff top recessions along the southern and eastern coasts of England, which are caused by sea abrasion, mass movements and water erosion (Figure 2.9). On the other hand, the lahars monitored by the latter are typically triggered by the failure of a tephra dam in the former outlet of the lake or by the collapse of part of the rim of a crater lake. Other possible triggers may include eruptions that have ejected water from the crater lake.

Figure 2.9 Coastal landslide occurred in Scarborough, south-eastern coast of England *(McInnes and Moore 2011)*

Type(s) of landslide

Figure 2.10 shows the types of landslides monitored in the Lo-LEWS described herein. Almost all the systems—28 out of 29—deal with one type of landslide: this is not surprising, as systems operating at slope scale are designed and managed according to the characteristics of the landslide under surveillance, which in turn strongly influence the choices on the parameters to be monitored and the monitoring methods. The most investigated phenomena are debris flows (8) and rockslides (6). In two cases (AS_2014_P and OC_2005_P) only generic statement that the systems address rainfall-induced landslide is reported. Furthermore, neither the types of landslide under investigation nor the style of movement is mentioned for six systems.

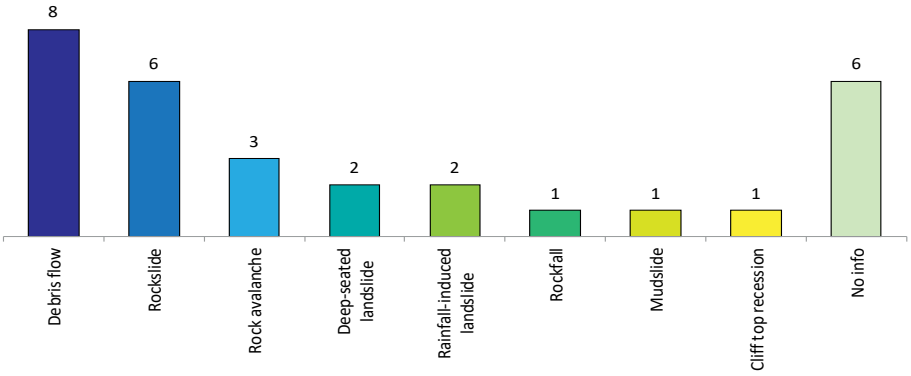

Figure 2.10 Type of landslide under surveillance within the Lo-LEWS reviewed herein. Total is higher than 29 because two different type of landslides are considered in EU_2010c_A *(Pecoraro et al. 2018)*

A peculiar system is operational in Preonzo, Switzerland (EU_2010c_A), where a series of retrogressive rockslides and rock avalanches are being monitored as a part of an extremely complex phenomenon (Figure 2.11).

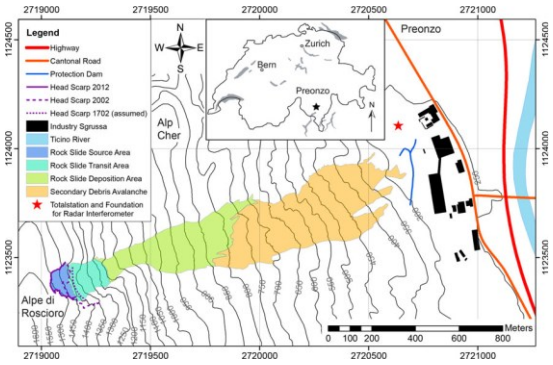

Figure 2.11 Map of the Preonzo 2012 trigger, propagation, and deposition areas. Elements at risk (industrial area of Sgrussa, cantonal road, A2 highway) are also shown *(Loew et al. 2016)*

2.3.3 Warning model

The landslide model is part of the warning model, whose two other components are warning criteria and warning levels. Table 2.4 lists the main characteristics of the warning models developed within the 29 Lo-LEWS: warning criteria, warning parameters, and warning levels.

Table 2.4 Information on warning model developed within the Lo-LEWS reviewed by *Pecoraro et al. (2018).* Legend: *HM:* Heuristic method; *CL:* Correlation law; *PM:* Probabilistic model

ID	Warning criterion	Warning parameters	Warning levels
AS_1977_N	Power law: velocity vs. failure time (CL)	Velocity	2
AS_1991_P	Empirical correlation with acoustic emission (HM)	Acoustic emission	2
AS_2002_A	Rainfall intensity or cumulated rainfall (CL)	Rainfall intensity or accumulated rainfall	2
AS_2004_A	Empirical correlation with displacement, pore water pressure, strains (HM)	Displacement, pore water pressure, strains	4
AS_2005_A	Empirical correlation with seismic acceleration, stream flow, displacement, water quality, rainfall (HM)	Seismic acceleration, stream flow, displacement, water quality, rainfall	3
AS_2007_P	Correlation with antecedent rainfall and displacement (CL)	Antecedent rainfall, displacement	3
AS_2014_P	Empirical velocity thresholds (HM)	Velocity	4
EU_1995_P	Correlation with acoustic emission (HM)	Acoustic emission	2
EU_1997_A	Empirical thresholds (HM)	Displacement, groundwater level	2
EU_2000_A	Correlation with acoustic emission (HM)	Acoustic emission	2
EU_2000b_A	Rainfall intensity-duration (CL)	Rainfall	2
EU_2002_A	Pre-defined thresholds based on rate of movement (HM)	Displacement	3
EU_2003_A	Rainfall and displacement thresholds (HM)	Rainfall, displacement	3
EU_2004_A	Velocity level (HM)	Velocity	5
EU_2006_P	Power law: velocity vs. failure time (CL)	Velocity	3
EU_2007_A	No info	No info	No info
EU_2007b_P	Empirical velocity thresholds (HM)	Velocity	3
EU_2007c_P	Empirical correlation with pore water pressure and displacement (HM)	Pore water pressure, displacement	3
EU_2008_A	Empirical thresholds (HM)	Displacement, rainfall, groundwater level	5
EU_2009_A	Empirical displacement thresholds (HM)	Displacement	3
EU_2009b_A	Velocity level (HM)	Velocity	5
EU_2010_A	Empirical displacement thresholds (HM)	Displacement	4
EU_2010b_A	Rain intensity-duration law (CL)	Rainfall	2
EU_2010c_A	Correlation law: velocity vs. time of failure (CL)	Velocity	4
NA_1998_A	Correlation with acoustic emission (HM)	Acoustic emission	3
NA_2005_A	Empirical velocity-based thresholds (HM)	Velocity	4
NA_2009_N	Discriminant analysis of rainfall events (PM)	Rainfall	5
OC_2000_A	Correlation with absolute lake level (HM)	Absolute lake level	6
OC_2005_P	Intensity-duration (CL)	Rainfall	3

Warning criteria

A warning criterion can be defined as a functional relationship whereby the occurrence of the landslides under surveillance is related to the parameters being monitored (e.g., displacements, rainfall). Figure 2.12 displays that twenty-seven of the 29 identified systems employ empirical models, which can be further subdivided into heuristic methods (19 cases) and correlation laws (8 cases). On the other hand, a probabilistic model has been developed in North Vancouver, Canada (NA_2009_N). No information is available for the system dealing with La Valette landslide, France (EU_2007_A).

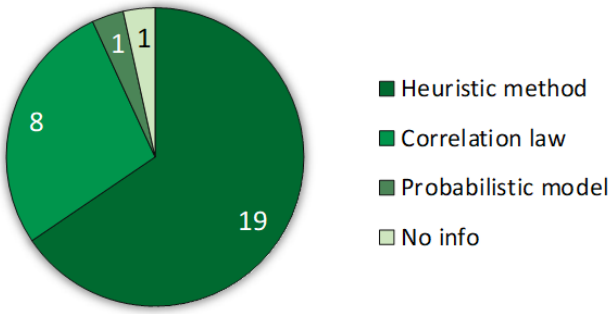

Figure 2.12 Warning criteria adopted within the Lo-LEWS reviewed by *Pecoraro et al. (2018)*

Heuristic approaches rely on the identification of the conditions which lead to slope instability by analyzing monitoring data and landslide activity. The threshold values are typically defined through an expert judgment, without any rigorous statistical, mathematical or physical criterion. An example is represented by the system employed at Lake Sarez, Tajikistan (AS_2005_A), where long-term monitoring data have been collected since the international "Lake Sarez Risk Mitigation project" was launched in 2000. The acquired historical observations have been analyzed and multiple thresholds have been implemented considering the following parameters: seismic acceleration, stream flow, displacement, water quality, and rainfall; in addition, the system is supported by visual observations of the landslide activity (Di Biagio and Kjekstad 2007). Another example is the system employed in Torgiovannetto, Italy (EU_2007b_P) empirically-based movement rate thresholds (mm/day) have been defined considering measurements from a network of extensometers installed within the

rockslide body (Figure 2.13). The thresholds for each extensometer have been derived by analysing the most critical periods of the whole dataset and their reliability has been assessed by performing a back analysis supported by expert judgement and interpretation. Moreover, the system is designed to be flexible, since the thresholds can be modified as soon as new data become available (Intrieri et al. 2012).

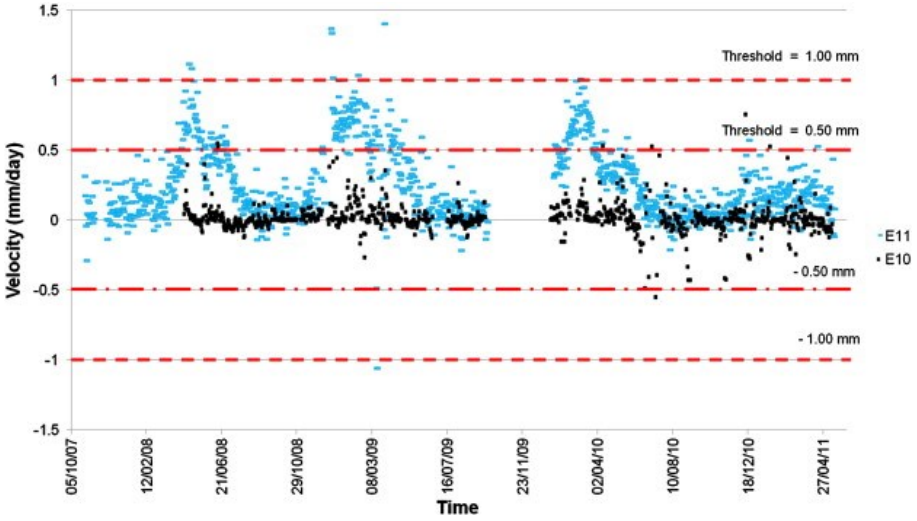

Figure 2.13 Example of extensometers data used for defining the thresholds in Torgiovannetto *(Intrieri et al. 2012)*

Eight systems employ correlation laws derived from a statistical analysis of historical data. For weather-induced landslides, thresholds are defined as the lower-bound limit to the rainfall conditions which resulted in slope instability plotting two representative variables (e.g., intensity, duration, antecedent rainfall, accumulated rainfall) in Cartesian, semi-logarithmic or logarithmic coordinates. In some cases, the thresholds are refined by considering also the rainfall events that did not results in landslides. Intensity-duration *(ID)* thresholds have been defined for four systems: Taiwan torrents (AS_2002_A), Illgraben catchment (EU_2000b_A), Bagnaschino (EU_2010b_A), Wollongong (OC_2005_P). A peculiar model has been applied in Banjarnegara (AS_2007_P), where the algorithm is based on two different monitoring parameters: antecedent rainfall in 24 and 72 h and cumulative displacements. On the other hand, systems addressing rockslides—Ruinon (EU_2006_P) and Preonzo

(EU_2010c_A)—employ a power law defined assuming that a catastrophic event would be preceded by an "accelerating creep" behaviour (Crosta and Agliardi 2003; Loew et al. 2016). In both the cases, the failure time t_f, i.e. the time interval between the beginning of the monitoring activity and the collapse of the unstable slope, has been derived by a power-law relationship obtained by time-integrating the equation which relates the displacement acceleration $\ddot{\Omega}$ of a material close to failure to the velocity $\dot{\Omega}$ (Figure 2.14a,b).

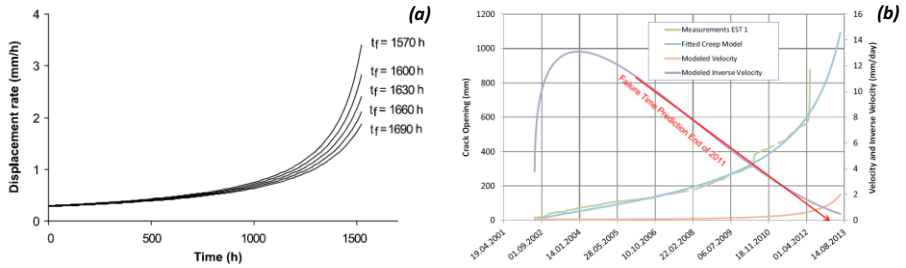

Figure 2.14 Failure time calculated from rate of movement in (a) Ruinon *(Crosta and Agliardi 2003)* and (b) Preonzo *(Loew et al. 2016)*

Finally, the system operational in North Vancouver (NA_2009_N) from 2009 to 2011 employed a probabilistic model for the definition of the thresholds. Indeed, a discriminant function analysis was conducted to identify the rainfall variables which provide the best predictive discriminatory power and variance. The outcomes of the correlation matrix suggested that the most intercorrelated rainfall variables are the antecedent and the intensity. These parameters allow the classification of a rainstorm into landslide triggering *(LS)* or non-landslide triggering *(NLS)* groups. The difference between the classification scores of each group, ΔCS, can be assumed as a reasonable proxy for the likelihood of debris flows occurrence because it represents the distance to the centroid of each data population (Jakob et al. 2012).

Warning parameters

Warning parameters can be considered as variables representative of the landslide behaviour, whose critical values must be identified for the definition of the thresholds to be implemented. As expected, displacements (in terms of rate of movement, velocity and acceleration) are the primary parameters for 15 systems, as they provide direct evidence

of the state of activity of the landslide under surveillance- Besides, meteorological parameters have been considered for 8 systems addressing weather-induced landslides. It is worth mentioning that variables not included in the warning model have been investigated in a large number of cases (21). The need for additional information may be attributed to the willingness to evaluate the landslide model, towards possible updates of the adopted warning model. For example, although the thresholds developed for the rock avalanche under surveillance at Turtle Mountain (NA_2005_A) are based on rate of movement (primary parameters), displacement and cracking (secondary parameters) and rainfall (tertiary parameters) are also monitored (Froese and Moreno 2014).

Warning levels

Figure 2.15 shows that the majority of the 29 Lo-LEWS employ two (8 cases) or three (10 cases) warning levels. Indeed, as stated by Medina-Cedina and Nadim (2008) the definition of many thresholds could lead to a needless complexity not necessarily improving the reliability of the system. However, several systems deployed in the 2000s employ four warning levels (6 cases) or more (4 cases). The highest number of warning levels, from base level (ordinary state) to level 5 (risk characterized by a conditional probability of 100%), is adopted at Mt. Ruapehu (OC_2000_A).

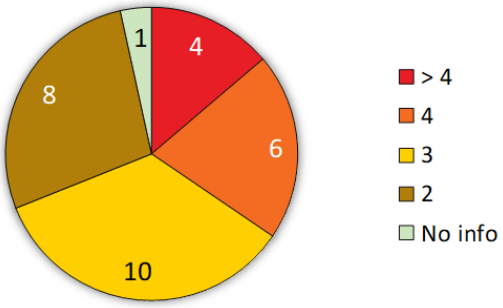

Figure 2.15 Number of warning levels adopted within the Lo-LEWS reviewed by *Pecoraro et al. (2018)*

In North Vancouver (NA_2009_N), the warning model was designed to avoid sudden transitions between the four warning levels: no watch, watch I/watch II, warning I, warning II (Figure 2.16). Therefore, each level was

preceded by the level that was higher or lower in the hierarchy, without skipping any step. Moreover, each level was typically maintained for at least six consecutive hours, otherwise an override was issued to avoid confusion to the system users. No information on this issue is available for the system employed for La Valette landslide (EU_2007_A).

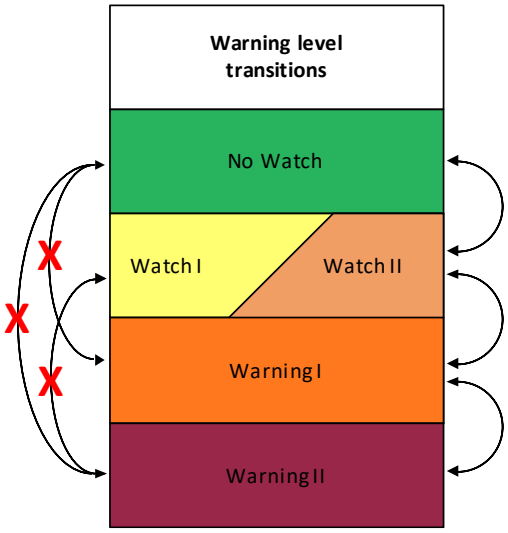

Figure 2.16 Warning level transitions and switches that allow transitions from one warning level to another *(Jakob et al. 2012)*

2.3.4 Warning system

The landslide model and the warning model are embedded in the warning system, which refers both to technical issues and social aspects. Table 2.5 summarizes the main characteristics of the warning models developed within the 29 Lo-LEWS: lead time, warning statements, media employed to spread the warnings to the recipients, as well as decision-making process for issuing a warning. All these aspects vary significantly among the systems depending both on the warning level and on the aims for which they are designed and managed.

Table 2.5 Information on warning system of Lo-LEWS reviewed by *Pecoraro et al. (2018)*

ID	Lead time	Warning statement	Information tools	Decision-making
AS_1977_A	24 hours	Public	No info	No info
AS_1991_P	Few seconds	Internal	No info	No info
AS_2002_A	< 1 hour	Internal	Triggering signal	No info
AS_2004_A	No info	Public	Website	Government
AS_2005_A	< 1 hour	Public	Warning messages	Control centre
AS_2007_P	1 to 24 hours	Public	Web pages	No info
AS_2014_P	24 hours	Public	Web pages	Experts judgement
EU_1995_N	Few seconds	Internal	No info	No info
EU_1997_A	No info	Internal	Automatic phone calls	No info
EU_2000_A	20 to 60 minutes	Public	Flood lights	No info
EU_2000b_A	Few seconds	Public	Flashing lights, sirens	Automated alert signals
EU_2002_A	No info	Internal	Automatic phone calls	Road authorities
EU_2003_A	24 hours	Internal	Warning messages	Expert group
EU_2004_A	24 hours	Public	Web pages, public meetings, newspapers, television, radio, sirens, automatic phone calls	Early Warning Centre
EU_2006_P	24 hours	Public	No info	No info
EU_2007_A	No info	Public	No info	Local risk managers
EU_2007b_P	24 hours	Internal	Automatic notification	No info
EU_2007c_P	24 hours	Public	Two traffic lights, SMS	Experts
EU_2008_A	1 to 3 hours	Internal	Warning SMS, direct call	Civil Protection Department of the Ancona Municipality
EU_2009_A	1 hour	Public	Warning messages, traffic lights	Civil Protection
EU_2009b_A	> 24 hours	Public	SMS, emails, electronic warning siren	Early Warning Centre
EU_2010_A	No info	Internal	SMS, direct call	Technical personnel of the Alice Bel Colle Municipality
EU_2010b_A	No info	Public	No info	No info
EU_2010c_A	> 1 hour	Internal	SMS	Cantonal officers and automatic alarms
NA_1998_A	40 minutes to 3 hours	Public	Warning messages, television, radio, sirens	Automated system
NA_2005_A	24 hours	Internal	Warning messages, phone calls	Municipal and provincial emergency managers
NA_2009_N	6 hours	Public	Warning messages	Warnings updated automatically
OC_2000_A	5 to 30 minutes	Internal	Pagers, phone calls, internet	Decision-making authorities
OC_2005_P	6 hours	Public	Web pages	No info

Lead time

The lead time can be described as the interval between the beginning of a landslide event and the time when a warning is issued. Therefore, it must be necessarily longer than the response time needed to undertake the appropriate actions in case of emergency. According to Calvello (2017), systems operating at slope scale can be classified into two main categories: alarm systems and warning systems. The former typically detect process parameters (e.g. acoustic signal) of a phenomenon already in progress providing a very short lead time, on the order of seconds or minutes; on the contrary, the latter monitor triggering factors (e.g. rainfall) before the beginning of a landslide event, thus ensuring a longer lead time, typically more than one hour. Eight of the 29 Lo-LEWS presented herein can be considered alarm systems, as the lead time varies from few seconds to several minutes. Most of them deal with debris flows, such as the prototype system employed in the Moscardo catchment (EU_1995_P) in 1995 and 1996 for research purposes. The four seismic detectors installed at a distance of about 20 meters from the torrent channel were capable to detect three events occurred during the period of analysis in near-real-time, i.e. few seconds before the arrival of the debris flows front (Figure 2.17).

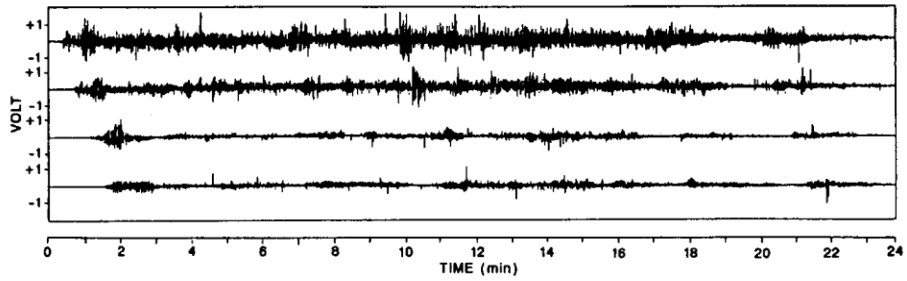

Figure 2.17 Seismic measurements from a geophone installed in the Moscardo catchment on 5 July 1995 *(Arattano 1999)*

Conversely, fifteen systems can be considered warning systems, as the lead time varies from 1 to 24 h. Indeed, they typically address landslides which evolve slowly in the initial phase, but can be characterized by movement rates rapidly increasing before a general failure stage (e.g. rockslides, deep-seated landslides). As an example, the lead time is expected to be 24 h in Swabian Alb (EU_2007c_P), where a limit-equilibrium model was integrated into a semi-automated prototype early warning system in the

context of the ILEWS project, aimed at assessing the stability conditions of the slow-moving landslide under surveillance every 24 h (Figure 2.18). Information on the provided lead time is not available for the remaining six systems.

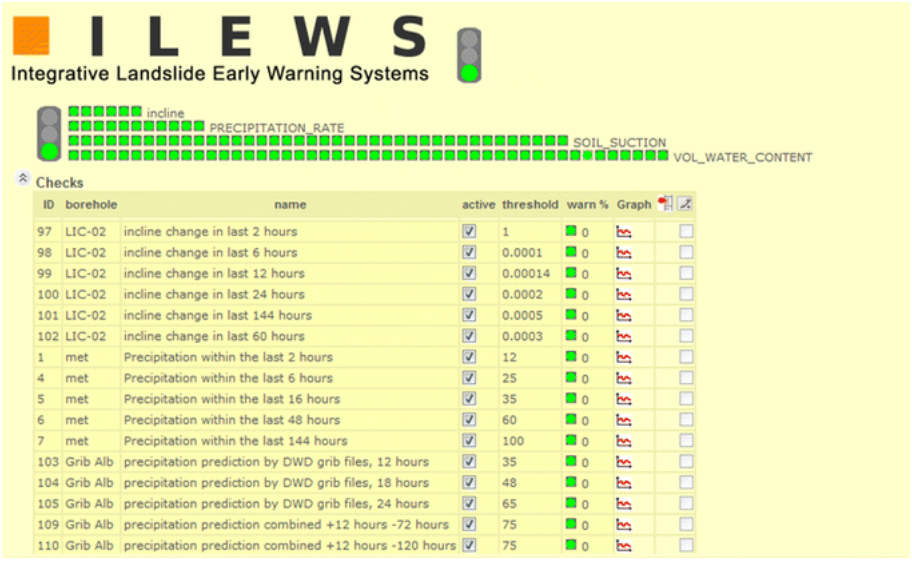

ID	borehole	name	active	threshold	warn %	Graph
97	LIC-02	incline change in last 2 hours	☑	1	0	
98	LIC-02	incline change in last 6 hours	☑	0.0001	0	
99	LIC-02	incline change in last 12 hours	☑	0.00014	0	
100	LIC-02	incline change in last 24 hours	☑	0.0002	0	
101	LIC-02	incline change in last 144 hours	☑	0.0005	0	
102	LIC-02	incline change in last 60 hours	☑	0.0003	0	
1	met	Precipitation within the last 2 hours	☑	12	0	
4	met	Precipitation within the last 6 hours	☑	25	0	
5	met	Precipitation within the last 16 hours	☑	35	0	
6	met	Precipitation within the last 48 hours	☑	60	0	
7	met	Precipitation within the last 144 hours	☑	100	0	
103	Grib Alb	precipitation prediction by DWD grib files, 12 hours	☑	35	0	
104	Grib Alb	precipitation prediction by DWD grib files, 18 hours	☑	48	0	
105	Grib Alb	precipitation prediction by DWD grib files, 24 hours	☑	65	0	
109	Grib Alb	precipitation prediction combined +12 hours -72 hours	☑	75	0	
110	Grib Alb	precipitation prediction combined +12 hours -120 hours	☑	75	0	

Figure 2.18 ILEWS status control highlighting the parameters monitored and the thresholds for issuing the daily alerts *(Thiebes et al. 2014)*

Warning statements

Table 2.5 shows that in 12 cases only internal statements are planned, hence the information is not directly spread to the public in an early stage, but it is targeted to competent authorities, such as politicians, scientists, government institutions, civil protection agencies, or infrastructure authorities. For example, in the system designed for assessing the Ancona Landslide in Italy (EU_2008_A) a team of engineers, geologists, technical experts and urban planners have access year-round the values of the monitored parameters. Moreover, a special task force, named "Centro Operativo di Controllo" (COC), is in charge of coordinating the emergency actions established in case a warning is issued (Figure 2.19). The COC is an interagency structure, which involves experts from other municipality departments as well as experts from other local institutions and organizations and is coordinated by the Major of Ancona who is responsible for all risk mitigation measures (Cardinaletti et al. 2011).

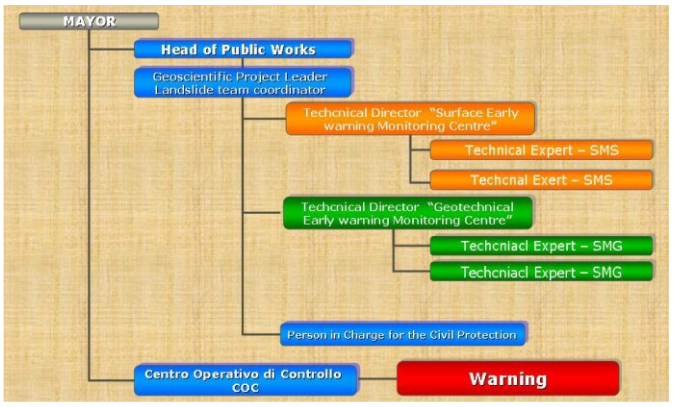

Figure 2.19 Organization of the structure designed for assessing the Ancona Landslide *(Cardinaletti et al. 2011)*

Differently, in the remaining 17 cases the systems are designed to directly inform and warn the population of a possible occurrence of a landslide, prompting them to move to safer places. For example, in Wollongong (OC_2005_P) a web-based software to provide real-time graphical updates of the monitoring data as well as the issued warnings has been developed as a joint initiative of the research time in charge of managing the prototype system and University of Wollongong Centre for Educational Development and Interactive Resources (CEDIR). Figure 2.20 presents the home page of the website reporting a map of the monitoring stations and a list of the monitored sites in the upper left part of the page (Flentje and Chowdhury 2005).

Figure 2.20 Home page of the website dedicated at spreading information on landslides under surveillance in Wollongong *(Flentje and Chowdhury 2005)*

Information tools

Figure 2.21a,b displays the communication strategies developed within the 29 Lo-LEWS described herein. Warning messages, typically sent as an SMS, are the most used tool—13 out of 29—, because many recipients can be easily informed even in emergency situations and the latency between a decision to alert to message receipt is minimized. In nine cases, warning signals, such as traffic lights and sirens, are adopted along road and railways threated in mountainous environments. Moreover, manually or automated phone calls have been also employed in Lo-LEWS deployed before 2000, while internet-based tools, such web pages and email, have been used in more recent systems. Although many communications tools are available, redundancy has been often overlooked in the reviewed Lo-LEWS, because only 21% of them combine two techniques and 14% more than two techniques. However, two relevant exceptions are represented by the systems operational in Åknes (EU_2004_A), and at Mt. Rainier (NA_1998_A), where several techniques—SMS sent in Norwegian, English, and German; warning messages on website, automated phone calls, newspapers, radio/television news ads; warning sirens in the former; warning messages, radio/television news ads, warning sirens in the latter—are combined and evacuation drills are also conducted.

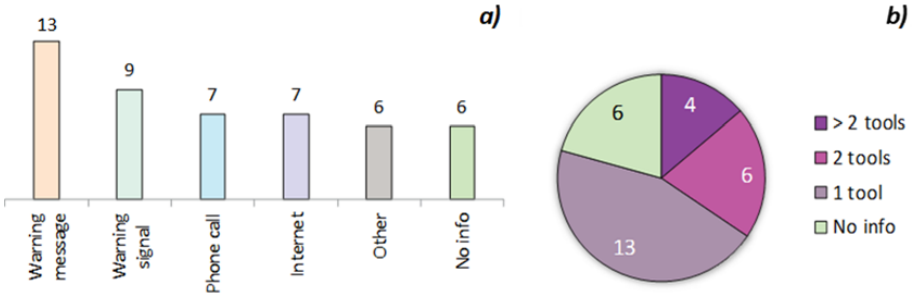

Figure 2.21 Communication tools used (a) and their redundancy (b) within the Lo-LEWS reviewed by *Pecoraro et al. (2018)*

Decision-making process

In a number of cases—11 out of 29—information on criteria for issuing or canceling an alert are not available. However, in the majority of the documented cases (14) the alerts are issued manually by system managers, experts or local authorities. The only documented exceptions are: Illgraben catchment (EU_2000_A), for which alert signs are activated by

a detection system; Preonzo (EU_2010c_A), where the highest level of warning is issued by cantonal officials supported by an automated alert system based on crack meters (Figure 2.22); Mt. Rainier (NA_1998_A), where the alerts are issued by a computer base station, after analyzing the signals from the field stations; and North Vancouver (NA_2009_N), where the warning levels were updated hourly combining rainfall measures from a rain gauge and rainfall forecasts.

Figure 2.22 Downstream view of two radar sensors for measuring flow depth as employed in the Illgraben catchment *(Badoux et al. 2009)*

2.4 REVIEWS ON TERRITORIAL LANDSLIDE EARLY WARNING SYSTEMS

2.4.1 Reviews on territorial landslide early warning systems

Piciullo et al. (2018) prepared a review on 24 Te-LEWS operational worldwide. The information was retrieved from different sources: international journals and publications, scientific reports, web pages, and gray literature, and, in some cases, personal contacts of the authors with system managers. Figure 2.23 provides a summary of the location and the state of activity of the reviewed systems.

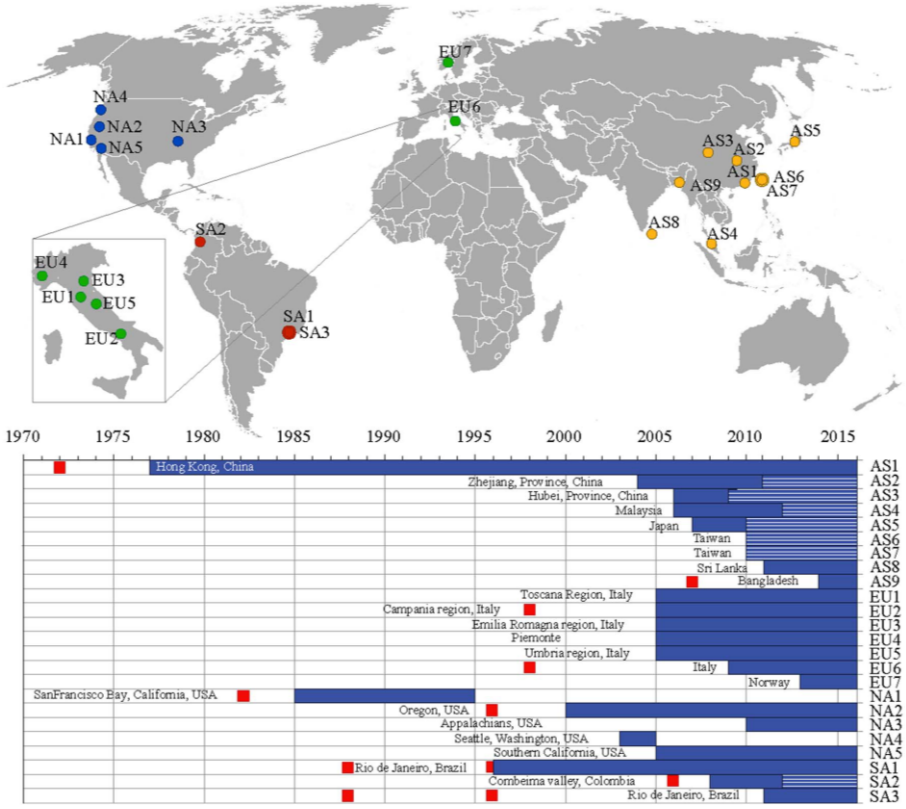

Figure 2.23 Territorial landslide early warning systems operational worldwide: location and period of activity. Legend: red squares: dates of catastrophic landslide events; dark blue: period of activity, retrieved from reliable references; light blue: period of activity, assumed by authors *(Piciullo et al. 2018)*

Only few experiences at regional scale have been carried out before 2005: the majority of the systems have been designed and managed in USA (NA1, NA2, NA3, NA4), even though other examples are reported in Asia (AS1, AS2) and in South America (SA1). On the other hand, in the last decade many other systems have been employing around the world, in Asia and in Europe, particularly in Italy (6 cases). In 9 cases out of 24, systems have been employed after catastrophic landslide events (red squares in Figure 2.23), causing many victims and significant economic losses. Only two of the reviewed systems are no longer active, both of them located in the USA and employed in the San Francisco Bay (NA1)

and in the city of Seattle, Washington (NA4). The former terminated because the institution in charge of operating the system, i.e. the National Weather Service, experienced a net staff reduction, while the latter was operational under an informal agreement between USG, NWS and the city of Seattle for four years, in the period 2002-2005.
The reported territorial LEWS operate at three different territorial levels: national (AS4, AS5, AS7, EU6, EU7), regional (AS2, AS3, AS6, AS8, AS9, EU1, EU2, EU3, EU4, EU5, NA1, NA2, NA3, NA5, SA2), and municipal (AS1, NA4, SA1). The warning area varies by orders of magnitude, even among systems operating at the same level. The majority of the reviewed systems (18) are designed to forecast the possible occurrence of landslides on natural slopes. Only in few cases (AS8, AS9, SA1, SA3) both natural and man-made slopes are considered. Hong Kong (AS1) is the only reported example of a system exclusively designed for man-made slopes, grouped into four main categories: cut slopes, rock slopes, fill slopes, and retaining walls. Although all the reported Te-LEWS deal with weather-induced landslides, in some cases (9) they also consider other natural disasters, such as: hurricanes, floods, typhoons, and snow avalanches.
The main characteristics of the reviewed systems have been analyzed and discussed according to a conceptual model organized in four main tiles: setting, modelling, warning, and response. Besides, the authors presented some considerations and insights on criteria for assessing the success of the systems, i.e. the efficiency and the effectiveness.

2.4.2 Regional LEWS operational in Italy

Pecoraro and Calvello (2016) described the 21 LEWS designed and operated by the Italian regions as a part of the hydrogeological risk mitigation strategy. The report has been prepared for the Project of National Relevance (PRIN) "Landslide risk mitigation through sustainable countermeasures". Information was gathered from a variety of sources, including national and regional laws, technical reports and web pages of the institutions in charge of managing the systems.
The regional LEWS have been introduced by a national law on landslide and flood risk management (DPCM 2005), as a response to a catastrophic landslide event that occurred in Sarno in 1998 (Cascini 2004). The Italian Civil Protection System is constituted by an early warning national office (called Central Functional Centre, CFC) and a network of 21 Regional Centres (called Periferic Functional Centres, CFP), whose main activities

are the prediction, monitoring and evaluation of critical flooding and landslide events resulting from heavy rainfalls and (seldom) snowmelt. Moreover, the CFP are in charge of designing and operating the regional LEWS (Figure 2.24).
The study is organized into two parts. Firstly, the structure of the Central Functional Centre is described reporting: the general organization, the responsibilities of the different actors involved in hydrogeological risk management, the criteria for defining the warning zones and the thresholds for landslide occurrence, the procedures for spreading the warnings, as well as the tasks assigned to the CFP. In the second part the authors summarized and discussed the main aspects related to the design and the implementation of the regional LEWS, such as: types of natural hazards under surveillance; number of warning zones; monitoring systems; warning criteria and number of warning levels; communication tools. Table 2.6 reports some of the abovementioned aspects as well as the year of the most recent update for each system.

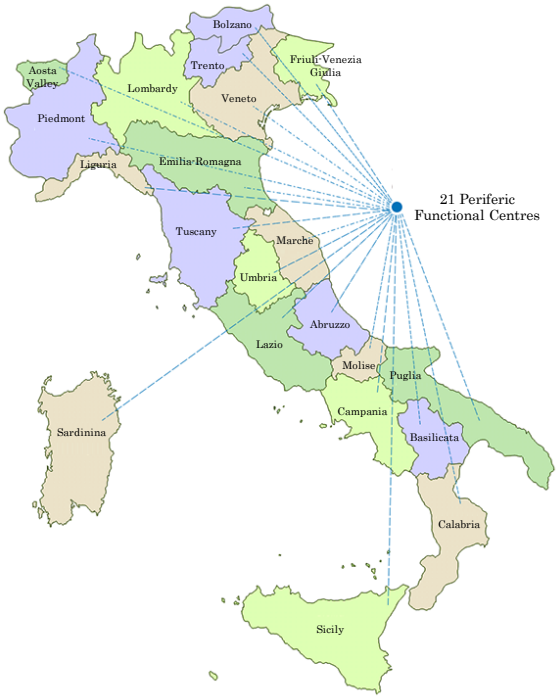

Figure 2.24 Functional Centres in charge of designing and operating regional LEWS in Italy *(Pecoraro and Calvello 2016)*

Table 2.6 Regional LEWS operational in Italy: natural hazards addressed; warning zones; communication tools *(Pecoraro and Calvello 2016)*

Regional LEWS	Natural hazards	Warning zones	Communication tools
Abruzzo	Landslides, heavy rainfall, floods, heat waves, snow, wind, storm tides	6	Email, certified email, website
Aosta Valley	Landslides, heavy rainfall, heat waves, snow, snow avalanches, storm tides	4	Fax, email, website
Autonomous Province of Bolzano	Landslides, heavy rainfall, snow avalanches	1	Website, fax, SMS, email
Autonomous Province of Trento	No info	1	Fax, SMS, phone call, website, TV
Basilicata	Landslides, heavy rainfall, floods, heat waves, snow, wind, storm tides	3	Fax, website, SMS, email, PEC
Calabria	Landslides, heavy rainfall, floods, heat waves, snow, wind, storm tides	6	Fax, website
Campania	Landslides, heavy rainfall, floods, heat waves, snow, wind, storm tides	8	Fax, website
Emilia-Romagna	Landslides, heavy rainfall, floods, heat waves, snow, wind, storm tides	8	Fax, email, SMS, website
Friuli-Venezia Giulia	Landslides, heavy rainfall, floods, snow, snow avalanches	4	Email, certified email, SMS, website
Lazio	Landslides, heavy rainfall, floods	7	SMS, website
Liguria	Landslides, heavy rainfall, floods, heat waves, snow, wind, storm tides	5	Email, PEC, SMS, Facebook, Twitter, websites
Lombardy	Landslides, heavy rainfall, floods, heat waves, snow, snow avalanches, wind	8	Phone call, fax, SMS, website
Marche	Landslides, heavy rainfall, floods, heat waves, snow, wind, storm tides	4	Fax, website
Molise	Landslides, heavy rainfall, floods, heat waves, snow, wind, storm tides	3	Fax, website
Piedmont	Landslides, heavy rainfall, floods, heat waves, snow, fog	11	Fax, website, phone call
Puglia	Landslides, heavy rainfall, floods, heat waves, snow, wind, storm tides	9	Fax, website, SMS, email, certified email
Sardinia	Landslides, heavy rainfall, floods, snow, wind, storm tides	7	SMS, email, website
Sicily	Landslides, heavy rainfall, floods	9	Email, SMS, website
Tuscany	Landslides, heavy rainfall, floods, snow, wind, storm tides	26	Fax, email, SMS, phone call, website
Umbria	Landslides, heavy rainfall, floods, snow, ice	6	Fax, website
Veneto	Landslides, heavy rainfall, floods, snow, snow avalanches	8	Fax, email, SMS, website

2.4.3 Rainfall thresholds for landslide occurrence

Segoni et al. (2018a) reviewed the rainfall thresholds defined for landslide occurrence in the last 9 years. The authors examined all published papers presenting studies on the definition of thresholds, including the contributions on their employment into prototypal or operational LEWS. However, the research was restricted exclusively to peer-reviewed papers written in English and published in journals in order to guarantee the accessibility and the readability to all the reviewed works. They identified 115 thresholds described in 107 papers (two or more thresholds were presented in some articles). Figure 2.25 displays that literature contributions report rainfall thresholds for a large variety of countries.

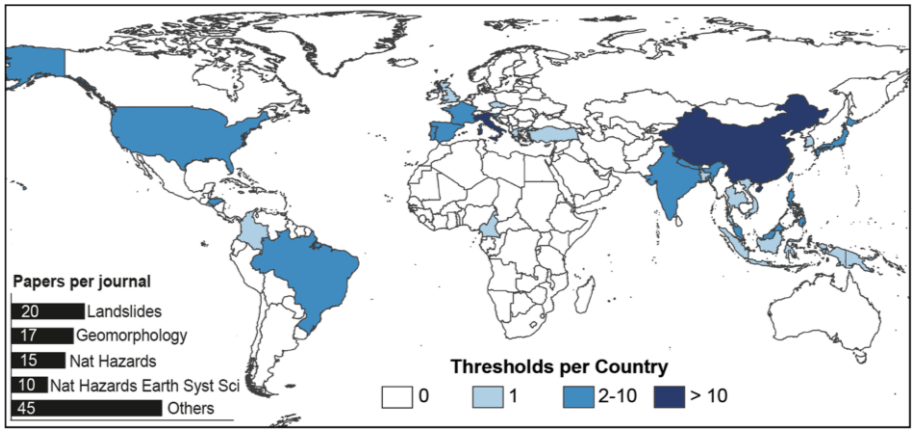

Figure 2.25 Geographical distribution of the analyzed rainfall thresholds. Countries colored based on the number of published thresholds. In the inset in the bottom left, the number of papers per scientific journal in which they were published. *(Segoni et al. 2018a)*

The large majority of them are defined in Europe and Asia (52 and 36%, respectively); 9% of the reported thresholds are located in the Americas, while Africa and Oceania are only marginally represented in this dataset (1% each). The authors stated that this distribution partially reflects the distributions of landslide hazard and risk across the world. Besides, they noted that Africa and central/south America start to focus on the issue of landslide forecasting only recently, thus the scientific progress in this field is still advancing.

On the other size, in North America the low number of papers (3%) is mainly related to a landslide risk lower than other continents, as all the

thresholds are implemented (or to be implemented) within operational LEWS. About half of the papers describe thresholds located in two countries: Italy (35%) and China (14%). According to the authors, this can be explained again with the high exposure to landslide risk of these two countries. This statement is also confirmed by considering that about half (53%) of the thresholds operational into LEWS relates to test sites located in Italy, while half of the papers which describe study areas in China reports prototypal or operational LEWS.
Figure 2.26 reveals that the number of thresholds published in international journal in the last years is increasing, because splitting the surveyed time interval into 3-year periods, more than half of the works (55%) were published in the 2014-2016 (20 papers in 2014, 24 in 2015, and 20 in 2016), while 22% both in the 2008-2010 and in the 2011-2013. Moreover, among the 59 thresholds employed within early warning systems (40 prototypes and 19 operational), 33 of them (56%) were published in the 2014-2016. These outcomes can be interpreted as a proof that researches on rainfall thresholds and on their employment within LEWS are pressing issues in the scientific community.

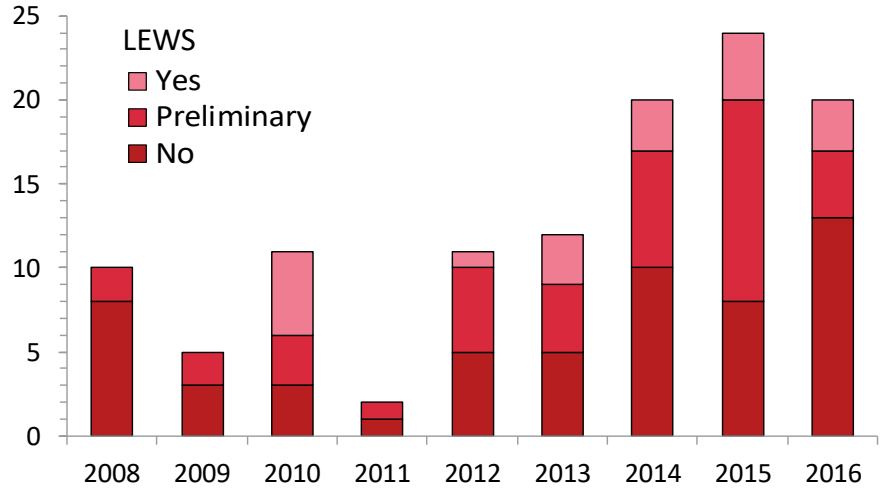

Figure 2.26 Bar chart showing the number of thresholds published in scientific journals from 2008 to 2016. Each year, the number of thresholds implemented in a LEWS (Yes), the preliminary thresholds (Preliminary), and thresholds not deemed to be part of a LEWS (No) are also shown by means of different colored bars *(Segoni et al. 2018a)*

Data collected on rainfall thresholds were grouped into four categories: publication details, geographical distribution and uses, dataset features, threshold definition. In each category the authors selected descriptive information to characterize each one of the 115 thresholds in order to define the most important steps needed to obtain replicable and reliable thresholds with a high predictive capability.
Regarding this review, it should be noted that only information on rainfall thresholds implemented into operational or prototypal Te-LEWS—45 out of 115—are presented and discussed in Chapter 3.

3 MONITORING STRATEGIES AND WARNING MODELS

Monitoring strategies and warning models are fundamental technical aspects to be taken into account in order to define an efficient LEWS. Over the last decades, many systems have been operational both at regional and local scale all around the world, as reported in the literature reviews introduced in Chapter 2. These valuable experiences provide the means for describing these aspects and for investigating their role in the success/failure of a LEWS.
This Chapter is organized into three main parts. Section 3.1 analyses the monitoring strategies developed within operational Lo-LEWS. Successively, Section 3.2 reports and discusses information on monitoring strategies and warning models developed within Te-LEWS for weather-induced landslides. Finally, Section 3.3 highlights several questions that need to be addressed for improving the performance of warning models implemented within LEWS for weather-induced landslides.

3.1 MONITORING STRATEGIES WITHIN LO-LEWS

(based on Pecoraro et al. 2018)

3.1.1 Classification of monitoring instruments

Monitoring is a crucial continuous activity within a LEWS. Indeed, monitoring is necessary to investigate landslide occurrence and activity as well as to define thresholds and alert criteria to be adopted within a warning model in the design phase. Besides, triggering parameters need to be continuously monitored in order to assess the probability of thresholds exceedance in the operational phase. Mikkelsen et al. (1996) stated that monitoring of landslides represents a considerable challenge for

geotechnical engineers and elaborated the first classification presented in the literature, differentiating monitoring techniques in: surface movement measurements, ground displacement measurements, groundwater monitoring and others. Besides, the instruments can be further classified into manually and automated, based on how the measurements are performed. According to Savvaidis (2003), landslide monitoring techniques can be differentiated in: remote sensing, photogrammetric, ground-based geodetic, satellite-based geodetic, and geotechnical. Their applicability varies from case to case depending on several factors, such as: expected risk, accessibility of the area, potential for damage, and availability of resources. In a report of the ClimChAlp project, Komac et al. (2008) individuated four main categories for slope monitoring methods: geodetic, geotechnical, geophysical and remote sensing. The author also discussed the possible fields of application, considering surface extension, coverage, and predominant morphology. Baroň et al. (2012) described the parameters monitored for different types of landslides and presented some relevant examples from test sites in Europe. Recently, Stähli et al. (2015) presented an overview of the technologies typically used in EWS for weather-induced landslides operational worldwide. They also discussed the applicability of such technologies to alarm, warning and forecasting systems.

Besides global reviews on monitoring strategies, literature contributions also exist on specific issues. For example, Arattano and Marchi (2008) reviewed the sensors applied for debris flow monitoring. According to them, the warning devices can be subdivided into three main classes: i) advance warning systems, predicting the possible occurrence of an event before its occurrence through the monitoring of the triggering factors; ii) event warning systems, monitoring a debris flow while in progress and providing an alarm; and iii) post-event warning systems, detecting a debris flow already occurred allowing the appropriate risk mitigation measures (e.g., stopping the traffic on a railway). Furthermore, Scaioni et al. (2014) presented a classification of remote sensing techniques for geotechnical investigation, also discussing about their applicability to the different types of landslides. Applications are classified into three main classes: i) landslide recognition, classification, and post-event analysis; ii) landslide monitoring (i.e., monitoring the activity of existing landslides); and iii) landslide susceptibility and hazard assessment. Michoud et al. (2012) described the techniques for landslide detection (i.e. new landslides recognition from space or airborne imagery), characterization (i.e. retrieving information on

failure mechanism and volume involved), rapid mapping (i.e. fast semi-automatic image processing for changes detection and/or target detection; hotspot mapping) and long-term monitoring (i.e. processing data for retrieving deformation patterns). Stumpf et al. (2012) provided criteria for the selection of the most suitable remote sensing technologies based on: type of landslide, rate of movement, scales of analysis and risk management strategy. Tofani et al. (2012) described and evaluated the most innovative landslide remote sensing techniques, aiming at addressing their future scientific and technological developments.

By elaborating the literature contributions described herein, Calvello (2017) classified the landslide monitoring instruments in terms of parameters, activities and methods of monitoring (Table 3.1). The monitoring strategies adopted within the Lo-LEWS presented herein are analysed and discussed according to this classification.

The monitored activities are classified into three main categories: (i) deformation, i.e. direct monitoring of the actual kinematic behaviour of a landslide; (ii) groundwater and soil moisture, i.e. monitoring of the pore water pressure conditions which could lead to an activation or an acceleration of a landslide; and (iii) trigger, i.e. monitoring the external process responsible of activating or accelerating a landslide. For each activity a certain number of monitoring parameters can be defined.

The monitoring methods are classified in six main categories: (i) geotechnical, identifying ground geomorphologic evolution and providing measurements of ground displacements, soil deformation, groundwater level and total stress in the soil; (ii) hydrologic, measuring the distribution and the movement of the water on and below ground surface; (iii) geophysical, monitoring changes in the landslide mass, observing physical parameters of soil or rock mass (e.g. density, acoustic/elastic parameters, resistivity, etc.); (iv) geodetic, assessing landslide displacements by measuring horizontal and vertical angles as well as by tracking GPS distances; (v) remote sensing, monitoring surface displacements and characterizing the slope instability factors without any physical contact with the landslide mass; (vi) meteorological, measuring the weather parameters that may trigger a landslide (e.g., rainfall, snowmelt) and/or influence its behaviour (e.g., wind, air temperature).

Table 3.1 Instruments used for landslide monitoring within LEWS, classified considering the parameters and the activities monitored and the monitoring methods (modified from *Calvello 2017*)

Monitored activity	Monitored parameter	Monitoring method					
		Geotechnical	Hydrologic	Geophysical	Geodetic	Remote sensing	Meteorological
Deformation	Displacements	Inc BExt EExt DMS Tilt			GPS Int TotS	Cam GbLiD ALiD GbSAR InSAR UAV	
	Strains	OptF EExt		Geoph			
	Cracking	Crack				GbLiD ALiD	
	Mass balance					GbLiD ALiD	
	Microseismicity / Acoustic emission			Acc Seis Geoph		GPR	
	Rockfall event frequency					GbLiD ALiD	
Groundwater	Pore water pressure	Piez					
	Groundwater level	PS					
	Suction	Tens TPsy		ElCS ThCS			
	Soil water content			TDR		Sat	
Trigger	Weather					Sat	RG WS
	Earthquake			Acc Seis Geoph			
	Volcanic activity			Acc Seis Geoph		InSAR	
Other	Atmospheric tides						Bar
	Stream flow		WL M Hyd				
	Water quality		SprS				

← Legend: Inc: Inclinometer; BExt: Borehole extensometer; DMS: "Differential monitoring of stability" column; Tilt: Tiltmeter; GPS: Global positioning satellite; Int: Interferometer; TotS: Total station; Cam: Camera; GbLiD: Ground-based LIDAR; ALiD: Airborne LIDAR; GbSAR: Ground-based synthetic aperture radar; InSAR: Interferometric synthetic aperture radar; UAV: Unmanned air vehicle; OptF: Optic fiber; EExt: Embedded extensometer; Geoph: Geophone; Crack: Crackmeter; Acc: Accelerometer; Seis: Seismometer; GPR: Ground penetrating radar; Piez: Piezometer; PS: Perforated standpipe; Tens: Tensiometer; TPsy: Thermocouple psychrometer; ElCS: Electrical conductivity sensor; ThCS: Thermal conductivity sensor; TDR: Time domain reflectometer; Sat: Satellite sensor; RG: Rain gauge; WS: Weather Station; Bar: Barometer; WLM: Water level meter; Hyd: Hydrometer; SprS: Spring sampling

3.1.2 Activities and parameters monitored

Monitored parameters can be defined as "phenomenon indicators or factors related to slope (area of interest), which could be quantified and monitored in time" (Baroň et al. 2012). A key issue for any LEWS operational at local scale is the understanding of the behaviour of such site-specific parameters and, especially, the evaluation of their role as early warning indicators by identifying their critical values (i.e., thresholds) through an advanced knowledge of their temporal evolution. Figure 3.1a displays the parameters monitored in the 29 Lo-LEWS reviewed herein and Figure 3.1b presents the information in terms of monitored activities based on the classification introduced in Table 3.1. As expected, the large majority of the systems—27 out of 29—monitor deformation, expressed in terms of displacement (15 cases), velocity (8 cases), acoustic emissions (8 cases), cracking (4), acceleration (2), and strain (1). Indeed, they show direct evidence of active deformations and movements in the slope, providing relevant information for early warning purposes. Although displacements are investigated in the large majority of the cases, velocity and acceleration are more commonly considered for describing the kinematic behaviour of landslides in rock. In addition, a large number of Lo-LEWS monitor triggering parameters (21 cases), especially rainfall (20 cases), because they can be assumed as the main triggering factor for the majority of the investigated landslides. Groundwater conditions are investigated in 16 systems, mainly in terms of pore water pressure (8 cases) and groundwater level (7 cases), which are recorded at intervals related to the period of the year and to the soil characteristics. The groundwater regime may display rapid response to intense rainfall or a gradual rise/decline of the groundwater level during wet/dry seasons. Only in 5 cases other parameters have been employed. An example is the system

deployed at Lake Sarez, eastern Tajikistan (AS_2005_A), where the fluctuations of the lake level and the turbidity of the water represent significant landslide precursors.

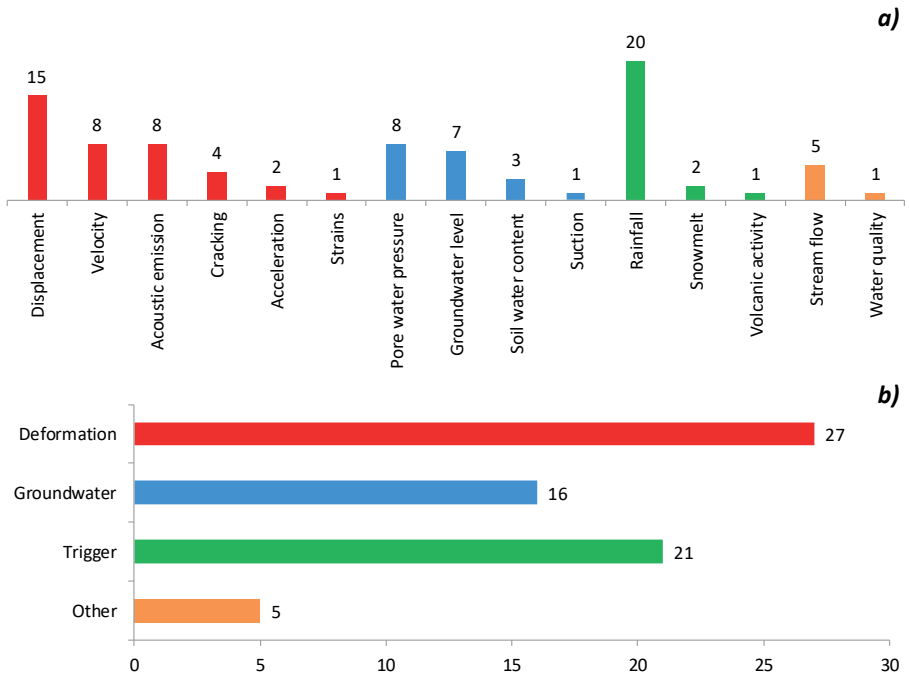

Figure 3.1 Inventory of the parameters (a) and the activities (b) monitored within the 29 reviewed Lo-LEWS according to the classification of Table 3.1 (modified from *Pecoraro et al. 2018*)

Further analyses have been carried out in order to determine the most investigated activities in relation to the type of landslide under surveillance (Figure 3.2). Although the number of records for several classes of landslides is quite limited, deformation activity has been investigated in all the cases. The two most common classes of landslides, i.e. debris flows and rockslides, employ very different parameters, even though the activity monitored is the same. Two parameters are concurrently or alternatively investigated for debris flows: rainfall (trigger activity) to predict an event before its occurrence, and acoustic emission (deformation activity) to detect a phenomenon while in progress. Conversely, displacement and rate of movement (deformation activity) have always been considered for

characterizing the state of activity of the rockslides. It is worth mentioning that in the majority of the cases, independently on the type of landslide under surveillance, groundwater and meteorological parameters are also investigated. This seems to suggest that redundancy of the monitored parameters is a crucial aspect to consider for better understanding the behaviour of the landslide and for improving the reliability of the system.

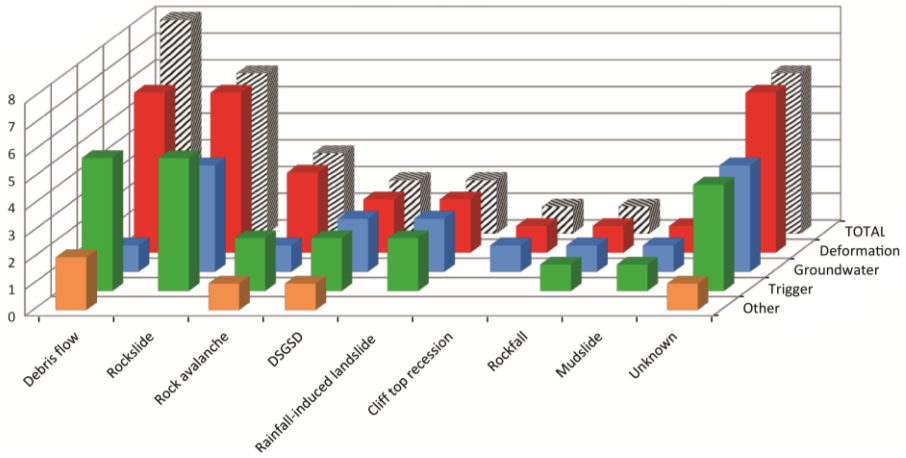

Figure 3.2 Monitored activities in relation to the type of landslide and to the group of parameters according to the classification of Table 3.1; totals are higher than 29, i.e. the total number of reviewed Lo-LEWS, because multiple parameters are monitored in some systems and two different types of landslides are considered in EU_2010c_A *(Pecoraro et al. 2018)*

3.1.3 Monitoring methods

The monitoring methods implemented within Lo-LEWS depend on the site-specific conditions of the slope to be investigated and, as a consequence, on the parameters monitored. Once the parameters more suitable for the landslide under surveillance are identified, the most appropriate monitoring instruments can be selected according to the following criteria: simplicity, robustness, reliability, and cost. Many types of monitoring instruments are available and allow the LEWS designers and managers to choose among several options for investigating each class of parameters. Figure 3.3a displays the monitoring instruments used within the 29 Lo-LEWS presented herein while Figure 3.3b summarizes

the monitoring methods according to the classification proposed in Table 3.1.

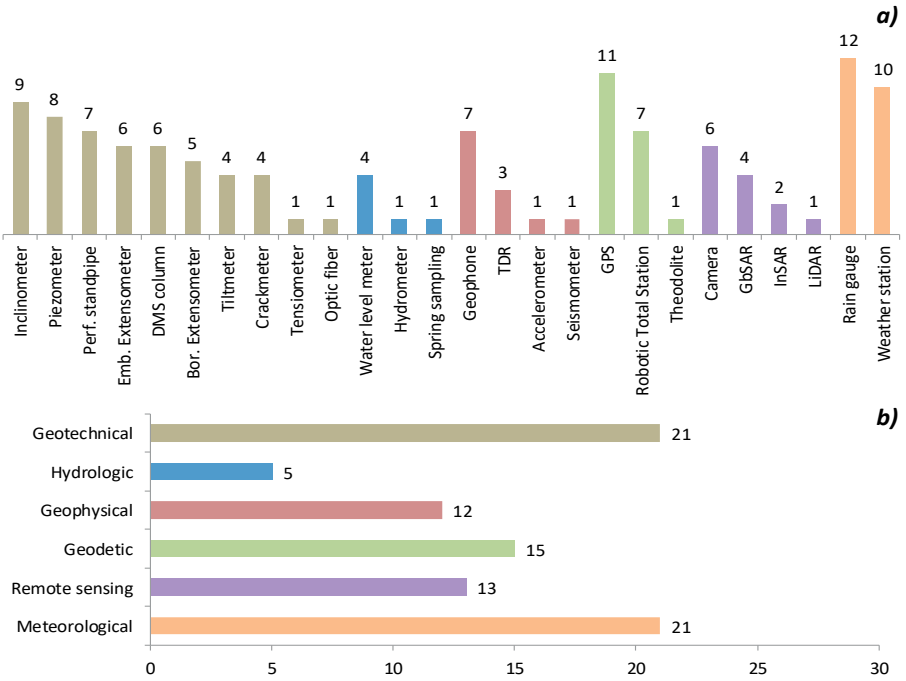

Figure 3.3 Inventory of the monitoring instruments (a) and methods (b) employed within the 29 reviewed Lo-LEWS according to the classification of Table 3.1 (modified from *Pecoraro et al. 2018)*

A large number of systems (23) employ more than one monitoring method, confirming that redundancy is a crucial aspect for developing monitoring strategies. A relevant example is represented by the system operational at Wushan Town, China (AS_2004_A), where the ground and deep displacements of a deep-seated colluvial landslide are monitored through geotechnical and geodetic methods (i.e., inclinometers and GPS). The system is also integrated by hydrologic (i.e., water level meter), geophysical (i.e., TDR), and meteorological sensors (i.e., a network of rain gauges). The most employed monitoring methods are geotechnical and meteorological, because both of them are considered in 21 systems. Geotechnical methods are used for measuring deformation and groundwater, mainly by means of traditional sensors (i.e., inclinometers, piezometers, perforated standpipes, and extensometers), which deliver

reliable data and are robust and cheap. However, systems addressing large and complex phenomena, often employ expensive instruments, such as differential monitoring of stability (DMS) columns (6 cases) which may provide profiles of horizontal and vertical displacements as well as pore water pressure measurements along monitored boreholes. Besides, in 13 systems geotechnical instruments are combined with geodetic sensors in order to achieve additional information on the absolute displacements of the landslides with respect to some reference points. GPS devices are preferred in the large majority of the cases (11), because they ensure reliable results and are flexible, since measurements are possible even during the night and under adverse weather conditions. As stated before, meteorological methods are also widely used, including both rain gauges (12 cases) and weather stations (10 cases). Remote-sensing techniques, especially cameras and ground-based synthetic aperture radars (GbSAR), are employed in a number of applications (13), because they allow updating the knowledge on the long-term behaviour of a landslide. However, these techniques are quite expensive and do not provide real-time data suitable for early warning purposes.
Monitoring methods are also analyzed in relation to the investigated landslide (Figure 3.4).

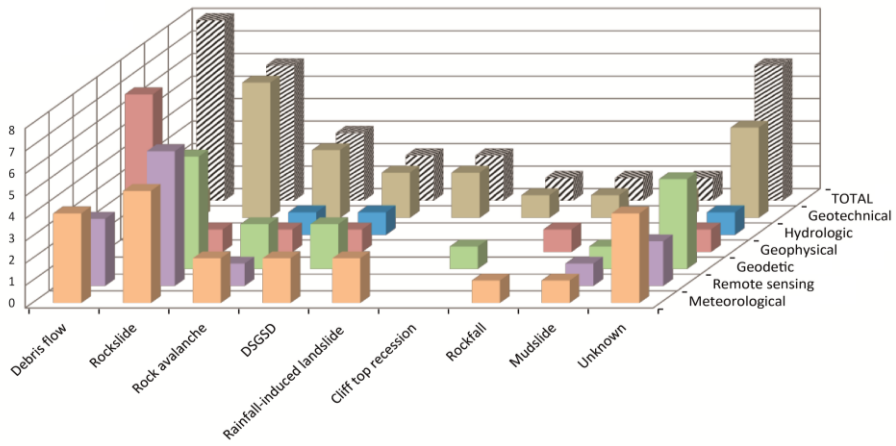

Figure 3.4 Monitoring methods grouped in relation to the type of landslide and to the group of instruments according to the classification of Table 3.1; totals are higher than 29, i.e. the total number of reviewed Lo-LEWS, because multiple monitoring methods are employed in some systems and two different types of landslides are considered in EU_2010c_A *(Pecoraro et al. 2018)*

Geotechnical methods are widely employed for all types of landslides, apart from debris flows monitoring. In these cases, monitoring strategies are based either on meteorological instruments for measuring the triggering factor (i.e., rainfall) or on geophysical instruments for recording the ground vibration produced by the moving mass of water and debris. Geotechnical and geophysical methods are often combined for monitoring the evolution of the rockslides. Furthermore, remote sensing techniques provide additional information in a certain number of cases. In particular, cameras are used for debris flows and GbSAR and interferometric synthetic aperture radars (InSAR) are employed for large and destructive phenomena, such as rockslides and deep-seated colluvial landslides.

3.1.4 Monitoring strategies

The performed analyses revealed that redundancy of monitoring strategies is a crucial aspect of operational Lo-LEWS. However, some parameters and instruments are more reliable than others for issuing an alert. Figure 3.5a,b presents the number of the parameters monitored and the monitoring instruments within the 29 Lo-LEWS described herein (in red colour in the Figure), highlighting which parameters and the instruments are directly used for issuing the alerts (in blue colour in the Figure). It should be noted that in seven cases, the exceedance of more than one parameter is considered to issue a warning. Therefore, the total number of parameters employed for warning purposes (40) exceeds the total number of systems. As expected, displacement and its derivates (velocity and acceleration) are the parameters most widely employed (25 cases). Besides, displacement and velocity are considered the main warning parameters in 18 cases. They are investigated through a variety of sensors, among which the highest warning potential can be attributed to GPS devices (9 cases), embedded extensometers (6 cases), and inclinometers (5 cases). Since other literature contributions (Baroň and Supper 2013; Michoud et al. 2013) indicate traditional instruments (e.g., inclinometers and extensometers) as the most reliable sensors for warning purposes, the widespread application of GPS techniques is quite surprising. On the other hand, recent studies demonstrated that these types of instruments are very suitable for landslide monitoring, as they proved to be accurate,

rapid, efficient, and cost-effective, especially when the study area is higher (Gullà et al. 2018, Song et al. 2018).

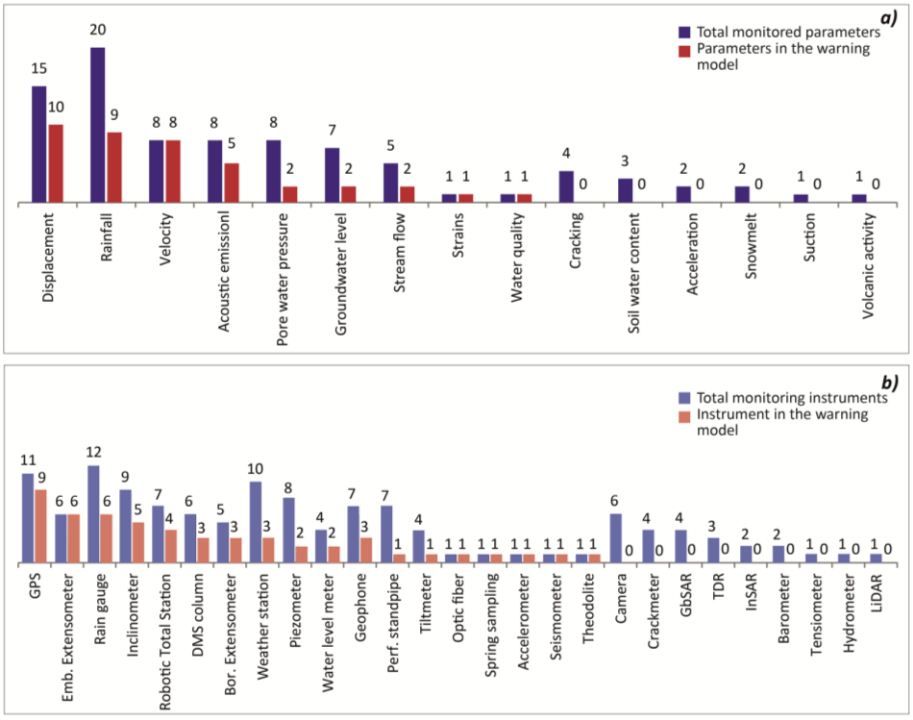

Figure 3.5 a) Total number of monitored parameters composing the monitoring networks and monitored parameters directly used to issue the warnings. b) Total number of instruments composing the monitoring networks and instruments directly used to issue the warnings *(Pecoraro et al. 2018)*

Rainfall is also widely considered (in 20 cases), since most of the investigated phenomena are weather-induced landslides. Rainfall is monitored by means either by rain gauges or weather stations, when additional parameters (e.g., snowmelt, and temperature) are required for landslides occurring in mountainous environments. Acoustic emissions are crucial for systems aimed at detecting debris flows in their initial stage. In a good number of applications (e.g., Arattano and Marchi 2008) they are monitored through geophones, which have demonstrated to be robust and reliable sensors. It is worth mentioning that a good number of instruments, although are part of several monitoring networks, have not been considered suitable for early warning. For example, data acquired by

remote sensing sensors have not been included in any warning model because they are still not mature enough for geotechnical applications, yet they have a high warning potential (Baroň and Supper 2013). Finally, although redundancy of monitoring strategies is only one of the aspects to be considered for designing a successful Lo-LEWS, it should be stressed that acquiring as more information as possible can improve the efficiency, the robustness, and the reliability of the systems.

3.2 MONITORING STRATEGIES AND WARNING MODELS WITHIN TE-LEWS

3.2.1 Monitoring strategies

A key technical issue for the operation of an effective Te-LEWS is the identification, measurement and monitoring of landslide precursors. Monitoring strategies are typically based on prediction and forecasting of meteorological parameters over appropriately defined homogenous warning zones.

Figure 3.6a displays that rainfall is the main monitored parameter for all the territorial systems reviewed by Piciullo et al. (2018). However, six Te-LEWS employ additional thresholds based on: soil water content (in 4 cases), pore water pressure (1) and hydrometric parameters (1). A relevant example is the prototype system deployed in the city of Seattle, Washington (NA4), where an antecedent water index representing the depth of water above or below the amount required to bring a 2-m-deep column of soil to "field capacity" was also monitored. As expected, in the large majority of the cases (22) automatic rain gauges are the most adopted instrument for providing information in near real-time (Figure 3.6b). The only exception is represented by the national LEWS operating in Japan (AS5), which does not employ a network of rain gauges as main tool for rainfall monitoring. Rainfall intensities used in the system are estimated by a Radar Automated Meteorological Data Acquisition System and distributed by the Japan Meteorological Agency. However, a number of systems (14) employ both data from a network of rain gauges and weather radar observations. Geotechnical instruments (i.e. piezometers and tensiometers) are considered in solely three cases: Malaysia (AS4), Norway

(EU7), and Seattle (NA4). They can provide supplemental data needed to determine the likelihood of a rainfall threshold-exceeding actually producing landslides, and are particularly valuable in areas where soil water conditions change significantly thorough the year, yet they may prove useful in other areas as well. Moreover, in addition to rainfall monitoring some systems employ weather forecasts, mainly using nowcasting estimates provided by different numerical meteorological models, typically developed and deployed at national level.

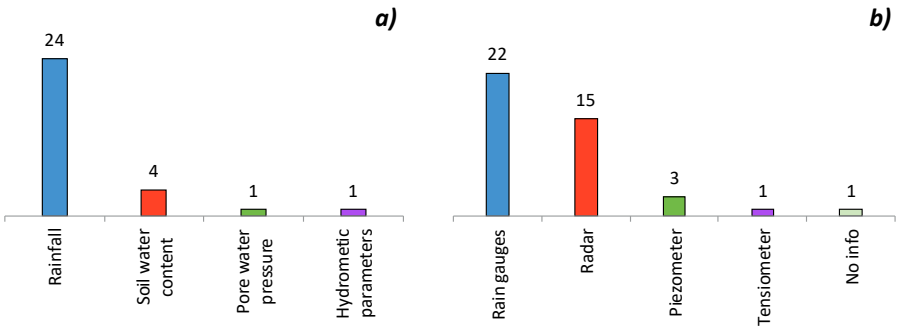

Figure 3.6 Monitored parameters (a) and monitoring methods (b) employed within the 24 Te-LEWS operational worldwide

Looking at the Italian regional systems (Pecoraro and Calvello 2016), rainfall is again the main parameter to be investigated in all the 19 cases for which this information is available (Figure 3.7a). On the other hand, soil water content is also considered a critical parameter for landslide triggering, as it is monitored in 12 cases. A peculiar example is represented by the system employed in the Umbria region, where the rainfall thresholds originally employed were successively combined with soil water content simulations derived by a physically-based model. Furthermore, snowmelt is also monitored in Aosta Valley and Emilia-Romagna, two mountainous regions where landslides may be triggered by prolonged rainfall as well as by rapid snowmelt from a sudden rise of the temperature. Figure 3.7b shows that rain gauges are employed by all the regional systems, even though in a number of cases (11) they are supported by weather radar observations and in three regions (i.e. Umbria, Liguria, and Veneto) satellite estimates are also used. Moreover, geotechnical instruments are part of the monitoring networks of the systems operational in: Aosta Valley (extensometers and inclinometers), Emilia-

Romagna (inclinometers and piezometers), Umbria (extensometers) and autonomous province of Trento (extensometers, inclinometers, and piezometers). However, geotechnical data have been mainly used for adjusting operational rainfall thresholds without being part of any warning model.

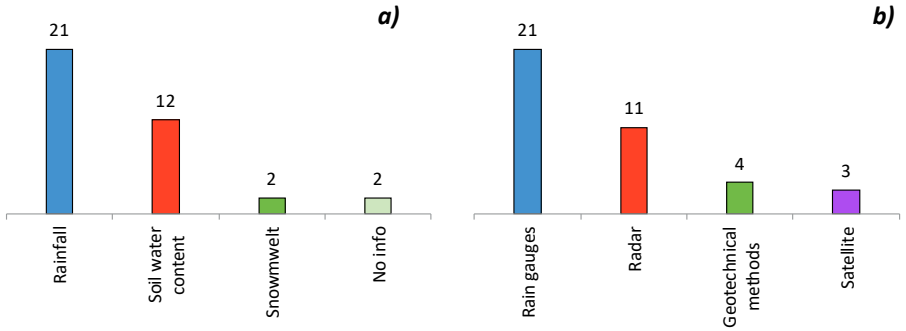

Figure 3.7 Monitored parameters (a) and monitoring methods (b) employed within the 21 regional LEWS operational in Italy

The review proposed by Segoni et al. (2018a) highlights that still the rain gauges are by far the most used instrument to obtain rainfall data for threshold analysis within the 45 Te-LEWS: 86.7% of the systems employ rain gauges, among which 6.7% combines rain gauges and radar measurements (Figure 3.8).

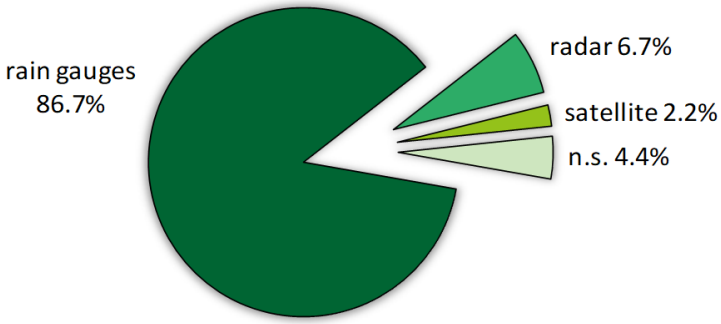

Figure 3.8 Sources of rainfall data used to define thresholds within the 45 Te-LEWS operational worldwide (modified from *Segoni et al. 2018a)*. Legend: n.s.: not specified

On the other hand, 6.7 and 2.2% of the rainfall measurements are provided only by radar and satellite measurements, respectively. In some circumstances, this is a forced choice, because no reliable rain gauge network exists in the studied area and satellite or radar measurements are the best choices available. Conversely, in other cases, the choice of using radar is an attempt to obtain rainfall measurement with higher spatial and temporal resolution and reduced uncertainties. The source of rainfall data is not clearly specified for the 4.4% of the systems. In 6 cases (13.3%), additional monitoring instruments, besides those used to obtain rainfall data for the threshold analysis, were used. In particular, in 3 cases (6.7%), they consist in other instruments used to measure rainfall, e.g., to integrate rainfall measures or to have redundancy of rainfall data. In two cases, the systems are equipped with instruments for temperature measurements. The use of temperature sensors is due to cope with snowmelt-induced landslides to take into account snow accumulation/melting phenomena in regional scale threshold analysis, or to model the degree of saturation in order to adjust operational rainfall thresholds. Only in one case piezometers are employed for providing additional information on pore water pressure variations.

3.2.2 Warning models

The warning model of a Te-LEWS for weather-induced landslides typically consists in defining one or more thresholds for landslide occurrence in a certain area of interest. The rainfall thresholds are typically based on correlation laws derived from a statistical analysis of historical data. According to Guzzetti et al. (2007), they can be differentiated into three main categories: A) thresholds that combine precipitation measurements obtained from specific rainfall events; B) thresholds that consider antecedent rainfall conditions; and C) other thresholds. The first category can be further subdivided, depending on the precipitation measurements, in: A1) intensity-duration; A2) rainfall event-duration; A3) total event rainfall; and A4) rainfall event-intensity.
Following this schematization, Figure 3.9 describes the thresholds defined within the 24 Te-LEWS reviewed by Piciullo et al. (2018). The majority of the systems (17) employ intensity-duration thresholds (A), whereas other thresholds (C) are used in 7 cases and antecedent conditions (B) are considered in 6 cases. Rainfall event-duration thresholds (A2) are deployed only in the system designed to address landslides along highways in

Taiwan (AS6). Ten systems employ one threshold, yet two thresholds are evaluated simultaneously in 7 cases. An example is the system operational in Rio de Janeiro (SA1), where a combination of antecedent condition of rainfall through the measurement of 24-h and 96-h cumulated rainfall was first considered. Successively, a third rainfall variable representing the intensity duration, i.e. the hourly rainfall, was added to the previous two. Other or two more complex thresholds are adopted in the remaining 7 cases, such as in Hong Kong (AS1). Japan (AS5), and Norway (EU7). The latter is a peculiar system, since the thresholds currently used have been derived from empirical tree-classification using 206 landslide events occurred throughout the country, as a function of two variables: relative water supply (derived from rainfall and snowmelt), and relative soil water content.

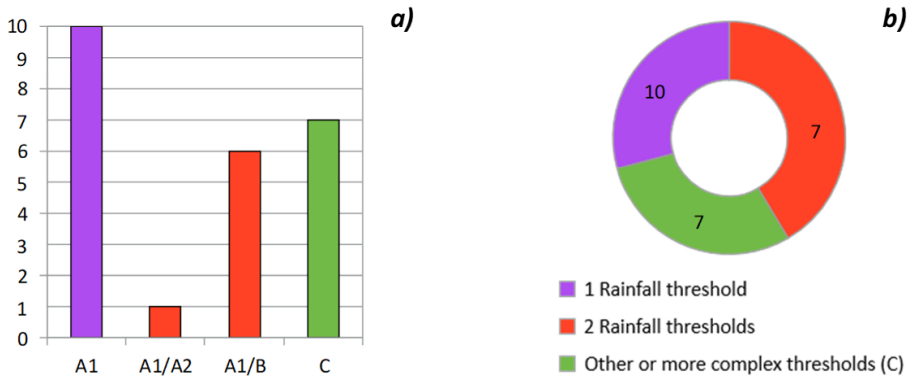

Figure 3.9 a) Classification (following the schematization by *Guzzetti et al. 2007)* and b) number of thresholds employed in the 24 Te-LEWS operational worldwide *(Piciullo et al. 2018)*

Figure 3.10 groups the thresholds employed within the 21 Italian regional LEWS (Pecoraro and Calvello 2016). Among the reviewed systems, only in Liguria and Marche two thresholds are combined: intensity-duration (A1) and antecedent conditions (B). On the other hand, one threshold is applied in 16 circumstances, equally distributed between intensity-duration (A1) and others (C). Among the latter, in six systems (Campania, Lazio, Lombardy, Sardinia, Sicily, and Umbria) rainfall precursors are related to returns period estimated on the basis of probabilistic analyses of historical rainfall. The values obtained for each type of precursor correspond to a different risk scenario, i.e. level of warning. A peculiar example of

thresholds definition is represented by the system operational in Emilia-Romagna. The model employed is called SIGMA, whose name reflects the central role assumed by standard deviations in the proposed methodology. The areas of the region susceptible to landslide events has been subdivided into territorial units, each one associated to a reference rain gauge. The time series of cumulated rainfall from 1 to 365 days have been derived for each rain gauge and the cumulative rainfall series are approximated by a standard Gaussian distribution. Proceeding in the same way for the number of cumulative rainfalls between 1 and 365 days, it is possible to build the precipitation curves (σ curves) associated with various probabilities of non-exceedance. Multiples of the standard deviation (σ) are used as thresholds to discriminate between ordinary and extraordinary rainfall events. In Aosta Valley, multiparametric thresholds have been defined by combining 30-day antecedent rainfall with quantitative weather forecasts (average and peak rainfall intensity, and snowmelt). In the remaining 3 cases, information on rainfall thresholds employed is not available.

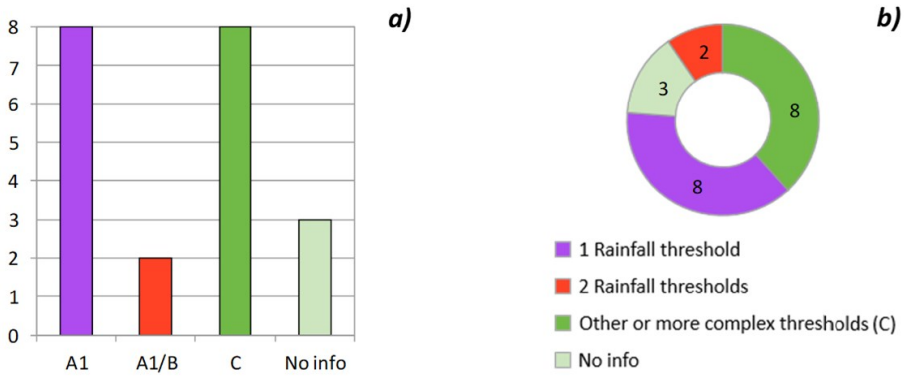

Figure 3.10 a) Classification (following the schematization by *Guzzetti et al. 2007)* and b) number of thresholds employed in the 21 regional LEWS operational in Italy

Segoni et al. (2018a) stated that the rainfall thresholds for landslide occurrence are characterized by three relevant features: source of landslide data, variables or parameters employed and methods used.
Regarding the landslide databases, 44% of the reviewed systems makes use of two or more sources of information, trying to compile a database as much complete as possible. As an instance, local newspapers usually

report with good temporal precision landslides that had a relevant impact on human infrastructures but very rarely provide reliable technical/scientific information (e.g., landslide type). On the contrary, scientific reports may be rich of details but sometimes they may not state clearly the exact moment or day of landslide occurrence. Figure 3.11a reports the distribution of landslide information source. The most used sources of information are reports (used in 19 cases), which can have various different origins: fire brigades, civil protection, local administration, technical offices, and scientific reports. News found in newspapers archives (14 cases) and/or on internet (5) are another relevant source of information. Furthermore, 12 systems make use of official databases released by different organizations, mainly governmental organizations, local authorities, or research institutions. Remote sensing can be a valuable tool to compile post-event catalogs or to constantly update large inventories, indeed surveys performed by remote sensing techniques were used in 5 circumstances. Historical records of various origin were taken into account for 3 systems, while in 2 cases are used datasets prepared for previous works. In 3 circumstances, the source of landslide data is not clearly defined.

The methods adopted for the definition of the thresholds in Te-LEWS reported by Segoni et al. (2018a) can be grouped into two classes: manual and statistical (Figure 3.11b). The former are applied in 55.6% of the cases in which the thresholds are actually drawn manually in several ways: delimiting the lower bound of the point cloud representing the triggering rainfall conditions, searching the best fit of the lower part of the cloud, or adopting a regression. The latter are used in 37.7% of the cases through the following approaches: frequentist analysis, partial duration series, return time calculations, or point density analysis. The methods are not clearly specified in 6.6% of the cases. Further proposals of thresholds using different methods have been presented in the literature, yet not employed in any operational or prototypal Te-LEWS. Among them, it is worth mentioning the probabilistic models based on Bayesian analyses tested by Berti et al. (2012) in the Emilia-Romagna region (Italy) and by Robbins (2016) in Papua Nuova Guinea.

Figures 3.11c,d display that three combinations of rainfall parameters are more commonly implemented into the reviewed systems: intensity-duration (A1), antecedent conditions (B), and others (C). The most used combination is intensity-duration (21 cases), whose definition follows a consolidated tradition which dates back to Caine (1980). The second most

used approach relies on antecedent conditions (11 cases), which can be derived using several combinations of rainfall measures, such as: daily rainfall and 15-day antecedent rainfall, 3- and 30-day antecedent rainfall, daily and 3-day cumulated rainfall. In some cases, rainfall measures are not used directly but processed to calculate antecedent rainfall indexes, in order to better account for the degree of saturation of the soil (e.g., Jaiswal and van Westen 2010). In 6 cases intensity-duration and antecedent are combined. Out of these categories, 7 systems employ a wide variety of parameters to define rainfall thresholds. As instance, the abovementioned regional system operational in Emilia-Romagna uses the standard deviation from the mean rainfall amount accumulated during progressively increasing time steps.

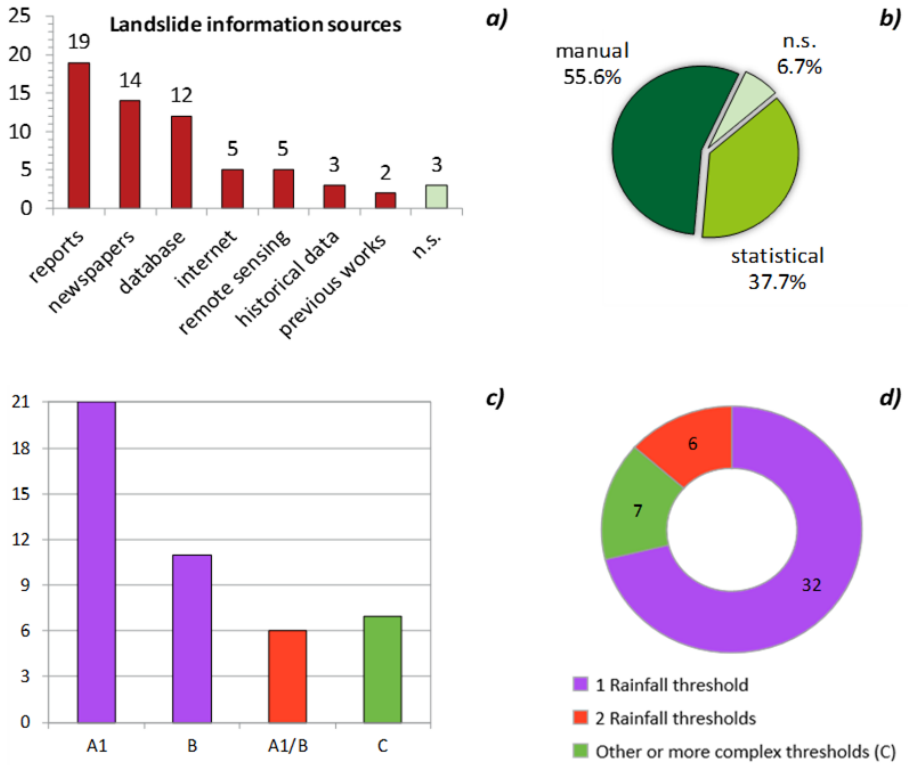

Figure 3.11 a) Information sources used to define the thresholds, b) methods used for drawing or defining the thresholds, c) classification (following the schematization by *Guzzetti et al. 2007)* and d) number of thresholds employed in the 45 Te-LEWS operational worldwide (modified from *Segoni et al. 2018a).* Legend: n.s.: not specified

3.3 OPEN ISSUES

The literature contributions reported herein describe many landslide early warning systems (LEWS) deployed to address weather-induced landslides both at regional and slope scale all around the world. The efficiency of a LEWS strongly depends on the monitoring strategies adopted and the method developed for the definition of the warning model. As already mentioned, monitoring strategies play a central role, both in the design and in the operational phase of a LEWS, as suitable parameters for monitoring must be identified and the most appropriate monitoring instruments selected according to a set of criteria, such as simplicity, robustness, reliability, and cost. On the other hand, the definition of the warning model also represents a crucial issue for scientists and managers involved in landslide risk management. In particular, there are no standard procedures indicating steps that cannot be neglected in order to ensure objectivity and reproducibility of the implemented method.

Warning models developed for weather-induced landslides are mainly based on correlation laws, for which thresholds are defined considering one or more combinations of the monitored parameters that have led (or not lead) to slope movements. Thresholds are drawn either by delimiting triggering and non-triggering conditions in cartesian planes or by statistically analyzing historical data. These methods do not typically include a quantitative assessment of the uncertainties correlated to the results, that may be due to incomplete or inadequate: input data, knowledge on the physical process, and reconstruction of the rainfall events (Berti et al. 2012, Robbins 2016).

The reliability of a warning model does not depend solely on the applied method, but also on the quantity and quality of the input data, i.e. historical landslide records and rainfall measurements (or other meteorological parameters). A landslide catalog that is regularly updated and as much complete as possible—not only in terms of number of events reported, but also in terms of information to be used in the analyses—is critical for supporting the calibration and the validation of a warning model (Battistini et al. 2013, Kirschbaum et al. 2015). Unfortunately, in many cases data on landslide occurrence are either not available or accessible only to a restricted number of scientists, technicians, and insiders (Segoni et al. 2018a).

Regarding rainfall measurements, the most used monitoring instruments are by far rain gauges, whose spatial density varies significantly from case

to case. Overall, decrease in gauge density leads to increased underestimation of rainfall, which in turn leads to large underestimation of the thresholds, especially in those based on the correlation between intensity and duration (Nikolopoulos et al. 2014, 2015).
As already mentioned, in almost all the cases only meteorological parameters are included within the warning model. However, meteorological monitoring does not allow to take into account critical soil properties controlling the initiation of the triggering process. Depending on these conditions, landslides may be triggered in response to a large variety of rainfall combinations. Therefore, although the integration of geotechnical parameters (e.g., pore water pressure, soil water content, ground deformation) within warning models for weather-induced landslides may be very challenging for some types of landslides, they can provide additional information to determine the likelihood of rainfall events actually triggering landslides (Baum and Godt 2010, Stähli et al. 2015, Calvello 2017).

4 THE PROPOSED METHODOLOGIES

In this Chapter the main elements to be considered in the development of a warning model for weather-induced landslides are summarized in a conceptual framework (Section 4.1). In particular, the influence of the input data and the necessary activities needed for obtaining reliable results are highlighted. Considering the proposed framework as well as the relevant aspects according to Section 3.3, two procedures are defined for the development of a probabilistic warning model (Section 4.2) and a multi-scalar warning model (Section 4.3). Their application to specific case studies is presented in Chapters 6 and 7, respectively.

4.1 CONCEPTUAL FRAMEWORK

The definition of a warning model for weather-induced landslides presents some critical issues, thus there are important steps that cannot be neglected. Figure 4.1 displays a conceptual framework that summarizes the main elements of the process: (i) input data, (ii) activities, and (iii) output.

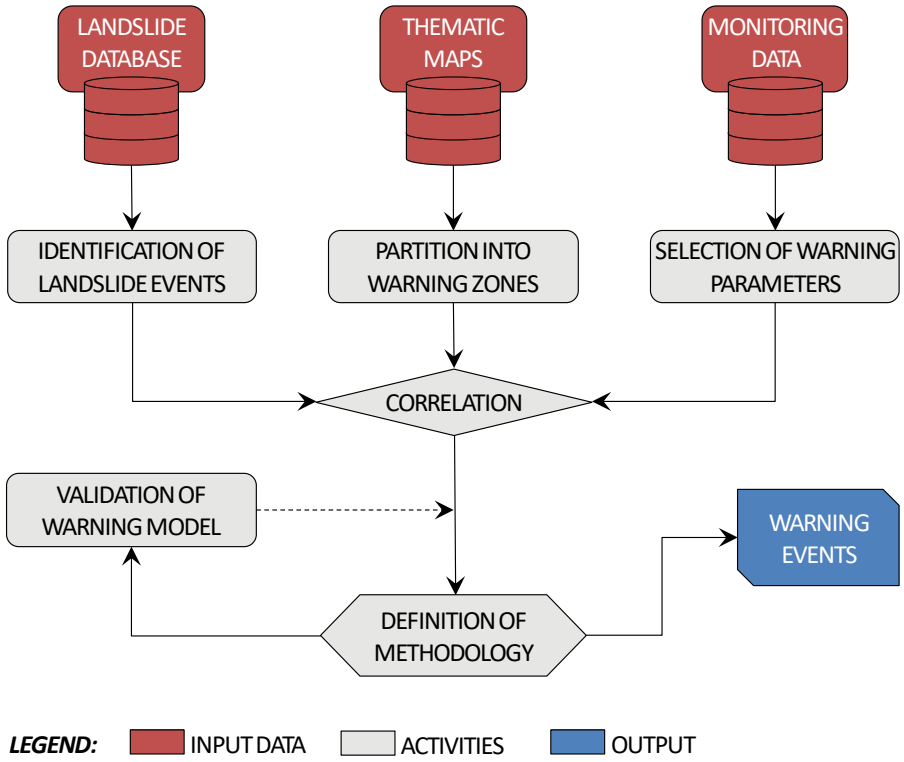

Figure 4.1 Conceptual framework highlighting the main elements needed for the definition of a warning model for weather-induced landslides

Input data

The reliability of a warning model significantly depends on the quantity and the quality of the input data, which can be derived by three different sources of information: thematic maps, landslide databases, and monitoring data. In addition, these details are also important in order to determine the most appropriate methodology and to assess the feasibility of a possible application to other case studies. Thematic maps can be used to highlight the main features of the study area, such as the areal extension and the geomorphological context (e.g., lithology, land use, and slope). The former provides an indication on the spatial scale of analysis, which in turn influences both the spatial extension of the landslide database and the choice of the most suitable monitoring methods. The latter is related to the types of landslides that may potentially occur within the study area and the mechanics of the triggering processes (Stähli et al. 2015, Calvello

2017, Segoni et al. 2018a). Regarding the landslide database, using a high and well-distributed number of recorded events (i.e., representative of a wide range of different triggering conditions) is recommended for the calibration of a warning model. In addition, landslide catalogs should be populated constantly and timely in order to allow a recalibration of the model when new data are available (Kirschbaum et al. 2015, Rosi et al. 2015, Battistini et al. 2017). Finally, monitoring data to be employed within warning models are typically represented by meteorological parameters, investigated through two different monitoring methods: in-situ monitoring and remote sensing (Pecoraro et al. 2018, Piciullo et al. 2018, Segoni et al. 2018a). Meteorological instruments deployed in-situ measure directly and continuously the monitored parameter (e.g., rain gauges for monitoring rainfall), thus they provide robust and reliable local observations. It should be stressed that the highest possible density of measurements is desirable, to better account for the spatial variability of the monitored parameters. The selection of the most representative local instrument(s) for a certain landslide event is not a trivial matter, therefore the design of the monitoring network for local observations should be based on quantitative and objective elements. On the other hand, recent technological advances in remote sensing methods (i.e. weather radars and satellite estimates) are encouraging their deployment for early warning purposes. In particular, they allow enhancing the spatial and the temporal resolution of the measurements (e.g., spatial resolution of weather radars can arrive to few km^2). They are particularly helpful in areas where reliable meteorological monitoring networks are not available. Furthermore, other monitoring data available in the study area (e.g., monitoring of geotechnical parameters) may provide fruitful information on the landslides under surveillance, thus they can be profitably used to complement the monitored meteorological parameters.

Activities

The main activities needed for the delimitation of the warning zones, the analysis and the correlation of the input data, and the definition and the validation of the warning model are herein described.

Partition into warning zones. A warning zone is the portion of territory alerted with the same warning level and it can be seen as the spatial discretization adopted for warnings (Calvello and Piciullo 2016). The aim is to divide the study area into territorial units characterized by meteorological and hydrogeological homogeneity. The criteria adopted for the definition of

the warning zones generally consider the hydro-geomorphological conditions of the area to be warned as well as the characteristics of the employed monitoring network, including factors like: number of monitoring instruments per unit area, climatic homogeneity, geology and geomorphology (Calvello 2017). In addition, some authors (Jaiswal and van Westen 2010, Segoni et al. 2014, Zhuang et al. 2014, among others) state that in large study areas characterized by heterogeneous climatic regimes and geomorphological characteristics each warning zone should be independently analyzed for the definition of a specific threshold.

Identification of landslide events. Landslide events necessary for the calibration of the warning model are retrieved from a landslides database according to data, classification, spatial and temporal characteristics of the landslide records. In some cases, the numerosity of the landslides triggered by the same weather conditions can be also considered, thus the landslide events can be differentiated into single landslide events and areal landslide events (Calvello and Pecoraro 2018). In particular, single landslide events refer to the occurrence of one landslide; areal landslide events are defined as a series of landslides grouped on the basis of their characteristics, so as to implicitly evaluate and classify the magnitude of a set of multiple phenomena occurring in a given area within a given time period. Regarding the types of landslides considered for the analyses, two different approaches can be followed. If the adopted landslide catalog reports a small number of records, all the weather-induced landslides that occurred in the study area in the analyzed time frame may be included to increase the number of landslides available for the analyses. Conversely, if a wide number of landslides is reported in the database, landslides triggered or favored by similar contour conditions (e.g., shallow landslides in loose soils) may be grouped and considered separately for the calibration of the thresholds in order to enhance the accurateness of the predictions. Finally, only landslides for which information on cause and on spatial and temporal characteristics is adequate should be considered, as a high degree of uncertainty in the dataset could result in a significant decrease in the performance of the warning model.

Selection of warning parameters. The monitoring data are processed and analyzed in order to determine the most suitable warning parameters, i.e. combinations of meteorological measurements that can provide an adequate description of the triggering event (e.g., a combination of rainfall intensity and duration for characterizing a rainfall event). Several aspects should be taken into account in order to select the warning parameters:

the types of landslides under surveillance, the geoenvironmental conditions of the study area, and the climatic regime. As an example, antecedent rainfall conditions would be more appropriate than rainfall intensity for systems dealing with deep-seated landslides in low-permeability soils.

Spatial-temporal correlation. The correlation between the landslide events and the warning parameters is based on their spatial and temporal characteristics. In particular, each landslide event occurring in a certain warning zone within a given time period is associated to a set of warning parameters, which are derived from the monitoring data collected in the same warning zone and can be considered representative of the weather conditions that triggered the landslide event. The reconstruction of the conditions responsible for landslides initiation is not a trivial matter as it can be characterized by a relevant degree of subjectivity and uncertainty (Segoni et al. 2018a). For this reason, a standard criterion should be set in advance to get objective and fully reproducible measures. To this aim, it could be useful to implement an algorithm that reconstructs the triggering and non-triggering conditions according to a reduced set of parameters to account for different physical settings and operational conditions (Melillo et al. 2015).

Definition of warning model. A warning model for weather-induced landslides can be defined using a variety of methods, classifiable into three main categories: heuristic, statistical, and probabilistic. Heuristic methods are based on the identification of the conditions which lead to the triggering of the landslides through a visual comparison between monitoring data and landslide occurrences. In these cases, threshold values are typically defined manually by expert judgment, without any statistical, mathematical or physical criterion. Statistical methods comprise a wide variety of techniques, such as: frequentist method, partial duration series, and point density analysis. Thresholds are typically drawn as the lower-bound limit to the conditions which resulted in slope instability plotting two representative variables (e.g., rainfall intensity and duration) in Cartesian, semi-logarithmic or logarithmic coordinates. In some cases, the thresholds are refined by considering also the rainfall events that did not results in landslides. Probabilistic approaches are aimed at identifying the probability of landslide occurrence associated to each combination of warning parameters. They provide objective and reproducible results which can be easily updated when new data become available.

Validation of warning model. In general terms, validation can be defined as "the process of determining the degree to which a model is an accurate representation of the real world from the perspective of the intended uses of the model" (Corominas and Mavrouli 2012). Validation is one of the most important issues in the definition of a warning model, as the assessment of the predictive capability needs to be adequately analyzed and supported by data (Calvello and Piciullo 2016, Piciullo et al. 2017b, Segoni et al. 2018a). Depending on the availability of data, validation can be performed either against the same dataset used to define the model (i.e., calibration and validation sets are not separated) or against a different dataset that can be separated spatially, temporarily or randomly from the calibration set. Different statistical methods have been developed and applied for performance evaluation; they are based on the computation of tools such as: contingency matrices, receiver operating characteristic (ROC) curves, and duration matrices. A contingency matrix is compiled to define true negatives (TN), true positives (TP), false negatives (FN), and false positives (FP) and to derive a series of statistical indicators, such as: efficiency index, threat score, odds ratio. A ROC analysis is devised to assess the overall performance of the model by computing the area under a curve drawn in the true positive rate vs false positive rate space, and other parameters (Metz 1978). A duration matrix takes into account the overlapping durations of warning levels and landslides events with the aim of determining, within a given time frame, the amount of time of adequate and inadequate behavior of the warning model (Calvello and Piciullo 2016). Alternative approaches adopted to quantify the performance of a warning model include: a quantitative comparison with other models aimed at demonstrating that the developed model is the best one for a specific case study; comparison between model outputs and real data counting only one or two statistical parameters (e.g., hits) and without building a contingency matrix; visual and qualitative assessments (e.g. visual comparison with landslide inventories).

Output

Warning events (i.e. the warning model output) are generated by evaluating appropriately defined warning criteria (i.e. the decision-making procedures required for issuing the warnings), in turn based on correlations between the warning parameters (i.e. the triggering factor) and the landslide events (i.e. the hazard for which warnings are issued). They are represented by a set of warning levels issued within each warning zone,

according to the magnitude of the expected impact. The number of warning levels can vary from a minimum of two (i.e., warning, no warning) to five or more (i.e., states with an increased probability of landslides). It is worth mentioning that the adoption of a high number of levels requires an adequate calibration of the thresholds as well as clear statements about the meaning of the issued warnings. Indeed, each warning level is associated to a series of characteristics of the landslide event, to a series of potential consequences and, thus, to a series of appropriate actions to be undertaken from relevant stakeholders (Calvello and Piciullo 2016, Calvello 2017, Pecoraro et al. 2018).
The proposed conceptual framework could be used as a reference for the development of a warning model for weather-induced landslides. Anyway, it should be stated that a warning model needs to be constantly evaluated, updated and upgraded to maintain or to increase its forecasting effectiveness. Sections 4.2 and 4.3 present two warning models developed according to the proposed framework and taking into account some of the issues highlighted in Chapter 3.

4.2 PROBABILISTIC WARNING MODEL

As highlighted in Section 3.3, warning models implemented within operational LEWS addressing weather-induced landslides are mainly based on heuristic and statistical methods. Some literature contributions (Berti et al. 2012, Robbins 2016) propose alternative approaches based on the adoption of probabilistic techniques to evaluate the probability of occurrence of landslides in a given area. However, a standardized procedure does not exist and these models have not yet been implemented within LEWS operational at real scale.
Figure 4.2 describes a methodology for the definition of a probabilistic warning model, following the conceptual framework introduced in Section 4.1. In particular, a probabilistic analysis is performed to assess the probability of landslide occurrence associated to each combination of the warning parameters within a certain study area. The proposed procedure includes: the identification of the main characteristics of the study area and the collection of the input data (Phase I), the correlation between the landslide events and the warning parameters (Phase II), and the application of the probabilistic methodology (Phase III).

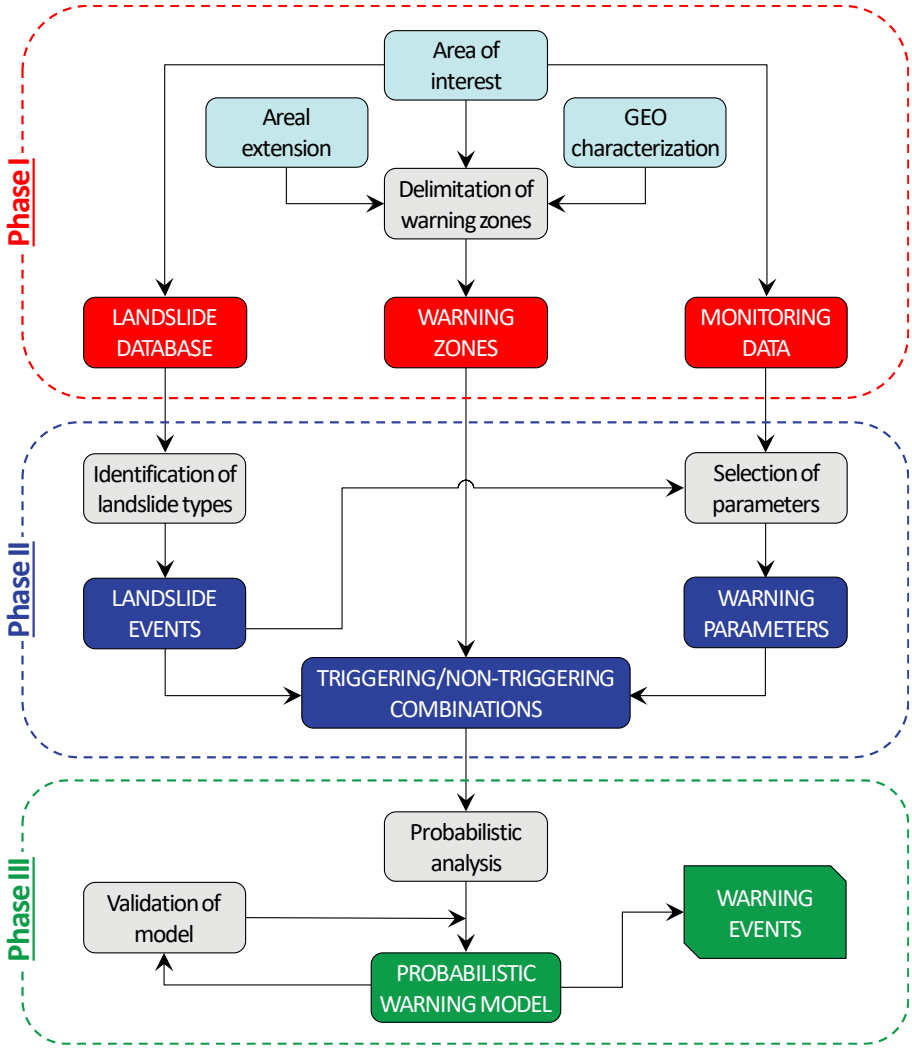

Figure 4.2 Flowchart of the proposed methodology for the definition of a probabilistic warning model for weather-induced landslides

In Phase I, information on the areal extension and on the geological, geomorphological, hydrogeological and geotechnical features of the area of interest is derived from thematic maps. The information is then used to determine the scale of analysis of the model and to define homogeneous warning zones based on the hydro-geomorphological conditions of the warned area, such as climatic regime, geology, and geomorphology. Moreover, input data to be employed within the warning model are

derived from landslide catalogs and monitoring networks available and accessible within the study area in the period of analysis. In Phase II, landslide events addressed by the warning model are selected from the available database and eventually grouped according to their characteristics. Records of questionable quality as well as landslides not clearly triggered by weather changes should not be considered. Besides, monitoring data are analyzed in order to identify combinations of warning parameters representative of the conditions which may lead to the possible initiation of the landslides. After the weather events have been defined, the landslide events that occurred within each warning zone are associated to the adopted combinations of warning parameters, and the weather events that resulted or did not results in landslides are identified. In Phase III, a probabilistic analysis is developed to compute the probability of landslide occurrence for each possible combination of warning parameters within the study area. This methodology allows to explicitly take into account information from all input data and to highlight the weather conditions corresponding to critical states of the system, i.e. conditions that are likely to trigger landslides. Finally, a validation of the model is performed in order to assess the predictive capability of the model so that, if necessary, some parameters can be modified when new data become available.

4.3 MULTI-SCALAR WARNING MODEL

Almost all the warning models presented and described in Chapter 3 are based on meteorological monitoring, typically employing a network of rain gauges for measuring rainfall in order to predict weather-induced landslides by investigating their triggering factor. However, mechanisms that lead to slope instability are often influenced by numerous factors (e.g. slope gradient, soil properties, land use), thus there is not always a direct relationship between meteorological parameters and landslide initiation. Therefore, some authors (Baum and Godt 2010, Stähli et al. 2015, Calvello 2017) propose to integrate monitoring of geotechnical parameters within the warning model, to obtain additional information useful to determine rainfall events actually triggering landslides.
Figure 4.3 presents a methodology for the definition of a multi-scalar warning model that combines monitoring data collected at regional and

slope scale. The main aim is to improve the performance of the regional warning model by integrating information from local observations. The proposed procedure can be schematized into three successive steps: collection of the input data and classification of the warning zones (Phase I), application of the regional warning model (Phase II), and integration of local observations (Phase III).

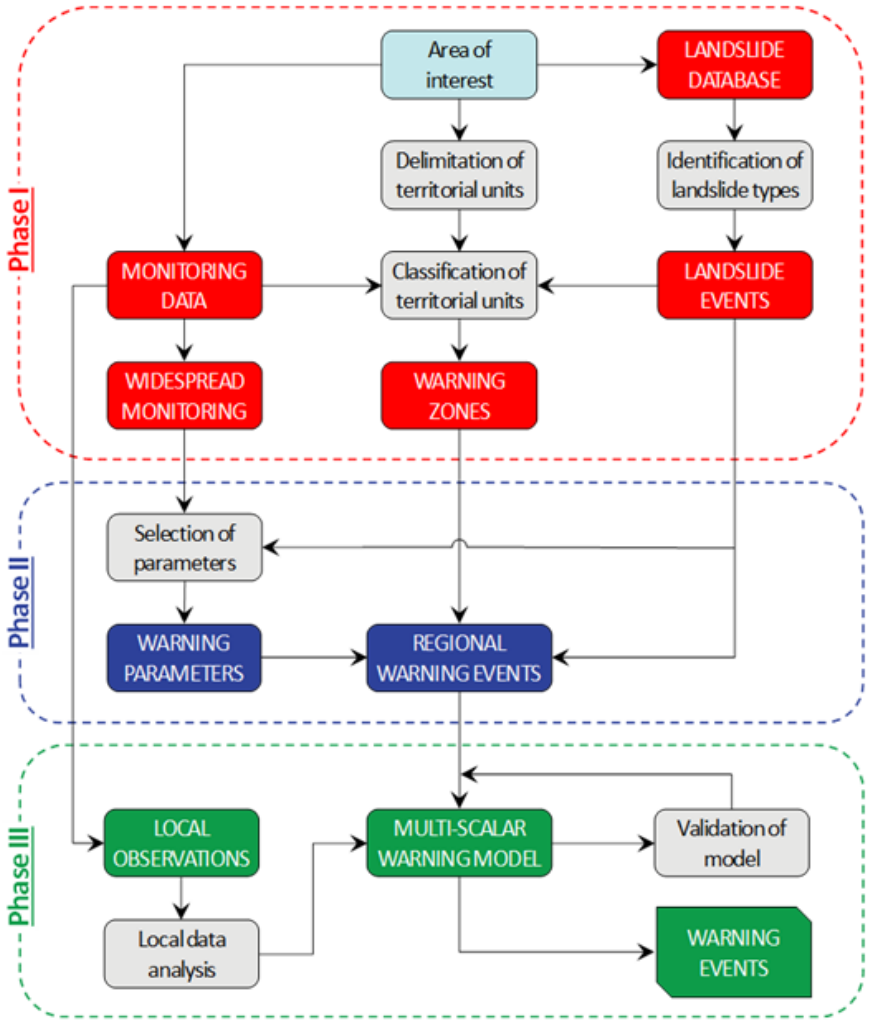

Figure 4.3 Flowchart of the proposed methodology for the definition of a multi-scalar warning model for weather-induced landslides

In Phase I, information on landslides that occurred within the area of analysis are retrieved from available landslide catalogs in order to select the types of landslides of interest for the warning model (i.e., landslide events). The most appropriate monitoring data, in terms of widespread meteorological measurements and local observations, are also collected in this phase. The area of analysis is divided into territorial units of appropriate areal extension (i.e. the warning zones adopted in the model) considering the scale of analysis, intermediate between regional scale and slope scale, so that information from widespread monitoring and local observations may be profitably combined. The territorial units are classified considering two criteria: the occurrence of landslide events in the period of analysis and the availability of relevant information from monitoring instruments in the proximity of the landslide source areas. Following this classification, the most representative territorial units are identified. In Phase II, the regional warning model developed employing only meteorological data is applied. The performance of the issued warning events (i.e., combinations of warning parameters exceeding pre-defined thresholds) is then evaluated through a comparison with the landslide events that occurred in the period of analysis. In Phase III, the regional warning events are assessed by using the information derived from the local observations within each warning zone. The multi-scalar warning model is validated by means of statistical indicators and, if necessary, it is recalibrated. The obtained results can be also extended to other areas, identified as similar to the warning zones used for the development of the multi-scalar warning model.

5 APPLICATIONS OF PROBABILISTIC WARNING MODEL

This Chapter presents the application of the probabilistic warning model defined in Section 4.2 aimed at determining the rainfall conditions critical for landslide initiation. Firstly, Section 5.1 summarizes the main steps necessary for the development of the model. Then, Section 5.2 and 5.3 describe the open-access data employed for this research, coming from a non-conventional landslide inventory and a rainfall satellite monitoring mission. A two-dimensional Bayesian methodology for the definition of rainfall probabilistic thresholds is proposed in Section 5.4. Finally, the results carried out applying this procedure to Emilia-Romagna and Campania regions (Italy) are presented and discussed (Sections 5.5 and 5.6, respectively).

5.1 PROBABILISTIC WARNING MODEL: WORKFLOW

Two probabilistic warning models have been developed and tested in two different Italian regions, Emilia-Romagna and Campania, following the procedure described in Section 4.2. Although some differences exist between the two applications, the flowchart showed in Figure 5.1 summarizes the main common steps: delimitation of the warning zones and collection of the input data (Phase I), correlation between landslides and rainfall events (Phase II), calibration and validation of the probabilistic warning model (Phase III).

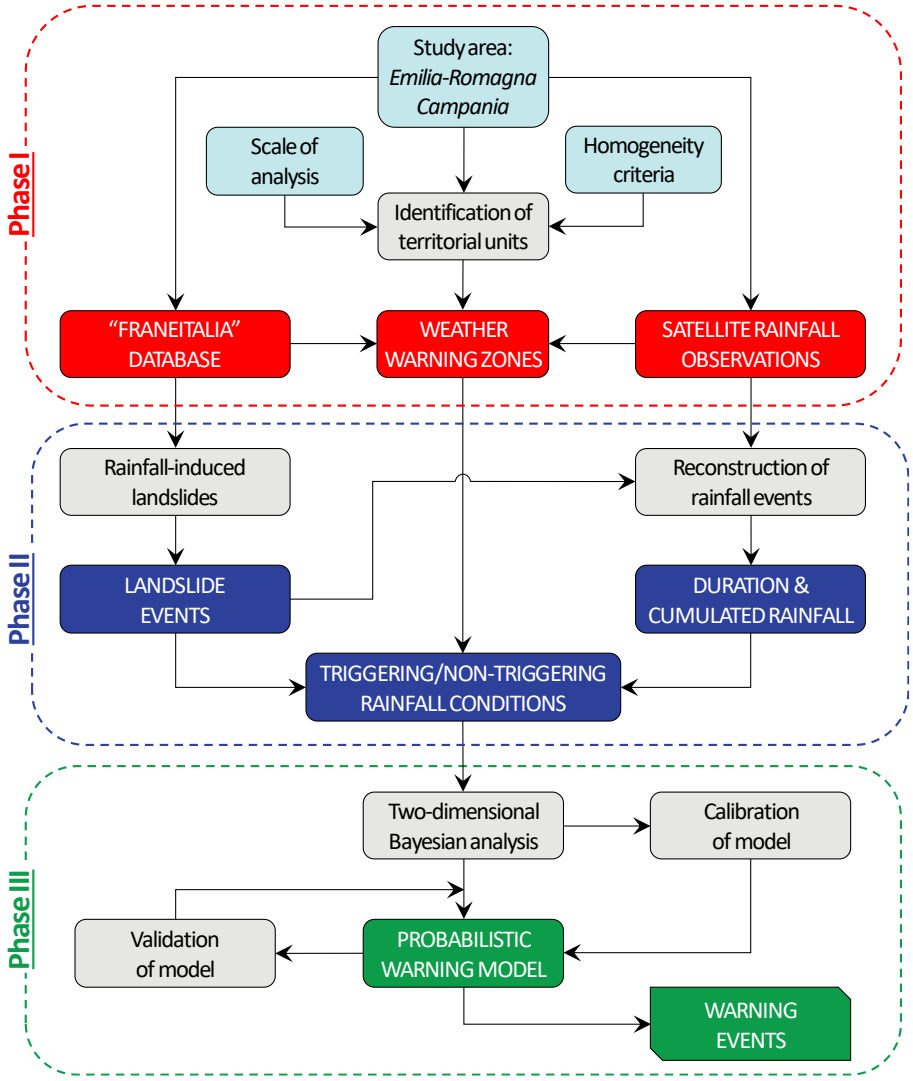

Figure 5.1 Flowchart of the proposed methodology for the definition of the probabilistic warning models for rainfall-induced landslides applied to the Emilia-Romagna and Campania case studies

In Phase I, the weather warning zones defined by the regional civil protection agency are considered as the most appropriate territorial units in relation to the scale of analysis and a series of homogeneity criteria. The analyses are conducted using open-access input data: landslide records

from a catalog of Italian landslides retrieved from online news; and rainfall measurements from satellite monitoring.
In Phase II, shallow rainfall-induced landslides in loose soils are selected from the database. Moreover, rainfall measurements are processed in order to reconstruct the rainfall events considering duration and cumulated rainfall as variables. To this aim, two different procedures are employed for the two case studies. Landslides and rainfall events are analyzed in order to define spatial-temporal correlations within each territorial unit and to differentiate between triggering and non-triggering rainfall conditions.
In Phase III, a probabilistic approach based on a two-dimensional Bayesian analysis is developed to calculate the landslide probability associated to the different types of rainfall events recorded in the database. Following this methodology, the rainfall conditions more likely to trigger landslides are identified, allowing to highlight critical levels of rainfall and to determine probabilistic thresholds for landslide initiation. Finally, the thresholds are validated employing two different procedures for the two case studies.

5.2 LANDSLIDE DATABASE: THE "FRANEITALIA" PROJECT

(based on Calvello and Pecoraro 2018)

5.2.1 Methodology

"FraneItalia" is a geo-referenced open access catalog of recent landslides affecting the Italian territory. The catalog has been developed consulting online news sources from 2010 onwards and includes both fatal landslide events and events that did not produce physical harm to people. Landslide events are classified considering two numerosity categories and three consequence categories. The numerosity categories are: single landslide events (SLE), for records only reporting one landslide; and areal landslide events (ALE), for records referring to multiple landslides triggered by the same cause in the same geographic area. Both SLEs and ALEs are divided in three consequence classes according to whether the event produced

victims and/or missing people (C1, very severe), injured persons and/or evacuations (C2, severe), or did not cause any physical harm to people (C3, minor). The "FraneItalia" catalog supplement already existing landslide catalogs and inventories in Italy, including landslide inventory maps produced by river basin authorities and databases of recent landslides developed using news articles as sources of information.

Information retrieved from online news sources on landslides that occur in Italy have been collected and organized within the new national landslide catalog, following a methodology organized in seven successive steps.

(i) Selection of sources. A certain number of online news media, published in Italian language, were preliminarily screened in order to compare the consistency and the quality of the outcomes. As a result of this activity, the following two news aggregators were selected as sources of information for the catalog: 1) Google Alert, GA (http://www.google.com/alerts), a web service that sends daily emails when it finds web pages or news articles that match users' search term(s); 2) the Italian Civil Protection press review, CP (http://ilgiornaledellaprotezionecivile.it/), a selection of articles available in pdf format collected daily from national, regional and local press.

(ii) Identification of effective keywords. Both the selected news aggregators may be searched employing a Boolean keyword approach. Key landslide terminology was assessed to select the terms that are more commonly used in Italian language to deal with landslide events. As a result of this activity, the two keywords selected for the searches are: "frana" (the Italian word for "landslide") and "frane" (the Italian word for "landslides").

(iii) Collection of relevant news articles. When one of the two search terms appears in daily searches conducted on the two information sources, the related online article is flagged as a potential entry for the landslide catalog. If the article refers to a new landslide event a record is added to the landslide database. If the article refers to a landslide event already existing in the database, the relative record is updated.

(iv) Identification of landslide categories. Landslide events are classified considering two numerosity categories and three consequence categories. The two numerosity categories are: single landslide events (SLE), for records only reporting one landslide; and areal landslide events (ALE), for records referring to multiple landslides triggered by the same cause in the same geographic area (at most coincident with an administrative Province). The latter category is used to simplify collection and reporting

of the landslide records for the numerous cases when many landslides are mentioned together in the news. The consequence classification is based on the severity of the effects to human life, not considering other consequence measures (e.g., economic loss, environmental damage). The three categories are: very severe consequences (C1), for landslide events with victims and/or missing people; severe consequences (C2), for events with injured persons and/or evacuations; minor consequences (C3), for landslide events that did not cause physical harm to people.
(v) Definition of other fields of database. Information on the landslide events collected in the catalog always include: data on the spatial location of the event, day of occurrence of the landslide(s), source(s) of information, and number of landslides in case of ALEs. Additional information may include: onset and duration of the landslide event, landslide characteristics, phase of activity, details on the consequences.
(vi) Mining of information from the articles. For each record of the database, i.e. for each inventoried landslide event, as much information as possible is obtained from the articles in relation to each field.
(vii) Geo-referencing of the events. A single set of geographic coordinates (WGS84 datum) is assigned to each record of the database, both for single and areal landslide events. The following categories of spatial positions are considered for SLEs: i) certain, if the news source clearly specifies the position of the landslide; ii) approximated, when the position of the landslide can be inferred, although it is not clearly indicated; iii) unknown, when the only information reported is the name of the municipality affected by the landslide. In the latter case, the geographic coordinates of the town hall are assigned. For ALEs, the assigned geographic coordinates are only meant to represent a point within the area affected by the landslide event and are thus useful only for maps drawn at national scale.

5.2.2 Database structure

The FraneItalia catalog was constructed adopting PostgreSQL version 9.6, an open source Relational DataBase Management System, with the PostGIS extension version 2.3. Tables, fields and relationships—designed in a logical model—were translated into PostgreSQL physical tables, fields, and one-to-one relationships. Figure 5.2 shows all the fields of the database. Each reported landslide event is characterized by 40 unique fields, which are grouped in 9 thematic tables: main info; spatial information; temporal information; landslide characteristics;

consequences to people, structures, infrastructures, cars and other elements; and source. Not all fields are mandatory.

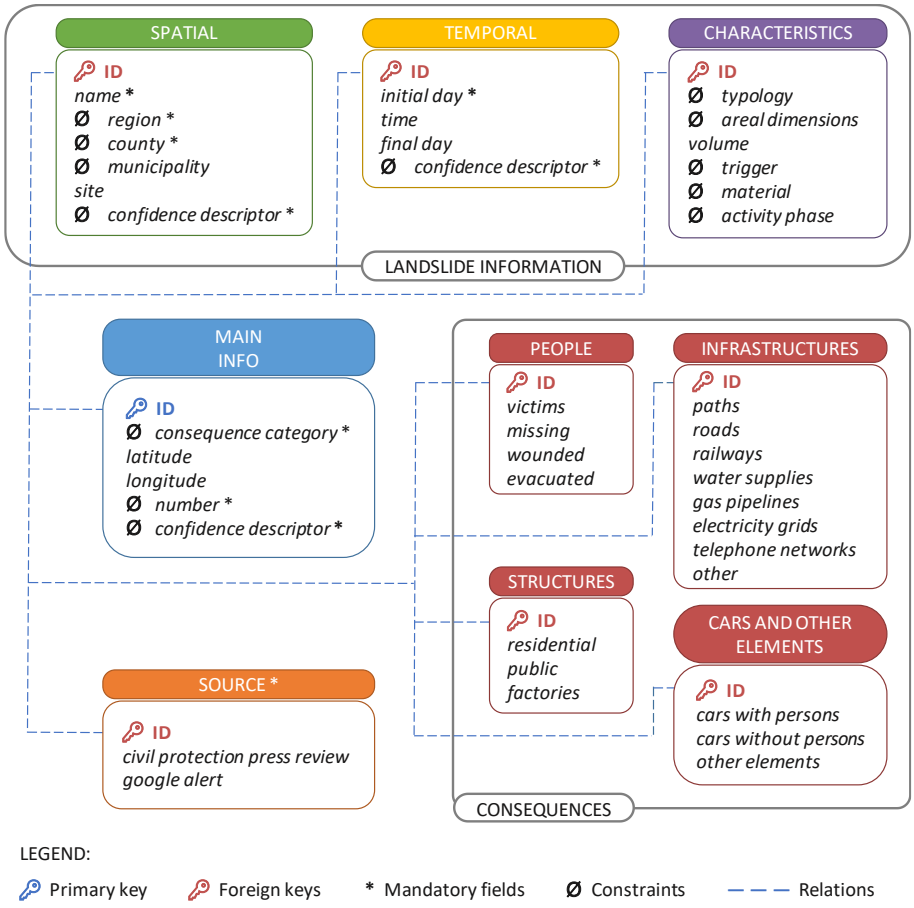

Figure 5.2 Structure of the "FraneItalia" landslide database *(Calvello and Pecoraro 2018)*

Inspection of Figure 5.2 reveals that the core of the catalog structure is the main info table, that maintains a unique hierarchical relation with tables containing information on the landslides, their consequences and the sources of information, i.e. links to online articles. The tables are connected through the identification code (ID), which is unique for each record and whose format is designed to highlight the landslide event category and the initial date of the event. The name of the landslide event

is not a compulsory entry and, when possible, it quotes the terms most commonly used to refer to the event. The landslide categories, as already mentioned, are based on landslide numerosity and on the consequences to human life of the landslide event. Both SLEs and ALEs are divided in three consequence classes. Further compulsory information for each record are the geographical coordinates of the landslide event and the source(s) of data. When the GA service is used, the references are the web addresses of the online news articles. When the CP press review is used, the references include the day (the press review is published each working day), the type (5 daily reviews are published in relation to the geographical location of the source: national, northern Italy, central Italy, southern Italy, main islands) and the pages of the PDF documents reporting the information. Finally, data visualization and editing in the FraneItalia database are allowed through a specific procedure that exploits QGIS software (QGIS Development Team, 2018) as a client, and a dedicated data visualization web interface.

According to many authors (e.g., Guzzetti 2000, Kirschbaum et al. 2010, among others), characterizing landslide events from news reports and other text-based sources is challenging, as information varies widely in terms of both accuracy and availability, resulting in possible biases and uncertainties affecting the catalog. Compulsory information in the FraneItalia catalog include the geographical coordinates and the date of each landslide event, as well as the number of landslides of ALEs. If, for a given record of the database, the needed data are not directly reported in any news, the operator is requested to compile the related fields using his/her own judgement to infer from the available sources. The uncertainty of the position of SLEs is specified by means of three confidence descriptors associated to the geographical coordinates of the landslide event, named: certain (Sd1); approximated (Sd2); municipality (Sd3). In the latter case, the operator has to identify the municipality wherein the landslide event occurred and assign to the event the geographical coordinates of the town hall. The geographic coordinates attributed to ALEs are always indicative (Sd4) and are only meant to approximately identify the geographical region affected by the mentioned landslides. A second source of uncertainty may result from lack of detailed information on the time of the event. In the vast majority of cases, the day of the landslide event is reported in the news; quite often, a general indication of the time of occurrence (e.g., "in the morning") is also available; sometimes, the date of the event is not reported and the news

article only generically refers to the event as a past occurrence (e.g., "few days ago"). The temporal uncertainty related to the occurrence of the landslide events is specified by means of two confidence descriptors, named: certain (Td1), when the news sources report at least the day of the event; estimation (Td2), when the operator has to interpret the news reports to assign a date to the event. In the first case, if more information on the time of the event is reported the "time" field is also filled, either by inserting the hour of the event or by specifying a time range (e.g., "in the morning"). In both cases, if the landslide event lasts longer than one day, the final day of the event is also reported. Finally, the uncertainty associated to the number of landslides in ALEs is specified by means of two descriptors, named: reported (Nd1), when the news reports that number; and estimation (Nd2), when the operator has to infer from the news to assign it. Most typically ALEs are due to extreme weather conditions triggering, in one or more days, multiple landslides over wide areas. In these cases, the news typically identifies the area affected by the events and highlights the landslide(s) that produced the highest consequences, only rarely reporting a number that can be considered representative of all the landslides occurring during the areal event.

Four types of constraints are adopted to guarantee the correctness and semantic integrity of the inserted records. A first group of constraints is adopted to ensure the appropriateness of the information related to the landslide numerosity class (SLE or ALE) and to the number of landslides within a landslide event (i.e. the number of landslides must be equal to one for SLEs and higher than one for ALEs). A second constraint limits the values of the possible choices of the confidence descriptors that quantify the uncertainties related to the number of landslides, their location and their time of occurrence. Next, geographical data are validated by means of a dictionary valid for Italy (first level for the regions, second level for the counties, and third level for the municipalities). Finally, lists of pre-identified values are adopted to standardize and harmonize the following characteristics of the landslide events: typology, areal dimensions, trigger, material, and activity phase.

Table 5.1 reports how the two selected news aggregators, GA and CP, were used to populate the FraneItalia catalog from January 2010, i.e. the beginning of the survey, to December 2017, i.e. the end of the period reported herein. The CP was predominantly used for a series of reasons. The daily press reviews from the Civil Protection are stored as an online archive accessible at a later date. When the study started, at the end of

2012, it was thus possible to go back in time and set January 2010, the month of first available CP press reviews, as starting date. On the contrary, the daily GA service has to be activated from a user. Therefore, GA was fully operational for the FraneItalia catalog only from January 2013. To overcome this limitation, the Google News search engine was also used to look for landslide news published in the year 2012. Yet, the search results were conditioned by the availability of the original online news when the searches were performed, i.e. first few months of 2013. Moreover, it has been empirically found that GA results depend on the location of the user as well as on its "habits" when using the Google search engine. The same GA search queries may thus generate different sets of online news articles for different users. Another important advantage of CP over GA is that the searches and the data entries performed using CP are less time-consuming. Indeed, the daily press reviews are already organized in 5 searchable PDF documents: one document collecting news of national relevance, mainly from countrywide news sources; the other four documents referring to news from Northern Italy, Central Italy, Southern Italy and the main Islands, respectively. This aspect of the CP, i.e. non-automatic pre-processing of online news from personnel of the civil protection, which may be considered a time-saving asset of this news aggregator, turned into a drawback when the civil protection agency either did not provide the press reviews (end of 2014) or performed limited reviews (November 2015). In summary, the CP was used to populate the FraneItalia catalog throughout the considered time period whenever available, whereas GA was only used in 2013, from September 2014 to February 2015, in November 2015 and, by means of the Google News search engine, from January 2011 to December 2012.

Table 5.1 News aggregators used to populate FraneItalia from January 2010 to December 2017 ***(Calvello and Pecoraro 2018)***

News aggregator	Period
Civil protection daily press review (CP)	From January 2010 to August 2014; from January 2015 to December 2017
Google Alert service (GA)	From January 2011 to December 2012 (via Google News search engine); year 2013; from September 2014 to February 2015; November 2015

5.2.3 Database contents

The FraneItalia catalog currently spans from January 2010 to December 2017, containing a total of 8931 landslides, grouped in 4231 SLEs and in 938 ALEs (Table 5.2). About 2% of the 5169 landslide events had very severe consequences to human life (C1), 14% of the records refer to events with severe consequences to human life (C2), while the vast majority of records deals with landslide events that had minor consequences to human life (C3).

Table 5.2 Landslides inventoried in the "FraneItalia" catalog from 2010 to 2017

Year	Single Landslide Events (SLE)				Areal Landslide Events (ALE)				Number of landslides
	C1	C2	C3	TOT	C1	C2	C3	TOT	
2010	12	100	498	610	2	36	171	209	1584
2011	16	60	302	378	4	20	68	92	821
2012	9	51	393	453	2	14	85	101	949
2013	12	77	538	627	1	39	114	154	1503
2014	15	111	844	970	3	36	144	183	1936
2015	9	63	377	449	2	17	58	77	801
2016	5	43	368	416	1	5	59	65	801
2017	3	45	280	328	1	13	43	57	536
TOT	81	550	3600	4231	16	180	742	938	8931

Figure 5.3 reveals that the sites affected by landslides are not equally distributed in Italy. SLEs are abundant in many regions and, as expected, there is a clear evidence of a correlation between an increasing density of landslide events and the location of the main Italian mountain chains, the Alps and the Apennines. ALEs are more common in the eastern sectors of the Alps (Lombardy and Veneto regions) and in the central and northern sectors of the Apennines (Tuscany, Liguria, Emilia-Romagna, and Marche regions). Among the southern regions, the one most affected by both single and areal events are Campania, Calabria and Sicily. The highest number of landslides reported in the database occurred in Toscana, mainly as a consequence of a series of major areal events triggered by heavy rainstorms. The lowest number of events is recorded in Puglia, whose territory mainly comprises plains. Most of the other regions experiencing a large number of landslides are located in northern Italy (Veneto, Lombardy, Emilia-Romagna and Liguria). In particular, Lombardy is the region most affected by SLEs, mainly occurring in the Alpine area where the presence of high relative relief and outcropping

rocks, such as granite, metamorphic rocks, massive limestone and dolomite, facilitate rock falls, rock slides and rock avalanches (Guzzetti, 2000).

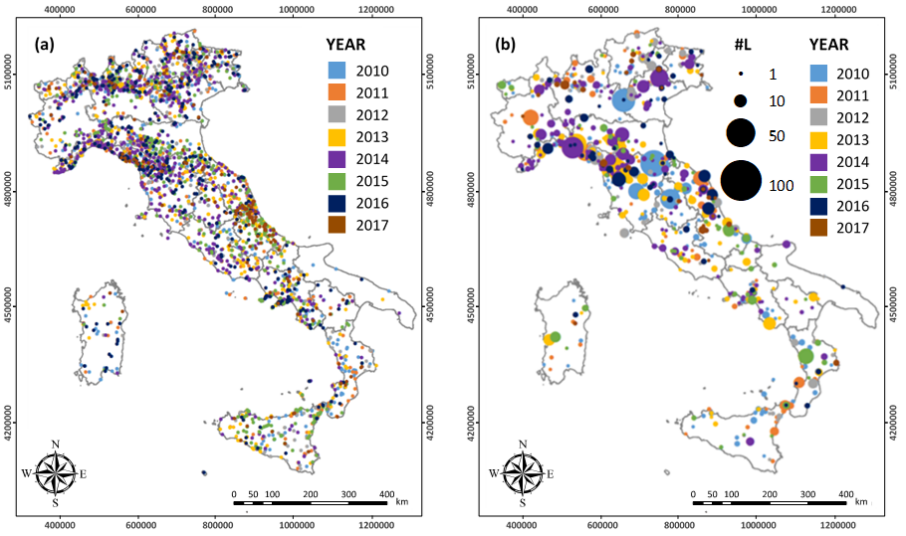

Figure 5.3 The "FraneItalia" landslide catalog for the period 01/01/2010–31/12/2017: (a) SLE records; (b) ALE records *(Calvello and Pecoraro 2018).* Legend: *#L* = Number of landslides

Figure 5.4 reports that in several regions (Lombardy, Veneto and Piedmont) a non-negligible number of events occurred in the summer, possibly in relation to extreme rainfall events or snowmelt processes in the Alpine environment. On the contrary, in most parts of central and southern Italy (e.g., Emilia-Romagna, Campania, and Sicily) a considerable number of landslides occurred during the autumn and winter seasons. These findings are consistent with the different seasonal failure scenarios reported by Cascini et al. (2014) for the Campania region: distributed or widespread first-time shallow slides triggered by frontal rainfall and propagating as debris flows or debris avalanches between November and May; local erosion phenomena and small first-time shallow slides triggered by isolated convective storms between June and August; widespread erosion phenomena triggered by hurricane-like rainfall, often turning into hyperconcentrated flows, between September and October.

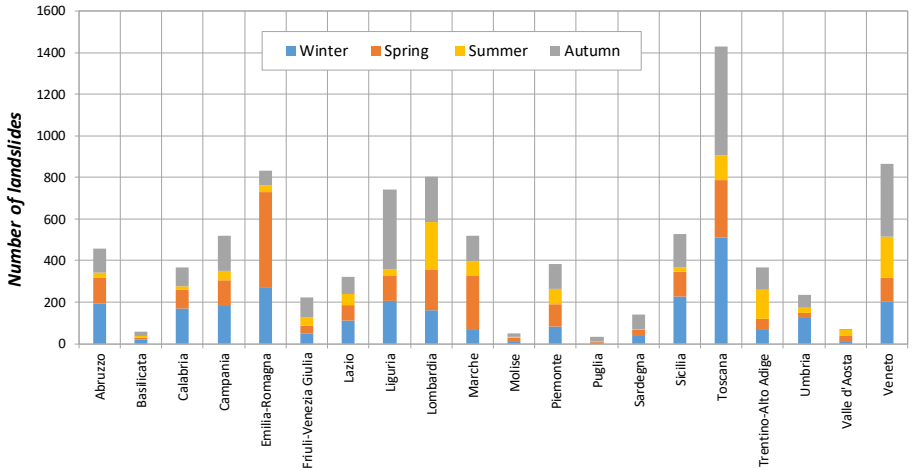

Figure 5.4 Number of landslides inventoried in the 20 Italian regions, differentiated per season *(Calvello and Pecoraro 2018)*

5.3 SATELLITE RAINFALL MEASUREMENTS

5.3.1 Global Precipitation Measurement (GPM) mission

Precipitation data have been derived from the satellite-based Global Precipitation Measurement (GPM) mission, co-led by the National Aeronautics and Space Administration (NASA) and the Japan Aerospace Exploration Agency (JAXA). GPM mission aims at improving the knowledge of Earth's water and energy cycles, improving the forecasting of extreme events that cause natural disasters, and extending current capabilities of using satellite precipitation information to directly benefit society (Hou et al. 2014). The GPM Core Observatory is designed to work with and anchor a constellation of satellites and ground systems from partner agencies located in the United States, Japan, Europe, and India (Figure 5.5).

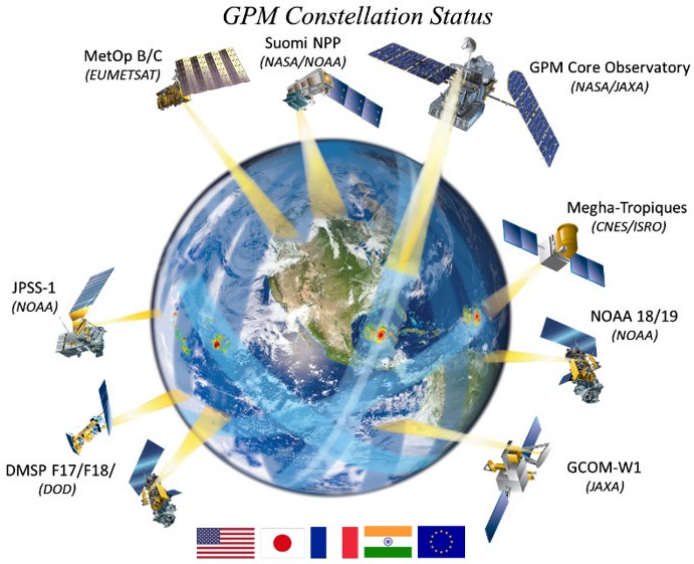

Figure 5.5 Constellation of satellites and international partners participating in the GPM mission (https://pmm.nasa.gov/GPM)

The mission was launched on 27 February 2014 and was a successor of the Tropical Rainfall Measuring Mission (TRMM), which provided data on heavy to moderate rainfall in Earth's tropics and subtropics from 1997 to 2015. TRMM data were used to obtain multiyear sets of tropical and subtropical rainfall observations; develop a better understanding of the interactions between sea, air, and land masses and their influence on global rainfall and climate, improve the modelling of tropical rainfall processes, and enhance satellite rainfall measurement techniques. GPM improves on TRMM's capabilities in a number of aspects. Although GPM employs only two instruments—a Dual-frequency Precipitation Radar (DPR) and a radiometer called GPM Microwave Imager (GMI)—versus the five instruments on TRMM, they are some of the most advanced instruments for monitoring precipitation from the space. Therefore, their combination provides an increased sensitivity to light rain rates as well as more reliable information on particle drop size distribution. One of the most significant evolutions in GPM data is its broader global coverage. While TRMM collected data in tropical and subtropical regions between roughly 35° north and south latitude, GPM collects data between approximately 60° north and south latitude. This allows GPM's instruments to collect data on storms as they form in the tropics and move into the middle and high

latitudes. A significant GPM data enhancement over TRMM is its design as a Core Observatory that coordinates data collection from a constellation of partner satellites, rather than as a single satellite. The GPM Core Observatory calibrates the data from almost a dozen orbiting U.S. and international satellites that observe precipitation, ensuring a uniform structure to the data collected from these satellites. The number of partner satellites in the constellation will change over time as new satellites are launched and older satellites are decommissioned (Kirschbaum et al. 2017).

GPM provides a wide variety of products retrieved combining data from active and passive instruments in the Integrated Multisatellite Retrievals for GPM (IMERG). This algorithm intercalibrates, merges, and time-interpolates "all" satellite microwave precipitation estimates in the GPM constellation, then incorporates microwave-calibrated satellite estimates and precipitation gauge analyses (Huffman et al. 2018). IMERG uses the GPM Combined Instrument precipitation estimate to intercalibrate all available microwave data, similar to the TMPA approach, yet an advanced time-interpolation scheme is employed in order to follow the estimated motion of the precipitation systems. Precipitation datasets are available at a variety of levels which denote the amount of data processing, from raw data (level 1) to model outputs mathematically derived using the raw data as input (level 3). Precipitation data used in this research have been derived from the IMERG version 5 (v05b), which includes gridded precipitation data collected every 30 min at a 0.1° × 0.1° (~10km × 10km) spatial resolution, currently covering the latitude band 60°N–60°S (Table 5.3).

Table 5.3 Technical characteristics of the GPM products used in this research *(Huffman et al. 2018)*

Integrated Multi-satellite Retrievals for GPM	
Basic acronym	IMERG
IMERG version	05b
GPM Level	3
Spatial resolution	0.1° × 0.1°
Temporal resolution	30 minutes
Coverage	Gridded, 60°N–60°S
Latency	4 h (NRT/Early run)

5.3.2 Analysis of rainfall data

Satellite rainfall data retrieved from GPM database have been analyzed through Google Earth Engine (GEE), a cloud-based platform for planetary-scale environmental data analysis. GEE allows users to download and upload global satellite imagery as well as to carry out the analysis of large datasets (Gorelick et al. 2017). The data catalog hosts a large repository of publicly available geospatial datasets, including observations from a variety of satellite and aerial imaging systems, environmental variables, weather and climate forecasts, land cover, topographic and socio-economic datasets. Users can access and analyze data from the public catalog as well as their own private data. The remote sensing datasets required for large scale analyses are downloaded via a web-based application programming interface (API) instantly using Google's high-performance parallel computation service. Analysis is performed using an interactive development environment Earth Engine (EE) Code Editor, which enables rapid prototyping and visualization of results (Figure 5.6).

Figure 5.6 Components of the Earth Engine Code Editor at ***https://code.earthengine.google.com/***

Code is typed by the user through the JavaScript code editor, which formats and highlights the code, underlines code with problems, and offers code completion hints for Earth Engine functions. Above the code editor are buttons for running the script, saving the script, resetting the

output map and console, and getting a link to the script. Asset manager in the left panel is used to upload and manage user's own image assets in Earth Engine. The Map panel in the API returns the geographic region visible in the Code Editor; customizations are available for this display using the Map functions. Console output allows to print and export something for the script, such as text, objects, or charts.
Figure 5.7 displays the methodology developed for analyzing the IMERG version 5 (v05b) GPM-Level 3 Final Run products available from the Earth Engine Weather catalog.

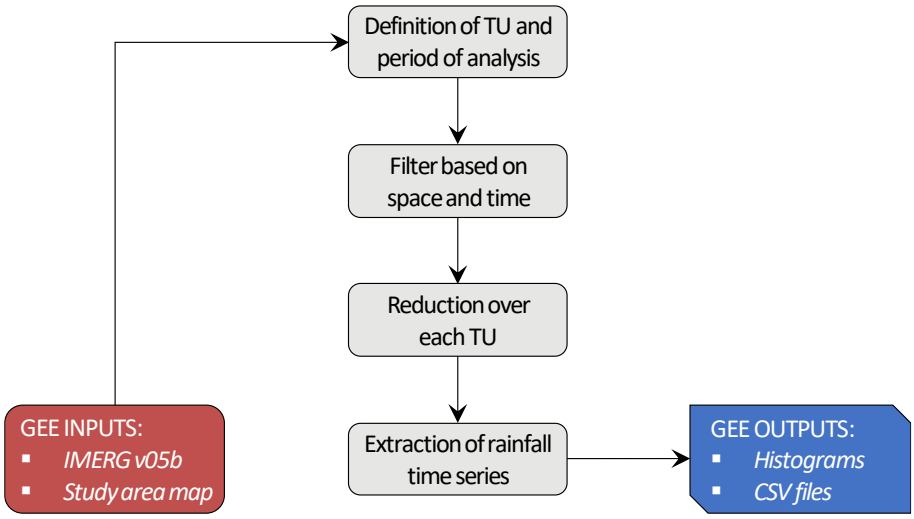

Figure 5.7 Methodology developed for analyzing the GPM rainfall data using GEE

To this aim, a script has been created and run through the Earth Engine Code Editor. Firstly, the rainfall dataset has been imported in the script and visualized in the map. Once the study area is partitioned into territorial units (TU), a Fusion Table containing geometry and other thematic information is created and imported in the script. Rainfall data have been filtered taking into account spatial (i.e., the areal extension of each territorial unit) and temporal (i.e., the period of analysis) criteria. Subsequently, a "reducer" has been applied in order to calculate statistics over each territorial unit. Reduction is a function which aggregates all the information derived from the pixels included in each territorial unit into a compact representation of the pixel data (e.g., "min", "max", "mean").

Finally, plots are generated using the chart function, which allows viewing and exporting them in multiple formats (e.g., comma-separated values, portable network graphics).

5.4 BAYESIAN PROBABILISTIC ANALYSIS

The probabilistic analysis is aimed at highlighting the critical levels of rainfall corresponding to different probabilities of landslide occurrence, in order to provide a quantitative assessment of the threshold reliability. The definition of the probabilistic model is based on the Bayesian theory and on the computation of conditional probabilities. The conditional probability can be defined as the probability of an event (i.e., a landslide event) given that (by assumption, presumption, assertion or evidence) another event has occurred (i.e., a rainfall event characterized by a certain magnitude, expressed in terms of rainfall parameters).
In principle, the Bayes' approach is suited to handle multidimensional analysis with n-variables, for example, the combined effect of rainfall duration, rainfall intensity and antecedent precipitation on landslide triggering. However, multidimensional data are difficult to visualize and analyze, therefore it is often more efficient to restrict the analysis to the two-dimensional cases. In such cases, the posterior landslide probability can be evaluated considering the joint probability of two rainfall parameters appropriately identified, as follows:

$$P(L|A,B) = \frac{P(L)\times P(A,B|L)}{P(A,B)} \qquad (5.1)$$

where: $P(L|A,B)$ is the posterior landslide probability, i.e. the conditional probability of a landslide event L given the joint probability of the two rainfall parameters A and B; $P(L)$ is the prior probability, i.e. the probability of a landslide event L; $P(A,B|L)$ is the likelihood, i.e. the conditional probability of A and B given the occurrence of a landslide event L; $P(A,B)$ is the marginal probability, i.e. the joint probability of A and B.
Bayesian probabilities are usually based on relative frequencies, which can be computed by:

$$P(L) = \frac{N_L}{N_R} \qquad (5.2)$$

$$P(A,B) = \frac{N_{(A,B)}}{N_R} \quad (5.3)$$

$$P(A,B|L) = \frac{N_{(A,B|L)}}{N_L} \quad (5.4)$$

where: N_L is the total number of landslide events that occurred in the period of analysis; N_R is the total number of rainfall events recorded in the period of analysis; $N_{(A,B)}$ is the number of rainfall events characterized by specific values of A and B; $N_{(A,B|L)}$ is the number of rainfall events characterized by specific values of A and B that resulted in landslides. The frequency distributions for specific classes of rainfall events that resulted in landslides and did not result in landslides can be converted into probabilities using this approach.

Figure 5.8 shows an application of equation *(5.1)* to a sample dataset, considering duration *(D)* and cumulated rainfall *(E)* as rainfall parameters. All the thirty rainfall events are plotted in the duration-cumulated rainfall plane, which is divided into four regions delimited by the D and E values (Figure 5.8a). Equation *(5.1)* is then computed separately for each region obtaining probabilistic information in the DE plane (Figure 5.8b).

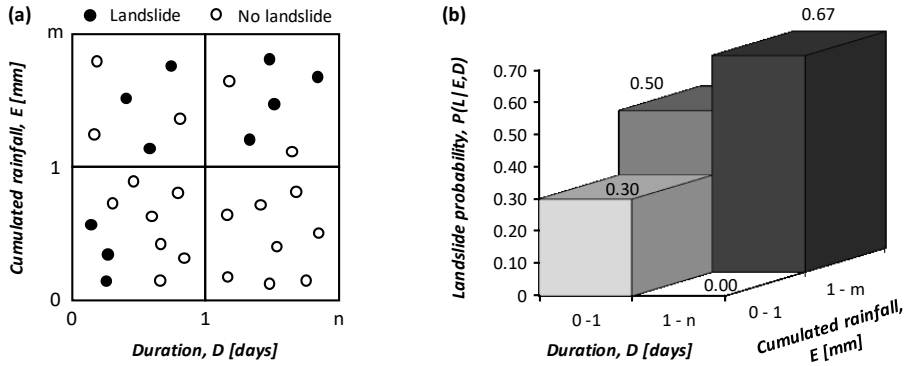

Figure 5.8 Example of two-dimensional Bayesian analysis. (a) Rainfall intensity-duration plot showing rainfall that did and did not result in landslides. (b) Histogram of conditional landslide probability for four different combinations of duration and cumulated rainfall

For example, in the upper-left cell 3 rainfall events out of 6 resulted in landslides, which means that $P(D,E|L) = 3/10 = 0.30$ and $P(D,E) = 6/30 = 0.20$. The prior landslide probability is $P(L) = 0.33$ and the posterior landslide probability is $P(L|D,E) = 3/6 = 0.50$ (Figure 5.8b).

Any pair of parameters can be considered in two-dimensional Bayesian analysis (e.g., peak rainfall intensity, total event rainfall, antecedent rainfall), and their significance can be assessed by comparing the computed posterior landslide probability with the prior landslide probability.
The Bayesian method described herein is similar to that used by Berti et al. (2012) in the Emilia-Romagna region (Italy). However, some differences exist between the two methodologies when applied to real case studies. These differences are related to the source of the rainfall data, the reconstruction of the rainfall events, the algorithm adopted for processing the data, and the computation of the final probabilities (see Sections 5.5 and 5.6 for further details).

5.5 CASE STUDY 1: EMILIA-ROMAGNA REGION, ITALY

5.5.1 Study area

The Emilia-Romagna region in northern Italy is bordered by the Apennines mountains on the south and on the west, by the Adriatic Sea on the east and by the Po River on the north. The northern and eastern portions of its territory are dominated by a wide flat area constituted by the alluvial plain of the Po, the largest Italian river. The southern and western portions of the region are occupied by the Apennines Chain, with a maximum altitude of 2165 m a.s.l. (Segoni et al. 2018b). The very complex geological setting of the study area is directly related to the formation of the Apennines, whose evolution began in the Cretaceous when two separated continental blocks (the European plate and the Adria microplate) collided. The bedrock geology is constituted by three main rock types: clastic rocks, flysch, and clays units (Martelloni et al. 2012). The study area is characterized by a typical Mediterranean climate with two distinct periods: warm and dry summers (approximately from May to October) and mild/cool and wet winters (approximately from November to April). The average annual precipitation is 1300-1400 mm, varying from a minimum of 500-600 mm in the foothills to more than 2000 mm in areas along the Po River. The mountainous part of the Emilia-Romagna region is strongly affected by landslides, especially rotational–translational slides,

slow earth flows, and complex movements. However, the frequency of rapid shallow landslides is markedly increasing in the last few years (Berti et al. 2012). This can be explained considering that shortest and more intense rainfalls, typically the main triggering factor of shallow landslides and debris flows in the Emilia-Romagna region, became more frequent in the Mediterranean area due to climate change (Floris et al. 2010).
The operative warning system for flood and landslide risk is currently based on the division of the region in eight districts, called warning zones (Figure 5.9); these areas have been defined following homogeneity criteria, including: physiography, lithology, precipitation regime, and administrative boundaries. The mean extension of the warning zones is about 3000 km^2, resulting in a medium scale approach that represents a compromise between operational and scientific constraints (Martelloni et al. 2012). The warning zones that include up to 20 municipalities can be further subdivided, obtaining a more detailed partitioning during operational phases (Pecoraro and Calvello 2016). The model employed for the rainfall thresholds definition is called SIGMA, whose name reflects the central role assumed by standard deviations in the proposed methodology. The areas of the region susceptible to landslide events has been subdivided into territorial units, each one associated to a reference rain gauge. The time series of cumulated rainfall from 1 to 365 days have been derived for each rain gauge. Precipitation curves (σ curves) associated with various probabilities of non-exceedance are built and the multiples of the standard deviation *(σ)* are used as thresholds to discriminate between ordinary and extraordinary rainfall events (Martelloni et al. 2012).

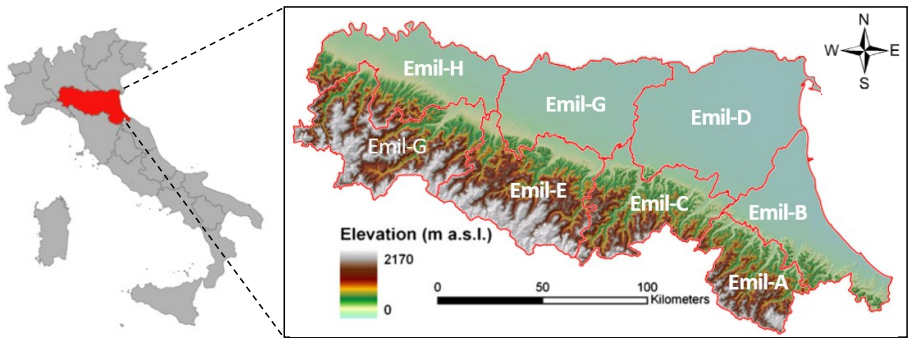

Figure 5.9 The eight warning zones of the Emilia-Romagna region. The elevation map is also reported

5.5.2 Territorial units and available datasets

The most appropriate territorial units for the spatial-temporal analyses can be considered the eight weather warning zones defined by the regional civil protection agency (see Figure 5.9), as they represent a good compromise between the purposes of this study and the spatial discretization of the input data (i.e., landslide records and rainfall measurements). Indeed, weather warning zones are deemed to be significantly homogeneous areas for the expected meteorological and hydrogeological events that may occur within them. On the other size, the geographical accuracy of the landslide records is affected by a certain degree of uncertainty. In particular, the location of SLEs is usually approximated (e.g., in some cases only the municipality where the landslide occurred is known), whereas for ALEs it is only indicative of the geographical area interested by multiple landslides (see Section 5.2.2 for further details). Therefore, adopting wide weather warning zones as territorial units may reduce the effect of biased spatial information on the reliability of model outputs. Finally, weather warning zones also represent appropriate territorial units for the rainfall analyses, considering the spatial resolution of the satellite rainfall estimates employed in this work (i.e., 0.1° × 0.1°, corresponding to ~10km × 10km).

The dataset used to analyze this case study includes information on landslide occurrences and satellite rainfall measurements from March 2014 to December 2015. The FraneItalia database reports 115 landslide events occurred in Emilia-Romagna in the period of analysis. However, 13 landslides have been not included in the dataset: nine of them cannot be considered rainfall-induced landslides, as they are reported as human- or earthquake-induced landslides or landslides for which the trigger is not known; the remaining four are classified as landslides in rock, for which the correlations with rainfall could be weak or inexistent. Among the 102 landslide events included in the dataset, 78 are classified as SLEs and the remaining 24 as ALEs (Figure 5.10). Almost all the reported records are concentrated in the south-western part of the region (especially in warning zones *Emil-A, Emil-B, and Emil-E*). In addition, *Emil-G* was affected by 6 major ALEs triggered by heavy rainstorms. Conversely, only a small number of SLEs occurred in the northern part. This distribution was expected, as in Emilia-Romagna landslide prone areas are mainly concentrated in the southern and western portions dominated by steep

slopes, while the northern and eastern areas are widely flat (see Section 5.5.1 for further details).
Satellite rainfall estimate products used for this research were derived from the NASA Global Precipitation Measurement (GPM) mission. In particular, precipitation data from the last current version (IMERG 05b) have been acquired from public satellite imagery datasets available on Google Earth Engine. For the purposes of this study, precipitation measurements have been aggregated at hourly temporal resolution and the mean values over each territorial unit have been calculated.

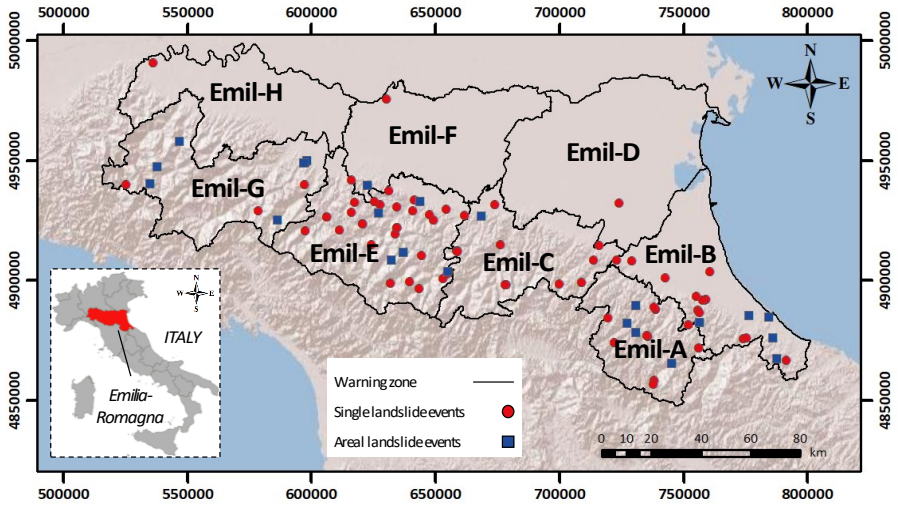

Figure 5.10 Shaded relief map of the eight warning zones of the Emilia-Romagna region showing the 102 rainfall-induced "FraneItalia" landslide records from March 2014 to December 2015, differentiated in single (red circles) and areal landslide events (blue squares). The inset shows the location of the Emilia-Romagna region in Italy

5.5.3 Correlation between landslides and rainfall events

The definition of the correlation between landslides and rainfall events in Emilia-Romagna required the reconstruction of the rainfall events in order to pass from a series of hyetographs to a point cloud in a graph reporting triggering and non-triggering combinations of rainfall parameters (Segoni et al. 2018a). Duration *(D)* and cumulated rainfall *(E)* have been identified as the most appropriate rainfall parameters. Indeed, as demonstrated by Berti et al. (2012) they are representative of the triggering conditions for

shallow rainfall-induced landslides in Emilia-Romagna, characterized by a predominance of fine-grained soils in the shallow soil layers. D is represented by the time between the moment, or period, of landslide initiation (rainfall end time, T_E) and the time when the rainfall event started (rainfall start time, T_S), i.e., $D = T_E - T_S$ (Rossi et al. 2017). T_E coincides with the end of the rainfall event in case the landslide occurs after the end of the rainfall events (Brunetti et al. 2010). The definition of T_S is often difficult particularly when rainfall is not continuous, as a dry period (i.e., a period without rainfall or with rainfall below a predefined threshold) between two successive rainfall values needs to be identified to separate different rainfall events. To this aim, Figure 5.11 shows the "standard" detection algorithm adopted for this case study. The procedure needs three main steps to define a rainfall event based on its attributes (i.e., D and E). In the first step, all the isolated rainfall events have been detected considering a minimum period without rain (Figure 5.11a). To account for different meteorological regimes in Italy, two minimum periods have been considered: a two-day (48 h) interval for the "warm" spring-summer period (April-September) and a four-day (96 h) interval for the "cold" period (October-March). Successively, isolated rainfall measurements that did not exceed a minimum value $E_R = 1\,mm$ have been excluded, because they have been considered not relevant for possible landslide initiation (Figure 5.11b). The triggering and non-triggering rainfall conditions have been identified according to the two aforementioned standards (Figure 5.11c,d). Regarding triggering rainfall conditions, landslides typically occur before the end of the rainfall event, thus the rainfall after the landslide occurrence cannot be considered relevant for the initiation of the slope failure. On the contrary, when landslides fail after the end of the rainfall period, the rainfall associated to the landslide corresponds to the cumulated rainfall of the entire event.

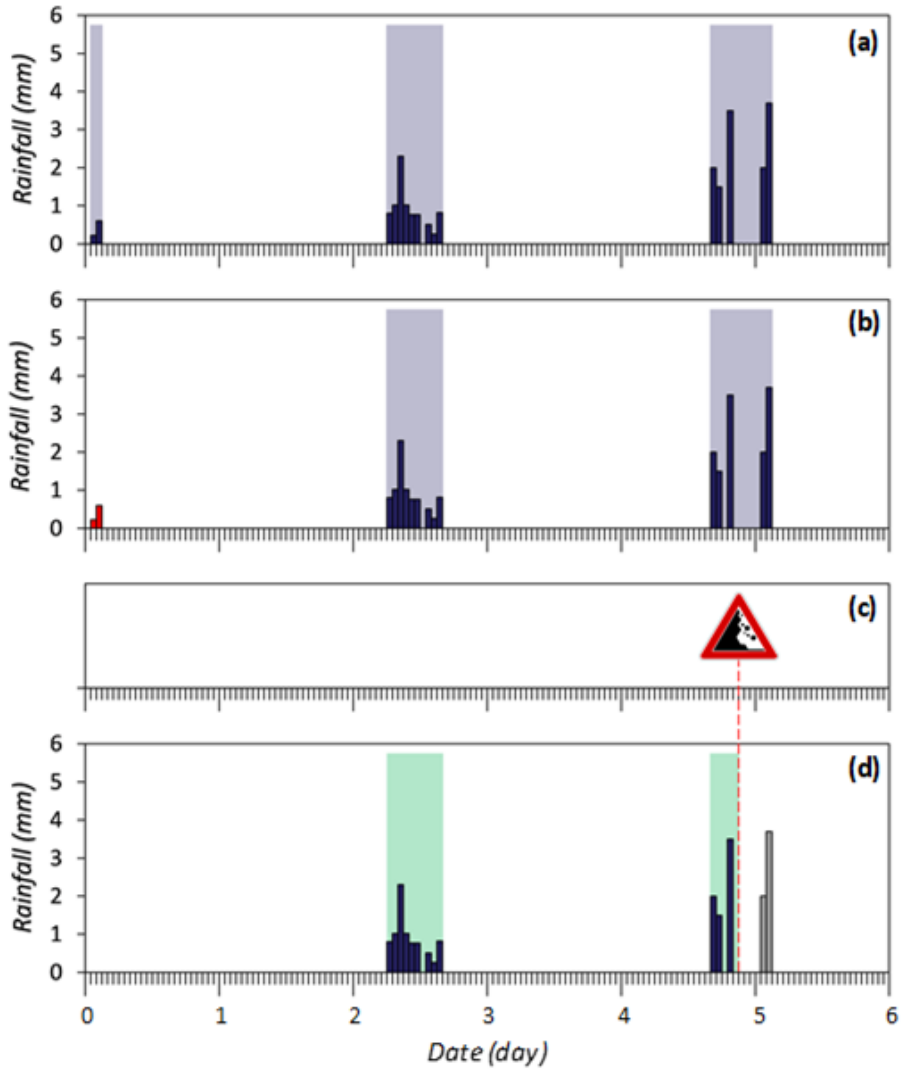

Figure 5.11 Example of the application of the standard algorithm for the reconstruction of rainfall events. a) Detection of rainfall events (highlighted by blue-shaded areas) grouping hourly rainfall measurements (blue bars). b) Exclusion of irrelevant rainfall events (red bars). c) Identification of landslide events (highlighted by the warning sign). d) Differentiation between triggering and non-triggering rainfall events (highlighted by green-shaded areas)

Following this approach, 1029 rainfall conditions *(D,E)* have been reconstructed and plotted in log-log coordinates (Figure 5.12). The 102

rainfall conditions responsible for the triggering of the 78 SLEs (red circles in Figure 5.12) and the 24 ALEs (blue squares in Figure 5.12) are in the range of duration $1 \leq D \leq 67\ h$ and in the range of cumulated rainfall $1.1 \leq E \leq 969\ mm$. Of course, the non-triggering rainfall conditions reconstructed in the same period are 927 (grey circles in Figure 5.12). These rainfall events are in the ranges of $1 \leq D \leq 79.5\ h$ and $1 \leq E \leq 963.5\ mm$. The graph does not show a clear distinction between triggering and non-triggering rainfall events, thus the application of conventional methods for the definition of a rainfall threshold is extremely difficult and a probabilistic approach seems to be more appropriate. The probabilistic analyses have been performed grouping SLEs and ALEs in a unique dataset (ALEs affecting several territorial units have been preliminarily separated and distributed among the territorial units where they occurred).

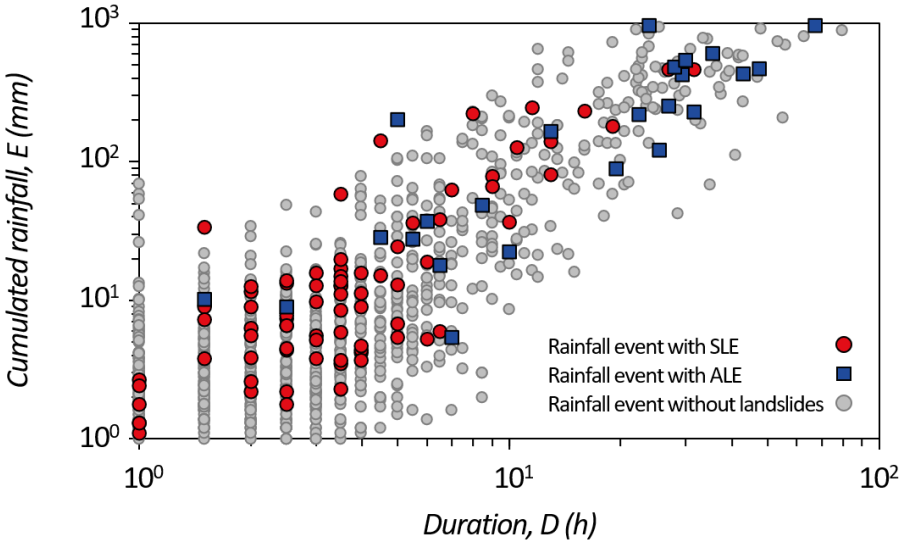

Figure 5.12 Rainfall duration *(D)* vs. cumulated rainfall *(E)* in Emilia-Romagna from March 2014 to December 2015. Red circles are 78 *ED* rainfall conditions associated with the triggering of SLEs. Blue squares are the 24 *ED* rainfall conditions associated with the triggering of ALEs. Grey circles are 927 *ED* rainfall conditions for which information on triggered landslides is not available. Data are in log-log coordinates

5.5.4 Calibration of the model

The definition of the probabilistic warning model is based on a two-dimensional Bayesian analysis to evaluate the conditional probability of landslide occurrence given the joint probability of two rainfall parameters (*D* and *E*). Following the procedure described in Section 5.4, equation *(5.2)* has been applied in order to compute the prior landslide probability, *P(L)* using the data reported in Section 5.5.3:

$$P(L) = \frac{N_L}{N_R} = \frac{102}{1029} = 0.10$$

Then, the *DE* plane reported in Figure 5.12 has been divided in 6x10 cells, a reasonable compromise between the resolution of the rainfall parameters and the numerosity of the rainfall events in each class. Figure 5.13 displays the posterior landslide probabilities, *P(L|D,E)* calculated applying equation *(5.1)*.

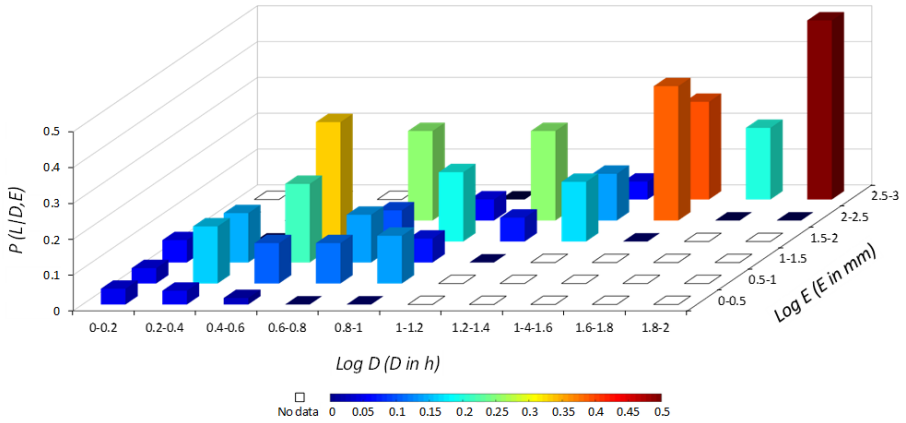

Figure 5.13 Histogram of posterior landslide probability, *P(L|D,E)* as a function of duration *(D)* and cumulated rainfall *(E)*

The rainfall conditions that resulted in landslides (i.e., posterior probability greater than zero) are concentrated in groups of cells. In particular, the landslide probability generally increases with both duration and cumulated rainfall. Indeed, the maximum value (0.50) is reached for rainfall events represented by the highest classes of both duration $(1.8 \leq log(D) \leq 2)$ and cumulated rainfall $(2.5 \leq log(E) \leq 3)$. However, a secondary peak can also be observed for rainfall events characterized by short-duration

and high-accumulation ($0.4 \leq log(D) \leq 0.8;\ 2.5 \leq log(E) \leq 3$). The "no landslides" combinations (dark blue cells in Figure 5.13) embed all the rainfall conditions for which $P(L|D,E) = 0$, because no landslide events are reported in the FraneItalia catalog $(N_{(D,E)} = 0)$. Moreover, a number of rainfall conditions (mainly short-duration, high-accumulation and very long-duration, low- to moderate-accumulation) have never been recorded (white cells in Figure 5.13).
Successively, the posterior landslide probabilities have been interpolated onto a 2D plot so that the probabilities across the log-log plane can be better visualized. Figure 5.14 confirms that long-duration, high-accumulation rainfall events show the highest landslide probabilities $(P(L|D,E) = 0.2)$. Besides, three secondary peaks $(P(L|D,E) > 0.2)$ can be also observed: two of them in the proximity of the main peak and another in correspondence of short-duration, middle-accumulation rainfall events. This could suggest that two different types of rainfall events are more likely to trigger landslides.

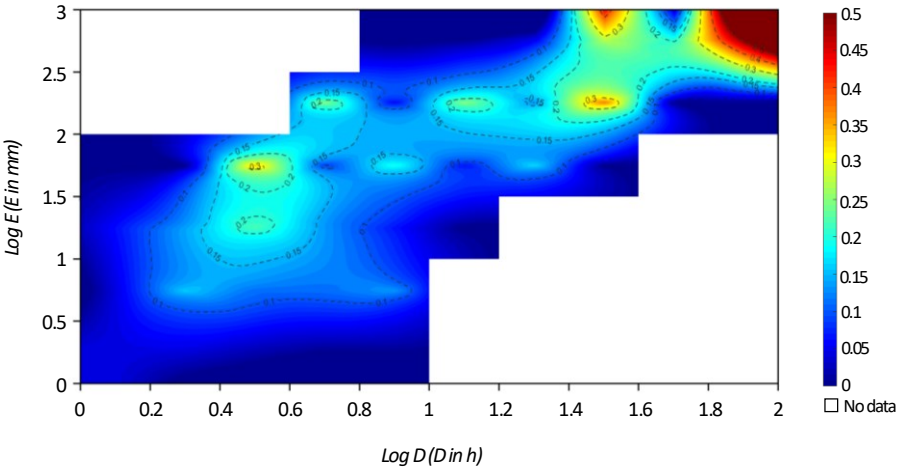

Figure 5.14 Posterior landslide probabilities obtained considering the rainfall events reported in Figure 5.12. Lines of equal probability are also drawn

Landslide probabilities have been further processed in order to draw lines of roughly equal landslide probability (i.e., isolines) in the log-log plane. They represent rainfall events characterized by different duration and magnitude, which result in the same probability of landslide occurrence and can be used as thresholds for early warning purposes. To this aim,

Berti et al. (2012) stated that a reasonable criterion for setting the threshold would be the observation of an abrupt increase in the probability of failure, which indicates a radical change in the state of the system. In this case, $(P(L|D,E) = 0.15)$ can be considered as an appropriate threshold, because above this line the landslide probability rapidly increases for different ranges of duration and cumulated rainfall.

5.5.5 Comparison with other regional thresholds in Emilia-Romagna

For validation purposes, the new probabilistic rainfall threshold obtained has been quantitatively compared with other *ED* rainfall thresholds defined for the same region: the environmental thresholds defined by Peruccacci et al. (2017) and the regional threshold derived by the probabilistic model developed by Berti et al. (2012).
Peruccacci et al. (2017) defined regional thresholds for Italy considering environmental subdivisions based on topography, lithology, land-use, land cover, climate, and meteorology. Threshold curves are represented by power law equations linking E (in mm) to D (in h):

$$E = (\alpha \pm \Delta\alpha) \times D^{(\gamma \pm \Delta\gamma)} \qquad (5.5)$$

where a is a scaling parameter (the intercept), γ is the slope (the scaling exponent) of the power law curve, and Δa and $\Delta\gamma$ are the uncertainties associated to a and γ, respectively. Table 5.4 reports the main characteristics of the environmental thresholds determined for Emilia-Romagna, calculated at 5% exceedance probability.

Table 5.4 Environmental *ED* thresholds for the Emilia-Romagna region defined by *Peruccacci et al. (2017)*

Environmental information	Code	Threshold	Label
Topographic provinces	P4	$E = (8.6 \pm 0.5) \times D^{(0.36 \pm 0.01)}$	$T_{5,P4}$
Lithological complexes	PO	$E = (8.2 \pm 0.7) \times D^{(0.35 \pm 0.02)}$	$T_{5,PO}$
Lithological complexes	TC	$E = (9.0 \pm 0.8) \times D^{(0.37 \pm 0.02)}$	$T_{5,TC}$
Pedological regions	B	$E = (8.3 \pm 0.9) \times D^{(0.38 \pm 0.02)}$	$T_{5,B}$
Pedological regions	C	$E = (14.8 \pm 3.2) \times D^{(0.26 \pm 0.05)}$	$T_{5,C}$
CORINE Land Cover classes	FA	$E = (6.9 \pm 0.5) \times D^{(0.45 \pm 0.02)}$	$T_{5,FA}$
Köppen-Geiger climate regions	Cfa	$E = (7.8 \pm 0.7) \times D^{(0.41 \pm 0.02)}$	$T_{5,Cfa}$
Mean annual precipitation (MAP) regions	LO	$E = (7.9 \pm 0.4) \times D^{(0.37 \pm 0.01)}$	$T_{5,LO}$
Mean annual precipitation regions	HI	$E = (8.9 \pm 1.3) \times D^{(0.43 \pm 0.03)}$	$T_{5,HI}$

← Legend: P4: Apennine mountain system; PO: Post-orogenic sediment; TC: Terrigenous complex; B: Soil of the Apennines with temperate climate; C: Soil of the hills of northern Italy; FA: Forested and semi-natural area; Cfa: Temperate climate without dry season and with hot summer; LO: Low, 800 < MAP ≤ 1200 mm; HI: High, 1600 < MAP ≤ 2000 mm

Moreover, by analyzing the outputs of the probabilistic model developed by Berti et al. (2012), Peruccacci et al. (2017) derived an additional *ED* threshold *($T_{5,R}$)* described by the following power law:

$$E = (12.6 \pm 1.1) \times D^{(0.38 \pm 0.05)} \quad (5.6)$$

Figure 5.15 displays in a log-log plane the rainfall conditions occurred in the period of analysis, the probabilistic thresholds defined in Section 5.5.4 *($T_{15,P}$)* and the regional thresholds reported in literature. For the environmental thresholds defined by Peruccacci et al. (2017) only the lower *($T_{5,LE}$)* and the upper envelope *($T_{5,UE}$)* are reported. It should be stressed that the direct comparison of these regional thresholds is not appropriate, as they were defined using different methods and techniques, different landslide and rainfall information, and adopting different criteria to identify rainfall conditions that resulted in landslides. Considering these limitations, a back analysis has been carried out using the same rainfall and landslide datasets employed for the calibration phase in order to perform a quantitative comparison of the three approaches. To this aim, thresholds have been considered as binary classifiers of rainfall conditions that may result (or not result) in landslides. Adopting this assumption, a set of contingencies scores derived by standard contingency tables has been considered (Wilks 1995). A "true positive" *(TP)* refers to a *(D,E)* pair located above the threshold and resulted in (at least) one landslide; a "true negative" *(TN)* is a *(D,E)* point below the threshold that did not result in landslides; a "false positive" *(FP)* occurs when a *(D,E)* rainfall condition exceeded the threshold and landslides did not occur; a "false negative" *(FN)* occurs when a *(D,E)* rainfall condition were below the threshold and landslides occurred. Table 5.5 summarizes the four contingencies scores *(TP, TN, FP, FN)* for the different thresholds defined for Emilia-Romagna. The probabilistic threshold *($T_{15,P}$)* allows maximizing the number of *TP* (78), concurrently not increasing excessively the number of *FP* (217) with respect to the other thresholds. Although *($T_{5,UE}$)* and $T_{5,R}$ show the lowest values of *FP* (203 and 212, respectively), they miss a relevant number of landslide events (65 and 64, respectively). On the contrary, $T_{5,LE}$ results in a relevant number of *FP* (about 50% higher than the probabilistic threshold).

Concluding, the overall good performance of $T_{15,P}$ can be explained taking into account that it is more flexible than conventional thresholds typically represented by linear classifiers. This feature could be extremely useful in areas where slope response to rainfall is quite complex, i.e., when landslides are triggered by different rainfall conditions. Moreover, the probabilistic threshold can be easily updated as new landslide and rainfall data become available.

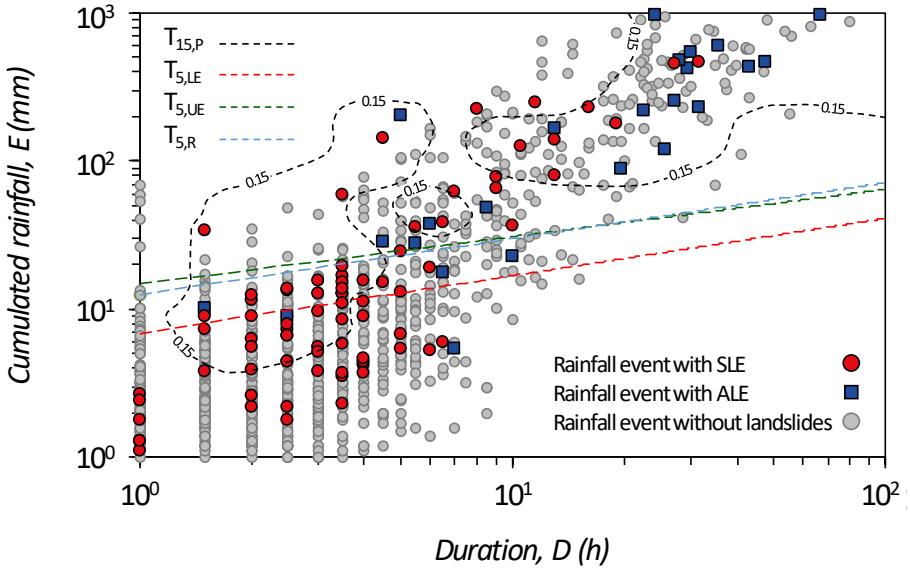

Figure 5.15 Comparison between the probabilistic threshold *($T_{15,P}$)* and the other rainfall thresholds reported in the literature for Emilia-Romagna in the log-log *DE* plane. Triggering and non-triggering rainfall conditions are also reported

Table 5.5 Contingencies scores calculated for the probabilistic threshold *($T_{15,P}$)* and for the other thresholds proposed in the literature for Emilia-Romagna. Best values are shown in italics

Threshold	Label	TP	FN	FP	TN
Probabilistic threshold	$T_{15,P}$	*78*	*24*	217	710
Environmental thresholds – LE *(Peruccacci et al. 2017)*	$T_{5,LE}$	58	44	320	607
Environmental thresholds – UE *(Peruccacci et al. 2017)*	$T_{5,UE}$	37	65	*203*	*724*
Regional threshold *(Berti et al. 2012)*	$T_{5,R}$	38	64	212	715

5.6 CASE STUDY 2: CAMPANIA REGION, ITALY

5.6.1 Study area

The Campania region in southern Italy extends from the Tyrrhenian Sea to the Southern Apennine Chain, covering about 13,500 km^2 and including 551 municipalities. The orographic setting is characterized by the presence of a central mountain ridge made up mainly of Mesozoic carbonates, elongated for more than 200 km in a NW–SE direction, with maximum peaks reaching 2000 m a.s.l. Strong volcanic activity was registered in the coastal plain with the growth of the Somma–Vesuvius and the Campi Flegrei volcanoes in the late Quaternary. Therefore, the landscape of the western portion of Campania is characterized by a wide flat area with isolated volcanic reliefs and islands. On the eastern side of the region, the carbonate ridges transition to hilly landscapes of lower elevation, mainly formed by Miocene and Pliocene flysch successions. In the remaining hilly part, stream catchments present lower mean longitudinal profiles, and wide alluvial plains linked to perennial river systems prevail (Vennari et al. 2016). The climatic regime is humid temperate with mean annual precipitation ranging from 1000 to 2000 mm (Longobardi et al. 2016). Due to the rugged topography of the region, severe storms are frequent in the region and result in abundant flash floods, debris flows and shallow landslides (Cascini et al. 2008), which may result in severe casualties as well as serious damage to urban areas and infrastructures (Piciullo et al. 2017b). Indeed, in the 50-year period 1950–2017, 288 persons were killed or went missing, 408 were injured, and more than 23,000 people were evacuated due to landslides in the region (http://polaris.irpi.cnr.it).

In Campania, a regional landslide early warning system has been designed and managed by the regional civil protection agency to deal with "hydraulic and geo-hydrological risks" (DPGR 299/2005). The strategy implemented within the system can be schematized into two main phases: wheatear forecast and environmental monitoring (Pecoraro and Calvello 2016). The first phase consists in issuing warnings based on the evaluation of possible consequences of hazardous hydrogeological phenomena, whose occurrences is predicted via numerical rainfall forecasts. To this aim, the Campania region is subdivided into eight warning zones for weather forecast and early warning purposes, according to homogeneity criteria, considering the following factors: hydrography, morphology,

precipitation regime, geology, land-use, hydraulic and hydrogeological events, and administrative boundaries. The second phase includes (i) the evaluation of meteorological and hydrological events and (ii) the hydrological and weather forecast at time intervals of 6 hours, through nowcasting techniques and rainfall-runoff modelling using real-time parameters. The environmental monitoring network encompasses 154 weather stations—14 of them located outside the boundaries of the Campania region—and a meteorological radar (Figure 5.16).

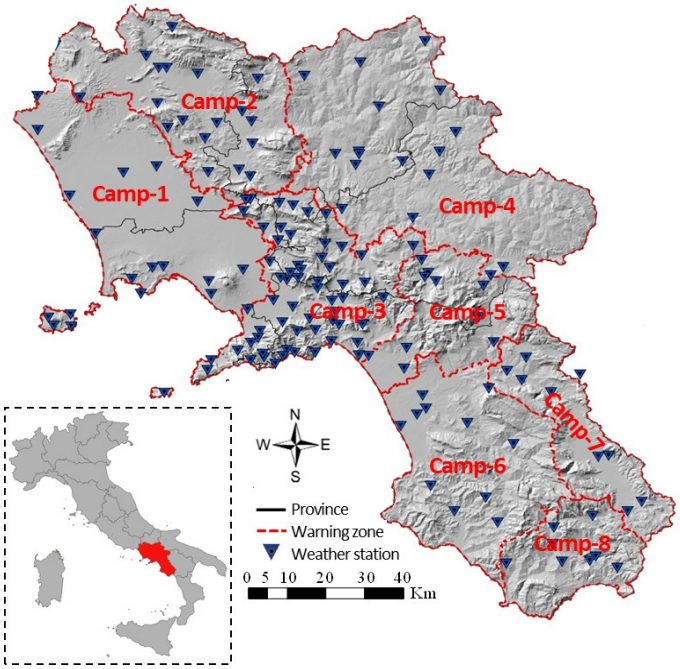

Figure 5.16 Warning zones and weather stations of the Campania region

5.6.2 Territorial units and available datasets

The eight weather warning zones defined by the regional civil protection agency (see Figure 5.16) have been identified as the most appropriate territorial units for the Campania region. This can be justified by the same reasons already reported for the Emilia-Romagna region in Section 5.5.2 (i.e., meteorological and hydrogeological homogeneity of weather warning zones, spatial accuracy of landslide records, and spatial discretization of rainfall measurements).

The dataset used for the Campania region includes data on landslide occurrences and satellite rainfall estimates from March 2014 to December 2017, derived from the same sources of information used for the Emilia-Romagna region.
Regarding landslide events, the FraneItalia database lists 151 events in Campania in the period of analysis. Eight records have not been included in the dataset: five of them were not triggered by weather conditions and the remaining three are classified as landslides in rock. Figure 5.17 reports the 143 rainfall-induced landslides considered for the analyses, differentiated between SLEs (124) and ALEs (19).

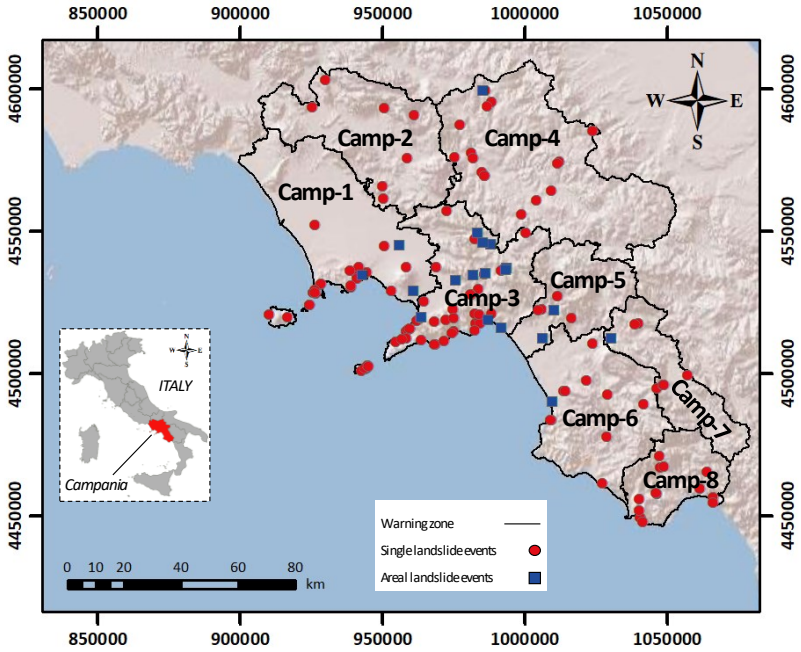

Figure 5.17 Shaded relief map of the eight warning zones of the Campania region showing the 143 rainfall-induced "FraneItalia" landslide records from March 2014 to December 2017, differentiated in single (red circles) and areal landslide events (blue squares). The inset shows the location of the Campania region in Italy

Camp-3 was the most affected warning zone, both in terms of single (38) and areal landslide events (11). This area is highly susceptible to shallow rainfall-induced landslides and debris flows, due to the presence of pyroclastic soil deposits mantling the carbonatic bedrock (Cascini et al.

2008). Indeed, it suffered some of the most catastrophic rainfall-induced landslide events in Europe, e.g., the events that occurred on 4–5 May 1998 over the slopes of the Pizzo d'Alvano massif (Piciullo et al. 2017b). *Camp-1* also experienced a significant number of landslide events (29 SLEs and 3 ALEs), mainly in the southern part characterized by the same geological context of *Camp-3*. Besides, a number of SLEs occurred over the slopes of the Apennines Chain in the north-eastern part of the region (*Camp-2* and *Camp-4*) and in correspondence of the Cilento mountains in the southern part (*Camp-6, Camp-7,* and *Camp-8*). The 143 rainfall-induced landslides in Campania have been divided into two subsets: (i) a calibration set, listing 98 landslide events that occurred between March 2014 and December 2016, used to define the probabilistic warning model, and (ii) a validation set, listing 45 landslide events that occurred in 2017, used to validate the model.

Regarding the satellite rainfall measurements, the IMERG precipitation data have been acquired from the database available in Google Earth Engine and the mean values at hourly temporal resolution have been calculated over each territorial unit of the Campania region, following the same procedure adopted for the Emilia-Romagna region.

5.6.3 Correlation between landslides and rainfall events

The methodology adopted for the definition of the correlation between landslides and rainfall events in Campania is similar to that described for Emilia-Romagna (see Section 5.5.3) and can be schematized into two main phases: the reconstruction of the rainfall events and the identification of triggering and non-triggering rainfall events. Duration *(D)* and cumulated rainfall *(E)* have been identified again as the most appropriate rainfall parameters, taking into account the types of landslides considered as well as the temporal accuracy of both the landslide and the rainfall datasets. The "algorithmic" approach developed by Melillo et al. (2015) has been applied to reconstruct the rainfall events and to identify triggering and non-triggering rainfall conditions. A reduced set of parameters to account for different physical settings and operational conditions has been considered. In particular, all the parameters are differentiated considering the "warm" springer-summer period, C_W, and the "cold" autumn-winter period, C_C (Table 5.6).

Table 5.6 Parameters used for the application of the algorithm developed by *Melillo et al. (2015)*

Step	Parameter name	Parameter value		Unit
		C_W	C_C	
S_0	G_S	0.2	0.2	mm
S_1	E_R	0.2	0.2	mm
S_1	P_1	3	6	h
S_2	P_2	6	12	h
S_3	P_3	1	1	mm
S_4	P_4	48	96	h

Parameters G_S, E_R and P_3 correspond to cumulated rainfall quantities, which are removed from the rainfall series under specific conditions described in the text. Parameters P_1, P_2 and P_4 are time intervals used to remove irrelevant amount of rain and to reconstruct the rainfall sub-events and rainfall events. The parameters in the algorithm depend on the climate period. Two climate periods are considered: C_W, a "warm" spring–summer period, and C_C, a "cold" autumn–winter period

The automated procedure employs the R open-source software (http://www.r-project.org) and is based on several steps. In the pre-processing step *(S_0),* the rainfall records lower than a predefined threshold G_S are considered noise and are set to $E_H = 0.0\ mm$. The remaining steps are differentiated into two main logical blocks. The first block performs the automatic reconstruction of the rainfall events and can be schematized in the following four steps: *(S_1)* detection of the isolated rainfall events considering a dry interval, P_1 and exclusion of irrelevant events that do not exceed a predefined threshold E_R (Figures 5.18a,b); *(S_2)* identification of rainfall sub-events proceeded and followed by dry periods with no rain, P_2 (Figure 5.18c); *(S_3)* exclusion of irrelevant sub-events, whose cumulated (total) rainfall, E_S is lower than a given threshold P_3 (Figure 5.18d); *(S_4)* identification of rainfall events, constituted either by a period of continuous rainfall or by an ensemble of periods considering a minimum dry period, P_4 (Figure 5.18e). Successively, in the second block the algorithm combines information on temporal occurrence of rainfall events and landslide events, performing three additional steps: *(S_5)* selection of triggering and non-triggering rainfall events (Figure 5.19a); *(S_6)* reconstruction of multiple aggregations of rainfall sub-events that are likely to trigger landslides (Figure 5.19b); *(S_7)* reconstruction of multiple aggregations of rainfall sub-events that did not trigger landslides (Figure 5.19c). All the triggering and non-triggering sub-events identified by the algorithm are equally possible. The second block has been slightly modified in order to reconstruct also the multiple aggregations of non-triggering rainfall sub-events, not provided in the original algorithm.

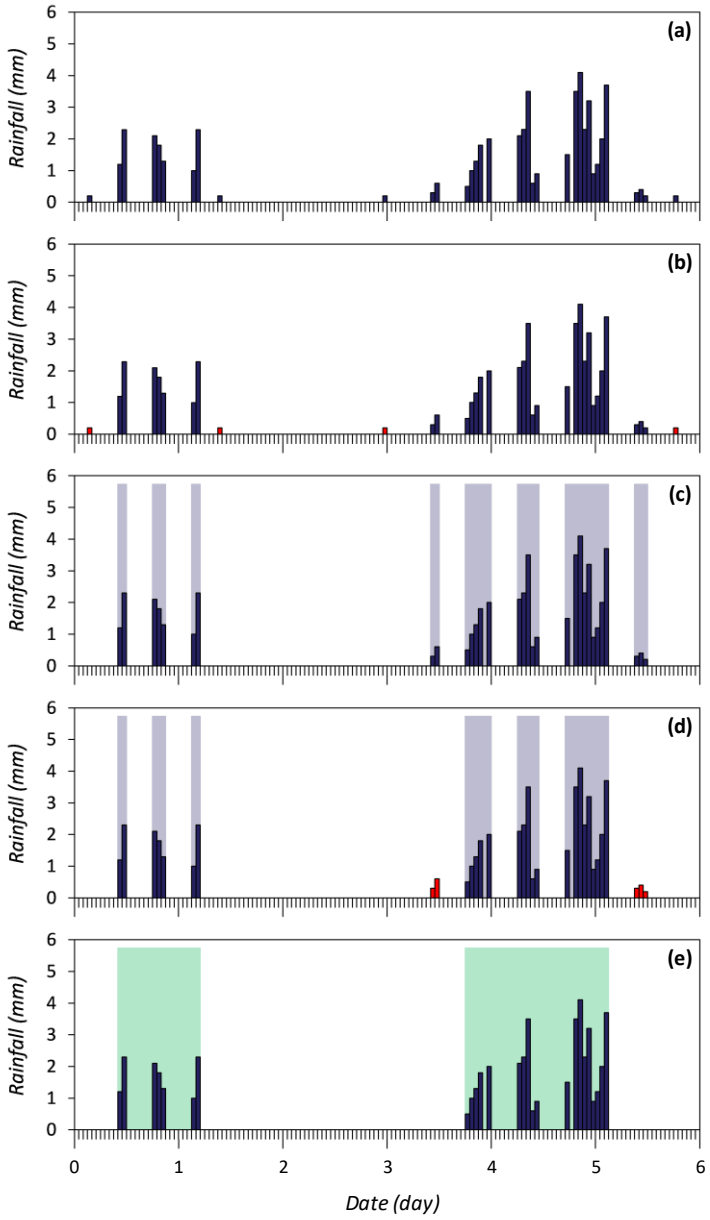

Figure 5.18 Example of the application of the automated algorithm for the reconstruction of rainfall events. a) Collection of hourly rainfall measurements (blue bars). b) Exclusion of the irrelevant isolated rainfall events (red bars). c) Identification of the rainfall sub-events (highlighted by blue-shaded areas). d) Selection of irrelevant sub-events (red bars). e) Identification of rainfall events (highlighted by green-shaded areas)

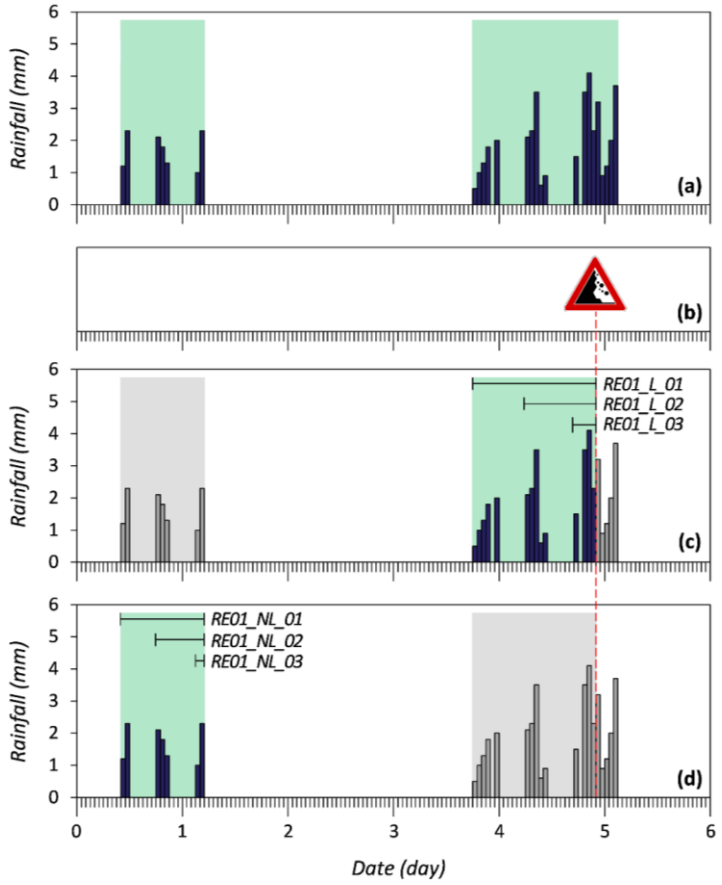

Figure 5.19 Example of the application of the automated algorithm for the reconstruction of rainfall events. a) Rainfall measurements (blue bars) and rainfall events identified by the first logical block of the algorithm (highlighted by green-shaded areas). b) Identification of landslide events (highlighted by the warning sign). c) Identification of the possible rainfall combinations for a triggering rainfall event (highlighted by green-shaded area). d) Identification of the possible rainfall combinations for two non-triggering rainfall events (highlighted by green-shaded areas)

Following this approach, 3431 rainfall conditions *(D,E)* have been reconstructed and plotted in log-log coordinates (Figure 5.20). The 479 rainfall conditions responsible for the triggering of 124 SLEs (red circles in Figure 5.20) and the 76 rainfall conditions responsible for 19 ALEs (blue squares in Figure 5.20) are in the range of duration $1 \leq D \leq 748\ h$ and in the range of cumulated rainfall $0.26 \leq E \leq 1916.74\ mm$. Of

course, the non-triggering rainfall conditions reconstructed in the same period are 2876 (grey circles in Figure 5.20). They are in the ranges of $1 \leq D \leq 1433\ h$ and $0.20 \leq E \leq 2096.98\ mm$. Due to the absence of a clear distinction between triggering and non-triggering rainfall conditions, also in this case a probabilistic analysis has been carried out to highlight rainfall conditions critical for landslide occurrence. To this aim, SLEs and ALEs have been grouped in a unique dataset (ALEs affecting several territorial units have been preliminarily separated and distributed among the territorial units where they occurred).

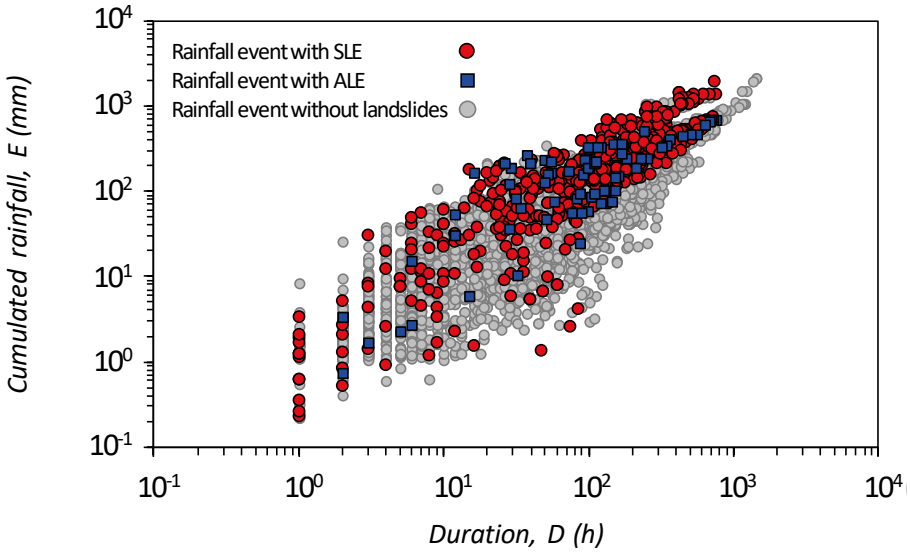

Figure 5.20 Rainfall duration *(D)* vs. cumulated rainfall *(E)* in Campania from March 2014 to December 2017. Red circles are 479 rainfall conditions associated with the triggering of SLEs. Blue squares are the 76 rainfall conditions associated with the triggering of ALEs. Grey circles are 2876 rainfall conditions for which information on triggered landslides is not available. Data are in log-log coordinates

5.6.4 Calibration of the model

The definition of the probabilistic warning model for this case study has been developed considering the calibration dataset defined in Section 5.6.2 comprising 98 landslide events and 824 rainfall events from Mach 2014 to

December 2016. According to the available data, the prior landslide probability, *P(L)* has been calculated as follows (equation *5.2*):

$$P(L) = \frac{N_L}{N_R} = \frac{98}{824} = 0.12$$

By applying the automated procedure described in Section 5.6.3, 431 triggering and 2255 non-triggering rainfall conditions have been identified. Once again, a Bayesian approach aimed at estimating the conditional landslide probability for different classes of D and E has been adopted. The marginal probability, *P(D,E)* and the likelihood, *P(D,E|L)* have been determined considering that the triggering and non-triggering rainfall conditions are expressed in terms of multiple combinations:

$$P(D,E) = \frac{\sum_i n_{i,(D,E)} \times f_i}{N_R} \quad (5.3')$$

$$P(D,E|L) = \frac{\sum_i n_{i,(D,E|L)} \times f_i}{N_L} \quad (5.4')$$

where: $n_{i,(D,E)}$ is the number of possible rainfall conditions characterized by specific values of D and E; $n_{i,(D,E|L)}$ is the number of rainfall events characterized by specific values of D and E that resulted in landslides; f_i is the relative frequency, defined as the inverse of the total number of possible aggregations of sub-events for a given rainfall event, n_{ss}; N_R and N_L are the total numbers of rainfall and landslide events, respectively.

Successively, the log-log plane represented in Figure 5.20 has been divided in 10x10 cells and the posterior landslide probability, *P(L|D,E)* has been calculated applying the equation *(5.1)* to each class. The 2D plot reported in Figure 5.21 highlights two main peaks of landslide probability, with maximum values higher than 0.70 in both the cases. This could suggest that two types of rainfall conditions are more likely to trigger landslides: long-duration $(2 \leq log(D) \leq 3)$ high-accumulation $(2.5 \leq log(E) \leq 3.5)$; and short-duration $(0 \leq log(D) \leq 1)$ high-accumulation $(-0.5 \leq log(E) \leq 0)$. This is probably due to the heterogeneity of the calibration dataset. Indeed, although all the records refer to shallow rainfall-induced landslides, they significantly differ in terms of triggering mechanism (different rainfall conditions lead to landslide initiation) and magnitude (both single and areal events have been grouped in the dataset). The duration of the rainfall events recorded in the period of analysis varies from 1 h $(log(D) = 0)$ to 1000 h $(log(D) = 3)$. This could indicate a

specific range of duration for possible landslide initiation, although more observations are needed to support this statement.
Figure 5.21 also displays a series of isolines (i.e., lines of roughly equal posterior probability), which allows better identifying relevant variations in the landslide probabilities. Indeed, as demonstrated in Section 5.5.4, a reasonable criterion for setting a probabilistic threshold could be an abrupt increase in landslide probability. Following this criterion, six possible thresholds have been proposed corresponding to posterior landslide probabilities varying from 0.05 to 0.5.
Threshold values higher than 0.5 have been not considered because they would result in a relevant number of missed events, a significant drawback for thresholds employed in an operative LEWS.

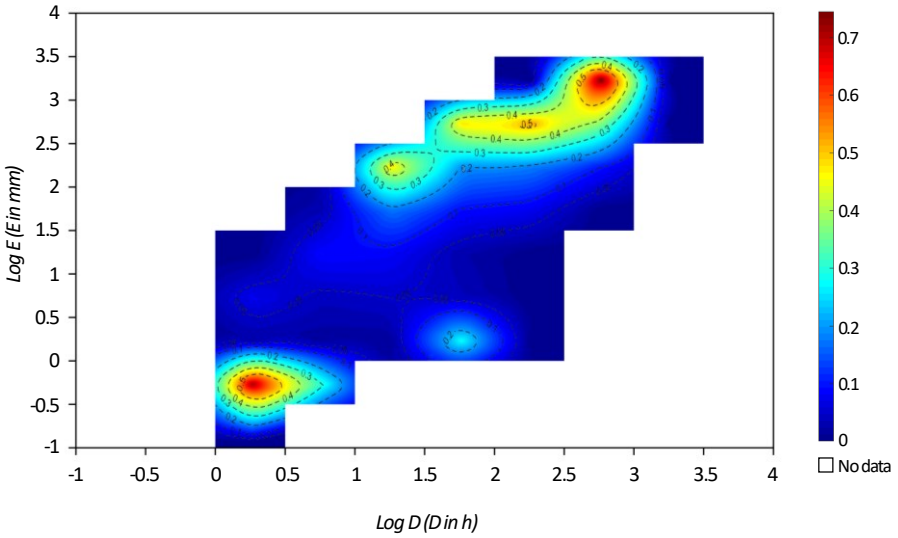

Figure 5.21 Posterior landslide probabilities obtained considering the rainfall events reported in Figure 5.20. Lines of equal probability are also drawn

5.6.5 Validation of the model

The probabilistic thresholds defined in this study have been validated using 45 landslide events and 311 rainfall events, from which 118 triggering and 621 non-triggering rainfall conditions have been identified (see Sections 5.6.2 and 5.6.3). For validation purposes, the method proposed by Gariano et al. (2015) that exploits a contingency table, a

receiver operating characteristic (ROC) analysis (Metz 1978) and the related skill scores has been adopted.
The contingencies scores *(TP, TN, FP, FN)* have been derived by standard contingency tables similarly to the procedure adopted in Section 5.5.5. Usually, the four possible outcomes of the contingency tables are computed aggregating the *(D,E)* data points by comparing the event occurrences and the model predictions. Conversely, for this case study the rainfall conditions used for computing the contingency table are characterized by a certain probability of occurrence (varying from 0 to 1 depending on the number of possible aggregations), thus the contingencies scores have been calculated aggregating their relative frequencies.
By combining *TP, TN, FP,* and *FN,* four skill scores have been calculated, namely: (i) the probability of detection score, $POD = \frac{TP}{TP+FN}$, (ii) the probability of false detection score, $POFD = \frac{FP}{FP+TN}$, (iii) the probability of false alarm score, $POFA = \frac{FP}{TP+FP}$, and (iv) the Hanssen and Kuipers (1965) skill score, $HK = \frac{TP}{TP+FN} - \frac{FP}{FP+TN} = POD - POFD$.
The ROC analysis has been performed constructing a ROC plot that shows *POD* against *POFD*. In the ROC plane, each point represents the predictive capability of a single probabilistic threshold and the ROC curve is obtained varying the landslide probability associated to the rainfall threshold. The best prediction performance corresponds to the upper left corner of the ROC plot (perfect classification). A meaningful indicator for describing the threshold performance is the Euclidean distance δ between the point representing the threshold on the ROC curve and the perfect classification point. A random guess would give a point along the "no gain" line, the diagonal line from the left bottom to the top right corners of the ROC plot. In particular, the shorter the distance δ, the more reliable is the threshold and, consequently, the higher the warning model prediction skill.
Figure 5.22 shows the ROC curve for the 6 considered thresholds. Each blue dot represents a threshold determined for a different posterior landslide probability. For the 6 *(POD, POFD)* pairs, the Euclidean distance δ from the perfect classification (red dot in Figure 5.22) has been calculated. Table 5.7 summarizes the four contingencies *(TP, FP, FN, TN)* and the four skill scores *(POD, POFD, POFA, HK)* for the six probabilistic thresholds. Among them, $T_{5,P}$ exhibits the highest *POD* (i.e., a low number

of *FN*), yet it also shows the highest *POFD* and *POFA* (i.e., a significant number of *FP*). On the contrary, thresholds defined with $P(L|D,E) \geq 0.2$ are characterized by a low number of *TP* (i.e., values from 13.67 to 3.50). In general, the highest value for HK and the lowest values for *POFA* and δ were obtained by $T_{10,P}$ that can be considered the optimal threshold, representing the best compromise between the minimum number of incorrect landslide predictions *(FP, FN)* and the maximum number of correct predictions *(TP, TN)*. It is worth mentioning that a further improvement for the probabilistic warning model developed herein can be achieved by combining more than one threshold in a multi-level warning model, in relation to the scope and the operational characteristics of the LEWS.

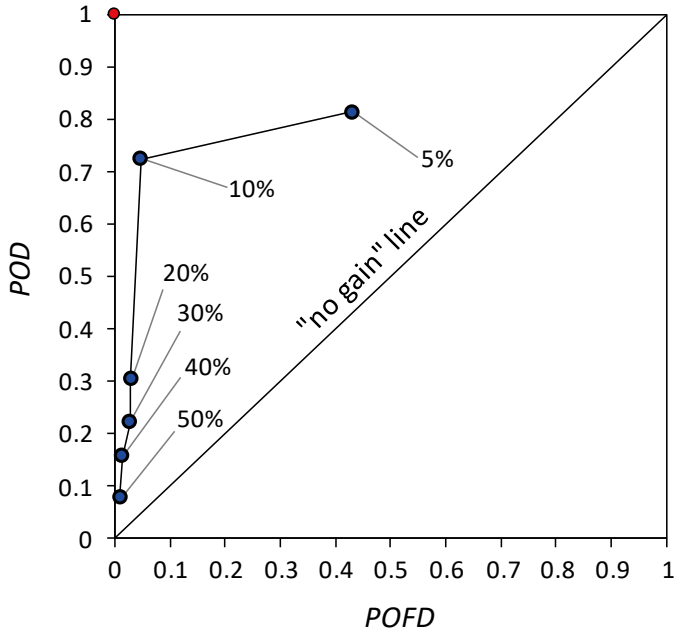

Figure 5.22 ROC curve drawn considering the 6 employed thresholds. Each *POFD-POD* pair (blue dot) corresponds to a threshold defined considering a given probability (label value). The "no gain" line and the perfect classification point (red dot, upper left corner) are also shown

Table 5.7 Contingencies *(TP, FP, FN, TN)* and skill scores (*POD, POFD, POFA, HK, δ)* calculated for the probabilistic thresholds defined herein. Best scores are shown in italics

Label	P(L|D,E)	TP	FN	FP	TN	POD	POFD	POFA	HK	δ
$T_{5,P}$	0.05	36.58	8.42	114.21	151.79	*0.81*	0.43	0.76	0.38	0.47
$T_{10,P}$	0.10	32.58	12.42	12.61	253.39	0.72	0.05	*0.28*	*0.68*	*0.28*
$T_{20,P}$	0.20	13.67	31.33	7.51	258.49	0.30	0.03	0.35	0.28	0.70
$T_{30,P}$	0.30	10.00	35.00	7.18	258.82	0.22	0.03	0.42	0.20	0.78
$T_{40,P}$	0.40	7.08	37.92	3.65	262.35	0.16	*0.01*	0.34	0.14	0.84
$T_{50,P}$	0.50	3.50	41.50	2.32	263.68	0.08	*0.01*	0.40	0.07	0.92

6 APPLICATION OF MULTI-SCALAR WARNING MODEL

The Chapter focuses on the application of the multi-scalar warning model proposed in Section 4.3, which integrates widespread monitoring data and local observations collected at local scale in order to improve the performance of a warning model for weather-induced landslides in Norway. Firstly, Section 6.1 summarizes the main steps necessary for the development of the model. Section 6.2 provides a description of the study area as well as the main characteristics of the Norwegian national LEWS. Section 6.3 presents the 30 test areas selected for the analyses and Section 6.4 shows the results obtained applying the regional warning model. Finally, the calibration and the validation of the multi-scalar warning model are reported in Sections 6.5 and 6.6, respectively.

6.1 MULTI-SCALAR WARNING MODEL: WORKFLOW

The methodology presented in Section 4.3 for the definition of a multi-scalar warning has been specifically adapted to the case study. To this aim, Figure 6.1 presents a flowchart organized in three successive steps: identification of the test areas (Phase I), application of the warning model employed in the Norwegian national LEWS (Phase II), calibration and validation of the multi-scalar warning model (Phase III).

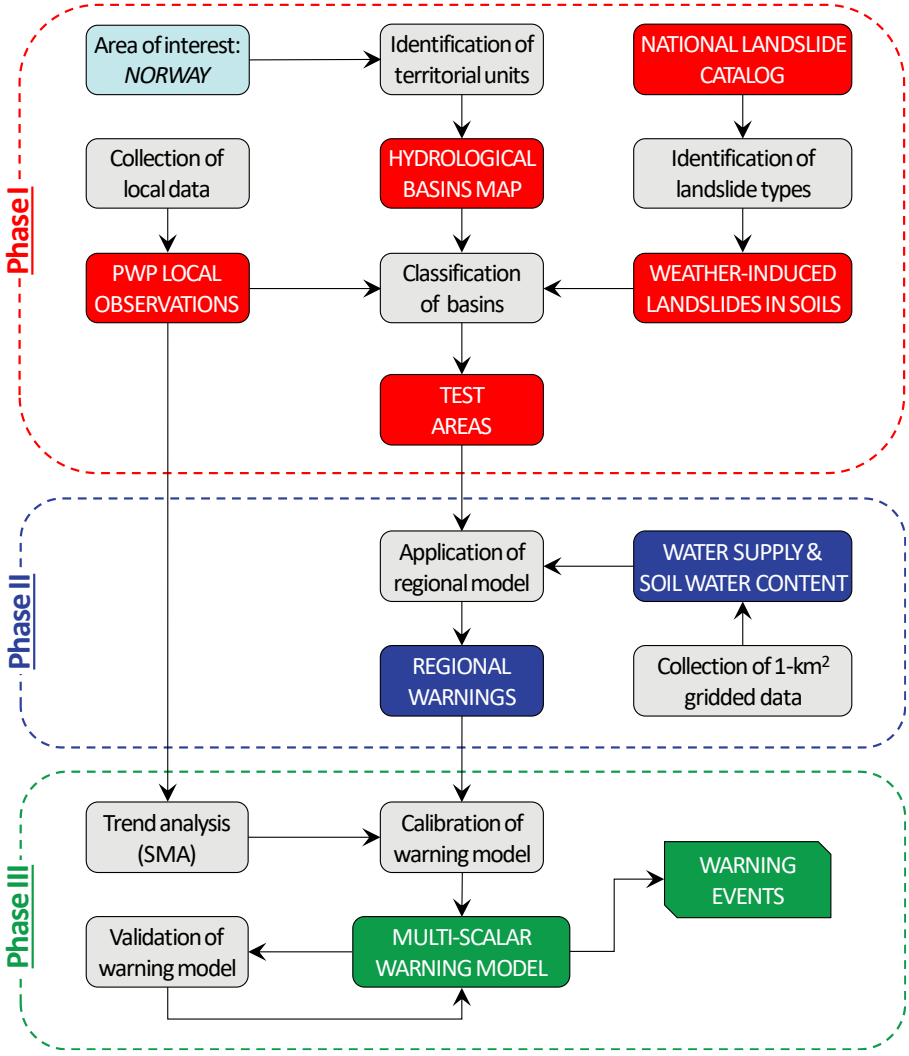

Figure 6.1 Flowchart of the proposed methodology for the definition of a multi-scalar warning model for weather-induced landslides applied to the Norwegian case study

In Phase I, the Norwegian hydrological basins have been identified as the most appropriate territorial units for the purpose of this study. They have been classified according to two main criteria: the occurrence of weather-induced landslides in soils and the availability of a relevant number of pore water pressure observations in the shallow soil layers in the proximity of the landslide source areas. Data on landslide occurrences have been

retrieved from a National landslide catalog containing more than 60,000 entries. The pore water pressure measurements have been collected at local scale from boreholes installed by the Norwegian Geotechnical Institute (NGI) for a variety of geotechnical projects. According to these criteria, 30 territorial units have been selected as potentially useful for the analyses.
In Phase II, the warning model employed in the Norwegian national LEWS has been applied to the 30 selected test areas. The daily combinations of relative water supply and relative soil water content, available as 1-km^2 gridded data, have been compared to the warning levels employed by the regional model. Therefore, for each test area the days with warnings have been identified and, in these cases, the level of warning has been defined.
In Phase III, the warning events issued by applying the regional model have been used for the calibration and validation of the multi-scalar warning model. For calibration purposes, the pore water pressure observations have been preliminarily analyzed in order to determine potential trends adopting a simple moving average (SMA) calculation. Then, the most appropriate indicators have been identified. Finally, the model has been validated using statistical indicators derived from contingency tables.

6.2 CASE STUDY: NORWAY

6.2.1 Physical setting

Norway is divided into 18 counties and 422 municipalities and covers an area of ~ 385,000 km^2 on the western and northern part of the Scandinavian Peninsula. The mainland is characterized by a very elongated shape which stretches from latitude 58°N to more than 71°N (Svalbard north to 81°N), including more than 490,000 km of rivers and streams and about 450,000 lakes. Rivers are relatively short and steep in Western Norway, whereas they are long and gently sloping further south. Approximatively 30% of the land area consists of mountains (with an average elevation of 460 m a.s.l.) and 6.7% of the country is covered by steep slopes. Large areas from the southern tip to the Russian border are

dominated by the Scandinavian Mountains, whose highest peaks reach 2500 m.a.s.l. (Jaedicke et al., 2009). Caledonian orogenesis and later recurring glaciations have created an alpine fjord landscape along most of the Norwegian Atlantic coast. The overall development of the geomorphology can be summarized as erosion process during the late Palaeozoic and Mesozoic, major uplift during the Cenozoic with maximum uplift in the western areas and glacial erosion during the Pleistocene (Etzelmüller et al. 2007). However, the Norwegian landscape has been largely determined by surface processes occurred during the Quaternary era, especially by the action of glaciers, which eroded a lot of bedrock and transported sediments, forming deep valleys, steep mountains and glacial fjords. The country is commonly divided into four physiographic regions: Eastern and Southern Norway (containing extensive areas with forest, gentle valleys and rich arable land); Western Norway (characterized by deep fjords penetrating 200 km inland or more); Central Norway (comprising a gentle landscape with rounded hills and mountains); Northern Norway (consisting of a mixture of valleys, numerous fjords, alpine mountains extending all the way to the coast and many large islands). In geological terms, Norway is situated along the western margin of the Baltic shield covered by Caledonian nappes in the west. The bedrock of the Baltic shield is dominated by Precambrian basement rocks (e.g., granites, gneisses, amphibolites, and meta-sediments) in the southern and south-eastern part of the country (Fredin et al. 2013). Continuous till deposits cover large areas of the valley sides and floors, although fluvial and glaciofluvial deposits as well as marine clays are widespread (Figure 6.2).

The latitudinal elongation, the rugged topography and the exposure to the Atlantic lead to large climatic differences throughout the country. Along the coast, the climate is kept much milder than in other regions by the warm North Atlantic Current of the Gulf Stream. Conversely, inner regions are characterized by a more continental climate. According to the Köppen climate classification, three different climate types can be identified in Norway: warm temperate humid climate (southern regions), cold temperate humid climate (mid and northern regions), and polar climate (northern coastal areas and mountainous regions). Precipitation types can be classified into three main categories: frontal, orographic, and showery. The average annual precipitation is about 1400, yet the distribution is non-uniform throughout the country. In Western Norway, annual precipitation may exceed 5000 mm, mainly concentrated in autumn

and early winter, whereas some valleys in the eastern part receive less than 300 mm per year, mainly in terms of showery precipitation during summer.

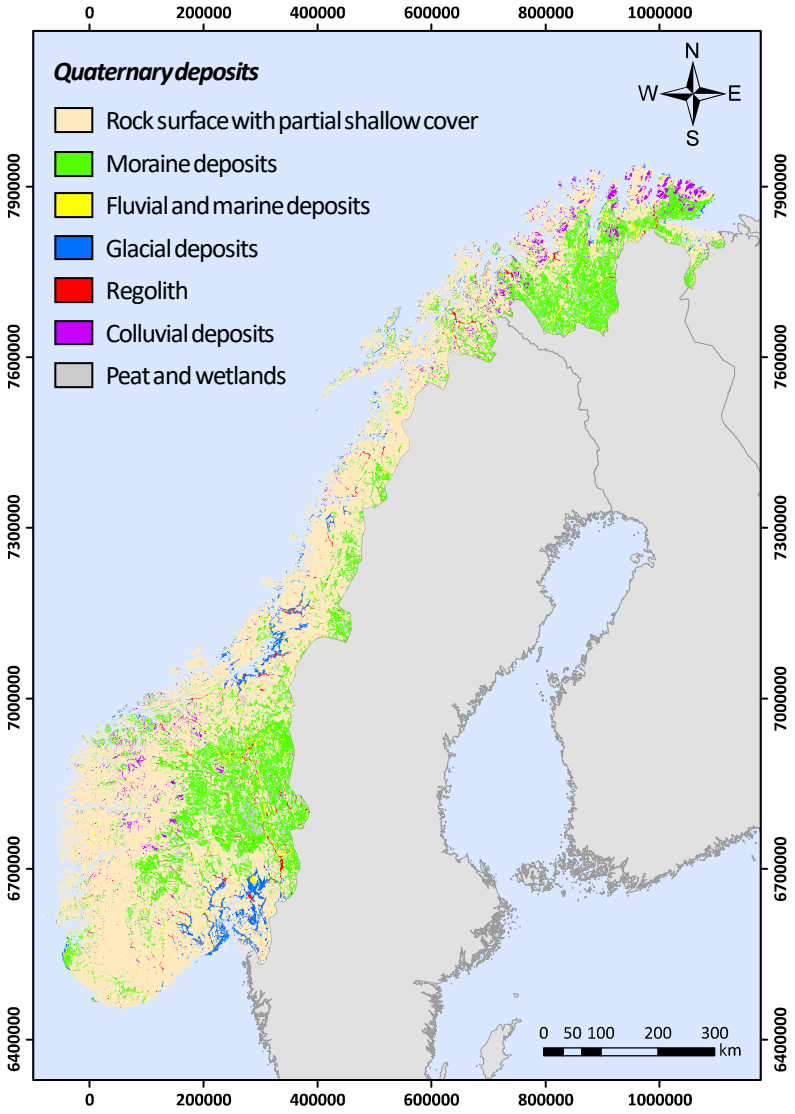

Figure 6.2 Overview of quaternary deposits in Norway. Source: www.ngu.no

Steep slopes, various soil and climatic properties, and the presence of loose sediments provide a basis for the triggering of several types of

weather-induced landslides in soils, including slides in various materials, debris flows, debris slides, slush flows, and shallow landslides (Figure 6.3).

Figure 6.3 Examples of weather-induced landslides in Norway. a) Debris slides and debris flows. Veikledalen, Kvam, June 2011. b) Debris flow. Mjåland, Rogaland, June 2016. c) Flash flood. Notodden, Telemark, July 2011. d) Slushflow. Troms, May 2010 ***(Krøgli et al. 2018)***

Weather-induced landslides are typically triggered by rainfall and snowmelt, or their combination, resulting in intense or long-duration water supply and high soil water content. In these conditions soil cohesion decreases significantly, increasing the probability of landslide occurrence. Steep slopes covered by Quaternary loose sediments are highly exposed to landslide risk, yet landslide may also occur in gentle slopes covered by snow as well as in embankments along roads and railways. In addition, some events are triggered from or initiated as rockfalls or slush flows, developing into, for example, debris flows as they propagate downslope (Piciullo et al. 2017a). Although shallow landslides constitute a substantial threat to Norwegian society, there are limited comprehensive estimates of human and economic losses (Krøgli et al. 2018). According to Furseth

(2006), at least 230 fatalities can be associated to such slope failures over the last 500 years. A recent report prepared by Haque et al. (2016) showed that 12 people died in Norway in the period 1995-2016 because of weather-induced landslides (slush flows in 7 cases and debris flows or debris avalanches in the remaining 5 cases). Economic consequences are mainly associated to disruption of road and railway networks, although there are no reliable estimates of the total cost to society of weather-induced landslides. Furthermore, according to the Intergovernmental Panel on Climate Change (Hanssen-Bauer et al. 2017) the number of annual landslide events in Norway is expected to increase as the Northern Europe will probably experience higher intensity and frequency of heavy precipitation in the future.

6.2.2 The national LEWS

In 2009, the Norwegian Water Resources and Energy Directorate (NVE) started developing a national LEWS as part of a national programme for landslide risk management. The main aim of the system is to analyze and forecast extreme hydro-meteorological conditions, in order to warn appropriately and in time the authorities about the possible occurrence of catastrophic shallow landslides, such as debris flows, debris slides, debris avalanches and slush flows. The system was officially launched in the autumn of 2013, as a joint initiative across public agencies between NVE, the Norwegian Meteorological Institute (MET), the Norwegian Public Road Administration (NPRA), and the Norwegian Rail Administration (Bane NOR). The service is operative year-round performing daily a landslide hazard assessment at a regional level (i.e., for a county and/or group of municipalities). Predictions of the systems are based on the forecasting of hydro-meteorological conditions responsible for landslides initiation. Because of the sparse monitoring network and the relative short measurement periods, a distributed version of the hydrological HBV model (Beldring et al. 2003) has been employed to describe the water balance on a national scale. Therefore, Norway has been divided into more than 385,000 1-km^2 grid cells and each cell is treated as a separate basin in order to simulate water balance. In particular, the model uses rainfall and temperature as input data and simulates a number of hydro-meteorological parameters, such as: runoff, snowmelt, groundwater, soil saturation, and frost depth. In the development phase of the EWS, hazard threshold levels were calibrated through a statistical analysis of historical landslides and

different hydro-meteorological conditions. The thresholds currently adopted in the EWS were proposed by Colleuille et al. (2010), by combining simulations of water supply (rainfall and snowmelt) and soil water content (both expressed as relative values normalised to annual averages and maxima over a 30-year reference period, respectively). Thresholds were statistically derived from empirical tree classification considering 206 landslides events from different parts of the country (Figure 6.4). Piciullo et al. (2017a) analyzed the warnings issued in Western Norway in the period 2013–2014, confirming an overall good performance of the adopted thresholds. However, in the last years NVE has been conducting a revision and an update of the adopted thresholds in collaboration with NGI, using statistical analysis of various hydro-meteorological data for registered and dated landslide events (Devoli et al. 2018).

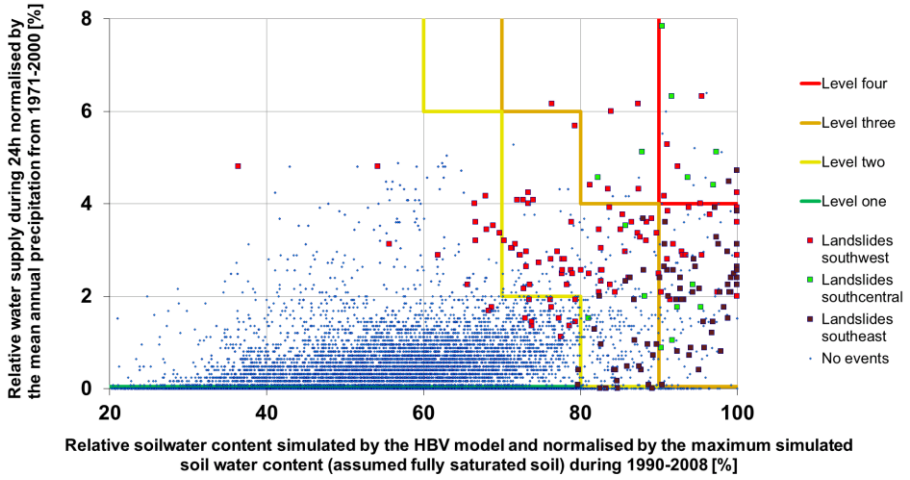

Figure 6.4 Hydrometeorological hazard thresholds used in the Norwegian national LEWS *(Colleuille et al. 2010)*

Decision-making procedures are not only based upon hazard threshold levels, but are also supported by hydro-meteorological and real-time landslide observations as well as landslide inventory and susceptibility maps (Figure 6.5). Real-time observations of rainfall, air temperature, water discharge, and ground water level are used in the daily landslide hazard assessment to check the performance of the hydrological model and to avoid overestimation or underestimation of hydro-meteorological

conditions in certain regions and in certain seasons. Real-time discharge data are used to automatically assimilate and correct the modelled streams discharge in order to provide more reliable information about debris flow hazards. The landslide inventory provides information for different types of analyses, such as: definition of the thresholds, calibration of the warning model, and evaluation of warning system performance. Event information is reported by roads/railways authorities or municipalities and obtained from media and from a real-time database (maintained by NVE and other public agencies). The database contains more than 65,000 events from early 1900s onwards, yet about 70% of the registrations are recorded after 2000. Two susceptibility maps covering the whole country are also used as supportive data for setting warning levels. The first map displays the first-order catchments more susceptible to landslides in soil (e.g., debris avalanches, debris flows, shallow soil slides, clay slides and quick-clay slides) combining several variables (e.g., cover map, land cover, and average annual rainfall). Forecasters use this map in the initial phase to perform a more accurate assessment (Bell et al. 2014). The second map indicates the modelled potential source and runout areas for debris avalanches and small debris flows at 1:50,000 scale (Fischer et al. 2012).
At least two times a day, a landslide expert on duty (as member of a rotation team) uses the aforementioned information to qualitatively perform a nationwide assessment of landslide warning levels: green (1), yellow (2), orange (3), and red (4). Warning levels also indicate the recommended awareness, providing information on the severity of the predicted landslide events (i.e., numerosity and areal extension) and on the mitigation measures that should be initiated or undertaken by the users. Assessment and updates of warning levels are published on the warning portal http://www.varsom.no/ for the three coming days. In case yellow, orange, or red warning levels are exceeded, warning messages are also sent to emergency authorities (regional administrative offices, roads and railways authorities) and media. Warning zones are not static warning areas, as their extent and position are dynamic and can change from day to day, depending on current hydro-meteorological conditions.

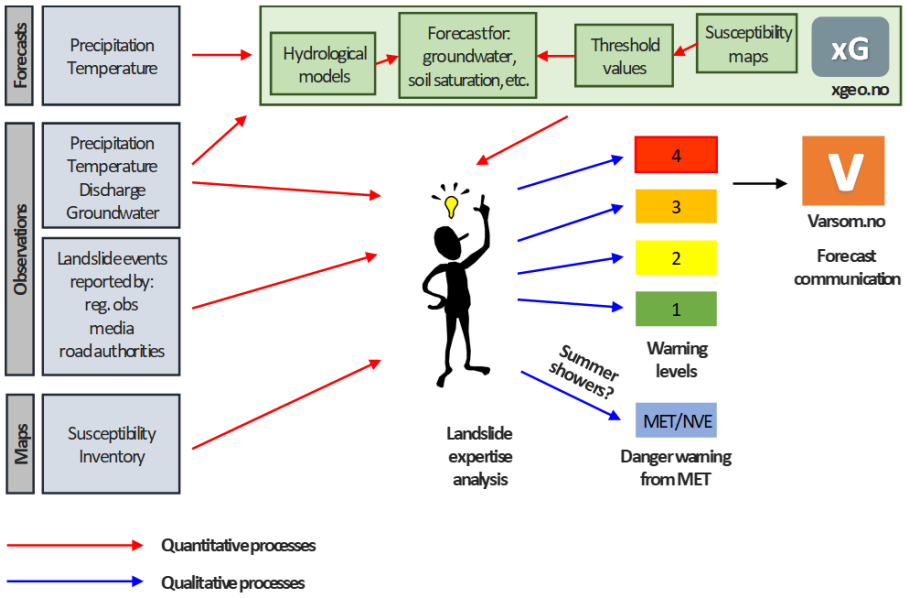

Figure 6.5 Conceptual framework of the national LEWS. Red arrows indicate quantitative processes; blue arrows indicate qualitative processes (modified from *Krøgli et al. 2018*)

6.3 TERRITORIAL UNITS AND AVAILABLE DATASETS

The Norwegian hydrological basins have been considered as the most appropriate minimum territorial units for applying the multi-scalar warning model. Indeed, the catchment scale is an intermediate scale of analysis between small areas (e.g., single slopes) and very wide areas (e.g., a municipality, a region or a nation). Within these units, both the widespread meteorological monitoring data employed in the national EWS and local pore water pressure observations may provide meaningful information for the definition of the warning model. In addition, at catchment scale the whole process area of the landslides is automatically considered. This allows reducing the uncertainty related to the location of the considered landslides. The national catchment database REGINE, compiled by the Norwegian Mapping Authority, displays the delimitation and classification of the Norwegian hydrological basins. The Norwegian water system is divided into 22,545 basins, defined as polygons which cover the whole country. The shape and the size of each unit is determined

by watersheds and intersections in the water system, e.g., tributary river junctions, lakes, and reservoirs. The subdivisions of the water system areas form a hierarchy, as each territorial unit may be characterized by a different structure. Indeed, the drainage area may vary by orders of magnitude, ranging from less than 10^{-4} km^2 for basins draining a well-defined small torrent (e.g., the Vasstøylsåni basin in the south-eastern part of Norway) to more than 10^4 km^2 for large river basins (e.g., the Pasvikelva basin in the proximity of the Russian border). However, only 554 basins out of 22,545 (2.46%) cover an area larger than 100 km^2. Conversely, the extension of the large majority of the basins (57.40%) is smaller than 10 km^2, whereas the remaining part of them (40.14%) drain an area between 10 and 100 km^2. Therefore, the extension of the majority of the basins seem to represent an appropriate scale of analysis for the purpose of this study.

The test areas have been identified according to two main criteria: the occurrence of shallow landslides in loose soils and the availability of a relevant number of pore water pressure measurements. The data on landslide occurrences were retrieved from the national landslide database (www.skrednett.no), which contains more than 60,000 entries (represented by point locations) covering the whole country over the last five hundred years (Figure 6.6). A relevant number of registrations (16,346) are recorded in the period of analysis, i.e. from January 2013 to June 2017, among which 1481 can be considered weather-induced landslides in loose soils. 658 of these records (44.43%) are categorized as landslides in soil, not otherwise specified due to lack of further documentation; 654 (44.16%) are classified as debris flows, debris avalanches or mudslides; 113 (7.63%) are reported as soil slides in artificial slopes (cuts and fillings along road and railway lines); 43 (2.90%) are slush flows and the remaining 13 (0.88%) are clay slides. Registrations recorded by road and railway authorities are usually reported as points where landslides affect transportation networks, thus often far away from the source area. In addition, further uncertainties may result from: errors in classifying the type of landslide event, lack of spatial and/or temporal information, and double registrations. Because of these limitations, landslide records characterized by a questionable quality were removed from the dataset used herein.

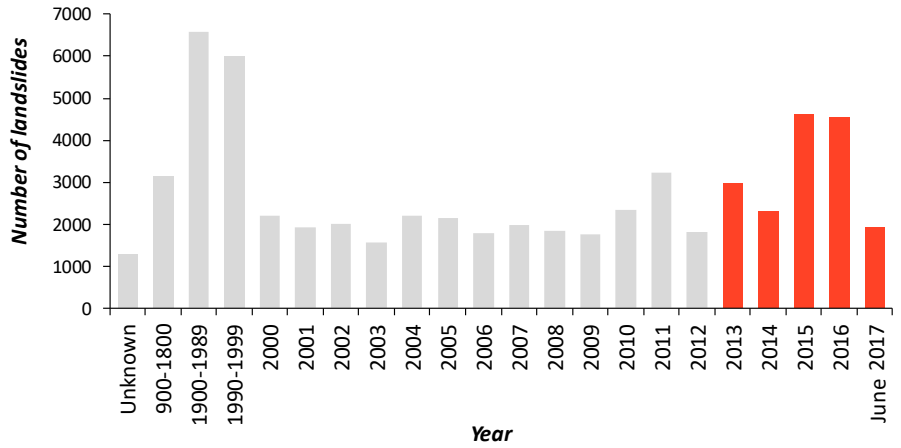

Figure 6.6 Landslides reported in the national landslide catalog (landslide occurred in the period of analyses are marked in red)

The pore water pressure measurements were collected at local scale analysing data from 41,706 boreholes installed by NGI for a variety of geotechnical projects throughout Norway not specifically aimed at early warning purposes, such as: geotechnical site characterization of soils; slope stability analysis; efficiency evaluation of surface drainage works; monitoring of road and railway embankments. The piezometers considered representative of conditions which led to the triggering of the landslides have been selected taking into account their spatial proximity to the landslides that occurred in the period of analysis, and the installation in the shallow soil layers or in areas characterized by the presence of loose sediments, according to a quaternary deposit map at 1:50,000 scale (www.ngu.no). It should be mentioned that data from only electric piezometers have been considered, as they provide longer and more reliable data series.

According to the criteria of selection, 30 Norwegian hydrological basins have been identified as potential useful for the analyses. Figure 6.7 displays that the majority of them (16 out of 30) are distributed along the western coast of Norway: three are situated in the southern part (SW in Figure 6.7), twelve in the central part (CW1 and CW2 in Figure 6.7), and one in the northern part (NW in Figure 6.7). All of them are dominated by narrow fjords and steep mountainsides and are characterized by the presence of shallow marine deposits covering weathered and altered bedrock. The remaining 14 basins are concentrated in the south-eastern part of Norway

(SE in Figure 6.7), an area highly prone to landslides due to long-term infiltration from large amounts of rain and/or snow in autumn and winter and presence of various shallow Quaternary deposits (especially moraine materials). The main characteristics of the study areas are summarized in Table 6.1.

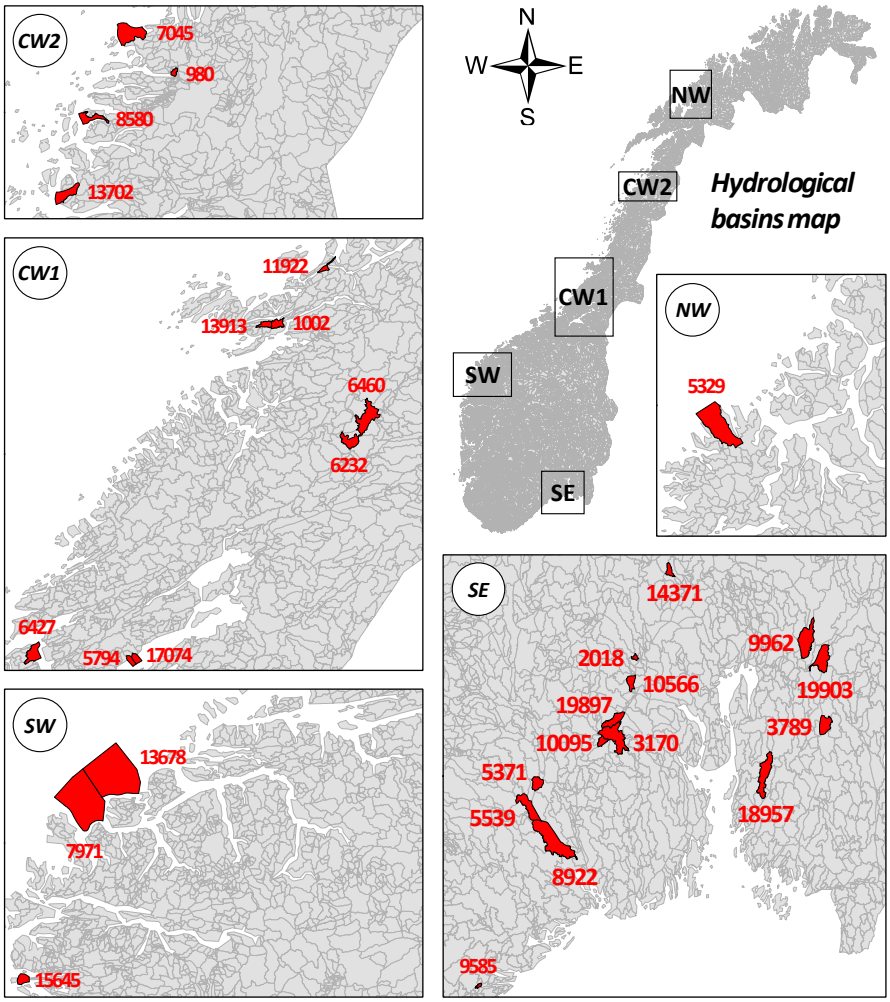

Figure 6.7 Location of the 30 test areas

Table 6.1 Name, area, loose sediments, landslides occurred, and piezometers available within the 30 test areas

ID	Name	Area [km²]	Loose sediments [%]	Weather-induced landslides	Piezometers
980	Fykanåga/Glomfjorden, Gåsværfjorden og Sørfjorden	5.58	23	3	7
1002	Horvereidelva	14.04	55	4	6
2018	Simoa/Drammensvassdraget	3.69	65	4	8
3170	Numedalslågen	64.00	38	3	10
3789	Glommavassdraget	27.13	59	5	8
5329	Senja Vest	136.66	17	6	8
5371	Skiensvassdraget	18.21	52	4	9
5539	Skiensvassdraget	38.88	53	5	8
5794	TrondheimsfJorden Vest	8.08	63	3	6
6232	Namsen	26.48	31	4	7
6427	Ytre Trondheimsfjorden: Agdenes Fyr-geitaneset	30.02	22	4	7
6460	Namsen	56.51	47	3	7
7045	Fykanåga/Glomfjorden, Gåsværfjorden og Sørfjorden	65.47	29	3	6
7971	Hareidlandet og Gurskøya	269.15	7	3	8
8580	Vestre Svartisen og Rødøy kommune	23.08	19	4	8
8922	Skiensvassdraget	104.55	51	6	12
9585	Vegårsvassdraget og Gjerstadvassdraget/ kyst Kragerø-Tromøya	2.45	52	4	7
9962	Leira/Nitelva/ Glommavassdraget	57.76	62	7	13
10095	Numedalslågen	10.09	39	3	8
10566	Drammensvassdraget	14.38	66	4	8
11922	Vikna og Kyst Foldfjorden-Bindalsfjorden	7.64	72	3	7
13678	Hareidlandet og Gurskøya	307.18	10	4	6
13702	kyst Utskarpen-nesna-tonnes	33.45	17	3	8
13913	Horvereidelva	10.58	41	5	7
14371	Simoa/Drammensvassdraget	9.43	69	5	6
15645	Oselvvassdraget/Flora kommune	15.25	27	3	6
17074	TrondheimsfJorden Vest	9.83	78	3	6
18957	Mossevassdraget	51.39	36	6	10
19897	Vestfosselva/ Drammensvassdraget	25.08	30	5	9
19903	Glommavassdraget	43.46	46	6	14

The majority of the basins situated in the south-eastern part of Norway (10 out of 14) cover an area smaller than 50 km^2; on the contrary, three out of the four basins with an area higher than 100 km^2 are distributed along the western coast. The shallow soil layers are significantly characterized by the presence of Quaternary loose deposits highly prone to landslides, which cover more than half of surface in 11 cases out of 30. A total of 125 weather-induced landslides in soils occurred in the 30 test areas between January 2013 and June 2017: in the majority of them (25 out of 30) the number of landslides varies between 3 and 5, yet four basins were interested by 6 landslides and the remaining one by 7 landslides. Finally, pore water pressure measurements recorded in the period of analysis were derived from 240 boreholes, whose numerosity within the test areas varies between 7 and 14.

6.4 APPLICATION OF THE REGIONAL WARNING MODEL

The regional warning model employed within the Norwegian EWS has been applied to the 30 test areas identified in Section 6.3. However, the model has been slightly modified because several aspects need to be taken into account, including: the scale of analysis, the definition of the regional warning events, and the meaning of the warning levels. Indeed, the Norwegian EWS employs variable minimum territorial units, varying from a small group of municipalities (hundreds or thousands of km^2) to several administrative regions (tens of thousands of km^2). Thus, extent and position of warning zones are dynamic and may change day by day, depending on hydrometeorological conditions. Conversely, the minimum territorial units adopted herein are the Norwegian hydrological basins, which are predefined static warning areas ranging from few km^2 to more than 100 km^2. In the Norwegian EWS, relative water supply (rain and snowmelt) and relative soil saturation/groundwater conditions are combined for the definition of a hydro-meteorological index, which is compared with statistically-defined thresholds. Then, a qualitatively daily assessment of landslide warning levels is performed by an expert on duty supported by susceptibility maps and real-time observations. On the contrary, in this study the hydrometeorological index is directly compared with the warning thresholds and a refinement of the model is performed by using local monitoring data, as it will be described in Sections 6.5 and

6.6. In both the cases four warning levels are adopted: green *(WL_1)*, yellow *(WL_2)*, orange *(WL_3)*, and red *(WL_4)*, although the classification criteria are rather different. In the Norwegian EWS, the principle behind the criteria is that rare hydrometeorological conditions are expected to cause more landslides and possibly higher damages. In addition, the criteria contain information on the expected number of landslides per area, as well as hazard signs indicating landslide activity. On the other hand, the classification criteria adopted in this study are not correlated to the number of expected landslides and the extension of the hazardous area in each territorial unit, but provide an indication on the probability of landslide occurrence, i.e. null *(WL_1)*, moderate *(WL_2)*, high *(WL_3)*, and very high *(WL_4)*.

The assessment of the warning events resulting from the application of the regional warning model within any territorial unit can be schematized into two phases. Figure 6.8 reports an example of application referring to the Horvereidelva basin. Firstly, the daily forecasts of water supply and relative soil water content are retrieved from the open-access web portal www.xgeo.no, where they are displayed as raster data at 1-km^2 resolution. Successively, hydro-meteorological indexes are evaluated calculating the average values of all the grid cells comprised within each territorial unit. Finally, the daily average values are compared with the warning levels employed by the regional model, in order to identify the days with warnings as well as to define, in these cases, the level of the warning.

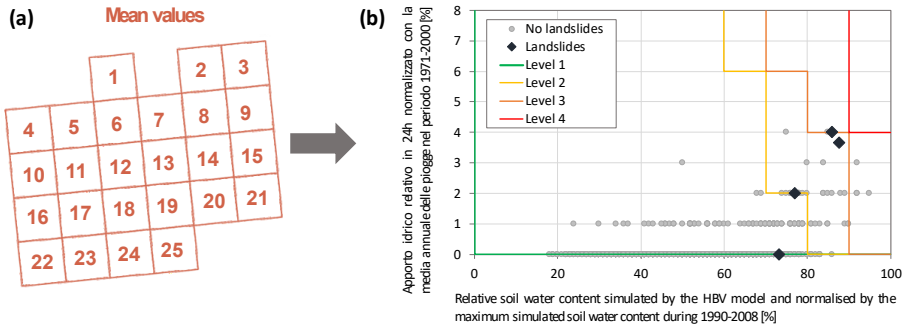

Figure 6.8 Example of application of the regional warning model to the Horvereidelva basin: a) collection of 1-km^2 meteorological gridded data and b) comparison of daily hydrometeorological indexes with the regional warning thresholds

The results are reported in a correlation matrix, which lists the landslide events occurred in relation to warning events. Table 6.2 reports a 2x4 correlation matrix related to the four levels of warning *(WL_1, WL_2, WL_3,* and *WL_4)* and to the presence or absence of a landslide. Twenty-six of the 125 landslide events which affected the test areas between January 2013 and June 2017 occurred when the warning model was in level 1, i.e. when no warnings were issued. For the other 99 occurrences the warning model was in level 2 in 57 cases, in level 3 in 37 cases and in level 4 in the remaining 5 cases. In the period of analysis, 695 daily warnings have been issued: the majority being level 2 "moderate warnings" (560 events), 130 events being level 3 "severe warnings", with the rest of them being level 4 "very severe warnings" (5 events).

Table 6.2 Results obtained applying the regional warning model employed in the national LEWS to the 30 test areas

	WL_1	WL_2	WL_3	WL_4
Landslides	26	57	37	5
No landslides	41622	503	93	0

The 695 warnings issued by applying the regional model were divided into two subsets: (i) a calibration set used to define the multi-scalar model, listing 457 warnings issued within 20 territorial units, and (ii) a validation set used to validate the model, listing 238 warnings issued within the remaining 10 territorial units. The two subsets have been defined with similar characteristics in terms of: areal distribution of the territorial units, numerosity of landslides, and availability of piezometers.

6.5 CALIBRATION OF THE MULTI-SCALAR WARNING MODEL

6.5.1 Definition of the model

The pore water pressure observations collected at local scale have been used to assess the warning events issued by applying the regional model. In particular, pore water pressure variations have been analyzed in order to determine significant upward (and downward) trends indicating local conditions which may lead (or not lead) to the triggering of a landslide

within a territorial unit in response to a given weather event. However, the records are typically characterized by a significant short-term variability. Therefore, before being used, they have been statistically processed in order to smoot the short-term fluctuations and to make the identification of potential trends possible. Moving averages are simple and common smoothing techniques widely used in time series analysis. They are used to determine new series, whose values are comprised of the average of a given number of observations in the original time series. A fundamental parameter is the time period (i.e., the window length) of the moving average, as it defines the number of observations to be used to calculate the values of the new time series. The "moving" part in the moving average is due to the fact that the window defined by the window length slides along the time series in order to calculate the average values. Several types of moving averages—e.g., simple moving average (SMA), cumulative moving average (CMA), weighted moving average (WMA), and exponential moving average (EMA)—can be used, depending on the purpose of the analysis, the types of data, and the time periods.

In this study, the simple moving average of the recorded pore water pressures at a given day *(u_i)* has been calculated, over the number of days of a specified time period *(n),* as follows:

$$u_i = \sum_{k=i-n+1}^{i} \frac{p_k}{n} \quad (6.1)$$

where p_k is the pore water pressure recorded at day *k*. Then, two indicators of pore water pressure variations have been defined, as follows:

$$\Delta u_i = u_i - u_{i-n} \quad (6.2)$$

$$\Delta u_i^* = \frac{\Delta u_i}{\Delta u_{imax}} \quad (6.3)$$

where Δu_i is the difference between the simple moving averages calculated considering a length equal to n days and referring to days *i* and *i–n;* and Δu_i^* is the same difference normalized by the maximum difference observed in the dataset, Δu_{imax}. Figure 6.9 displays an example of application of this technique considering a time period *(n)* equal to 2 days.

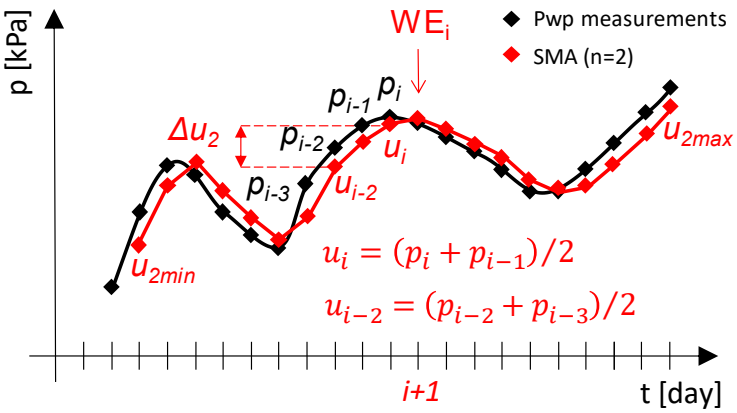

Figure 6.9 Example of application of simple moving average to a pore water pressure data series considering a time period of 2 days

The multi-scalar warning model is based on a 2-step procedure developed using the above-defined indicators (Figure 6.10). In the first step, the differences between the simple moving averages referring to days *i* and *i–n* are evaluated. In case they do not show a clear trend, the warning level issued by the regional model *(WL_0)* is maintained. Otherwise, a second step is performed wherein the normalized simple moving average differences are compared with predefined thresholds (i.e., a lower threshold, *LT* and an upper threshold, *UT)*.

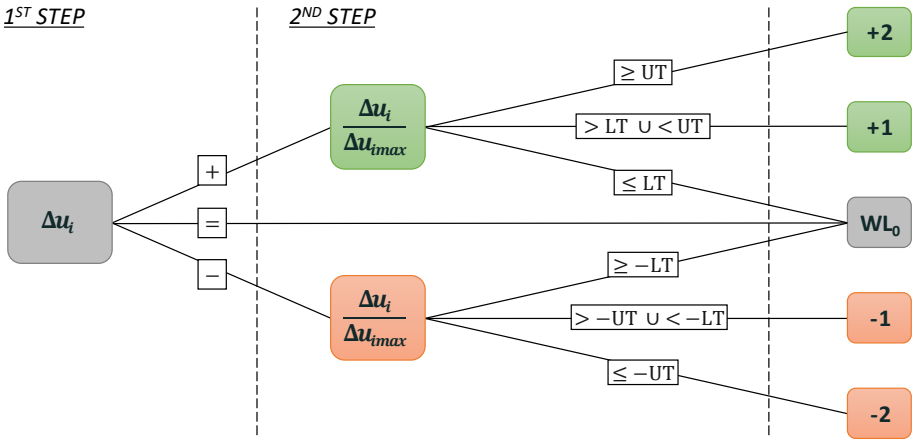

Figure 6.10 Scheme of the methodology developed for analyzing pore water pressure observations. The numbers to the right indicate the change from the original warning level *(WL_0)* of the new warning model

Three final outcomes are possible: the confirmation of the same warning level issued by the regional warning model, an increase of the warning level, a decrease of the warning level. No more than two warning level variations are allowed.

6.5.2 Calibration of the model parameters

The multi-scalar warning model presented in Figure 6.10 has been calibrated using the 457 warnings issued when the regional warning model is applied. To this aim, two parametric analyses have been carried out, respectively for identifying the most appropriate time period *(n)* for calculating the simple moving average indicators, and for setting the values of the two thresholds *(LT* and *UT)* to be adopted in the second step of the procedure.

In the first parametric analysis, the possible trends of Δu_i have been evaluated over time periods *(n)* of 1, 2, 3, 4, 5, 6, 7, and 14 days. Short time periods have been considered because pore water pressure variations representative of possible landslide initiation in shallow loose sediments are typically recorded few days before a landslide event. Besides, a short-term moving average allows identifying possible significant trends without any significant temporal lag between the original and the average data series caused by longer window lengths. Tables 6.3 and 6.4 show, respectively, the comparison between the moving average trends considering the 69 warning events during which landslides occurred (Table 6.3) and the 388 warning events that are not associated to known landslides (Table 6.4). It is worth highlighting that in the first case an "uptrend" can be considered as a correct indicator (i.e., a trend suggesting that an increase of the warning level may be appropriate), whereas in the second case a "downtrend" is a sign of coherence with the data (i.e., a trend suggesting that a decrease of the warning level or a withdraw of the warning may be appropriate). In both the cases, "no trend" indicates that the moving average differences do not show a clear trend. Regarding "severe" *(WL_3)* and "moderate" *(WL_2)* warning events associated to landslides, a number of moving average differences (i.e., Δu_4, Δu_5, Δu_6, Δu_7, and Δu_{14} for WL_3; Δu_3, Δu_4, Δu_5, Δu_6, and Δu_{14} for WL_2) provide similar results, with a percent difference between correct and incorrect indicators greater than 50%. On the other size, considering both "severe" *(WL_3)* and "moderate" *(WL_2)* warning events not associated to landslides,

the best performance has been clearly obtained using Δu_{14}, *as* this time period produces the maximum number of downtrends (41 for WL_3 and 206 for WL_2) as well as the minimum number of uptrends (17 for WL_3 and 80 for WL_2). "Very severe" warning events (WL_4) cannot be evaluated in this case because only two events were issued in the considered time frame, both of them associated to the occurrence of a landslide.
Successively, the trends of each moving average difference have been grouped according to the correctness of the indication provided, regardless of the warning level issued from the regional model. On this issue, correct indicators are represented by uptrends associated to warning events issued when landslides occurred and downtrends associated to warning events issued when landslides did not occur. Conversely, incorrect indicators are represented by uptrends associated to warning events issued when landslides did not occur and downtrends associated to warning events issued when landslides occurred. "No trend" indicators refer again to moving average differences that do not show a clear trend. Figure 6.11 highlights that the percent difference between correct and incorrect indicators increases with the length of the time period. Indeed, Δu_{14} shows the highest value of this difference (42%), as 66% are correct indicators (301 out of 457), 24% are incorrect indicators (110), and the remaining 10% (46) do not show any trend.

Table 6.3 Number of uptrends (up), downtrends (down), and no trends per each moving average difference considering warning events that resulted in landslides. The number of warning events issued for each warning level is reported in round brackets

Indicator	WL_2 (37)			WL_3 (30)			WL_4 (2)		
	up	down	no trend	up	down	no trend	up	down	no trend
Δp_1	25	7	5	17	8	5	0	1	1
Δu_2	26	8	3	19	7	4	0	2	0
Δu_3	25	8	4	22	5	3	0	1	1
Δu_4	27	6	4	23	4	3	0	2	0
Δu_5	29	5	3	21	5	4	0	2	0
Δu_6	29	4	4	21	4	5	0	2	0
Δu_7	28	4	5	20	6	4	0	2	0
Δu_{14}	30	6	1	24	5	1	0	2	0

Table 6.4 Number of uptrends (up), downtrends (down), and no trends per each moving average difference considering warning events that did not resulted in landslides. The number of warning events issued for each warning level is reported in round brackets

Indicator	WL_2 (327)			WL_3 (61)			WL_4 (0)		
	up	down	no trend	up	down	no trend	up	down	no trend
Δp_1	138	120	69	25	25	11	0	0	0
Δu_2	133	126	68	22	29	10	0	0	0
Δu_3	127	130	70	27	28	6	0	0	0
Δu_4	130	130	67	27	28	6	0	0	0
Δu_5	118	141	68	26	30	5	0	0	0
Δu_6	117	147	63	24	31	6	0	0	0
Δu_7	100	171	56	22	29	10	0	0	0
Δu_{14}	80	206	41	17	41	3	0	0	0

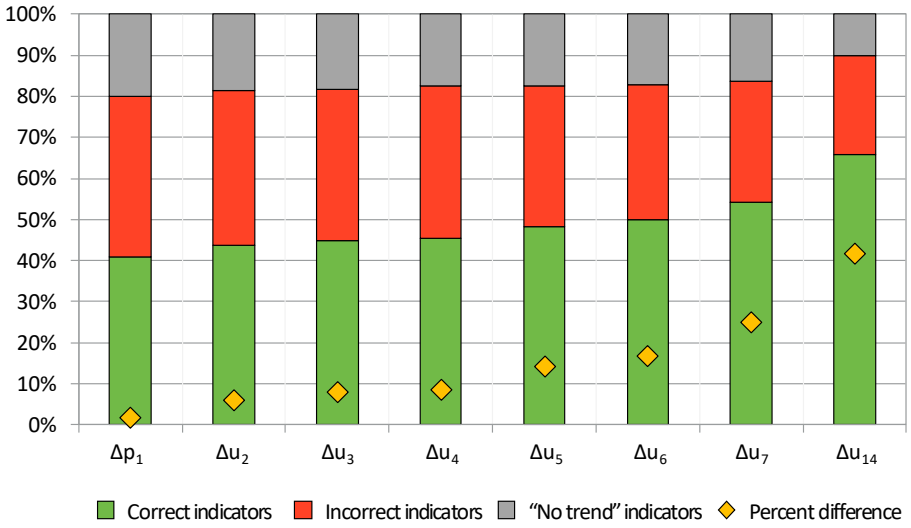

Figure 6.11 Simple moving average differences calculated using time periods *(n)* of 1, 2, 3, 4, 5, 6, 7, and 14 days

The second parametric analysis has been conducted using exclusively Δu_{14} in order to identify the two thresholds to be employed in the second step of the procedure. In particular, six combinations have been defined, considering three values of the lower threshold, *LT* (i.e., ± 5%, ± 10% and ± 15%) and two values of the upper threshold, *UT* (i.e., ± 25% and ± 30%). Table 6.5 summarizes the correlation matrices obtained

considering the six thresholds combinations and the regional warning model.

Firstly, the analysis reveals that the model is extremely sensitive to variations of *LT,* resulting in large differences among the three pairs of combinations $\Delta u_{14,5,25}^{*}-\Delta u_{14,5,30}^{*}$, $\Delta u_{14,10,25}^{*}-\Delta u_{14,10,30}^{*}$, and $\Delta u_{14,15,25}^{*}-\Delta u_{14,15,30}^{*}$. This can be explained considering that the large majority of the level transitions in the period of analysis are 1-level transitions caused by the exceedance of *LT*.

Therefore, each pair of combinations employing the same *LT* have been compared with the regional warning model. The best-performing combination is $\Delta u_{14,10,25}^{*}-\Delta u_{14,10,30}^{*}$, which allows to significantly increase the number warning levels concurrent with landslides (a total of 22 between WL_3 and WL_4, issued in both cases), both minimizing the number of WL_4 and significantly reducing the number of WL_3 and WL_2 in absence of landslides. As expected, the highest number of level transitions has been observed for $\Delta u_{14,5,25}^{*}-\Delta u_{14,5,30}^{*}$, resulting in a significant number of relocations from WL_2 to WL_3 and WL_4 in case of landslide occurrences and in an increase of withdraws when landslides did not occur (WL_1). However, the large amount of WL_3 and WL_4 in absence of landslides (a total of 66 in both the cases) is a sign of a relevant number of severe model errors. Regarding $\Delta u_{14,5,25}^{*}-\Delta u_{14,5,30}^{*}$, the low number of correct level transitions is due to the high value of the *LT,* although the thresholds combinations show an overall good performance.

Table 6.5 Correlation matrices computed for the regional warning model (RM) and for six thresholds combinations

Label	Landslides				No landslides			
	WL_1	WL_2	WL_3	WL_4	WL_1	WL_2	WL_3	WL_4
RM	13	37	30	2	27,191	327	61	0
$\Delta u^{*}_{14,5,25}$	17	9	27	29	27,349	164	54	12
$\Delta u^{*}_{14,5,30}$	16	10	30	26	27,347	166	57	9
$\Delta u^{*}_{14,10,25}$	16	11	30	25	27,318	221	36	4
$\Delta u^{*}_{14,10,30}$	15	12	33	22	27,316	223	39	1
$\Delta u^{*}_{14,15,25}$	15	19	31	17	27,279	250	46	4
$\Delta u^{*}_{14,15,30}$	14	20	34	14	27,277	252	49	1

Further analyses have been carried out on the best-performing combinations (i.e., $\Delta u_{14,10,25}^{*}-\Delta u_{14,10,30}^{*}$) in order to determine correct (i.e., an increase of the warning level in presence of a landslide or a decrease of

the warning level in absence of a landslide) and incorrect level transitions (i.e., a decrease of the warning level in presence of a landslide or an increase of the warning level in absence of a landslide). Figure 6.12 shows that the differences between the two thresholds combinations are minor. On the other hand, $\Delta u_{14,10,25}^{*}$ shows a higher number of correct 2-level transitions (13), whereas no incorrect 2-level transitions occur employing $\Delta u_{14,10,30}^{*}$.

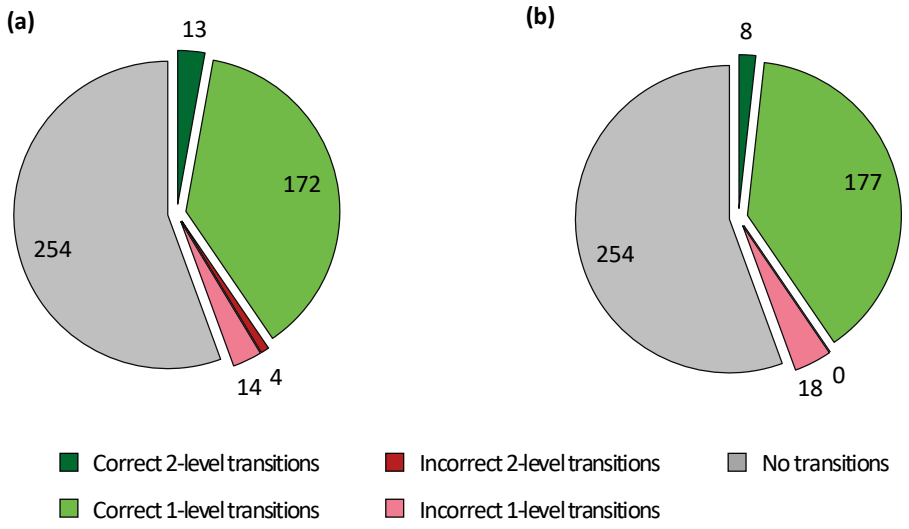

Figure 6.12 Comparison between $\Delta u^{*}_{14,10,25}$ (a) and $\Delta u^{*}_{14,10,30}$ (b) considering number and level of transitions with respect to the regional warning model

6.6 VALIDATION OF THE MULTI-SCALAR WARNING MODEL

6.6.1 Performance criteria and indicators

The validation of the warning model has been developed using statistical indicators derived from contingency tables, following a procedure widely adopted in literature. In a preliminary phase, the warnings issued and the landslides occurred have been retrieved from the validation dataset and reported in a correlation matrix. It is worth mentioning that the relative importance assigned to the different types of errors by the system managers is a key issue to consider to properly validate the model. Figure

6.13 reports a graphical representation of a more comprehensive analysis of the correlation matrix based on a set of two performance criteria, both of them assigning a meaning to all the elements of the matrix.

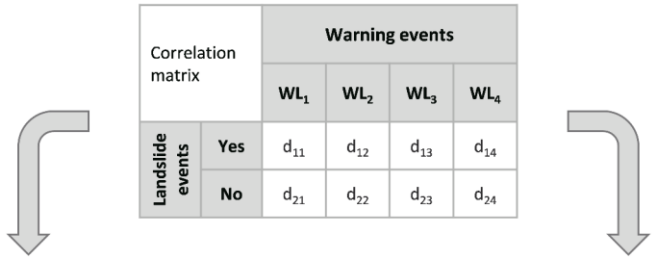

a) Alert classification criterion

Landslide events	Warning events: WL_1	WL_2	WL_3	WL_4
Yes	MA	CA	CA	CA
No	TN	FA	FA	FA

b) Grade of accuracy criterion

Landslide events	Warning events: WL_1	WL_2	WL_3	WL_4
Yes	Red	Yel	Gre	Gre
No	Gre	Gre	Red	Red

Figure 6.13 Alert classification (a) and grade of correctenss (b) performance criteria used for the analysis of the correlation matrix (modified from *Calvello and Piciullo 2016)*

The "alert classification" criterion (Figure 6.13a) employs an alert classification scheme derived from a standard contingency table, and identifies correct alerts *(CA),* false alerts *(FA),* missed alerts *(MA),* and true negatives *(TN).* The issuing of one of the three highest levels of warning *(WL_2, WL_3,* and *WL_4)* concurrently with the occurrence of at least one landslide is assumed as CA. FA and MA are incorrect predictions of the system: the first is related to the issuing of one of the three highest levels of warning *(WL_2, WL_3,* and *WL_4)* and the simultaneous absence of a landslide; the second refers to the occurrence of a landslide without any warning. *TN* represent the absence of both landslides and warning occurrences. The "grade of accuracy" criterion (Figure 6.13b) assigns a colour code to the components of the correlation matrix in relation to the agreement between a given warning event and a given landslide event. For instance, if one of the two highest *WL* is issued (i.e. *WL_3* or *WL_4)* and no landslides occur, this could be considered a significant error of the warning model. Using this criterion, the elements are classified in three colour-coded classes, as follows: green *(Gre)* for the elements which are assumed

to be representative of the best model response, yellow *(Yel)* for elements representative of minor model errors, red *(Red)* for elements representative of a significant model error. Starting from the two performance criteria, several performance indicators can be derived (Piciullo et al. 2017b). Table 6.6 lists the indicators considered in this study.

Table 6.6 Performance indicators used for the analysis (modified from *Calvello and Piciullo 2016)*

Performance indicator	Symbol	Formula	Criterion	Range	Best value
Efficiency index	I_{eff}	$(CA + TN)/\Sigma_{ij}d_{ij}$	a	[0, 1]	1
Hit rate	HR_L	$CA/(CA + MA)$	a	[0, 1]	1
Positive predictive power	P_{PW}	$CA/(CA + FA)$	a	[0, 1]	1
Odds ratio	OR	$(CA + TN)/(MA + FA)$	a	[1, +∞[	+∞
Missed alert rate	R_{MA}	$1 – HR_L$	a	[0, 1]	0
False alert rate	R_{FA}	$1 – PP_W$	a	[0, 1]	0
Error rate	ER	$(Yel + Red)/\Sigma_{ij}d_{ij}$	b	[0, 1]	0
Probability of serious mistakes	P_{SM}	$Red/\Sigma_{ij}d_{ij}$	b	[0, 1]	0

6.6.2 Performance evaluation

The results of the multi-scalar warning model have been validated considering the validation dataset (i.e., 238 regional warning events) in order to determine the optimal combination of thresholds. Table 6.7 shows the results obtained for the six combinations and the regional warning model considering the elements of each duration matrix in terms of alert classification and grade of accuracy. Once again, the model demonstrates a low sensitivity to the *UT,* thus the results have been analyzed considering the three pairs $\angle u_{14,5,25}^{*}–\angle u_{14,5,30}^{*}$, $\angle u_{14,10,25}^{*}–\angle u_{14,10,30}^{*}$, and $\angle u_{14,15,25}^{*}–\angle u_{14,15,30}^{*}$, which differ only for the *LT*. The combination $\angle u_{14,5,25}^{*}–\angle u_{14,5,30}^{*}$ shows the best performance for 4 indicators out of 7 (i.e., *TN, FA, Gre,* and *Yel).* However, looking at the remaining three indicators (i.e., *CA, MA,* and *Red)* the values are minor than those of the regional warning model. Therefore, the best-performing pair of thresholds combinations seems to be $\angle u_{14,10,25}^{*}–\angle u_{14,10,30}^{*}$, for which *TN, FA, Gre,* and *Yel* slightly differ from the pair $\angle u_{14,5,25}^{*}–\angle u_{14,5,30}^{*}$ and which improves the performance of the regional warning model considering *CA, MA,* and *Red,* three relevant indicators for an operative LEWS.

Table 6.7 Values of the correlation matrix elements in terms of "alert classification" (a) and "grade of accuracy" (b) criteria (Figure 6.13). Best values are shown in italics

Element	Criterion	RM	$\Delta u^*_{14,5,25}$	$\Delta u^*_{14,5,30}$	$\Delta u^*_{14,10,25}$	$\Delta u^*_{14,10,30}$	$\Delta u^*_{14,15,25}$	$\Delta u^*_{14,15,30}$
CA	a	*30*	27	27	*30*	*30*	*30*	*30*
TN	a	14,431	*14,538*	14,536	14,519	14,517	14,485	14,483
MA	a	*13*	16	16	*13*	*13*	*13*	*13*
FA	a	208	*113*	115	120	122	154	156
Gre	b	14,613	*14,636*	*14,636*	14,633	14,633	14,620	14,620
Yel	b	22	*2*	*2*	8	8	19	19
Red	b	34	40	40	*28*	*28*	30	30

Table 6.8 and Figures 6.14 and 6.15 show the results in terms of performance indicators for the six different threshold combinations and the regional warning model. Success (Figure 6.14) and error (Figure 6.15) performance indicators are plotted separately.

Among the success indicators, the efficiency index *(I_{eff})* is very high (slightly lower than 100%) for all the thresholds combinations and also for the regional warning model. However, the value slightly increases by applying the multi-scalar warning model, due to a higher number of *TN*. Regarding the hit rate *(HR_L),* it is worth mentioning that the application of the multi-scalar warning model cannot increase the total number of *CA,* thus in turn it cannot increase the value of HR_L. Therefore, it could be considered satisfactory that two pairs of combinations (i.e., $\Delta u^*_{14,10,25}$–$\Delta u^*_{14,10,30}$, and $\Delta u^*_{14,15,25}$–$\Delta u^*_{14,15,30}$) show the same value of the regional warning model. On the other hand, the low values of the pair $\Delta u^*_{14,5,25}$–$\Delta u^*_{14,5,30}$ are due to the transitions of three *CA* in *MA*. Although the application of the multi-scalar warning model leads to an increase of the positive predictive power *(P_{PW})* in all the cases, the values are relatively low (i.e., about 20% for the best-performing pair $\Delta u^*_{14,10,25}$–$\Delta u^*_{14,10,30}$), because in all the cases *FA* remain sensitively higher than *CA*. The odds ratio *(OR),* which can be considered as a rate between correct and predictions, is higher for the pair $\Delta u^*_{14,5,25}$–$\Delta u^*_{14,5,30}$ as a function of the reduction of *FA* and *MA* and the significant increment of *TN,* which balances the reduction of *CA*.

Concerning the error indicators, the very low values of the error rate *(ER)* and the probability of serious mistakes *(P_{SM})* in all the cases are principally dependent on the high values assumed by *TN*. The variations of the missed alert rate *(R_{MA})* and of the false alert rate *(R_{FA})* can be exactly related to those of the hit rate *(HR_L)* and the positive predictive power *(P_{PW}),* as

the former are the one's complement of the latter following the performance criteria defined in Section 6.1.
Concluding, the validation process confirms that $\Delta u_{14,10,25}^{*}$–$\Delta u_{14,10,30}^{*}$ are the optimal thresholds combinations and highlights that according to the available data and the criteria adopted herein the overall performance of $\Delta u_{14,10,25}^{*}$ is slightly better.

Table 6.8 Performance indicators obtained for each the regional warning model (RM) and for each combination of thresholds. Best values are shown in italics

Indicator	Criterion	RM	$\Delta u^{*}_{14,5,25}$	$\Delta u^{*}_{14,5,30}$	$\Delta u^{*}_{14,10,25}$	$\Delta u^{*}_{14,10,30}$	$\Delta u^{*}_{14,15,25}$	$\Delta u^{*}_{14,15,30}$
I_{eff}	a	0.9849	*0.9912*	0.9911	0.9909	0.9908	0.9886	0.9885
HR_L	a	*0.70*	0.63	0.63	*0.70*	*0.70*	*0.70*	*0.70*
P_{PW}	a	0.126	0.193	0.190	*0.200*	0.197	0.163	0.161
OR	a	65	*113*	111	109	108	87	86
M_{AR}	a	*0.30*	0.37	0.37	*0.30*	*0.30*	*0.30*	*0.30*
F_{AR}	a	0.874	0.807	0.810	*0.800*	0.803	0.837	0.839
ER	b	0.0047	0.0039	0.0039	*0.0033*	*0.0033*	0.0042	0.0042
P_{SM}	b	*0.002*	0.003	0.003	*0.002*	*0.002*	*0.002*	*0.002*

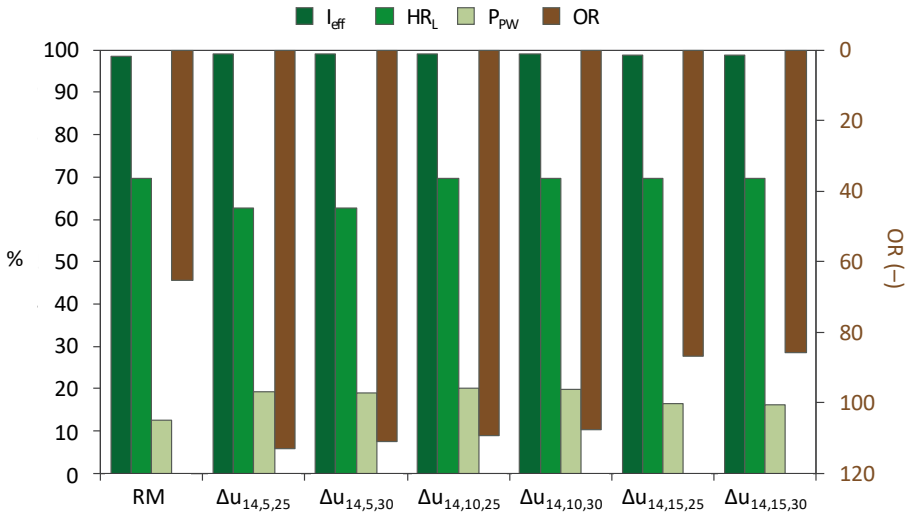

Figure 6.14 Bar chart showing the values of success indicators for each combination of thresholds. Efficiency index *(I_{eff})*, hit rate *(HR_L)*, and positive predictive power *(P_{PW})* values are shown as percentages (green bars). The absolute values for the odds ratio *(OR)* are also reported (brown bars, on secondary vertical axes in reverse order)

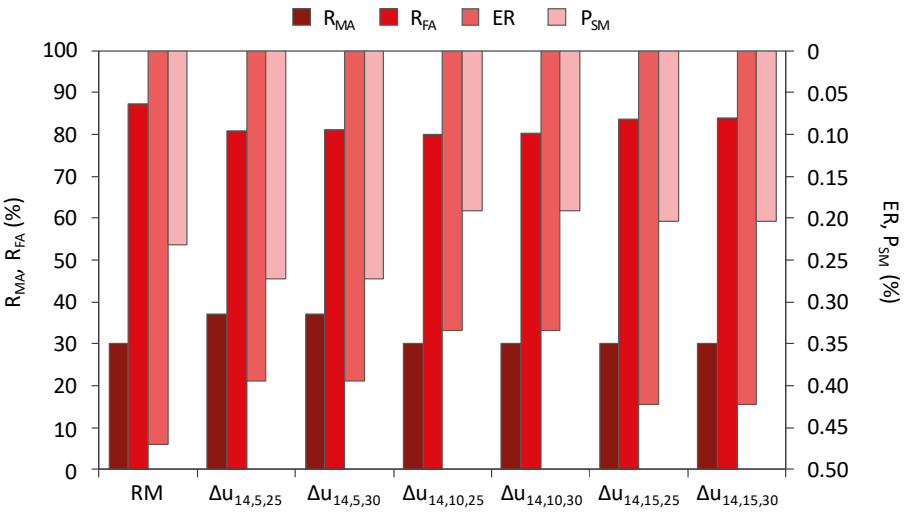

Figure 6.15 Bar chart showing the percentage values of error indicators for each combination of thresholds: missed alert rate *(R_{MA}),* false alert rate *(R_{FA}),* error rate (*ER)* and probability of serious errors *(P_{SM}).* The latter two are reported on secondary vertical axes in reverse order

7 CONCLUSIONS

The risk associated to weather-induced landslides cannot be mitigated only by means of structural mitigation measures, thus landslide early warning systems (LEWS) are being increasingly implemented in many parts of the world. LEWS differ widely depending on: the type of landslides, their predisposing and triggering factors, the scale of analysis—i.e., the size of the area covered by the system. The main aim of this PhD thesis was the definition of innovative methodologies for improving the performance of warning models employed in LEWS for weather-induced landslides.
Firstly, the main features of the landslides addressed in this work and the possible consequences for local communities, structures, and infrastructures were introduced. Information on systems operational both at local and regional scale were retrieved from literature contributions and their main characteristics were analyzed considering a structure based on a clear distinction among landslide model, warning model, and warning system. The monitoring strategies implemented within the reviewed LEWS were classified in terms of monitored parameters and monitoring instruments in relation to the types of landslides under surveillance. Many relevant aspects of the warning models were analyzed, including: the methods for the definition of the model, the warning parameters, the monitoring networks, and the number of warning levels. Warning models are typically based on empirical rainfall thresholds, defined by analyzing past rainfall events that have resulted or not in slope failures. However, these methods do not typically include a quantitative assessment of the uncertainties correlated to the results. Indeed, a questionable quality of the input data (i.e., historical landslide records and rainfall measurements) may significantly affect the outputs of the model. Moreover, meteorological monitoring does not allow to take into account critical soil properties controlling the initiation of the triggering process. Finally, despite the relevant number of recent applications, standard requirements for the definition of a reliable warning model do not still exist, thus some relevant aspects are often neglected by systems developers and managers, such as: reliability and completeness of the landslide catalog; adequate coverage

and spatial resolution of the monitoring network; robust and quantitative validation of the model.

To overcome these issues, a conceptual framework was introduced in order to highlight the main steps to be addressed for the definition of a reliable warning model for weather-induced landslides:

- collection of input data appropriate for the analyses to be carried out (i.e., landslide records, monitoring data, thematic maps of the study area);
- partition of the study area into territorial units characterized by hydrogeological and meteorological homogeneity;
- identification of the landslide events addressed by the warning model;
- selection of appropriate warning parameters depending on several factors, including the types of landslides, the geomorphological context, and the climatic regime;
- spatial-temporal correlation between landslides and weather events;
- calibration of the warning model using the most appropriate method on the basis of the available input data and the expected outputs;
- validation of the warning model in order to assess its predictive capability.

Following the general framework introduced, two innovative procedures were proposed for the definition of:

1. a probabilistic warning model, in order to obtain objective and reproducible probabilistic rainfall thresholds to consider the uncertainty of the input data as well as to quantitatively estimate the reliability of the results;
2. a multi-scalar warning model, whose main innovation is the integration between widespread meteorological monitoring data and pore water pressure observations collected at local scale.

Other innovations introduced by the procedures developed in this study, in relation to the warning models commonly adopted in LEWS described in the scientific literature, were: the use of "FraneItalia", a landslide inventory retrieved from online news, for defining correlations between landslides and rainfall events at regional scale; and the employment of rainfall measurements derived from satellite monitoring.

Probabilistic warning model

The probabilistic warning model was developed and tested in two different Italian regions, highly affected by weather-induced landslides: Emilia-Romagna and Campania. Although the two applications differ for a series of aspects, some common steps were developed. In a preliminary phase, the weather warning zones were identified as the most appropriate territorial units for the two case studies, considering the spatial uncertainty of the landslide records and the spatial resolution of the rainfall measurements. Then, a new landslide catalog was developed searching online news, and populated with landslide records since January 2010. To this aim, a series of constraints were adopted to ensure the appropriateness of the information, and the outputs were validated through a comparison with other landslide inventories already existing in Italy. Then, satellite rainfall measurements derived from the NASA Global Precipitation Measuring (GPM) mission and available from March 2014 onwards were collected and analyzed over the territorial units. Duration *(D)* and cumulated rainfall *(E)* were identified as the most appropriate rainfall parameters. Finally, the probabilistic warning model was developed by applying a Bayesian probabilistic approach, aimed at highlighting the critical levels of rainfall corresponding to different probabilities of landslide occurrence.

In Emilia-Romagna, the analyses were conducted using landslide records and monitoring data from January 2014 to December 2015. Rainfall events were reconstructed setting in advance some standards depending on the climatic characteristics of the study area. Then, a spatial-temporal correlation considering the landslides occurred in each territorial unit was developed to differentiate between triggering and non-triggering rainfall events. The Bayesian probabilistic analysis allowed to identify the highest value of landslide probability $(P(L|D,E) = 0.5)$ as well as three secondary peaks $(P(L|D,E) > 0.2)$. Therefore, two different rainfall conditions more likely to trigger landslides were identified and a probabilistic threshold was defined in correspondence of $P(L|D,E) = 0.15$. For validation purposes, a back analysis was conducted by comparing the new probabilistic threshold with other regional thresholds reported in the literature. A quantitative analysis was performed considering the thresholds as binary classifiers and using a set of contingency indicators. The overall good performance of the probabilistic

threshold showed that its flexibility can be extremely useful in areas where landslides are triggered by different rainfall conditions.
In Campania, the analyses were carried out between March 2014 and December 2017. Differently from Emilia-Romagna, rainfall events were reconstructed by adopting an "algorithmic" procedure. This allowed to explicitly account for the uncertainty in the reconstruction of the rainfall events, by assigning a relative frequency based on the number of possible aggregations for each rainfall event. The results indicated that two different rainfall conditions are more likely to trigger landslides. This can be explained considering the heterogeneity of the landslide dataset, in terms of types of movements and magnitude of the events. Following the same criterion adopted for Emilia-Romagna, six possible thresholds were identified for probability values varying from 0.05 to 0.50. Successively, the probabilistic thresholds were validated using a well-established procedure employing a ROC analysis and the related skill scores. In this case study, the parameters most affecting the results and crucial for the identification of the optimal threshold were: i) the probability of false alarm score, *POFA;* ii) the Hanssen and Kuipers (1965) skill score, *HK;* iii) the Euclidean distance, δ. They showed that $T_{10,P}$ is the best-performing threshold, representing a compromise between the minimization of incorrect landslide predictions and the maximization of the correct predictions. On the other hand, the high number of the landslide events detected considering higher thresholds (i.e., $T_{20,P}$ and $T_{30,P}$) seems to indicate that the model could be further improved by adopting a multi-level warning model combining different threshold values.

Multi-scalar warning model
The multi-scalar warning model was developed and applied considering Norway as the test area and the Norwegian hydrological basins as the most appropriate territorial units. The latter indeed represent an intermediate scale of analysis, where both widespread meteorological data and local pore water pressure observations may provide fruitful information. According to a set of criteria, 30 territorial units were selected for analyses. The regional warning model currently employed in the Norwegian national LEWS was applied, and the warnings issued were assessed considering local observations. The data series were preliminary analyzed in order to determine potential trends adopting a simple moving average (SMA) calculation. Two Indicators derived from these analyses (i.e., $\measuredangle u_i$ and $\measuredangle u_i^*$) were employed in a 2-step procedure for the definition of a new

multi-scalar warning model. In the calibration phase, two parametric analyses were performed for identifying the most appropriate time period *(n)* for calculating the simple moving average indicators, and for setting the values of the two thresholds to be adopted in the second step of the procedure (i.e., a lower threshold, *LT* for 1-level transition and an upper threshold, *UT* for 2-level transitions). Firstly, time periods varying from 1 to 14 days were evaluated and the best results were achieved considering a period of 14 days, as it produced the maximum number of correct predictions as well as the minimum number of incorrect predictions. Among the different combinations of thresholds evaluated, $\angle\!\!\!\perp u_{14,10,25}^{*}$–$\angle\!\!\!\perp u_{14,10,30}^{*}$ provided the best results. It should be mentioned that the model demonstrated a low sensitivity to the upper threshold, due to the small number of 2-level transitions recorded in the period of analysis. Two performance criteria employing statistical indicators derived from contingency tables were considered for validation purposes. The most useful indicators for determining the best-performing thresholds were: the efficiency index, I_{eff}; the false alert rate, R_{FA}; and the error rate, *ER*. They confirmed that $\angle\!\!\!\perp u_{14,10,25}^{*}$–$\angle\!\!\!\perp u_{14,10,30}^{*}$ are the optimal combinations of thresholds, and that slight differences can be observed among them. On the other hand, it is worth mentioning that all the considering thresholds allowed to enhance the performance of the currently adopted regional warning model, demonstrating that pore water pressure trends can provide useful indications for early warning purposes at regional scale. Of course, the results of the performed analysis should be considered specific for the regional warning model employed in Norway, although the proposed methodology can be applied to other case studies, upon adequately considering differences related to the regional warning model adopted, the geomorphological context, and the types of landslides under surveillance.

Concluding remarks and future perspectives

Concluding, some specific requirements and potential practical issues that LEWS managers would have to take into consideration when designing a warning model for weather-induced landslides, can be mentioned.

- The definition of a reliable warning model is strictly connected to the availability of rainfall and landslide datasets and to the accuracy of the information therein contained.

- Weather measurements alone can be not sufficient for a reliable prediction of landslide occurrence in complex geomorphological contexts. In these cases, geotechnical data collected at local scale can provide additional information, although the parameters need to be appropriately selected depending on the types of landslides under surveillance.
- Multi-level thresholds combinations can be adopted as a solution to be employed in a warning model.
- A continuous collection of data, an update of the adopted thresholds and periodic performance assessments are necessary to maintain the reliability of a warning model.

The results of this thesis raise new questions on future refinements for improving the prediction capabilities of warning models for weather-induced landslides. In the following, potential improvements are presented, and the prospects for applying the developed early warning applications in general are also discussed.

Both warning models developed in this study offer a huge potential for applications to other study areas. In particular the probabilistic warning model can be easily applied to other areas where the weather-induced landslides pose a significant risk. To this aim, the availability of landslide inventories and widespread monitoring data is crucial for the calibration and the validation of the model. Regarding the landslide inventory, the methodology adopted to define and populate the "FraneItalia" catalog from online news is deemed to be general and can be used to develop similar initiatives in other countries in order to supplement existing landslide inventories. On the other hand, the advances in satellite and ground-based radar technology are providing a great support to the development of reliable warning models, especially in areas where land-based monitoring networks are not available or their spatial resolution is not adequate. Of great benefit to future application of the multi-scalar warning model to other case studies could be a comprehensive investigation on the landslides under surveillance in order to define the most suitable parameters to be monitored for early warning purposes. In addition, the availability of a significant number of local observations is also crucial for the definition of a reliable warning model.

The methodologies proposed in this work are aimed at improving the efficiency of the warning models adopted within warning systems for weather-induced landslides. It must be noted, however, that they do not

tackle other aspects that are critical for the effectiveness of a LEWS, such as: communication strategies, public education, emergency action, and risk perception. Therefore, their design and operation necessarily require an interdisciplinary collaboration as well as the collaboration of hazard management officers, communities and other relevant stakeholders involved in the process of landslide risk management.

REFERENCES

Arattano M (1999) On the use of seismic detectors as monitoring and warning systems for debris flows. *Nat Hazards* 20:197–213. https://doi.org/10.1023/A:1008061916445

Arattano M, Marchi L (2008) Systems and sensors for debris-flow monitoring and warning. *Sensors* 8(4):2436–2452. https://doi.org/10.3390/s8042436

Badoux A, Graf C, Rhyner J, Kuntner R, McArdell BW (2009) A debris-flow alarm system for the alpine Illgraben catchment: design and performance. *Nat Hazards* 49:517–539. https://doi.org/10.1007/s11069-008-9303-x

Baroň I, Supper R (2013) Application and reliability of techniques for landslide site investigation, monitoring and early warning—outcomes from a questionnaire study. *Nat Hazards Earth Syst Sci* 13:3157–3168. https://doi.org/10.5194/nhess-13-3157-2013

Baroň I, Supper R, Ottowitz D (2012) SafeLand deliverable 4.6.: report on evaluation of mass movement indicators. *European project SafeLand, Grant Agreement No. 226479,* 382 pp. Available at: http://www.safeland-fp7.eu

Battistini A, Rosi A, Segoni S, Lagomarsino D, Catani F, Casagli N (2017) Validation of landslide hazard models using a semantic engine on online news. *Appl Geogr* 82:59–65. https://doi.org/10.1016/j.apgeog.2017.03.003

Battistini A, Segoni S, Manzo G, Catani F, Casagli N (2013) Web data mining for automatic inventory of geohazards at national scale. *Appl Geogr* 43:147–158. https://doi.org/10.1016/j.apgeog.2013.06.012

Baum RL, Godt JW (2010) Early warning of rainfall-induced shallow landslides and debris flows in the USA. *Landslides* 7(3):259–272. https://doi.org/10.1007/s10346-009-0177-0

Beldring S, Engeland K, Roald LA, Sælthun NR, Voksø A (2003) Estimation of parameters in a distributed precipitation runoff

model for Norway. *Hydrol Earth Syst Sci* 7:304–316. https://doi.org/10.5194/hess-7-304-2003

Bell R, Cepeda J, Devoli G (2014) Landslide susceptibility modeling at catchment level for improvement of the landslide early warning system in Norway. *Proceeding 3rd World Landslide Forum,* 2–6 June 2014, Beijing, China.

Berti M, Martina MLV, Franceschini S, Pignone S, Simoni A, Pizziolo M (2012) Probabilistic rainfall thresholds for landslide occurrence using a Bayesian approach. *J Geophys Res* 117:F04006. https://doi.org/10.1029/2012JF002367

Blikra LH, Kristensen L, Lovisolo M (2013) Subsurface monitoring of large rockslides in Norway: a key requirement for early warning. *Ital J Eng Geol Environ* 6:307–314. https://doi.org/10.4408/IJEGE.2013-06.B-28

Blong RJ (1973) A numerical classification of selected landslides of the debris slide-avalanche-flow type. *Eng Geol* 7: 99-144

Broccolato M (2010) I grandi movimenti di massa sul territorio valdostano: Il sistema di monitoraggio (in Italian). In: *Conference presentation,* Barzio, Italy

Brunetti MT, Peruccacci S, Rossi M, Luciani S, Valigi D, Guzzetti F (2010) Rainfall thresholds for the possible occurrence of landslides in Italy. *Nat Hazards Earth Syst Sci* 10:447–458. https://doi.org/10.5194/nhess-10-447-2010

Caine N (1980) The rainfall intensity-duration control of shallow landslides and debris flows. *Geografiska Annal* 62A:23–27

Calvello M (2017) Early warning strategies to cope with landslide risk. *Riv It Geotecnica* 2:63–91. https://doi.org/10.19199/2017.2.0557-1405.063

Calvello M, Pecoraro G (2018) FraneItalia: a catalog of recent Italian landslides. *Geoenviron Disasters* 5(13). https://doi.org/10.1186/s40677-018-0105-5

Calvello M, Piciullo L (2016) Assessing the performance of regional landslide early warning models: the EDuMaP method. *Nat Hazards Earth Syst Sci* 16:103–122. https://doi.org/10.5194/nhess-16-103-2016

Cardellini S, Osimani P (2008) Living with landslide: the Ancona case history and early warning system. In: *Proc of the 1st World Landslide Forum,* Tokyo, pp 473–476

Cardinaletti M, Cardellini S, Ninivaggi A (2011) The integrate landslide managing system of Ancona. *UNISDR PreventionWeb.* https://www.preventionweb.net/applications/hfa/lgsat/en/image/href/512. Accessed 23 October 2017

Cascini L (2004) The flowslides of May 1998 in the Campania region, Italy: the scientific emergency management. *Riv It Geotecnica* 38 (2): 11–44

Cascini L, Cuomo S, Guida D (2008) Typical source areas of May 1998 flow-like mass movements in the Campania region, Southern Italy. *Eng Geol* 96:107–125. https://doi.org/10.1016/j.enggeo.2007.10.003

Cascini L, Sorbino G, Cuomo S, Ferlisi S (2014) Seasonal effects of rainfall on the shallow pyroclastic deposits of the Campania region (southern Italy). *Landslides* 11 (5): 779–792 https://doi.org/10.1007/s10346-013-0395-3

Chae BG, Park HJ, Catani F et al (2017) Landslide prediction, monitoring and early warning: a concise review of state-of-the-art. *Geosci J* 21:1033–1070. https://doi.org/10.1007/s12303-017-0049-x

Clark AR, Moore R, Palmer JS (1996) Slope monitoring and early warning systems: application to coastal landslide on the south and east coast of England, UK. In: Senneset K (ed) Landslides, *7th International Symposium on Landslides,* Balkema, Rotterdam, pp 1531–1538

Colleuille H, Haugen LE, Beldring S (2010) A forecast analysis tool for extreme hydrological conditions in Norway. Poster presented in: *Proc of 6th world FRIEND 2010, Flow Regime and International Experiment and Network Data,* Fez (Morocco)

Corominas J, Mavrouli O (2012) SafeLand deliverable 2.8.: Recommended Procedures for Validating Landslide Hazard and Risk Models and Maps. *European project SafeLand, Grant Agreement No. 226479,* 162 pp. Available at: http://www.safeland-fp7.eu

Cotecchia V (2006) The second Hans Cloos lecture. Experience drawn from the great Ancona landslide of 1982. *Bull Eng Geol Environ* 45:1–41. https://doi.org/10.1007/s10064-005-0024-z

Crosta GB, Agliardi F (2003) Failure forecast for large rock slides by surface displacement measurements. *Can Geotech J* 40:176–191. https://doi.org/10.1139/t02-085

Crosta GB, Agliardi F, Rivolta C, Alberti S, Dei Cas L (2017) Long-term evolution and early warning strategies for complex rockslides by

real-time monitoring. *Landslides* 4(5):1615–1632. https://doi.org/10.1007/s10346-017-0817-8

Crosta GB, di Prisco C, Frattini P, Frigerio G, Castellanza R, Agliardi F (2014) Chasing a complete understanding of the triggering mechanisms of a large rapidly evolving rockslide. *Landslides* 11:747–764. https://doi.org/10.1007/s10346-013-0433-1

Crosta GB, Frattini P, Castellanza R, Frigerio G, di Prisco C, Volpi G, de Caro M, Cancelli P, Tamburini A, Alberto W, Bertolo D (2015) Investigation, monitoring and modelling of a rapidly evolving rockslide: the Mt. de la Saxe case study. In: *Engineering geology for society and territory,* vol 2. Springer, Berlin, pp 349–354. https://doi.org/10.1007/978-3-319-09057-3_54

Cruden DM (1991) A simple definition of a landslide. *Bulletin of IAEG,* 43: 27-29.

Cruden DM, Varnes DJ (1996) Landslide types and processes. *Landslides: Investigation and Mitigation, Special Report n. 247,* Washington: Transportation Research Board, pp 36-75

Del Ventisette C, Casagli N, Fortuny-Guasch J, Tarchi D (2012) Ruinon landslide (Valfurva, Italy) activity in relation to rainfall by means of GBInSAR monitoring. *Landslides* 9:497–509. https://doi.org/10.1007/s10346-011-0307-3

Devoli G, Tiranti D, Cremonini R, Sund M, Bøje S (2018) Comparison of landslide forecasting services in Piemonte (Italy) and in Norway, illustrated by events in late spring 2013. *Nat Hazards Earth Syst Sci* 18:1351–1372. https://doi.org/10.5194/nhess-18-1351-2018

DGR (2005) Deliberazione della Giunta Regionale dell'Emilia-Romagna n. 1427 del 12/09/2005: Attivazione del Centro Funzionale e procedure per la gestione del sistema di allertamento regionale ai fini di protezione civile (come previsto dal) DPCM 27 febbraio 2004. *Bollettino ufficiale della regione Emilia-Romagna (BURERC),* Emilia-Romagna, Italy (In Italian)

Di Biagio E, Kjekstad O (2007) Early warning, instrumentation and monitoring landslides. In: *Proc of the 2nd Regional Training Course, RECLAIM II,* Phulet, Thailand

DPCM, 2005. D27/02/2004, Direttiva Presidente Consiglio dei Ministri: Indirizzi operativi per la gestione operativa e funzionale del sistema di allertamento nazionale, statale e regionale per il rischio idrogeologico ed idraulico ai fini di protezione civile. In: *Gazzetta Ufficiale n. 59 del 11/03/2004,* Roma, Italy, 2004 (In Italian)

DPGR (2005) Decreto del Presidente della Giunta Regionale della Campania n. 299 del 30/06/2005: Il Sistema di Allertamento Regionale per il rischio Idrogeologico e Idraulico ai fini di protezione civile. *Bollettino ufficiale della regione Campania (BURC),* Campania, Italy (In Italian)

Etzelmüller B, Romstad B, Fjellanger J (2007) Automatic regional classification of topography in Norway. *Norwegian Journal of Geology* 87:167–180. Available at: http://www.geologi.no/njg/ (last access: 20 November 2018)

Fell R, Ho KKS, Lacasse S, Leroi E (2005) – A framework for landslide risk assessment and management. *Landslide Risk Management,* CRC Press, pp 3-25

Fischer L, Rubensdotter L, Sletten K, Stalsberg K, Melchiorre C, Horton P, Jaboyedoff M (2012) Debris flow modelling for susceptibility mapping at regional to national scale, in: *Landslides and Engineered Slopes,* edited by: Eberhardt E, Froese C, Turner K, Leroueil S, Protecting Society through Improved Understanding, CRC Press, pp. 723–729

Flentje P, Chowdhury RN (2005) Managing landslide hazards on the Illawarra escarpment. In: *Proc of the GeoQuest Symp on Planning for Nat Hazards,* pp 65–78

Flentje P, Chowdhury RN (2006) Observational approach for urban landslide management, engineering geology for tomorrow's cities. In: *Proc of the 10th International Association of Engineering Geology and the Environment Congress,* Nottingham (Paper no. 522)

Floris M, D'Alpaos A, Squarzoni C, Genevois R, Marani M (2010) Recent changes in rainfall characteristics and their influence on thresholds for debris flow triggering in the Dolomitic area of Cortina d'Ampezzo, north-eastern Italian Alps. *Nat Hazard Earth Syst Sci* 10:571–580. https://doi.org/10.5194/nhess-10-571-2010

Fredin O, Bergstrøm B, Eilertsen R, Hansen L, Longva O, Nesje A, Sveian H (2013) Glacial landforms and Quaternary landscape development in Norway. *Quaternary Geology of Norway* (Eds.: Olsen L, Fredin O, Olesen O, pp. 5-25. Geological Survey of Norway, Special Publication, Trondheim

Fredlund DG (1987) Slope stability analyses incorporating the effect of soil moisture suction. In: Anderson MG, Richards KS (eds), *Slope Stability,* Wiley and Sons, Chichester, pp 113–144

Froese CR, Moreno F (2014) Structure and components for the emergency response and warning system on Turtle Mountain, Alberta, Canada. *Nat Hazards* 70:1689–1712. https://doi.org/10.1007/s11069-011-9714-y

Froude MJ, Petley DN (2018) Global fatal landslide occurrence from 2004 to 2016. *Nat Hazards Earth Syst Sci* 18:2161–2181. https://doi.org/10.5194/nhess-18-2161-2018

Furseth A (2006) Slide accidents in Norway. *Tun Forlag,* Oslo, 207 pp. (in Norwegian)

Gariano SL, Brunetti MT, Iovine G, Melillo M, Peruccacci S, Terranova O, Vennari C, Guzzetti F (2015) Calibration and validation of rainfall thresholds for shallow landslide forecasting in Sicily, southern Italy. *Geomorphology* 228:653–665. https://doi.org/10.1016/j.geomorph.2014.10.019

Giuliani A, Bonetto S, Castagna S et al (2010) A monitoring system for mitigation planning: the case of "Bagnaschino" landslide in Northern Italy. *Am J Environ Sci* 6(6):516–522. https://doi.org/10.3844/ajessp.2010.516.522

Gorelick N, Hancher M, Dixon M, Ilyushchenko S, Thau D, Moore R (2017) Google earth engine: planetary-scale geospatial analysis for everyone. *Remote Sens Environ* 202:18–27. https://doi.org/10.1016/j.rse.2017.06.031

Guha-Sapir D, Below R, Hoyois PH (2018) EM-DAT: International Disaster Database, Université Catholique de Louvain, Brussels, Belgium. Available at: http://www.emdat.be, Accessed: 27 December 2018

Gullà G, Calcaterra S, Gambino P, Borrelli L, Muto F (2018) Long-term measurements using an integrated monitoring network to identify homogeneous landslide sectors in a complex geo-environmental context (Lago, Calabria, Italy). *Landslides* 15(8): 1503–1521. https://doi.org/10.1007/s10346-018-0974-4

Guzzetti F (2000) Landslide fatalities and the evaluation of landslide risk in Italy. *Engin Geol* 58: 89–107. https://doi.org/10.1016/S0013-7952(00)00047-8

Guzzetti F, Peruccacci S, Rossi M, Stark CP (2007) Rainfall thresholds for the initiation of landslides in central and southern Europe. *Meteorog Atmos Phys* 98:239–267. https://doi.org/10.1007/s00703-007-0262-7

Hanssen AW, Kuipers WJA (1965) On the relationship between the frequency of rain and various meteorological parameters. Koninklijk Nederlands Meteorologisch Institut Meded Verhand 81:2–15

Hanssen-Bauer I, Førland EJ, Haddeland I, Hisdal H, Mayer S, Nesje A, Nilsen JEØ, Sandven S, Sandø AB, Sorteberg A, Ådlandsvik B (2017) Climate in Norway 2100, a knowledge base for climate adaptation. *NCCS report,* 1. Available at: http://www.miljodirektoratet.no/Documents/publikasjoner/M741/M741.pdf (last access: 20 November 2018)

Haque U, Blum P, da Silva PF, Andersen P, Pilz J, Chalov SR, Malet JP, Auflič MJ, Andres N, Poyiadji E, Lamas PC, Zhang W, Peshevski I, Pétursson HG (2016) Fatal landslides in Europe. *Landslides* 13:1545–1554. https://doi.org/10.1007/s10346-016-0689-3

Honda K, Aadit S, Rassarin C et al (2008) Landslide early warning system for rural community as an application of sensor Asia. In: *Proc of the World Conference on Agricultural Information,* Tokyo, pp 283–288

Hou, A. Y., and Coauthors, 2014: The Global Precipitation Measurement Mission. *Bull Amer Meteor Soc,* 95, 701–722, https://doi.org/10.1175/BAMS-D-13-00164.1

Huang R, Huang J, Ju N, He C, Li W (2013) WebGIS-based information management system for landslides triggered by Wenchuan earthquake. *Nat Hazards* 65:1507–1517. https://doi.org/10.1007/s11069-012-0424-x

Huffman GJ, Bolvin DT, Braithwaite D, Hsu K, Joyce R, Kidd C, Nelkin EJ, Sorooshian S, Tan J, Xie P (2018) NASA Global Precipitation Measurement (GPM) Integrated Multi-satellite Retrievals for GPM (IMERG). *Algorithm Theoretical Basis Document (ATBD), version 5.2,* NASA, 30 pp. Available at: https://pmm.nasa.gov/sites/default/files/document_files/IMERG_ATBD_V5.2_0.pdf (accessed 14 January 2019)

Hungr O, Evans SG, Bovis MJ, Hutchinson JN (2001) A review of the classification of landslides of the flow type. *Environmental & Engineering Geoscience,* VII (3), pp 221 – 238

Hungr O, Leroueil S, Picarelli L (2014) The Varnes classification of landslide types, an update. *Landslides,* 11:167:194. http://dx.doi.org/10.1007/s10346-013-0436-y

Hutchinson JN (1988) Morphological and Geotechnical parameters of Landslides in relation to Geology and Hydrogeology. State of the

art Report. In: *Proc of the 5th Intl Symposium on Landslides,* Lausanne, Vol. 1, pp 3– 35

Intrieri E, Gigli G, Casagli N, Nadim F (2013) Landslide early warning system: toolbox and general concepts. *Nat Hazards Earth Syst Sci* 13:85–90. https://doi.org/10.5194/nhess-13-85-2013

Intrieri E, Gigli G, Mugnai F et al (2012) Design and implementation of a landslide early warning system. *Eng Geol* 147:124–136. https://doi.org/10.1016/j.enggeo.2012.07.017

IPCC – Intergovernmental Panel on Climate Change, 2014. (2014) Synthesis Report. *Contribution of Working Groups I, II and III to the Fifth Assessment Report of the Intergovernmental Panel on Climate Change,* Geneva, Switzerland, 151 pp

Itakura Y, Fujii N, Sawada T (2000) Basic characteristics of ground vibration sensors for the detection of debris flow. *Phys Chem Earth Part B* 25(9):717–720. https://doi.org/10.1016/S1464-1909(00)00091-5

Jaedicke C, Lied K, Kronholm K (2009) Integrated database for rapid mass movements in Norway. *Nat Hazards Earth Syst Sci* 9:469–479. https://doi.org/10.5194/nhess-9-469-2009

Jaiswal P, van Westen CJ (2010) Estimating temporal probability for landslide initiation along transportation routes based on rainfall thresholds. *Geomorphology* 112:96–105. https://doi.org/10.1016/j.geomorph.2009.05.008

Jakob M, Owen T, Simpson T (2012) A regional real-time debris-flow warning system for the district of North Vancouver, Canada. *Landslides* 9(2):165–178. https://doi.org/10.1007/s10346-011-0282-8

Ju NP, Huang J, Huang RQ, He CY, Li YR (2015) A real-time monitoring and early warning system for landslide in southwest China. *J Mt Sci* 12(5):1219–1228. https://doi.org/10.1007/s11629-014-3307-7

Keys HJR, Green PM (2008) Ruapehu lahar New Zealand 18 March 2007: lessons for hazard assessment and risk mitigation 1995–2007. *J Disaster Res* 3:284–285. https://doi.org/10.20965/jdr.2008.p0284

Kirschbaum DB, Adler R, Hong Y, Hill S, Lerner-Lam A (2010) A global landslide catalog for hazard applications: Method, results, and limitations. *Nat Hazards* 52:561–575 https://doi.org/10.1007/s11069-009-9401-4

Kirschbaum DB, Stanley T, Zhou Y (2015) Spatial and temporal analysis of a global landslide catalog. *Geomorphology* 249:4–15. https://doi.org/10.1016/j.geomorph.2015.03.016

Kirschbaum, D. B., Huffman, G. J., Adler, R. F., Braun, S., Garrett, K., Jones, E., et al. (2016). NASA's remotely-sensed precipitation: A reservoir for applications users. *Bulletin of the American Meteorological Society,* 98(6), 1169–1184

Komac M, Jemec M, Šinigoj J et al (2008) Slope monitoring methods: a state-of-the-art report. *ClimChAlp project, Deliverable WP6,* 165 pp https://www.lfu.bayern.de/geologie/massenbewegungen/projekte/climchalp/doc/engl_report_6.pdf Accessed 23 October 2017

Kristensen L, Blikra LH (2011) Monitoring displacement on the Mannen rockslide in Western Norway. In: *Proc of the 2nd World Landslide Forum,* Rome, 8 pp

Kristensen L, Blikra LH, Hole J (2010) Åknes: state of instrumentation and data analysis. *Åknes report 02-2010,* County Governor - Fylkesmannenno, 43 pp

Krøgli IK, Devoli G, Colleuille H, Boje S, Sund M, Engen IK (2018) The Norwegian forecasting and warning service for rainfall- and snowmelt-induced landslides. *Nat Hazards Earth Syst Sci* 18:1427–1450. https://doi.org/10.5194/nhess-18-1427-2018

Lacasse S, Nadim F (2011) Learning to live with geohazards: from research to practice. In: *Proc of GeoRisk 2011,* 26–28 June, Atlanta, pp 64–116. https://doi.org/10.1061/41183(418)4

LaHusen R (1998) Detecting debris flows using ground vibrations. *USGS Fact Sheet 236–96,* USGS (ed) Li D, Meng S, Sun J (2016) Prediction analysis of large-scale landslides in the three gorges reservoir. EJGE 21:2053–2063

Loew S, Gischig V, Moore J, Keller-Signer A (2012) Monitoring of potentially catastrophic rockslides. In: *Proc of the 11th International & 2nd North Am Symp on Landslides,* Taylor & Francis, London, pp 101–116

Loew S, Gschwind S, Gischig V, Keller-Signer A, Valenti G (2016) Monitoring and early warning of the 2012 Preonzo catastrophic rockslope failure. *Landslides* 14:141–154. https://doi.org/10.1007/s10346-016-0701-y

Longobardi A, Buttafuoco G, Caloiero T, Coscarelli R (2016) Spatial and temporal distribution of precipitation in a Mediterranean area

(southern Italy). *Environ Earth Sci* 75:189. https://doi.org/10.1007/s12665-015-5045-8

Manconi A, Giordan D (2015) Landslide early warning based on failure forecast models: the example of the Mt. de la Saxe rockslide, northern Italy. *Nat Hazards Earth Syst Sci* 15(7):1639–1644. https://doi.org/10.5194/nhess-15-1639-2015

Massey C, Manville V, Hancox GT et al (2010) Out-burst flood (lahar) triggered by retrogressive landsliding, 18 March 2007 at Mt. Ruapehu, New Zealand—a successful early warning. *Landslides* 7:303–315. https://doi.org/10.1007/s10346-009-0180-5

McArdell BW, Bartelt P, Kowalski J (2007) Field observations of basal forces and fluid pore pressure in a debris flow. *Geophys Res Lett* 34:L07406. https://doi.org/10.1029/2006GL029183

Medina-Cetina Z, Nadim F (2008) Stochastic design of an early warning system. *Georisk* 2:223–236. https://doi.org/10.1080/17499510802086777

Melillo M, Brunetti MT, Peruccacci S, Gariano SL, Guzzetti F (2016) Rainfall thresholds for the possible landslide occurrence in Sicily (southern Italy) based on the automatic reconstruction of rainfall events. *Landslides* 13(1):165–172. https://doi.org/10.1007/s10346-015-0630-1

Metz CE (1978). Basic principles of ROC analysis. *Seminars in Nuclear Medicine* 8:283–298. https://doi.org/10.1016/S0001-2998(78)80014-2

Michoud C, Abellán A, Derron MH, Jaboyedoff M (2012) SafeLand deliverable 4.1.: review of techniques for landslide detection, fast characterization, rapid mapping and long-term monitoring. *European Project SafeLand, Grant Agreement No. 226479,* 401 pp. Available at: http://www.safeland-fp7.eu

Michoud C, Bazin S, Blikra LH, Derron MH, Jaboyedoff M (2013) Experiences from site-specific landslide early warning systems. *Nat Hazards Earth Syst Sci* 13:2659–2673. https://doi.org/10.5194/nhess-13-2659-2013

Mikkelsen PE (1996) Field instrumentation. In: Turner AK, Schuster RL (eds), *Landslides investigation and mitigation, special report 247,* National Academy Press, Washington, DC, pp 278–316

Moore R, McInnes RG (2011) Cliff instability and erosion management in Great Britain: a good practice guide. Published by Halcrow Group Ltd.

Moreno F, Froese CR (2010) ERCB/AGS roles and responsibilities manual for the Turtle Mountain Monitoring Project, Alberta. ERCB. http://ags.aer.ca/publications/OFR_2017_04.html. Accessed 23 October 2017

Nikolopoulos EI, Borga M, Creutin JD, Marra F (2015) Estimation of debris flow triggering rainfall: influence of rain gauge density and interpolation methods. *Geomorphology* 243:40–50. https://doi.org/10.1016/j.geomorph.2015.04.028

Nikolopoulos EI, Crema S, Marchi L, Marra F, Guzzetti F, Borga M (2014) Impact of uncertainty in rainfall estimation on the identification of rainfall thresholds for debris flow occurrence. *Geomorphology* 221:286–297. https://doi.org/10.1016/j.geomorph.2014.06.015

Olivieri W, Lovisolo M, Crosta GB (2012) Continuous geotechnical monitoring for alert thresholds and hazard management. In: *Landslides and Engineered Slopes,* CRC Press, Taylor and Francis Group, pp. 1929–1934

OMIV (2017) Available at http://omiv2.u-strasbg.fr/monitored_lavalette.php. Accessed 23 October 2017

PCEM (2018) Available at https://www.piercecountywa.org/5888/Lahar-Warning-System. Accessed 05 September 2018

Pecoraro G, Calvello M (2016) Allertamento per il rischio da frana in Italia a scala regionale: analisi della normativa vigente. *Report project PRIN 2011 "Mitigazione del rischio da frana mediante interventi sostenibili",* 142 pp., in Italian. Available at: https://prinrischiodafrana.wordpress.com/interventi-di-mitigazione-non-strutturali/

Pecoraro G, Calvello M, Piciullo L (2018) Monitoring strategies for local landslide early warning systems. *Landslides,* Published online 24 October 2018. https://doi.org/10.1007/s10346-018-1068-z

Peruccacci S, Brunetti MT, Gariano SL, Melillo M, Rossi M, Guzzetti F (2017) Rainfall thresholds for possible landslide occurrence in Italy. *Geomorphology* 290:39–57. https://doi.org/10.1016/j.geomorph.2017.03.031

Petley D (2012) Global patterns of loss of life from landslides. Geology 40 (10):927–930. https://doi.org/10.1130/G33217.1

Piciullo L, Calvello M, Cepeda JM (2018) Territorial early warning systems for rainfall induced landslides. *Earth Sci Rev* 179:228–247. https://doi.org/10.1016/j.earscirev.2018.02.013

Piciullo L, Dahl M-P, Devoli G, Colleuille H, Calvello M (2017a) Adapting the EDuMaP method to test the performance of the Norwegian early warning system for weather-induced landslides. *Nat Hazards Earth Syst Sci* 17:817–831. https://doi.org/10.5194/nhess-17-817-2017

Piciullo L, Gariano SL, Melillo M, Brunetti MT, Peruccacci S, Guzzetti F, Calvello M (2017b) Definition and performance of a threshold-based regional early warning model for rainfall-induced landslides. *Landslides* 14:995–1008. https://doi.org/10.1007/s10346-016-0750-2

Pierson TC, Wood NJ, Driedger CL (2014) Reducing risk from lahar hazards: concepts, case studies, and roles for scientists. *J Appl Volcanol* 3:1–25. https://doi.org/10.1186/s13617-014-0016-4

Read RS, Langenberg W, Cruden D et al (2005) Frank Slide a century later: the Turtle Mountain monitoring project. In: Hungr O, Fell R, Couture RR, Eberhardt E (eds), *Landslide risk management,* Balkema, Rotterdam, pp 713–723

Robbins JC (2016) A probabilistic approach for assessing landslide-triggering event rainfall in Papua New Guinea, using TRMM satellite precipitation estimates. *J Hydrol* 541:296–309. https://doi.org/10.1016/j.jhydrol.2016.06.052

Rosi A, Lagomarsino D, Rossi G, Segoni S, Battistini A, Casagli N (2015) Updating EWS rainfall thresholds for the triggering of landslides. *Nat Hazards* 78:297–308. https://doi.org/10.1007/s11069-015-1717-7

Rossi M, Luciani S, Valigi D, Kirschbaum D, Brunetti MT, Peruccacci S, Guzzetti F (2017) Statistical approaches for the definition of landslide rainfall thresholds and their uncertainty using rain gauge and satellite data. *Geomorphology* 285:16–27. https://doi.org/10.1016/j.geomorph.2017.02.001

Sassa K, Luciano P, Yin YP (2009) Monitoring, prediction and early warning. In: *Proc of the 1st World Landslide Forum,* Tokyo, pp 351–375

Sättele M, Bründl M, Straub D (2012) A classification of warning system for natural hazards. In: *Proc of the 10th International Probabilistic*

Workshop, Institut für Geotechnik der Universität Stuttgart, pp 257– 270

Savvaidis PD (2003) Existing landslide monitoring systems and techniques. In: *Proc of the Conference from Stars to Earth and Culture,* Thessaloniki, Greece, pp 242–258

Scaioni M, Longoni L, Melillo V, Papini M (2014) Remote sensing for landslide investigations: an overview of recent achievements and perspectives. *Remote Sens* 6(10):9600–9652. https://doi.org/10.3390/rs6109600

Segoni S, Piciullo L, Gariano SL (2018a) A review of the recent literature on rainfall thresholds for landslide occurrence. *Landslides* 15:1483–1501. https://doi.org/10.1007/s10346-018-0966-4

Segoni S, Rosi A, Fanti R, Gallucci A, Monni A, Casagli N (2018b) A Regional-Scale Landslide Warning System Based on 20 Years of Operational Experience. *Water* 10, 1297. https://doi.org/10.3390/w10101297

Segoni S, Rosi A, Rossi G, Catani F, Casagni N (2014) Analysing the relationship between rainfalls and landslides to define a mosaic of triggering thresholds for regional scale warning systems. *Nat Hazards Earth Syst Sci* 14:2637–2648. https://doi.org/10.5194/nhess-14-2637-2014

Skempton AW (1953) The colloidal activity of clays. In*: Proc of the 3rd International Conference on Soil Mechanics and Foundation Engineering,* Zurich, pp 7-61

Song K, Wang F, Yi Q, Lu S (2018) Landslide deformation behavior influenced by water level fluctuations of the Three Gorges Reservoir (China). *Eng Geol* 247:58–68. https://doi.org/10.1016/j.enggeo.2018.10.020

Stähli M, Sättele M, Huggel C, McArdell BW, Lehmann P, van Herwijnen A, Berne A, Schleiss M, Ferrari A, Kos A, Or D, Springman SM (2015) Monitoring and prediction in early warning systems for rapid mass movements. *Nat Hazards Earth Syst Sci* 15:905–917. https://doi.org/10.5194/nhess-15-905-2015

Stumpf A, Kerle N, Malet JP (2012) SafeLand deliverable 4.4: guidelines for the selection of appropriate remote sensing technologies for monitoring different types of landslides. *European Project SafeLand, Grant Agreement No. 226479,* 91 pp. Available at: http://www.safeland-fp7.eu

Takeshi T (2011) Evolution of debris-flow monitoring methods on Sakurajima. *Int J Erosion Cont Eng* 4:21–31. https://doi.org/10.13101/ijece.4.21

Tamburini A (2005) EYDENET: a real time decision support system. In: *Conference presentation, at RiskHydrogeo,* Aosta, Italy

Tamburini A, Martelli D (2006) Displacement and rainfall threshold values for large landslide forecast in real time: the example of the "Becca di Nona" landslide (Aosta). In: *Conference presentation at RiskYdrogeo,* Saint Vincent, Italy

Thiebes B (2011) Landslide analysis and early warning – local and regional case study in the Swabian Alb, Germany. *PhD dissertation,* University of Vienna

Thiebes B, Bell R, Glade T, Jäger S, Mayer J, Anderson M, Holcombe L (2014) Integration of a limit-equilibrium model into a landslide early warning system. *Landslides* 11(5):859–875. https://doi.org/10.1007/s10346-013-0416-2

Thiebes B, Glade T (2016) Landslide early warning systems – fundamental concepts and innovative application. In: Aversa S, Cascini L, Picarelli L, Scavia C (eds), *Landslides and engineered slopes. Experience, theory and practice,* CRC Press, Napoli, pp 1903–1911

Thiebes B, Glade T, Bell R (2012) Landslide analysis and integrative early warning-local and regional case studies. In: *Proc of the 11th International & 2nd North American Symposium on Landslides,* Eberhardt E, Froese CR, Turner AK, Leroueil S (eds), Taylor & Francis, London, pp 1915–1921

Tofani V, Segoni S, Catani F, Casagli N (2012) SafeLand deliverable 4.5: evaluation report on innovative monitoring and remote sensing methods and future technology. *European Project SafeLand, Grant Agreement No. 226479,* 280 pp. Available at: http://www.safeland-fp7.eu

UNISDR (2006) Available at: http://www.unisdr.org/2006/ppew/info-resources/.https://volcanoes.usgs.gov/volcanoes/mount_rainier/. Accessed 05 September 2018

USGS (2018) Available at: https://volcanoes.usgs.gov/volcanoes/mount_rainier/. Accessed 05 September 2018

Varnes DJ (1978). Slope Movement Types and Processes. *Special Report 176: Landslides: Analysis and Control,* Schuster RL, Krizek RJ (eds), TRB, National Research Council, Washington, DC, pp 11–33

Varnes DJ (1984) Landslide hazard zonation: A review of principles and practice. *The International Association of Engineering Geology Commission on Landslides and Other Mass Movements 1984. Natural Hazards,* pp 3-63. Paris, France. UNESCO

Vennari C, Parise M, Santangelo N, Santo A (2016) A database on flash flood events in Campania, southern Italy, with an evaluation of their spatial and temporal distribution, *Nat Hazards Earth Syst Sci* 16:2485–2500. https://doi.org/10.5194/nhess16-2485-2016

Wang FW, Zhang YM, Huo ZT, Peng X, Araiba K, Wang G (2008) Movement of the Shuping landslide in the first four years after the initial impoundment of the Three Gorges Dam Reservoir, China. *Landslides* 5:321–329. https://doi.org/10.1007/s10346-008-0128-1

Wang S (2009) Time prediction of the Xintan landslide in Xiling Gorge, the Yangtze River. In: *Landslide disaster mitigation in Three Gorges Reservoir,* Wang F, Li T (eds), China, environmental science and engineering. Springer, Berlin, pp 411–431

Wilks DS (1995) Statistical methods in the atmospheric sciences. Academic Press, USA, 467 pp.

Yin HY, Huang CJ, Chen CY et al (2011) The present development of debris flow monitoring technology in Taiwan - a case study presentation. *Ital J Eng Geol Environ, Special issue,* pp. 307–314. https://doi.org/10.4408/IJEGE.2011-03.B-068

Yin Y, Wang H, Gao Y, Li X (2010) Real-time monitoring and early warning of landslides at relocated Wushan Town, the Three Gorges Reservoir, China. *Landslide*s 7:339–349. https://doi.org/10.1007/s10346-010-0220-1

Zhuang JQ, Iqbal J, Peng JB, Liu TM (2014) Probability prediction model for landslide occurrences in Xi'an, Shaanxi Province, China. *J Mt Sci* 11(2):345–359. https://doi.org/10.1007/s11629-013-2809-z

APPENDIX

A) LANDSLIDE EVENTS OCCURRED IN EMILIA-ROMAGNA AND CAMPANIA REGIONS

This Appendix reports the areal landslide events (ALEs) and the single landslide events (SLEs) categorized as weather-induced landslides in the FraneItalia database and used for the analyses carried out in Emilia-Romagna (Section 5.5) and Campania (Section 5.6). A total of 102 weather-induced landslide events occurred in Emilia-Romagna from March 2014 to December 2015, 24 of them classified as ALEs (Table A.1) and 78 as SLEs (Table A.2). On the other hand, Campania was affected from 143 weather-induced landslide events from March 2014 to December 2017, differentiated between 19 ALEs (Table A.3) and 124 SLEs (Table A.4).

The information reported for each ALE are: the identification code *(ID),* whose format is designed to highlight the landslide event category and the initial date of the event; the number of landslides; the confidence descriptor *Ndi* to differentiate between records for which the number of events is reported in the news reports or estimated by the operator; the county(-ies) affected from the landslides; the warning zone interested by the ALE.

Regarding the SLEs, the following information are included: the identification code *(ID)*; the geographic coordinates (WGS84 datum); the confidence descriptor *Sdi* associated to the accuracy of the geographic coordinates: certain, approximated, and municipality; the warning zone interested by the SLE.

Table A.1 Main information on ALEs occurred in Emilia-Romagna between March 2014 and December 2015

ID	Number	Ndi	County(-ies)	Warning zone
2014-04-03_ALE_C2_001	2	reported	Modena	Emil-E
2014-04-04_ALE_C3_001	3	reported	Reggio nell'Emilia	Emil-F
2014-04-28_ALE_C3_001	2	reported	Forlì-Cesena	Emil-B
2014-05-03_ALE_C3_002	9	reported	Parma	Emil-G
2014-05-16_ALE_C3_001	4	reported	Reggio nell'Emilia	Emil-E
2014-07-09_ALE_C3_002	4	estimation	Rimini	Emil-B
2014-10-13_ALE_C3_001	3	estimation	Piacenza	Emil-G
2014-10-15_ALE_C3_001	5	estimation	Parma	Emil-G
2014-11-17_ALE_C3_001	2	estimation	Forlì-Cesena	Emil-A
2015-02-25_ALE_C2_001	9	reported	Forlì-Cesena, Ravenna	Emil-A
2015-02-26_ALE_C2_001	2	reported	Parma	Emil-G
2015-02-26_ALE_C3_001	2	reported	Forlì-Cesena	Emil-A
2015-03-03_ALE_C3_001	2	reported	Modena	Emil-E
2015-03-05_ALE_C3_002	3	reported	Forlì-Cesena	Emil-A
2015-03-07_ALE_C3_001	3	reported	Rimini	Emil-B
2015-03-18_ALE_C3_001	2	reported	Rimini	Emil-B
2015-03-18_ALE_C3_002	2	estimation	Bologna	Emil-C
2015-03-20_ALE_C2_001	4	reported	Reggio nell'Emilia	Emil-F
2015-03-20_ALE_C3_001	2	estimation	Piacenza	Emil-G
2015-03-26_ALE_C3_003	5	estimation	Modena	Emil-E
2015-03-28_ALE_C3_001	4	reported	Rimini	Emil-B
2015-04-28_ALE_C3_001	4	reported	Modena	Emil-E
2015-09-14_ALE_C3_001	5	estimation	Piacenza	Emil-G
2015-11-20_ALE_C3_001	2	reported	Modena	Emil-E

Table A.2 Main information on SLEs occurred in Emilia-Romagna between March 2014 and December 2015

ID	Latitude	Longitude	Sdi	Warning zone
2014-03-19_SLE_C3_002	44.2140	11.2364	A	Emil-C
2014-04-02_SLE_C3_001	44.2693	10.9470	M	Emil-E
2014-04-04_SLE_C3_004	44.4982	10.4641	A	Emil-E
2014-04-04_SLE_C3_005	44.6488	10.9201	M	Emil-E
2014-04-26_SLE_C3_001	44.3762	10.5625	M	Emil-E
2014-05-02_SLE_C3_006	44.8747	9.3844	M	Emil-H
2014-05-09_SLE_C2_001	44.0064	11.9434	A	Emil-A
2014-05-12_SLE_C3_001	44.0444	12.1463	A	Emil-B
2014-05-14_SLE_C3_003	44.4796	11.0375	M	Emil-E
2014-05-15_SLE_C3_001	44.2140	11.2364	M	Emil-C
2014-05-20_SLE_C3_001	44.4843	10.3393	M	Emil-E
2014-06-02_SLE_C3_002	44.4839	10.3375	C	Emil-E
2014-06-09_SLE_C3_001	43.9565	12.1971	M	Emil-A
2014-06-26_SLE_C3_002	44.4372	10.6916	C	Emil-E
2014-07-30_SLE_C3_002	44.4548	10.5196	M	Emil-E
2014-08-03_SLE_C3_002	44.6676	10.8982	C	Emil-F
2014-09-19_SLE_C3_001	44.2904	11.8737	C	Emil-B
2014-10-10_SLE_C3_004	44.6114	9.3188	C	Emil-G
2014-10-13_SLE_C3_004	44.4340	10.2285	A	Emil-E
2014-11-11_SLE_C3_001	44.5370	10.4810	C	Emil-E
2014-12-15_SLE_C3_001	44.8377	10.0111	C	Emil-G
2015-02-04_SLE_C2_001	43.9833	12.4215	C	Emil-B
2015-02-06_SLE_C3_001	44.1333	12.2333	C	Emil-B
2015-02-07_SLE_C3_003	44.3533	11.7141	C	Emil-D
2015-02-07_SLE_C3_004	44.1041	11.9850	C	Emil-A
2015-02-11_SLE_C3_001	44.2225	12.0408	A	Emil-B
2015-02-14_SLE_C3_001	44.4333	10.4000	C	Emil-E
2015-02-19_SLE_C3_002	44.2154	11.2329	M	Emil-C
2015-02-21_SLE_C3_004	44.0794	11.7436	M	Emil-A
2015-02-21_SLE_C3_005	44.2994	11.6809	A	Emil-C
2015-02-24_SLE_C3_004	44.2303	10.6528	M	Emil-E
2015-02-24_SLE_C3_005	44.3463	10.9935	M	Emil-C
2015-02-24_SLE_C3_006	44.5403	10.7827	M	Emil-E
2015-02-26_SLE_C3_001	44.2128	11.5046	M	Emil-C
2015-02-27_SLE_C2_002	44.4995	10.7739	A	Emil-E
2015-02-27_SLE_C3_002	44.1131	11.9794	A	Emil-A

2015-02-27_SLE_C3_004	43.9862	11.7724	C	Emil-B
2015-02-27_SLE_C3_005	44.2146	11.6190	A	Emil-C
2015-02-28_SLE_C2_001	43.9863	12.4377	A	Emil-B
2015-02-28_SLE_C3_001	44.6009	10.5460	A	Emil-F
2015-02-28_SLE_C3_002	44.5262	10.6093	A	Emil-E
2015-03-02_SLE_C3_002	44.4547	10.5198	M	Emil-E
2015-03-02_SLE_C3_003	44.5092	9.9895	M	Emil-G
2015-03-04_SLE_C3_003	44.3459	10.9960	A	Emil-C
2015-03-04_SLE_C3_004	44.3336	10.8140	A	Emil-E
2015-03-05_SLE_C3_003	44.2689	10.9484	M	Emil-E
2015-03-05_SLE_C3_004	44.1368	12.2425	M	Emil-B
2015-03-08_SLE_C3_001	44.4146	10.6845	A	Emil-E
2015-03-17_SLE_C2_001	44.0499	12.2024	A	Emil-B
2015-03-18_SLE_C3_002	43.8958	12.6307	A	Emil-B
2015-03-19_SLE_C3_003	44.2427	10.9200	C	Emil-E
2015-03-26_SLE_C3_002	43.81773	12.2650	M	Emil-A
2015-03-26_SLE_C3_006	44.1333	12.2247	M	Emil-B
2015-03-26_SLE_C3_007	44.4372	10.6916	M	Emil-E
2015-03-27_SLE_C2_001	44.5772	10.6549	A	Emil-E
2015-03-27_SLE_C3_003	44.4372	10.6916	M	Emil-E
2015-03-27_SLE_C3_004	44.3651	11.2154	A	Emil-C
2015-03-27_SLE_C3_005	44.2962	11.7992	C	Emil-B
2015-03-30_SLE_C3_002	44.5032	10.9431	M	Emil-E
2015-04-02_SLE_C3_001	44.6200	10.4680	A	Emil-C
2015-04-09_SLE_C3_003	44.2600	10.9390	C	Emil-E
2015-04-11_SLE_C3_001	44.8000	10.3270	A	Emil-G
2015-04-15_SLE_C3_001	44.5100	11.8200	C	Emil-D
2015-04-20_SLE_C3_001	44.2695	10.9445	A	Emil-E
2015-04-20_SLE_C3_002	44.2383	12.2655	C	Emil-B
2015-04-21_SLE_C3_001	44.0980	12.1973	A	Emil-A
2015-04-22_SLE_C3_001	44.3447	10.9963	C	Emil-C
2015-05-04_SLE_C3_001	44.2355	10.7498	A	Emil-E
2015-05-12_SLE_C3_001	44.0069	11.9383	M	Emil-A
2015-05-29_SLE_C2_001	44.0878	12.2077	C	Emil-B
2015-10-01_SLE_C3_003	44.5167	10.6940	C	Emil-E
2015-10-29_SLE_C2_001	44.1493	12.1924	A	Emil-B
2015-11-16_SLE_C3_003	44.5388	10.5833	C	Emil-E
2015-11-22_SLE_C3_001	44.2073	10.7972	A	Emil-E
2015-12-01_SLE_C3_001	43.8391	11.9656	C	Emil-A

2015-12-07_SLE_C3_001	44.7487	10.9760	A	Emil-E
2015-12-15_SLE_C3_001	44.9212	10.6544	C	Emil-F
2015-12-15_SLE_C3_002	43.8261	11.9589	A	Emil-A

Table A.3 Main information on ALEs occurred in Campania between March 2014 and December 2017

ID	Number	Ndi	County(-ies)	Warning zone
2014-06-15_ALE_C2_001	1	reported	Avellino	Camp-3
2014-06-16_ALE_C3_001	2	estimation	Salerno	Camp-5
2014-07-30_ALE_C1_001	5	reported	Avellino, Napoli, Salerno	Camp-3
2014-09-01_ALE_C3_001	5	reported	Avellino	Camp-3
2014-09-12_ALE_C3_002	4	estimation	Salerno	Camp-6
2015-10-07_ALE_C3_001	3	estimation	Avellino	Camp-3
2015-10-11_ALE_C2_001	4	reported	Napoli	Camp-1
2015-10-19_ALE_C2_001	5	reported	Benevento	Camp-4
2015-10-20_ALE_C3_001	3	estimation	Salerno	Camp-3
2015-12-04_ALE_C3_001	8	estimation	Salerno	Camp-3
2015-12-04_ALE_C3_002	5	estimation	Salerno	Camp-5
2016-03-12_ALE_C3_002	5	estimation	Avellino	Camp-3
2017-09-02_ALE_C3_001	2	estimation	Salerno	Camp-3
2017-09-11_ALE_C3_001	5	estimation	Avellino, Salerno	Camp-3
2017-09-11_ALE_C3_001	5	estimation	Caserta	Camp-1
2017-11-07_ALE_C2_001	3	estimation	Napoli	Camp-1
2017-11-07_ALE_C3_002	5	estimation	Salerno, Napoli	Camp-3
2017-11-07_ALE_C3_003	2	estimation	Salerno	Camp-7
2017-11-07_ALE_C3_001	3	estimation	Napoli	Camp-3

Table A.4 Main information on SLEs occurred in Campania between March 2014 and December 2017

ID	Latitude	Longitude	Sdi	Warning zone
2014-04-09_SLE_C3_002	40.7974	14.0438	C	Camp-1
2014-05-05_SLE_C3_006	40.6329	15.3813	M	Camp-7
2014-06-15_SLE_C3_001	41.0035	14.9268	C	Camp-4
2014-06-15_SLE_C3_002	40.6332	15.3652	M	Camp-7
2014-06-18_SLE_C3_001	41.0305	14.6173	M	Camp-3
2014-06-19_SLE_C3_001	40.6644	15.1065	M	Camp-5
2014-07-22_SLE_C2_001	40.8518	14.2681	M	Camp-1
2014-07-30_SLE_C3_001	40.8232	14.7085	C	Camp-1
2014-09-07_SLE_C3_002	41.1200	14.3584	C	Camp-2
2014-09-11_SLE_C3_002	40.6857	14.5844	C	Camp-3
2014-09-11_SLE_C3_003	40.7935	14.0542	C	Camp-1
2014-09-13_SLE_C3_001	40.7170	14.6165	C	Camp-3
2014-09-21_SLE_C3_001	40.7389	15.0534	C	Camp-5
2014-11-14_SLE_C3_004	40.6594	14.4174	C	Camp-3
2014-11-22_SLE_C3_001	40.5462	14.2371	C	Camp-1
2014-12-04_SLE_C3_004	41.4653	14.1469	A	Camp-2
2014-12-28_SLE_C3_001	40.6112	14.5346	C	Camp-3
2014-12-29_SLE_C3_002	40.2114	15.4273	A	Camp-8
2015-01-03_SLE_C3_001	40.4375	15.0532	A	Camp-6
2015-01-24_SLE_C3_002	40.1400	15.1857	A	Camp-6
2015-01-26_SLE_C3_002	40.6697	14.7091	C	Camp-3
2015-01-27_SLE_C3_001	40.1764	15.4258	C	Camp-8
2015-02-01_SLE_C3_002	40.6277	14.3736	C	Camp-3
2015-02-01_SLE_C3_003	40.1500	15.6166	C	Camp-8
2015-02-02_SLE_C3_001	40.6500	14.6166	C	Camp-3
2015-02-04_SLE_C3_003	40.8410	14.2276	C	Camp-1
2015-02-04_SLE_C3_004	40.7500	14.5000	C	Camp-3
2015-02-04_SLE_C3_005	41.1333	14.7833	C	Camp-4
2015-02-04_SLE_C3_006	40.8702	14.2378	C	Camp-1
2015-02-05_SLE_C3_003	40.1000	15.5833	A	Camp-8
2015-02-09_SLE_C3_002	40.2833	15.2166	C	Camp-6
2015-02-10_SLE_C3_001	40.6214	14.5718	A	Camp-3
2015-02-10_SLE_C3_003	40.6666	14.4333	C	Camp-3
2015-02-11_SLE_C3_002	40.7000	14.9833	C	Camp-5
2015-02-12_SLE_C3_004	40.0223	15.3292	A	Camp-8
2015-02-19_SLE_C3_001	40.5480	14.2466	C	Camp-1

2015-02-25_SLE_C1_001	40.7244	13.9310	A	Camp-1
2015-03-02_SLE_C3_004	40.7369	13.8566	A	Camp-1
2015-03-05_SLE_C3_002	40.8345	14.2289	A	Camp-1
2015-04-01_SLE_C3_001	40.8067	14.1985	A	Camp-1
2015-04-24_SLE_C3_001	40.6633	14.4254	M	Camp-3
2015-04-27_SLE_C3_001	40.6985	14.9715	C	Camp-5
2015-05-12_SLE_C3_002	40.5813	15.1838	M	Camp-6
2015-07-27_SLE_C3_001	40.5414	14.2249	A	Camp-1
2015-08-10_SLE_C1_001	40.0220	15.3287	C	Camp-8
2015-09-28_SLE_C3_002	40.0943	15.4050	M	Camp-8
2015-10-12_SLE_C3_001	40.0957	15.4005	A	Camp-8
2015-10-19_SLE_C3_001	41.1442	14.7733	A	Camp-4
2015-10-20_SLE_C2_001	41.1951	14.6665	M	Camp-4
2015-11-13_SLE_C3_001	40.9303	14.3498	A	Camp-1
2015-11-29_SLE_C2_001	41.0441	14.9947	A	Camp-4
2016-02-11_SLE_C3_001	40.0705	15.6326	C	Camp-8
2016-02-11_SLE_C3_003	40.4658	15.1499	A	Camp-6
2016-02-14_SLE_C3_001	40.6842	14.7220	A	Camp-3
2016-02-14_SLE_C3_002	40.6679	14.7278	M	Camp-3
2016-02-14_SLE_C3_003	40.8225	14.0743	C	Camp-1
2016-02-14_SLE_C3_004	40.8228	14.0765	C	Camp-1
2016-02-29_SLE_C3_004	41.2033	14.4655	A	Camp-2
2016-03-06_SLE_C3_001	40.4242	15.4368	C	Camp-7
2016-03-08_SLE_C3_003	40.6974	14.7768	C	Camp-3
2016-03-25_SLE_C3_002	40.0087	15.3398	C	Camp-8
2016-04-08_SLE_C3_001	41.4002	14.8106	A	Camp-4
2016-04-24_SLE_C3_001	40.7753	14.7293	A	Camp-3
2016-04-26_SLE_C3_001	41.2067	14.7366	A	Camp-4
2016-04-27_SLE_C3_002	40.4163	15.2319	A	Camp-6
2016-05-11_SLE_C3_001	40.9359	14.7290	C	Camp-3
2016-05-11_SLE_C3_002	41.2979	14.6951	A	Camp-4
2016-07-25_SLE_C3_002	40.9433	14.9396	A	Camp-3
2016-08-02_SLE_C3_003	41.3621	14.8339	M	Camp-4
2016-08-02_SLE_C3_004	40.6468	14.7006	M	Camp-3
2016-09-11_SLE_C3_002	41.2497	15.2491	M	Camp-4
2016-09-18_SLE_C3_001	41.0708	15.0597	M	Camp-4
2016-09-18_SLE_C3_002	40.9152	14.7897	M	Camp-3
2016-09-19_SLE_C2_001	40.8052	14.0491	A	Camp-1
2016-09-20_SLE_C3_001	40.7000	14.7055	M	Camp-3

2016-09-27_SLE_C3_001	40.7593	14.0232	A	Camp-1
2016-10-03_SLE_C3_001	40.6666	14.4333	M	Camp-3
2016-10-05_SLE_C3_001	40.8533	14.5579	A	Camp-3
2016-10-10_SLE_C3_001	40.5558	14.2514	A	Camp-1
2016-10-19_SLE_C3_001	40.3499	14.9914	M	Camp-6
2016-10-24_SLE_C3_001	41.0113	14.0646	M	Camp-1
2016-10-30_SLE_C3_001	40.6957	14.7250	A	Camp-3
2016-11-13_SLE_C3_001	41.3666	14.3833	M	Camp-2
2016-12-06_SLE_C3_001	40.0800	15.3300	A	Camp-8
2016-12-10_SLE_C3_001	40.6282	14.4788	A	Camp-3
2016-12-21_SLE_C3_001	40.6825	14.5363	C	Camp-3
2017-01-03_SLE_C3_001	40.3486	14.9912	M	Camp-6
2017-01-18_SLE_C3_003	41.1333	14.7833	M	Camp-4
2017-01-20_SLE_C3_001	41.3500	14.8166	M	Camp-4
2017-02-25_SLE_C3_001	41.1902	14.7405	A	Camp-4
2017-02-26_SLE_C3_001	41.1599	15.0999	C	Camp-4
2017-03-08_SLE_C3_004	40.1785	15.4410	A	Camp-8
2017-03-09_SLE_C3_002	41.1564	15.0925	A	Camp-4
2017-04-04_SLE_C3_002	40.6352	14.4185	A	Camp-3
2017-05-22_SLE_C3_001	40.4586	15.5664	A	Camp-7
2017-07-13_SLE_C3_001	40.0462	15.3264	C	Camp-8
2017-07-21_SLE_C3_001	40.7593	14.0233	C	Camp-1
2017-07-26_SLE_C2_001	40.4342	15.4637	M	Camp-7
2017-07-31_SLE_C3_002	40.6333	14.4000	M	Camp-3
2017-08-03_SLE_C3_001	40.4333	15.4666	A	Camp-7
2017-08-17_SLE_C3_001	41.0805	14.3576	A	Camp-2
2017-08-18_SLE_C3_001	40.8590	14.2017	A	Camp-1
2017-09-02_SLE_C2_001	41.3388	14.5086	M	Camp-2
2017-09-08_SLE_C2_001	40.5505	14.2425	A	Camp-1
2017-09-08_SLE_C2_002	40.5488	14.2370	A	Camp-1
2017-09-12_SLE_C3_001	40.6887	14.4664	C	Camp-3
2017-09-19_SLE_C3_004	40.5562	14.2486	C	Camp-1
2017-09-20_SLE_C3_003	40.0529	15.6326	A	Camp-8
2017-09-22_SLE_C3_001	40.8127	14.2018	A	Camp-1
2017-09-26_SLE_C3_002	40.4361	15.0578	A	Camp-6
2017-09-27_SLE_C2_001	40.6445	14.6084	A	Camp-3
2017-10-01_SLE_C3_001	40.5556	14.2528	C	Camp-1
2017-10-17_SLE_C3_001	40.8221	14.7571	C	Camp-3
2017-10-22_SLE_C3_002	40.8224	14.7563	A	Camp-3

2017-10-23_SLE_C3_001	40.7626	14.6980	A	Camp-3
2017-11-10_SLE_C3_001	40.7980	14.0502	A	Camp-1
2017-11-10_SLE_C3_003	40.3789	15.3781	A	Camp-6
2017-11-10_SLE_C3_004	40.7617	14.6936	A	Camp-3
2017-11-11_SLE_C2_001	40.6960	14.4816	A	Camp-3
2017-11-12_SLE_C3_001	40.7872	14.3680	M	Camp-1
2017-11-30_SLE_C3_001	40.6894	14.6179	C	Camp-3
2017-11-30_SLE_C3_003	40.8293	14.8270	M	Camp-3
2017-12-17_SLE_C3_001	41.3833	14.0833	C	Camp-2
2017-12-18_SLE_C3_001	40.6111	14.5333	A	Camp-3

B) EXAMPLE OF A GOOGLE EARTH ENGINE SCRIPT FOR ANALYZING THE SATELLITE RAINFALL DATA

A script has been created and run through the Earth Engine Code Editor (*https://code.earthengine.google.com/*) in order to analyze the satellite rainfall data over each territorial unit (see Section 5.3.2). An example referring to the weather warning zone *Camp-8* in Campania region is reported herein:

```
// import the ImageCollection containing the satellite rainfall data from the GPM mission
var rain = ee.ImageCollection("NASA/GPM_L3/IMERG_V05");

// import the FeatureCollection derived from the shapefile of the weather warning zones of the Campania region
var Campania = ee.FeatureCollection('ft:1uguZfrRtmXZidhFpbzEL23v0xFcKLNLKhJM_5xDQ', 'geometry');

// select the weather warning zone Camp-8
var warningzone = Campania.filterMetadata('COD_AREA', 'equals', 'Camp-8');

// visualization options
Map.setCenter(13, 40, 7);
Map.addLayer(warningzone, {'color': 'FF0001'});
print (warningzone);

// filter the rainfall data by specifying the date and the rainfall variable
var rain = ee.ImageCollection("NASA/GPM_L3/IMERG_V05")
    .filterDate('2014-03-12', '2018-01-01')
    .select('precipitationCal');

// create and print a chart including the mean of the satellite rainfall data over the territorial unit
var mean = ui.Chart.image.series(rain, warningzone, ee.Reducer.mean(), 200);
```

```
print(mean);

// visualization options
Map.addLayer(rain, {opacity: 0.5, min: [0], max: [1], palette: 'FFFFFF,
0000FF'}, 'precipitationCal')
```

C) FACT SHEETS OF THE 30 NORWEGIAN HYDROLOGICAL BASINS

The multi-scalar warning model described in Chapter 6 has been calibrated and validated considering as test areas 30 Norwegian hydrological basins. A series of fact sheets have been prepared in order to provide a description of the test areas considered in this study. Each fact sheet can be divided into 5 main parts:

- *main characteristics,* showing a Quaternary deposit map of the shallow soil layers where the weather-induced landslides occurred and the piezometers available are also reported as well as a map indicating in which part of Norway the hydrological basin is situated (i.e., SE: southeast; SW: southwest; CW: central west; NW: northwest);
- *shallow soil layers,* indicating the surface of each hydrological basin and the soil profile in the shallow layers (i.e., loose sediments, no landslide materials, or bare rocks);
- *weather-induced landslides,* reporting the main features of the weather-induced landslides occurred within each basin: the date of occurrence of the landslide, a code indicating the type of landslide in the National landslide database (i.e., 133: slush flows: 140: landslides in soils, not specified: 141: clay slides; 142: debris flows: 143: mudslides: 144: debris avalanches: 160: soil slides in artificial slopes); the spatial accuracy of the landslide record (n.r.: "not reported" indicates that this information is not available in the database for some records);
- *pore water pressure data series,* representing the pore water pressure measurements available in the period of analysis for each hydrological basin. The depth of installation of the piezometers is also indicated;
- *correlation matrices,* listing the landslide events occurred in relation to the warning events issued by applying the regional warning model applied in the national LEWS and the multi-scalar warning model developed in Chapter 6.

FYKANÅGA basin (ID: 980) – CW2

Main characteristics:

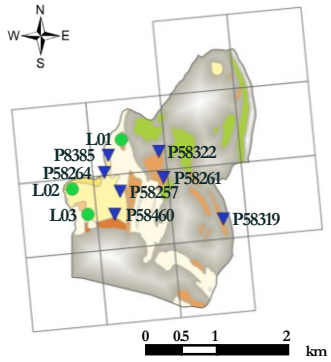

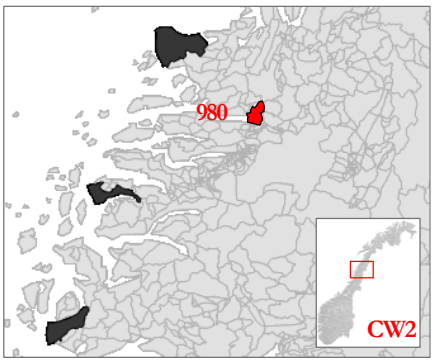

Quaternary deposits

- Moraine material, thick
- Moraine material, thin
- Terminal moraine
- Glaciofluvial deposits
- Weathered material
- Marine and fjord deposits, continuous
- Marine and fjord deposits, thin
- Marine and fjord deposits, thick
- No landslide materials
- Bare rocks

Legend

- xgeo grid
- Weather-induced landslides in soils (2013/01 – 2017/06)
- Piezometers

Shallow soil layers:

Area [km²]: ***5.58***
Loose sediments [%]: ***23***
No landslide materials [%]: ***14***
Bare rocks [%]: ***63***

Weather-induced landslides:

ID	*Date*	*Type*	*Spatial accuracy*
L01	2013/11/16	140	exact
L02	2014/03/12	160	exact
L03	2017/01/25	160	n.r.

FYKANÅGA basin (ID: 980) – CW2

Pore water pressure data series:

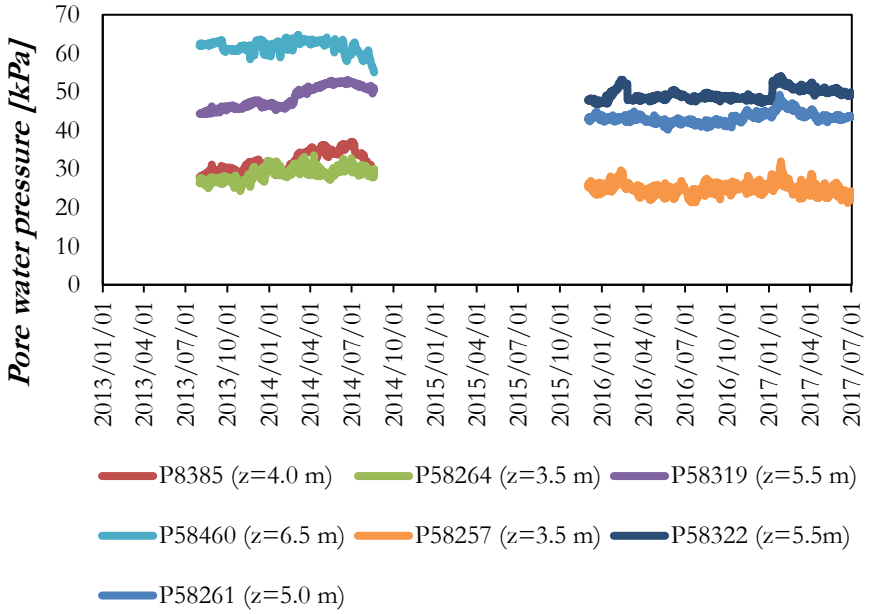

Correlation matrices:

Regional Warning Model	WL_1	WL_2	WL_3	WL_4
Landslides	3	0	0	0
No landslides	959	0	0	0

Multi-scalar Warning Model	WL_1	WL_2	WL_3	WL_4
Landslides	3	0	0	0
No landslides	959	0	0	0

HORVEIDELVA basin (ID: 1002) – CW1

Main characteristics:

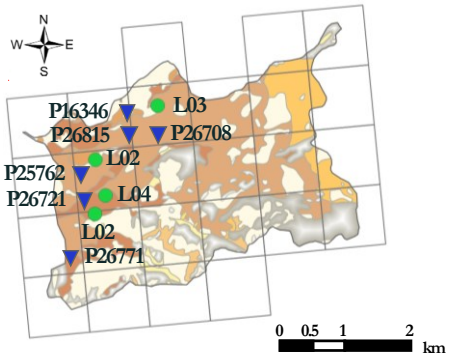

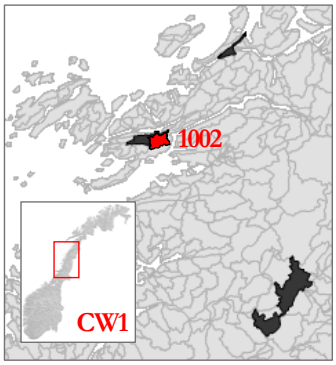

Quaternary deposits

- Moraine material, thick
- Moraine material, thin
- Terminal moraine
- Glaciofluvial deposits
- Weathered material
- Marine and fjord deposits, continuous
- Marine and fjord deposits, thin
- Marine and fjord deposits, thick
- No landslide materials
- Bare rocks

Legend

- xgeo grid
- Weather-induced landslides in soils (2013/01 – 2017/06)
- Piezometers

Shallow soil layers:

Area [km²]: ***14.04***
Loose sediments [%]: ***55***
No landslide materials [%]: ***18***
Bare rocks [%]: ***27***

Weather-induced landslides:

ID	*Date*	*Type*	*Spatial accuracy*
L01	2013/02/26	144	n.r.
L02	2014/10/30	140	10 m
L03	2015/10/03	140	exact
L04	2016/12/04	144	n.r.

HORVEIDELVA basin (ID: 1002) – CW1

Pore water pressure data series:

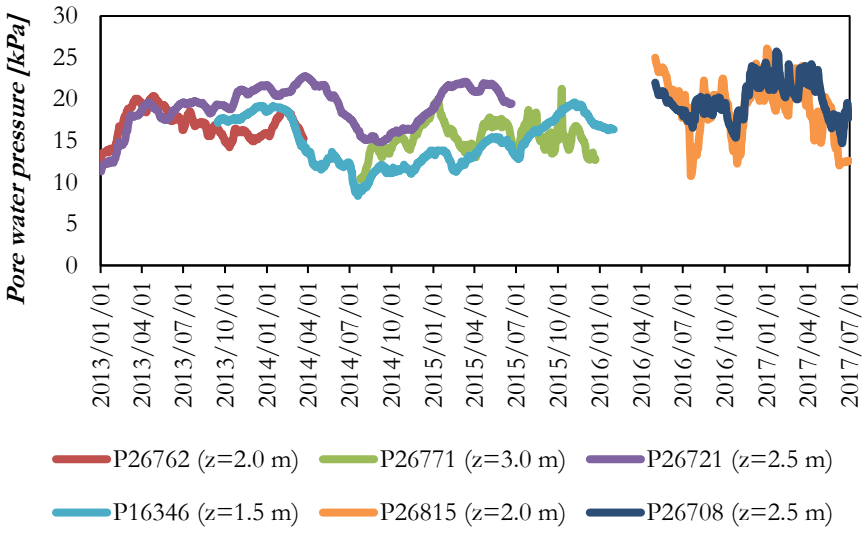

Correlation matrices:

Regional Warning Model	WL_1	WL_2	WL_3	WL_4
Landslides	2	2	0	0
No landslides	1525	16	7	0

Multi-scalar Warning Model	WL_1	WL_2	WL_3	WL_4
Landslides	2	0	1	1
No landslides	1536	7	5	0

SIMOA basin (ID: 2018) – SE

Main characteristics:

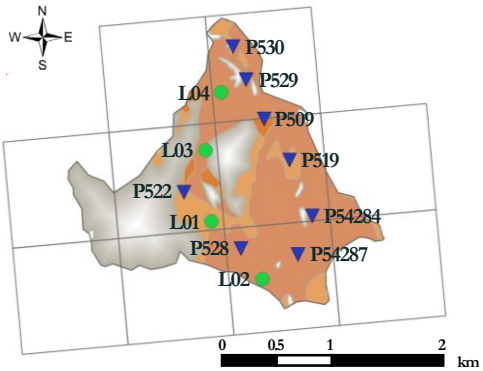

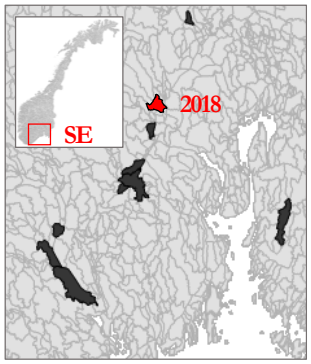

Quaternary deposits

- Moraine material, thick
- Moraine material, thin
- Terminal moraine
- Glaciofluvial deposits
- Weathered material
- Marine and fjord deposits, continuous
- Marine and fjord deposits, thin
- Marine and fjord deposits, thick
- No landslide materials
- Bare rocks

Legend

- xgeo grid
- Weather-induced landslides in soils (2013/01 – 2017/06)
- Piezometers

Shallow soil layers:

Area [km²]: ***3.69***
Loose sediments [%]: ***65***
No landslide materials [%]: ***0***
Bare rocks [%]: ***35***

Weather-induced landslides:

ID	*Date*	*Type*	*Spatial accuracy*
L01	2013/05/22	142	10 m
L02	2014/11/23	142	100 m
L03	2015/01/15	142	10 m
L04	2016/01/27	140	100 m

SIMOA basin (ID: 2018) – SE

Pore water pressure data series:

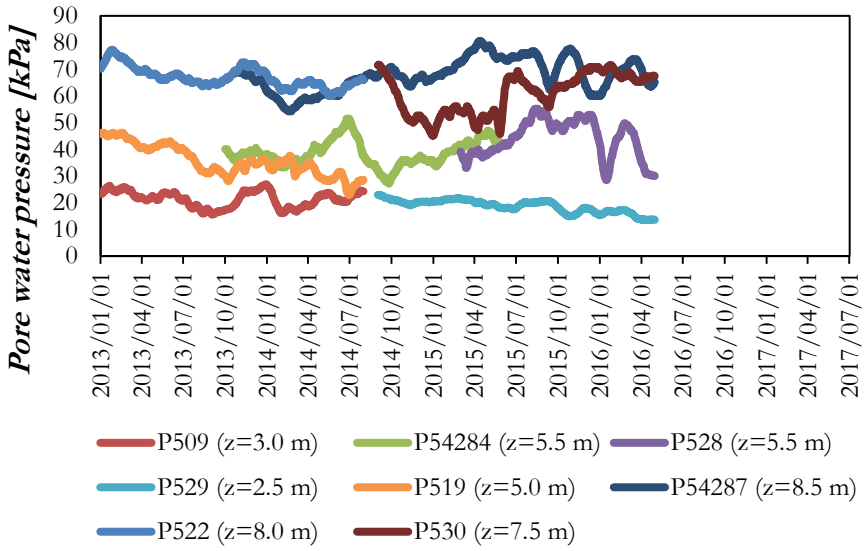

Correlation matrices:

Regional Warning Model	WL_1	WL_2	WL_3	WL_4
Landslides	2	2	0	0
No landslides	1187	24	1	0

Multi-scalar Warning Model	WL_1	WL_2	WL_3	WL_4
Landslides	2	1	1	0
No landslides	1199	13	0	0

NUMEDALSLÅGEN basin (ID: 3170) – SE

Main characteristics:

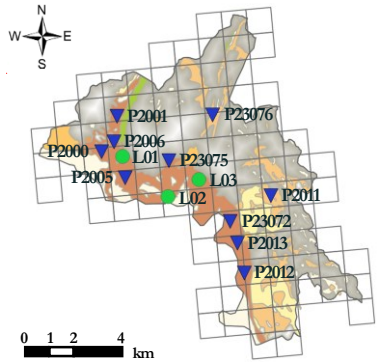

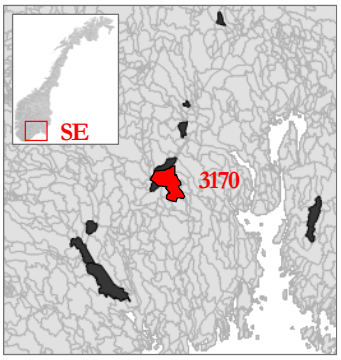

Quaternary deposits

- Moraine material, thick
- Moraine material, thin
- Terminal moraine
- Glaciofluvial deposits
- Weathered material
- Marine and fjord deposits, continuous
- Marine and fjord deposits, thin
- Marine and fjord deposits, thick
- No landslide materials
- Bare rocks

Legend

- xgeo grid
- Weather-induced landslides in soils (2013/01 – 2017/06)
- Piezometers

Shallow soil layers:

Area [km²]: ***64.00***
Loose sediments [%]: ***38***
No landslide materials [%]: ***9***
Bare rocks [%]: ***53***

Weather-induced landslides:

ID	*Date*	*Type*	*Spatial accuracy*
L01	2013/04/17	140	250 m
L02	2014/11/23	140	5000 m
L03	2016/03/28	144	n.r.

NUMEDALSLÅGEN basin (ID: 3170) – SE

Pore water pressure data series:

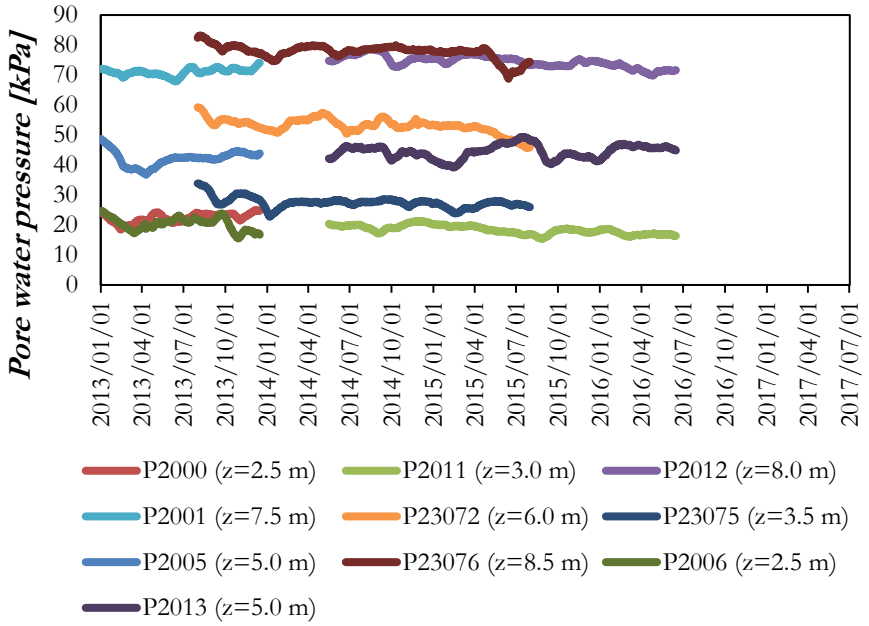

Correlation matrices:

Regional Warning Model	**WL₁**	**WL₂**	**WL₃**	**WL₄**
Landslides	0	3	0	0
No landslides	1250	9	0	0

Multi-scalar Warning Model	**WL₁**	**WL₂**	**WL₃**	**WL₄**
Landslides	0	2	1	0
No landslides	1256	3	0	0

GLOMMAVASSDRAGET basin (ID: 3789) – SE

Main characteristics:

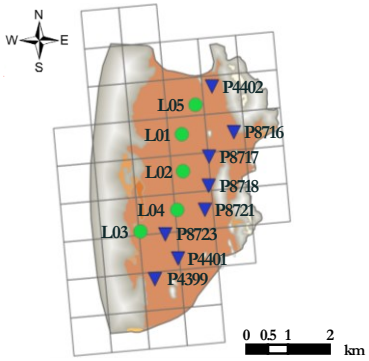

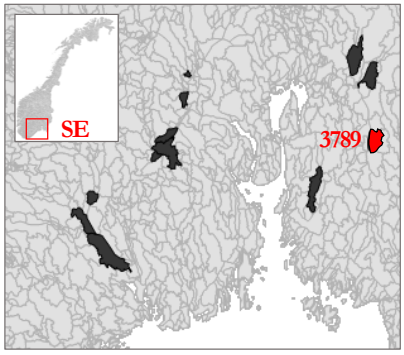

Quaternary deposits

- Moraine material, thick
- Moraine material, thin
- Terminal moraine
- Glaciofluvial deposits
- Weathered material
- Marine and fjord deposits, continuous
- Marine and fjord deposits, thin
- Marine and fjord deposits, thick
- No landslide materials
- Bare rocks

Legend

- xgeo grid
- Weather-induced landslides in soils (2013/01 – 2017/06)
- Piezometers

Shallow soil layers:

Area [km²]: ***27.13***
Loose sediments [%]: ***59***
No landslide materials [%]: ***1***
Bare rocks [%]: ***40***

Weather-induced landslides:

ID	*Date*	*Type*	*Spatial accuracy*
L01	2014/10/11	143	n.r.
L02	2014/10/28	143	n.r.
L03	2015/09/17	143	n.r.
L04	2016/01/29	141	n.r.
L05	2017/02/27	143	250 m

GLOMMAVASSDRAGET basin (ID: 3789) – SE

Pore water pressure data series:

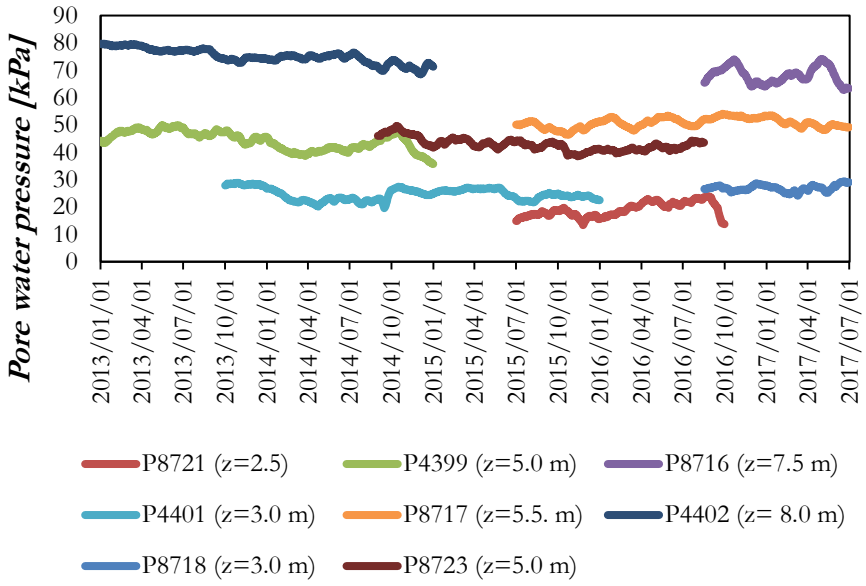

Correlation matrices:

Regional Warning Model	WL_1	WL_2	WL_3	WL_4
Landslides	0	4	0	1
No landslides	1580	44	13	0

Multi-scalar Warning Model	WL_1	WL_2	WL_3	WL_4
Landslides	0	1	2	2
No landslides	1604	22	11	0

SENJA VEST basin (ID: 5329) – NW

Main characteristics:

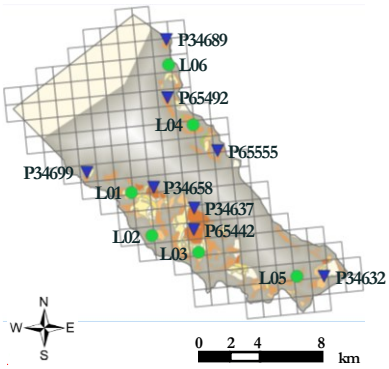

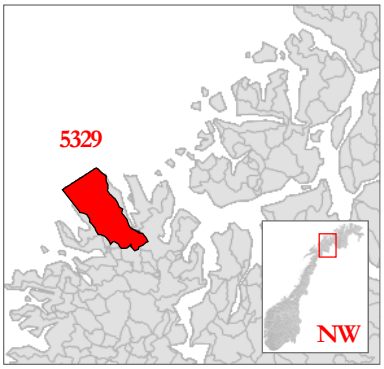

Quaternary deposits

- Moraine material, thick
- Moraine material, thin
- Terminal moraine
- Glaciofluvial deposits
- Weathered material
- Marine and fjord deposits, continuous
- Marine and fjord deposits, thin
- Marine and fjord deposits, thick
- No landslide materials
- Bare rocks

Legend

- xgeo grid
- Weather-induced landslides in soils (2013/01 – 2017/06)
- Piezometers

Shallow soil layers:

Area [km²]: ***136.66***
Loose sediments [%]: ***17***
No landslide materials [%]: ***19***
Bare rocks [%]: ***64***

Weather-induced landslides:

ID	*Date*	*Type*	*Spatial accuracy*
L01	2013/01/27	160	50 m
L02	2013/11/15	133	50 m
L03	2014/03/09	133	exact
L04	2014/12/03	140	exact
L05	2015/11/01	160	10 m
L06	2015/11/03	142	n.r.

SENJA VEST basin (ID: 5329) – NW

Pore water pressure data series:

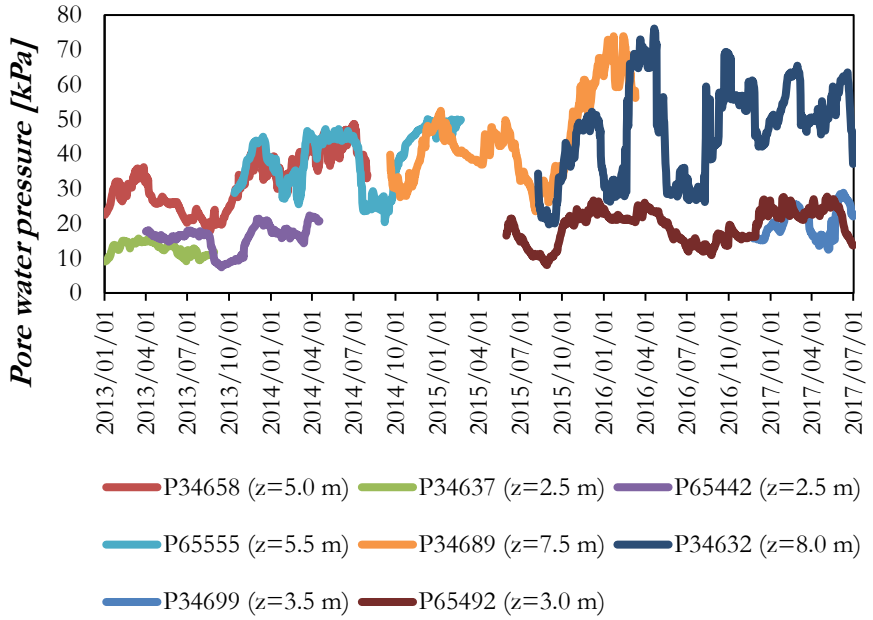

Correlation matrices:

Regional Warning Model	WL_1	WL_2	WL_3	WL_4
Landslides	4	2	0	0
No landslides	1626	10	0	0

Multi-scalar Warning Model	WL_1	WL_2	WL_3	WL_4
Landslides	4	0	2	0
No landslides	1629	7	0	0

SKIENSVASSDRAGET basin (ID: 5371) – SE

Main characteristics:

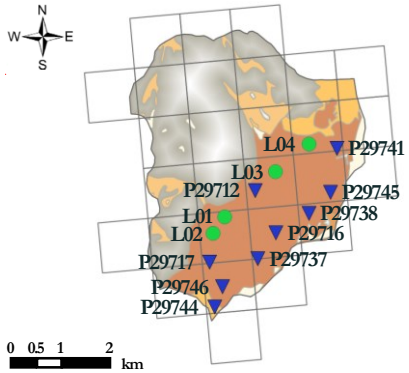

Quaternary deposits

- Moraine material, thick
- Moraine material, thin
- Terminal moraine
- Glaciofluvial deposits
- Weathered material
- Marine and fjord deposits, continuous
- Marine and fjord deposits, thin
- Marine and fjord deposits, thick
- No landslide materials
- Bare rocks

Legend

- xgeo grid
- Weather-induced landslides in soils (2013/01 – 2017/06)
- Piezometers

Shallow soil layers:

Area [km²]: ***18.21***
Loose sediments [%]: ***52***
No landslide materials [%]: ***2***
Bare rocks [%]: ***46***

Weather-induced landslides:

ID	*Date*	*Type*	*Spatial accuracy*
L01	2014/02/26	140	50 m
L02	2014/03/03	140	50 m
L03	2015/09/15	140	50 m
L04	2016/03/14	140	50 m

SKIENSVASSDRAGET basin (ID: 5371) – SE

Pore water pressure data series:

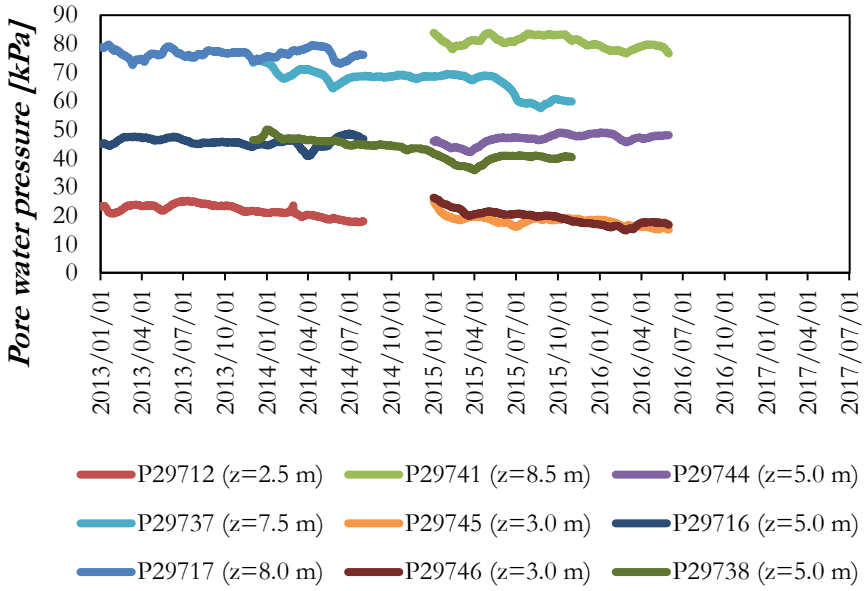

Correlation matrices:

Regional Warning Model	WL_1	WL_2	WL_3	WL_4
Landslides	0	4	0	0
No landslides	1224	17	2	0

Multi-scalar Warning Model	WL_1	WL_2	WL_3	WL_4
Landslides	0	2	2	0
No landslides	1228	12	3	0

SKIENSVASSDRAGET basin (ID: 5539) – SE

Main characteristics:

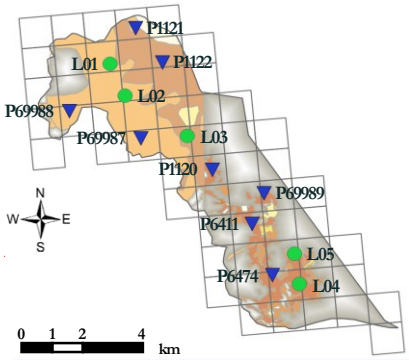

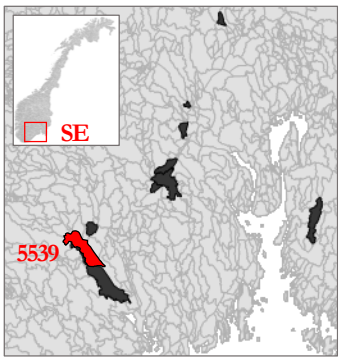

Quaternary deposits

- Moraine material, thick
- Moraine material, thin
- Terminal moraine
- Glaciofluvial deposits
- Weathered material
- Marine and fjord deposits, continuous
- Marine and fjord deposits, thin
- Marine and fjord deposits, thick
- No landslide materials
- Bare rocks

Legend

- xgeo grid
- Weather-induced landslides in soils (2013/01 – 2017/06)
- Piezometers

Shallow soil layers:

Area [km²]: ***38.88***
Loose sediments [%]: ***53***
No landslide materials [%]: ***2***
Bare rocks [%]: ***45***

Weather-induced landslides:

ID	*Date*	*Type*	*Spatial accuracy*
L01	2014/02/15	140	50 m
L02	2014/11/23	140	exact
L03	2015/09/15	140	50 m
L04	2015/09/17	140	exact
L05	2016/02/08	140	exact

SKIENSVASSDRAGET basin (ID: 5539) – SE

Pore water pressure data series:

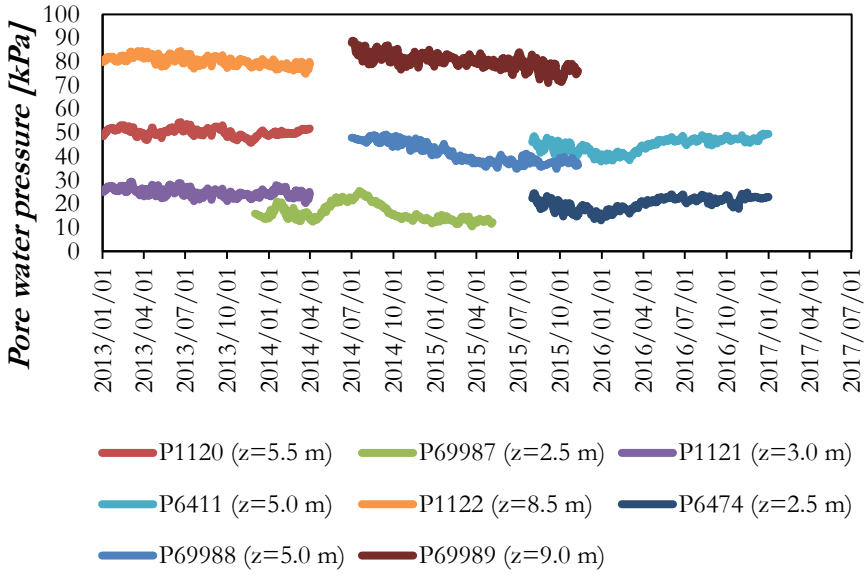

Correlation matrices:

Regional Warning Model	WL_1	WL_2	WL_3	WL_4
Landslides	0	3	2	0
No landslides	1432	24	0	0

Multi-scalar Warning Model	WL_1	WL_2	WL_3	WL_4
Landslides	0	2	1	2
No landslides	1449	7	0	0

TRONDHEIMSFJORDEN VEST basin (ID: 5794) – CW1

Main characteristics:

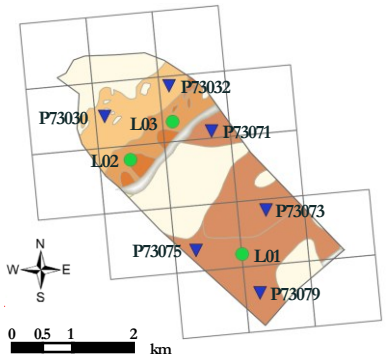

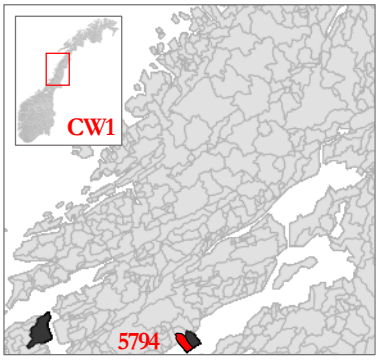

Quaternary deposits

- Moraine material, thick
- Moraine material, thin
- Terminal moraine
- Glaciofluvial deposits
- Weathered material
- Marine and fjord deposits, continuous
- Marine and fjord deposits, thin
- Marine and fjord deposits, thick
- No landslide materials
- Bare rocks

Legend

- xgeo grid
- Weather-induced landslides in soils (2013/01 – 2017/06)
- Piezometers

Shallow soil layers:

Area [km²]: ***8.08***
Loose sediments [%]: ***63***
No landslide materials [%]: ***34***
Bare rocks [%]: ***3***

Weather-induced landslides:

ID	*Date*	*Type*	*Spatial accuracy*
L01	2013/11/26	141	n.r.
L02	2014/12/30	140	10 m
L03	2015/12/06	140	exact

TRONDHEIMSFJORDEN VEST basin (ID: 5794) – CW1

Pore water pressure data series:

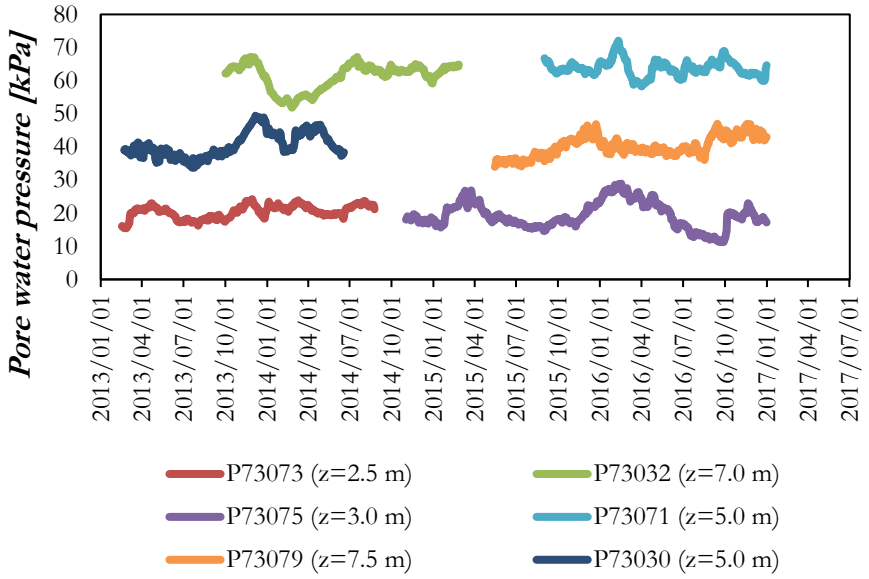

Correlation matrices:

Regional Warning Model	WL_1	WL_2	WL_3	WL_4
Landslides	3	0	0	0
No landslides	1411	1	0	0

Multi-scalar Warning Model	WL_1	WL_2	WL_3	WL_4
Landslides	3	0	0	0
No landslides	1411	1	0	0

NAMSEN basin (ID: 6232) – CW1

Main characteristics:

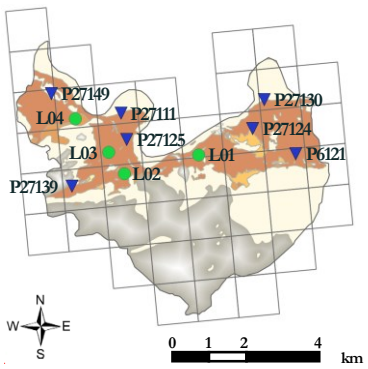

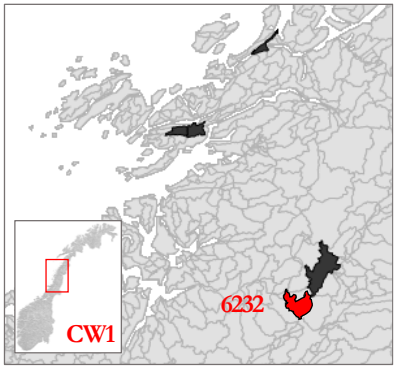

Quaternary deposits

- Moraine material, thick
- Moraine material, thin
- Terminal moraine
- Glaciofluvial deposits
- Weathered material
- Marine and fjord deposits, continuous
- Marine and fjord deposits, thin
- Marine and fjord deposits, thick
- No landslide materials
- Bare rocks

Legend

- xgeo grid
- Weather-induced landslides in soils (2013/01 – 2017/06)
- Piezometers

Shallow soil layers:

Area [km²]: ***26.48***
Loose sediments [%]: ***31***
No landslide materials [%]: ***35***
Bare rocks [%]: ***34***

Weather-induced landslides:

ID	*Date*	*Type*	*Spatial accuracy*
L01	2013/12/02	140	10 m
L02	2015/02/08	140	10 m
L03	2016/12/04	160	n.r.
L04	2017/02/18	140	10 m

NAMSEN basin (ID: 6232) – CW1

Pore water pressure data series:

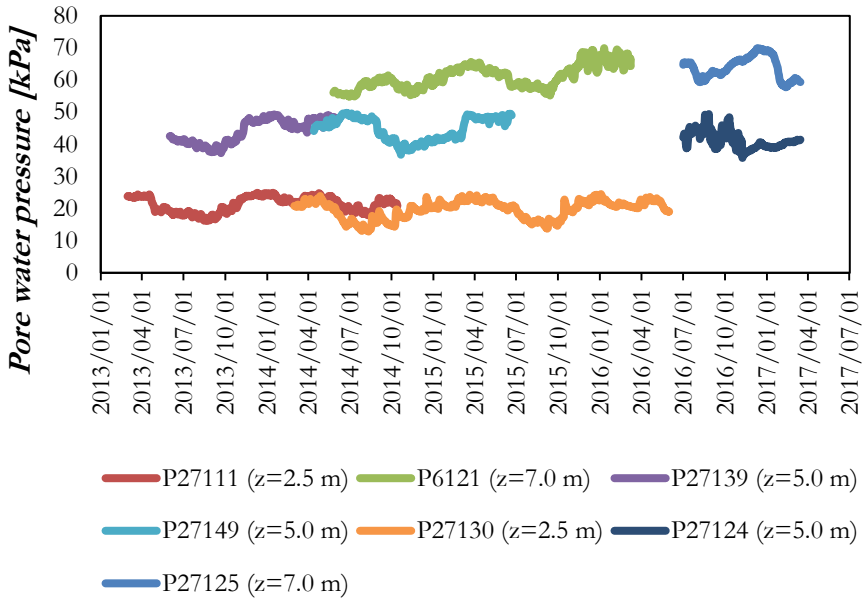

Correlation matrices:

Regional Warning Model	WL_1	WL_2	WL_3	WL_4
Landslides	0	3	1	0
No landslides	1439	4	0	0

Multi-scalar Warning Model	WL_1	WL_2	WL_3	WL_4
Landslides	0	1	3	0
No landslides	1439	4	0	0

YTRE TRONDHEIMSFJORDEN basin (ID: 6427) – CW1

Main characteristics:

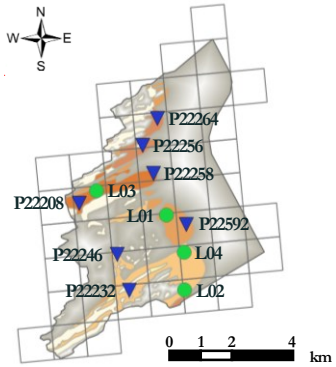

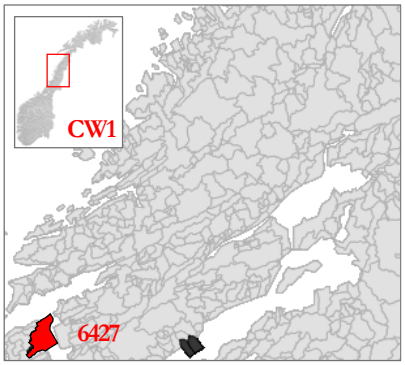

Quaternary deposits

- Moraine material, thick
- Moraine material, thin
- Terminal moraine
- Glaciofluvial deposits
- Weathered material
- Marine and fjord deposits, continuous
- Marine and fjord deposits, thin
- Marine and fjord deposits, thick
- No landslide materials
- Bare rocks

Legend

- xgeo grid
- Weather-induced landslides in soils (2013/01 – 2017/06)
- Piezometers

Shallow soil layers:

Area [km²]: ***30.02***
Loose sediments [%]: ***22***
No landslide materials [%]: ***8***
Bare rocks [%]: ***70***

Weather-induced landslides:

ID	*Date*	*Type*	*Spatial accuracy*
L01	2013/02/28	143	n.r.
L02	2013/11/15	142	500 m
L03	2016/01/15	140	exact
L04	2016/12/04	141	exact

YTRE TRONDHEIMSFJORDEN basin (ID: 6427) – CW1

Pore water pressure data series:

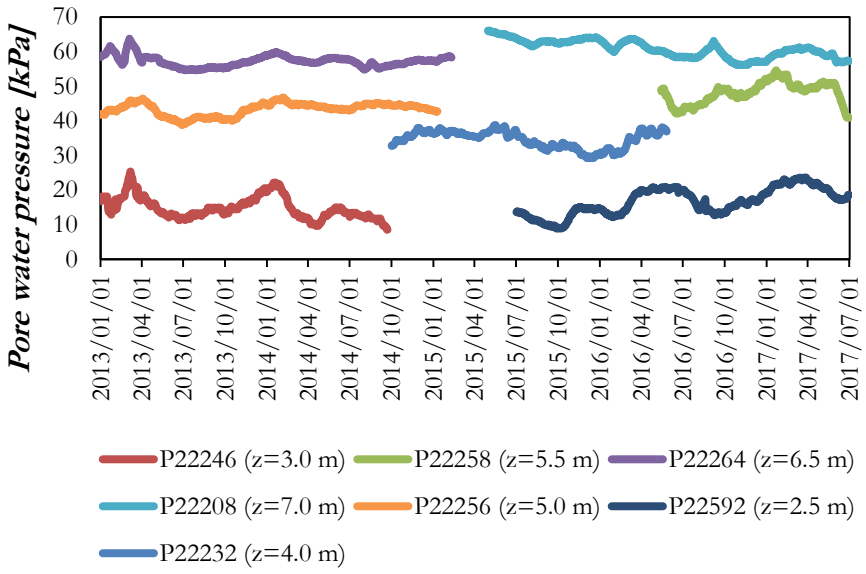

Correlation matrices:

Regional Warning Model	WL_1	WL_2	WL_3	WL_4
Landslides	4	0	0	0
No landslides	1638	0	0	0

Multi-scalar Warning Model	WL_1	WL_2	WL_3	WL_4
Landslides	4	0	0	0
No landslides	1638	0	0	0

NAMSEN basin (ID: 6460) – CW1

Main characteristics:

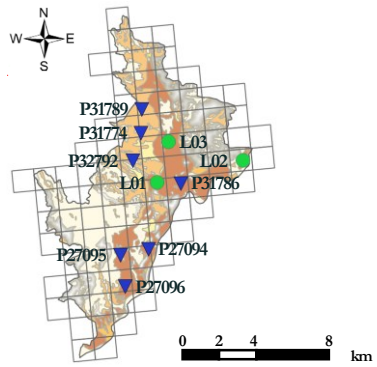

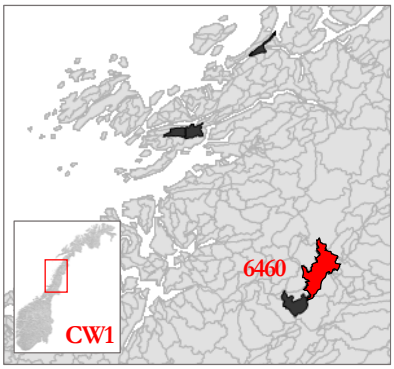

Quaternary deposits

- Moraine material, thick
- Moraine material, thin
- Terminal moraine
- Glaciofluvial deposits
- Weathered material
- Marine and fjord deposits, continuous
- Marine and fjord deposits, thin
- Marine and fjord deposits, thick
- No landslide materials
- Bare rocks

Legend

- xgeo grid
- Weather-induced landslides in soils (2013/01 – 2017/06)
- Piezometers

Shallow soil layers:

Area [km²]: ***56.51***
Loose sediments [%]: ***22***
No landslide materials [%]: ***8***
Bare rocks [%]: ***70***

Weather-induced landslides:

ID	*Date*	*Type*	*Spatial accuracy*
L01	2013/12/02	140	10 m
L02	2015/02/10	140	10 m
L03	2015/10/01	142	10 m

NAMSEN basin (ID: 6460) – CW1

Pore water pressure data series:

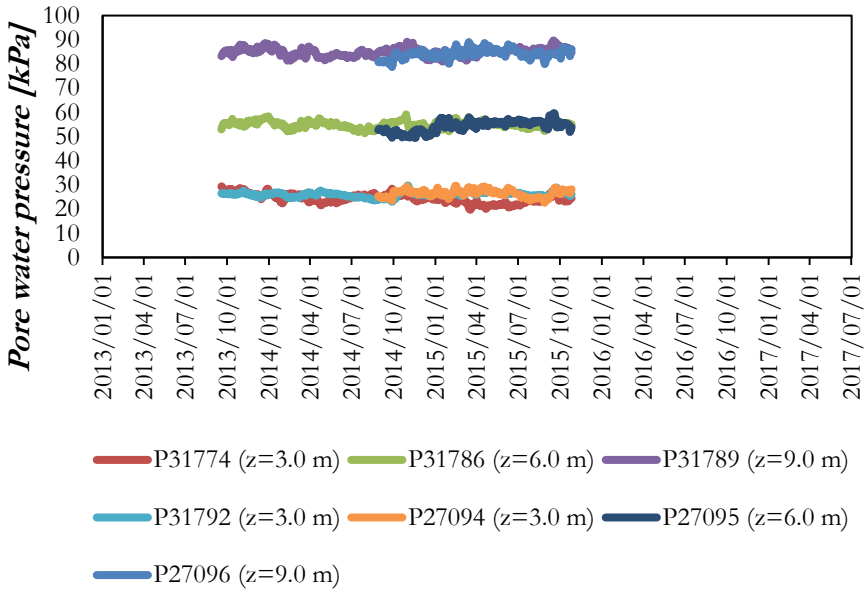

Correlation matrices:

Regional Warning Model	WL_1	WL_2	WL_3	WL_4
Landslides	0	3	0	0
No landslides	761	5	0	0

Multi-scalar Warning Model	WL_1	WL_2	WL_3	WL_4
Landslides	2	0	1	0
No landslides	763	3	0	0

FYKANÅGA basin (ID: 7045) – CW2

Main characteristics:

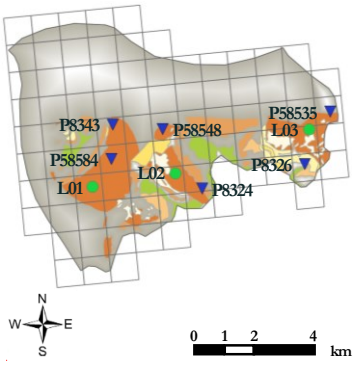

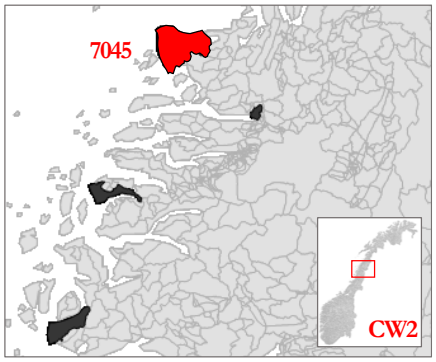

Quaternary deposits

- Moraine material, thick
- Moraine material, thin
- Terminal moraine
- Glaciofluvial deposits
- Weathered material
- Marine and fjord deposits, continuous
- Marine and fjord deposits, thin
- Marine and fjord deposits, thick
- No landslide materials
- Bare rocks

Legend

- xgeo grid
- Weather-induced landslides in soils (2013/01 – 2017/06)
- Piezometers

Shallow soil layers:

Area [km²]: ***65.47***
Loose sediments [%]: ***29***
No landslide materials [%]: ***2***
Bare rocks [%]: ***69***

Weather-induced landslides:

ID	*Date*	*Type*	*Spatial accuracy*
L01	2013/12/11	140	500 m
L02	2015/01/02	140	exact
L03	2017/01/25	144	exact

FYKANÅGA basin (ID: 7045) – CW2

Pore water pressure data series:

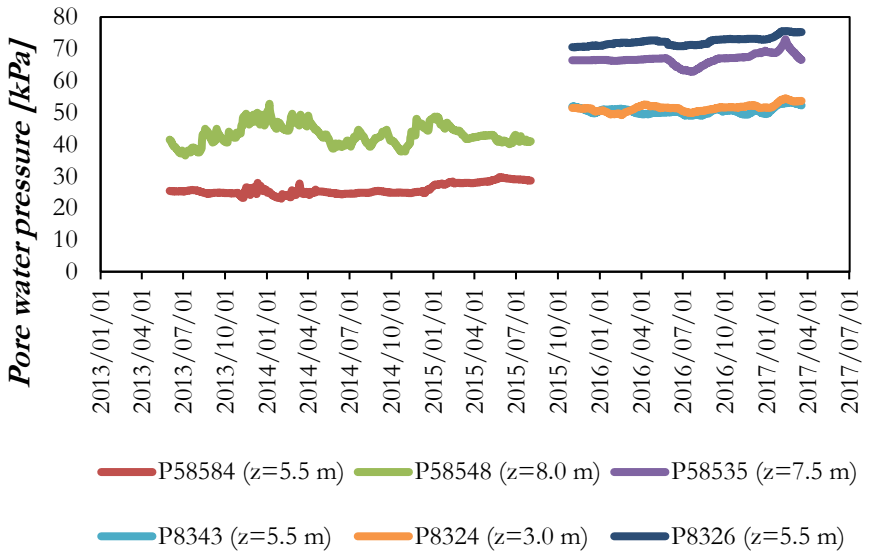

Correlation matrices:

Regional Warning Model	WL_1	WL_2	WL_3	WL_4
Landslides	2	1	0	0
No landslides	1294	0	0	0

Multi-scalar Warning Model	WL_1	WL_2	WL_3	WL_4
Landslides	2	0	1	0
No landslides	1294	0	0	0

HAREIDLANDET OG GURSKØYA basin (ID: 7971) – SW

Main characteristics:

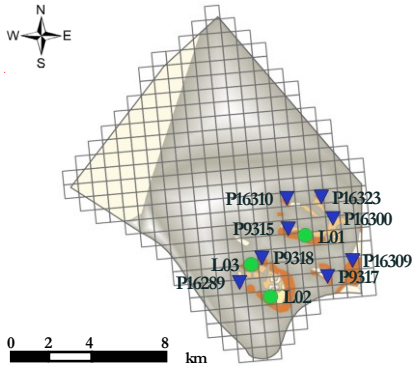

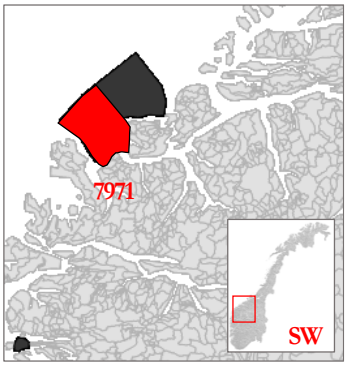

Quaternary deposits

- Moraine material, thick
- Moraine material, thin
- Terminal moraine
- Glaciofluvial deposits
- Weathered material
- Marine and fjord deposits, continuous
- Marine and fjord deposits, thin
- Marine and fjord deposits, thick
- No landslide materials
- Bare rocks

Legend

- xgeo grid
- Weather-induced landslides in soils (2013/01 – 2017/06)
- Piezometers

Shallow soil layers:

Area [km²]: ***269.15***
Loose sediments [%]: ***7***
No landslide materials [%]: ***16***
Bare rocks [%]: ***77***

Weather-induced landslides:

ID	*Date*	*Type*	*Spatial accuracy*
L01	2015/11/27	144	10 m
L02	2016/11/25	140	exact
L03	2017/01/19	140	exact

HAREIDLANDET OG GURSKØYA basin (ID: 7971) – SW

Pore water pressure data series:

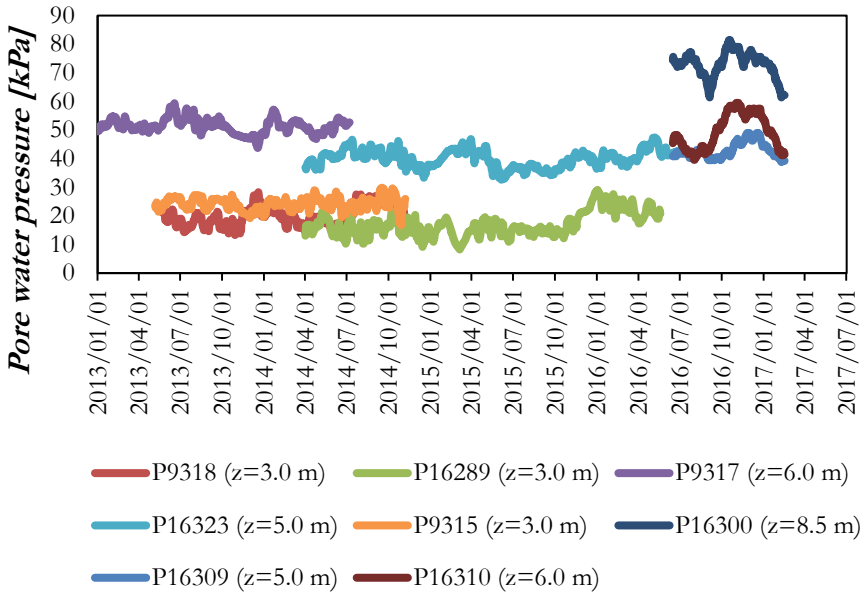

Correlation matrices:

Regional Warning Model	**WL_1**	**WL_2**	**WL_3**	**WL_4**
Landslides	0	0	3	0
No landslides	1473	27	4	0

Multi-scalar Warning Model	**WL_1**	**WL_2**	**WL_3**	**WL_4**
Landslides	0	2	0	1
No landslides	1485	15	3	1

VESTRE SVARTISEN basin (ID: 8580) – CW2

Main characteristics:

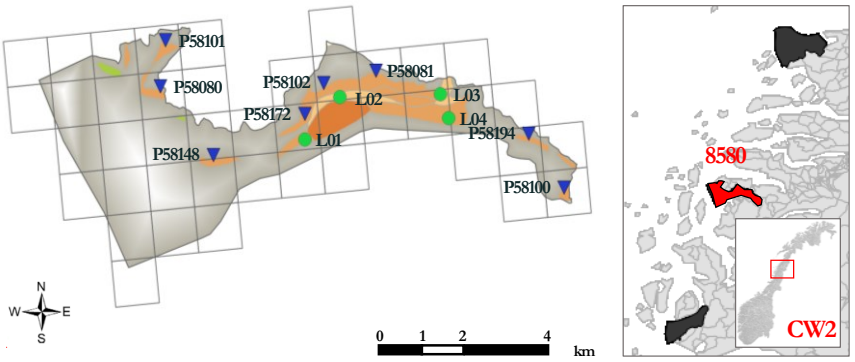

Quaternary deposits

- Moraine material, thick
- Moraine material, thin
- Terminal moraine
- Glaciofluvial deposits
- Weathered material
- Marine and fjord deposits, continuous
- Marine and fjord deposits, thin
- Marine and fjord deposits, thick
- No landslide materials
- Bare rocks

Legend

- xgeo grid
- Weather-induced landslides in soils (2013/01 – 2017/06)
- Piezometers

Shallow soil layers:

Area [km²]: ***23.08***
Loose sediments [%]: ***19***
No landslide materials [%]: ***0***
Bare rocks [%]: ***81***

Weather-induced landslides:

ID	*Date*	*Type*	*Spatial accuracy*
L01	2013/12/11	160	exact
L02	2014/03/13	160	exact
L03	2017/01/25	140	exact
L04	2017/01/26	142	n.r.

VESTRE SVARTISEN basin (ID: 8580) – CW2

Pore water pressure data series:

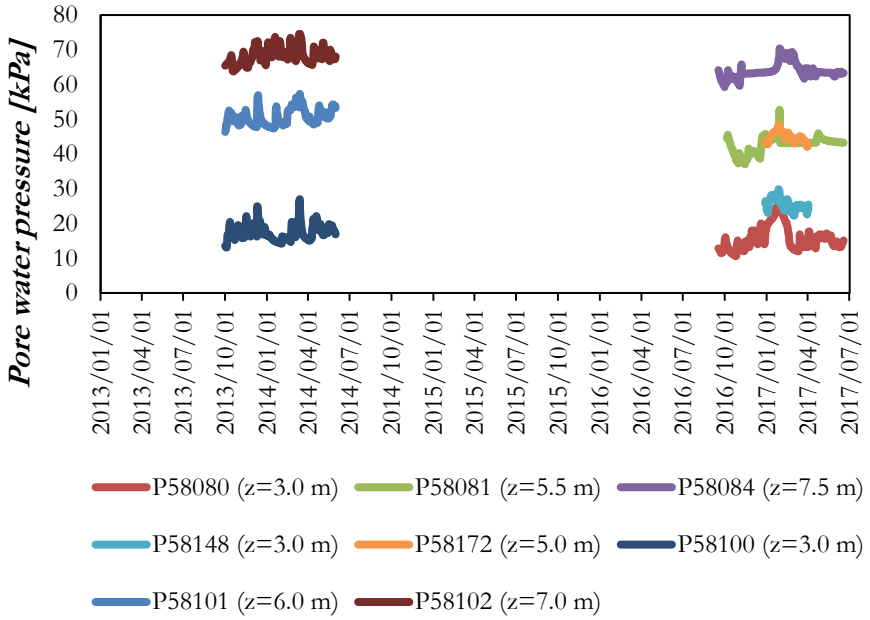

Correlation matrices:

Regional Warning Model	WL_1	WL_2	WL_3	WL_4
Landslides	1	2	1	0
No landslides	513	1	0	0

Multi-scalar Warning Model	WL_1	WL_2	WL_3	WL_4
Landslides	1	0	1	2
No landslides	514	0	0	0

SKIENSVASSDRAGET basin (ID: 8922) – SE

Main characteristics:

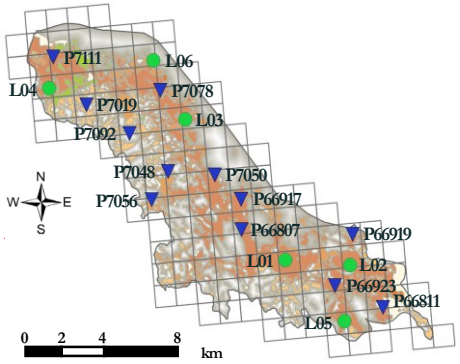

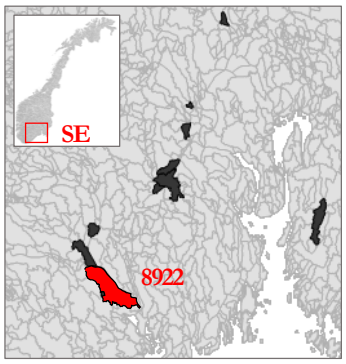

Quaternary deposits

- Moraine material, thick
- Moraine material, thin
- Terminal moraine
- Glaciofluvial deposits
- Weathered material
- Marine and fjord deposits, continuous
- Marine and fjord deposits, thin
- Marine and fjord deposits, thick
- No landslide materials
- Bare rocks

Legend

- xgeo grid
- Weather-induced landslides in soils (2013/01 – 2017/06)
- Piezometers

Shallow soil layers:

Area [km²]: ***104.55***
Loose sediments [%]: ***51***
No landslide materials [%]: ***2***
Bare rocks [%]: ***47***

Weather-induced landslides:

ID	*Date*	*Type*	*Spatial accuracy*
L01	2013/05/22	143	n.r.
L02	2014/01/06	140	exact
L03	2014/11/23	144	n.r.
L04	2015/09/01	140	50 m
L05	2015/09/02	144	n.r.
L06	2015/09/17	140	50 m

SKIENSVASSDRAGET basin (ID: 8922) – SE

Pore water pressure data series:

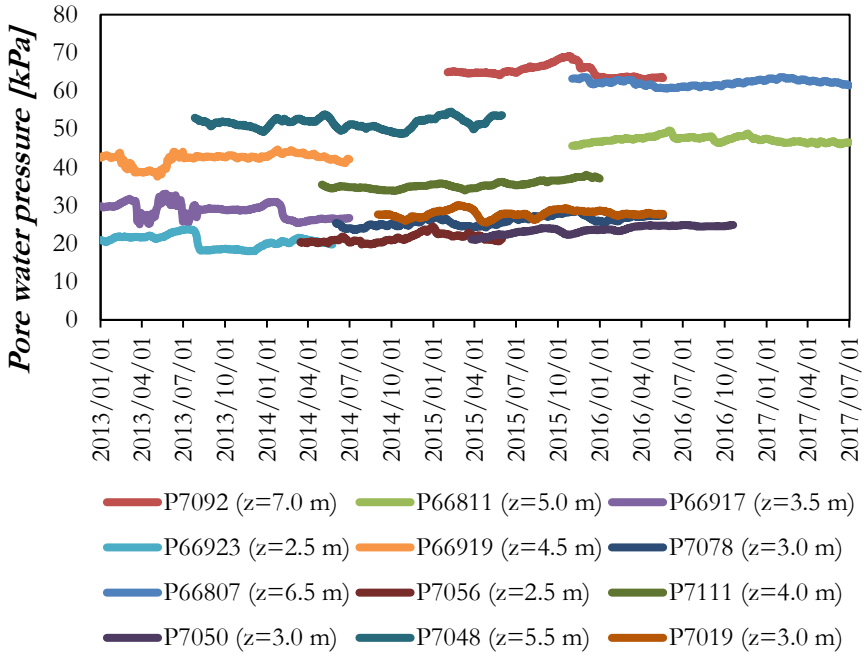

Correlation matrices:

Regional Warning Model	**WL_1**	**WL_2**	**WL_3**	**WL_4**
Landslides	0	4	2	0
No landslides	1609	26	1	0

Multi-scalar Warning Model	**WL_1**	**WL_2**	**WL_3**	**WL_4**
Landslides	0	0	4	2
No landslides	1616	20	0	0

VEGÅRSVASSDRAGET basin (ID: 9585) – SE

Main characteristics:

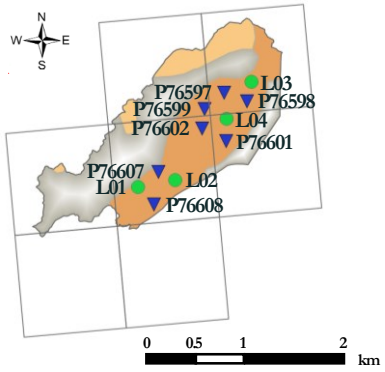

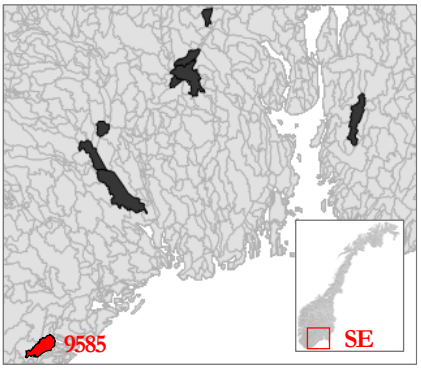

Quaternary deposits

- Moraine material, thick
- Moraine material, thin
- Terminal moraine
- Glaciofluvial deposits
- Weathered material
- Marine and fjord deposits, continuous
- Marine and fjord deposits, thin
- Marine and fjord deposits, thick
- No landslide materials
- Bare rocks

Legend

- xgeo grid
- Weather-induced landslides in soils (2013/01 – 2017/06)
- Piezometers

Shallow soil layers:

Area [km²]: ***2.45***
Loose sediments [%]: ***52***
No landslide materials [%]: ***0***
Bare rocks [%]: ***48***

Weather-induced landslides:

ID	*Date*	*Type*	*Spatial accuracy*
L01	2013/05/15	140	exact
L02	2014/10/18	144	n.r.
L03	2016/03/15	143	100 m
L04	2016/11/05	160	500 m

VEGÅRSVASSDRAGET basin (ID: 9585) – SE

Pore water pressure data series:

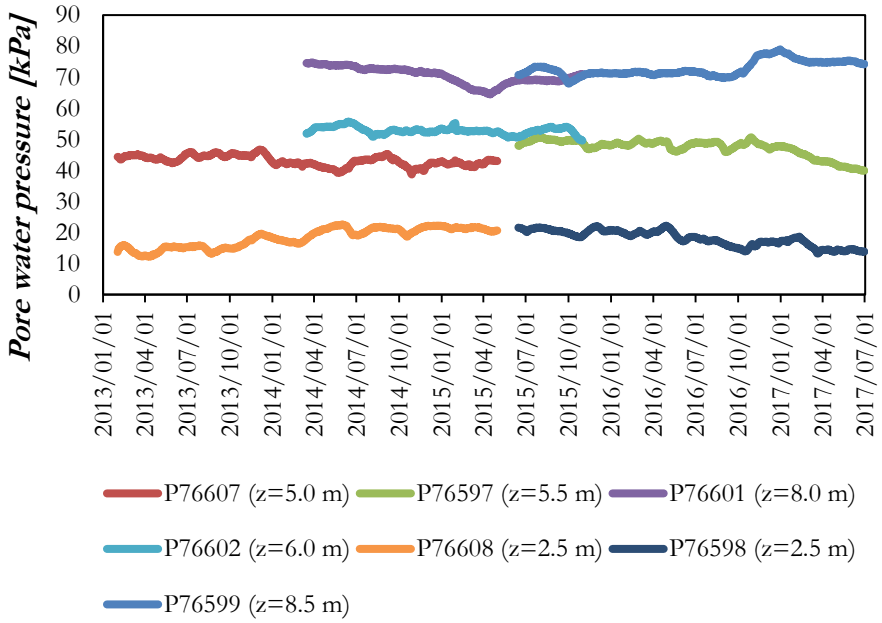

Correlation matrices:

Regional Warning Model	**WL_1**	**WL_2**	**WL_3**	**WL_4**
Landslides	0	3	0	1
No landslides	1560	35	12	0

Multi-scalar Warning Model	**WL_1**	**WL_2**	**WL_3**	**WL_4**
Landslides	0	1	2	1
No landslides	1579	23	5	0

LEIRA basin (ID: 9962) – SE

Main characteristics:

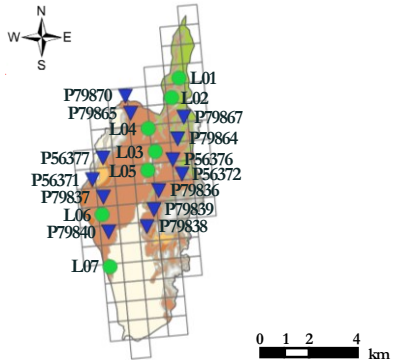

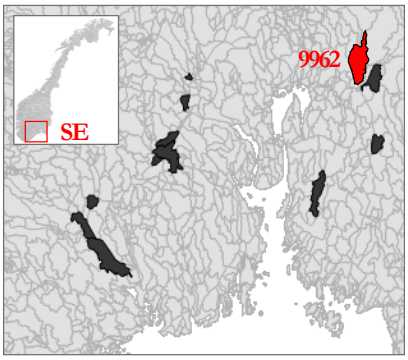

Quaternary deposits

- Moraine material, thick
- Moraine material, thin
- Terminal moraine
- Glaciofluvial deposits
- Weathered material
- Marine and fjord deposits, continuous
- Marine and fjord deposits, thin
- Marine and fjord deposits, thick
- No landslide materials
- Bare rocks

Legend

- xgeo grid
- Weather-induced landslides in soils (2013/01 – 2017/06)
- Piezometers

Shallow soil layers:

Area [km²]: ***57.76***
Loose sediments [%]: ***62***
No landslide materials [%]: ***25***
Bare rocks [%]: ***13***

Weather-induced landslides:

ID	*Date*	*Type*	*Spatial accuracy*
L01	2013/12/24	140	100 m
L02	2013/12/27	143	50 m
L03	2014/04/17	140	100 m
L04	2014/10/23	140	100 m
L05	2015/02/19	140	100 m
L06	2015/09/17	140	100 m
L07	2016/04/30	140	100 m

LEIRA basin (ID: 9962) – SE

Pore water pressure data series:

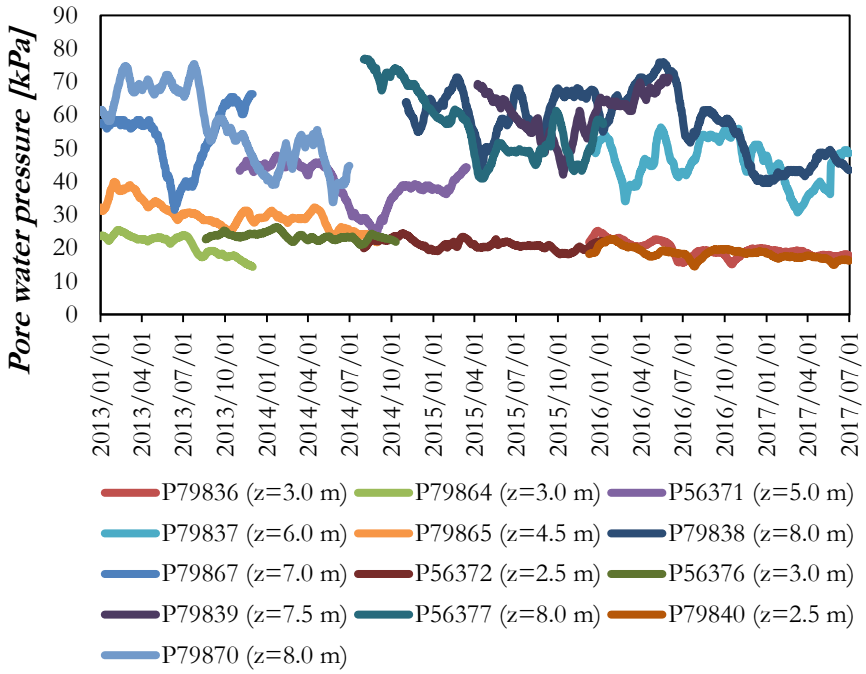

Correlation matrices:

Regional Warning Model	WL_1	WL_2	WL_3	WL_4
Landslides	1	4	2	0
No landslides	1589	31	15	0

Multi-scalar Warning Model	WL_1	WL_2	WL_3	WL_4
Landslides	1	1	3	2
No landslides	1608	20	7	0

NUMEDALSLÅGEN basin (ID: 10095) – SE

Main characteristics:

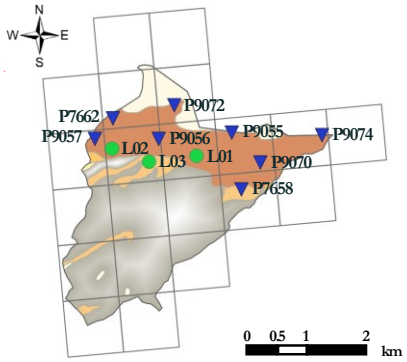

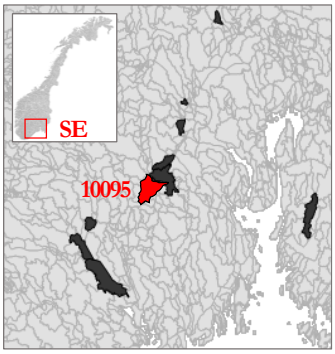

Quaternary deposits

- Moraine material, thick
- Moraine material, thin
- Terminal moraine
- Glaciofluvial deposits
- Weathered material
- Marine and fjord deposits, continuous
- Marine and fjord deposits, thin
- Marine and fjord deposits, thick
- No landslide materials
- Bare rocks

Legend

- xgeo grid
- Weather-induced landslides in soils (2013/01 – 2017/06)
- Piezometers

Shallow soil layers:

Area [km²]: ***10.09***
Loose sediments [%]: ***39***
No landslide materials [%]: ***7***
Bare rocks [%]: ***54***

Weather-induced landslides:

ID	*Date*	*Type*	*Spatial accuracy*
L01	2014/02/15	140	exact
L02	2015/01/15	140	50 m
L03	2016/03/28	160	50 m

NUMEDALSLÅGEN basin (ID: 10095) – SE

Pore water pressure data series:

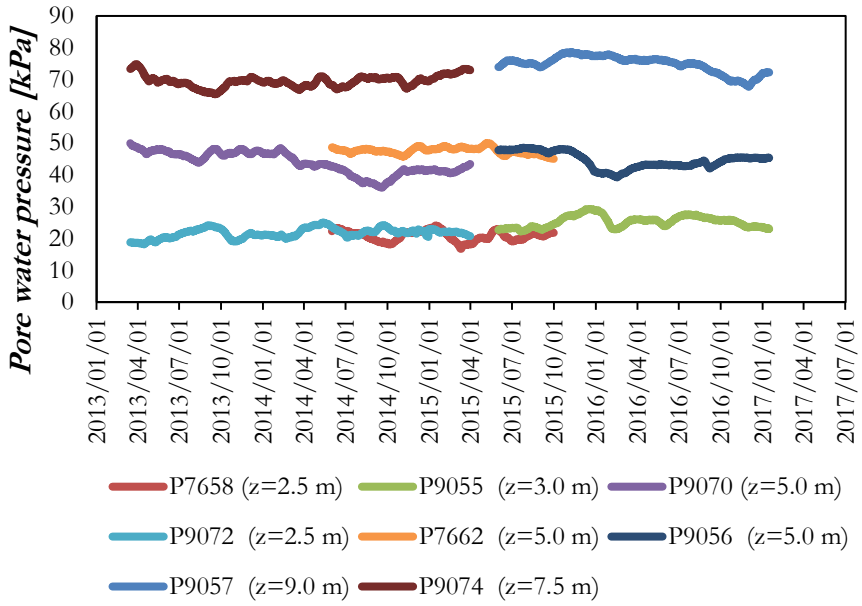

Correlation matrices:

Regional Warning Model	WL_1	WL_2	WL_3	WL_4
Landslides	0	2	1	0
No landslides	1366	34	0	0

Multi-scalar Warning Model	WL_1	WL_2	WL_3	WL_4
Landslides	0	1	2	0
No landslides	1386	14	0	0

DRAMMENSVASSDRAGET basin (ID: 10566) – SE

Main characteristics:

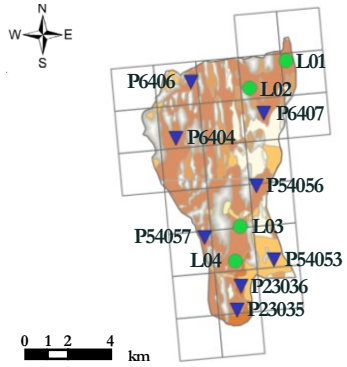

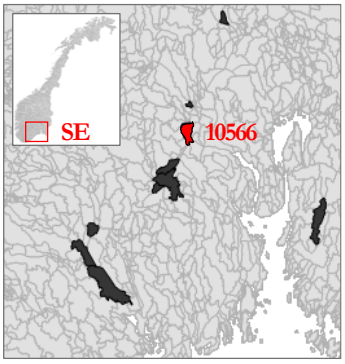

Quaternary deposits

- Moraine material, thick
- Moraine material, thin
- Terminal moraine
- Glaciofluvial deposits
- Weathered material
- Marine and fjord deposits, continuous
- Marine and fjord deposits, thin
- Marine and fjord deposits, thick
- No landslide materials
- Bare rocks

Legend

- xgeo grid
- Weather-induced landslides in soils (2013/01 – 2017/06)
- Piezometers

Shallow soil layers:

Area [km²]: ***14.38***
Loose sediments [%]: ***66***
No landslide materials [%]: ***8***
Bare rocks [%]: ***26***

Weather-induced landslides:

ID	*Date*	*Type*	*Spatial accuracy*
L01	2014/02/12	144	10 m
L02	2014/02/15	142	10 m
L03	2015/09/02	142	10 m
L04	2016/03/15	140	100 m

DRAMMENSVASSDRAGET basin (ID: 10566) – SE

Pore water pressure data series:

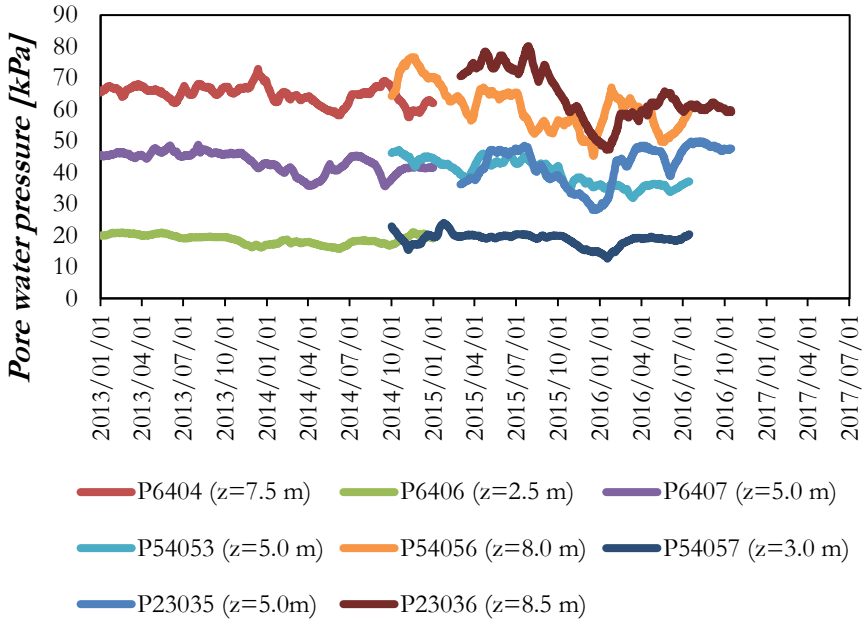

Correlation matrices:

Regional Warning Model	**WL_1**	**WL_2**	**WL_3**	**WL_4**
Landslides	1	2	1	0
No landslides	1363	17	0	0

Multi-scalar Warning Model	**WL_1**	**WL_2**	**WL_3**	**WL_4**
Landslides	1	1	1	1
No landslides	1367	13	0	0

VIKNA OG KYST FOLDFJORDEN basin (ID: 11922) – CW1

Main characteristics:

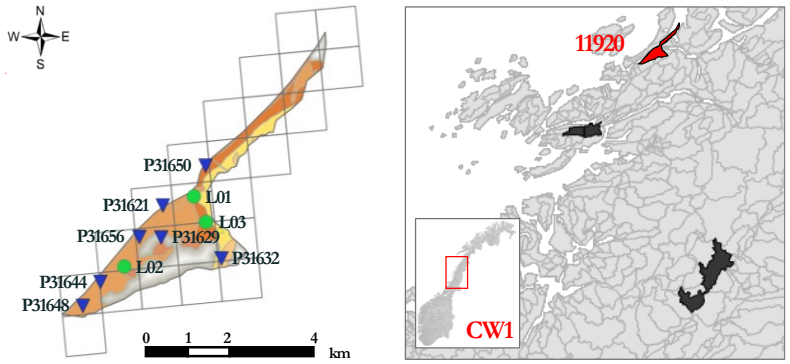

Quaternary deposits

- Moraine material, thick
- Moraine material, thin
- Terminal moraine
- Glaciofluvial deposits
- Weathered material
- Marine and fjord deposits, continuous
- Marine and fjord deposits, thin
- Marine and fjord deposits, thick
- No landslide materials
- Bare rocks

Legend

- xgeo grid
- Weather-induced landslides in soils (2013/01 – 2017/06)
- Piezometers

Shallow soil layers:

Area [km²]: ***7.64***
Loose sediments [%]: ***72***
No landslide materials [%]: ***0***
Bare rocks [%]: ***28***

Weather-induced landslides:

ID	*Date*	*Type*	*Spatial accuracy*
L01	2013/02/26	140	10 m
L02	2013/12/11	140	500 m
L03	2014/12/31	144	n.r.

VIKNA OG KYST FOLDFJORDEN basin (ID: 11922) – CW1

Pore water pressure data series:

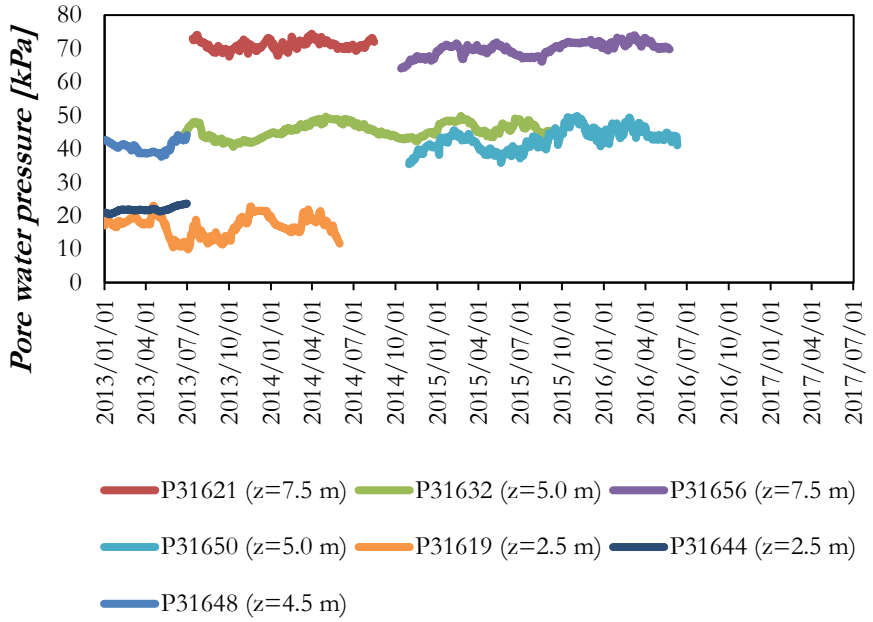

Correlation matrices:

Regional Warning Model	**WL_1**	**WL_2**	**WL_3**	**WL_4**
Landslides	0	0	3	0
No landslides	1234	16	4	0

Multi-scalar Warning Model	**WL_1**	**WL_2**	**WL_3**	**WL_4**
Landslides	0	0	2	1
No landslides	1234	16	4	0

HAREIDLANDET OG GURSKØYA basin (ID: 13678) – SW

Main characteristics:

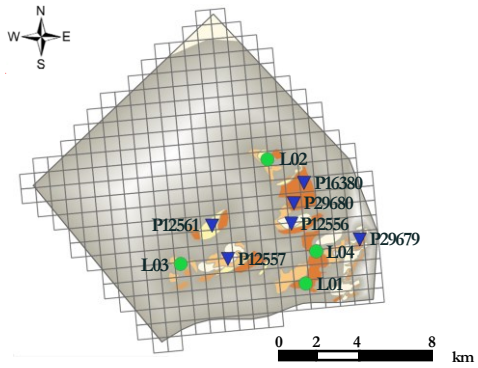

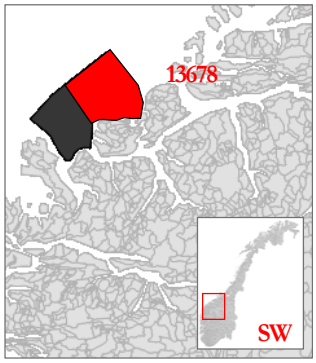

Quaternary deposits

- Moraine material, thick
- Moraine material, thin
- Terminal moraine
- Glaciofluvial deposits
- Weathered material
- Marine and fjord deposits, continuous
- Marine and fjord deposits, thin
- Marine and fjord deposits, thick
- No landslide materials
- Bare rocks

Legend

- xgeo grid
- Weather-induced landslides in soils (2013/01 – 2017/06)
- Piezometers

Shallow soil layers:

Area [km²]: ***307.18***
Loose sediments [%]: ***10***
No landslide materials [%]: ***3***
Bare rocks [%]: ***87***

Weather-induced landslides:

ID	*Date*	*Type*	*Spatial accuracy*
L01	2015/11/27	141	50 m
L02	2016/12/30	140	10 m
L03	2017/01/19	140	exact
L04	2017/01/20	142	n.r.

HAREIDLANDET OG GURSKØYA basin (ID: 13678) – SW

Pore water pressure data series:

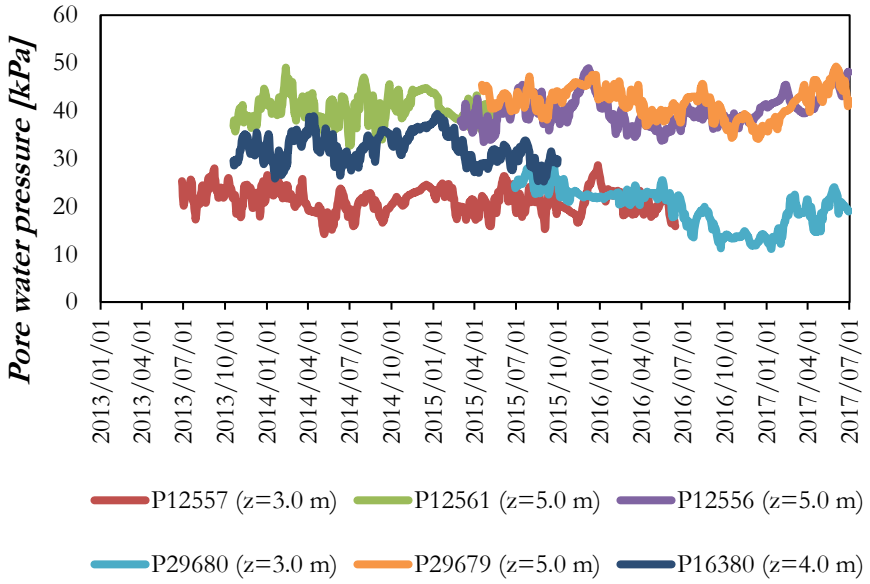

Correlation matrices:

Regional Warning Model	WL_1	WL_2	WL_3	WL_4
Landslides	0	1	3	0
No landslides	1441	19	0	0

Multi-scalar Warning Model	WL_1	WL_2	WL_3	WL_4
Landslides	0	0	4	0
No landslides	1447	13	0	0

KYST UTSKARPEN basin (ID: 13702) – CW2

Main characteristics:

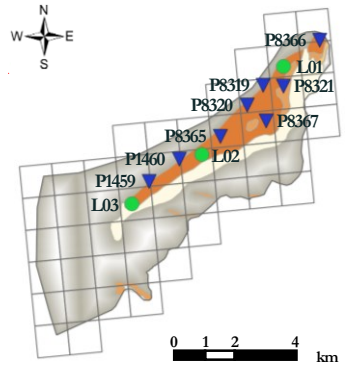

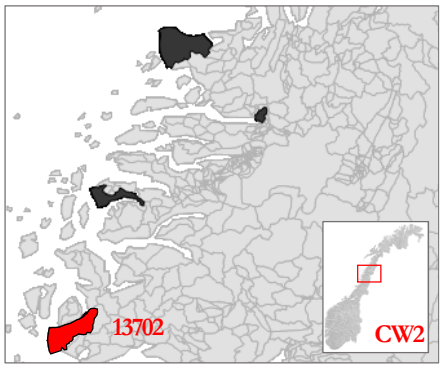

Quaternary deposits

- Moraine material, thick
- Moraine material, thin
- Terminal moraine
- Glaciofluvial deposits
- Weathered material
- Marine and fjord deposits, continuous
- Marine and fjord deposits, thin
- Marine and fjord deposits, thick
- No landslide materials
- Bare rocks

Legend

- xgeo grid
- Weather-induced landslides in soils (2013/01 – 2017/06)
- Piezometers

Shallow soil layers:

Area [km²]: ***33.45***
Loose sediments [%]: ***17***
No landslide materials [%]: ***12***
Bare rocks [%]: ***71***

Weather-induced landslides:

ID	*Date*	*Type*	*Spatial accuracy*
L01	2013/12/10	140	10 m
L02	2015/02/09	160	exact
L03	2017/01/26	142	n.r.

KYST UTSKARPEN basin (ID: 13702) – CW2

Pore water pressure data series:

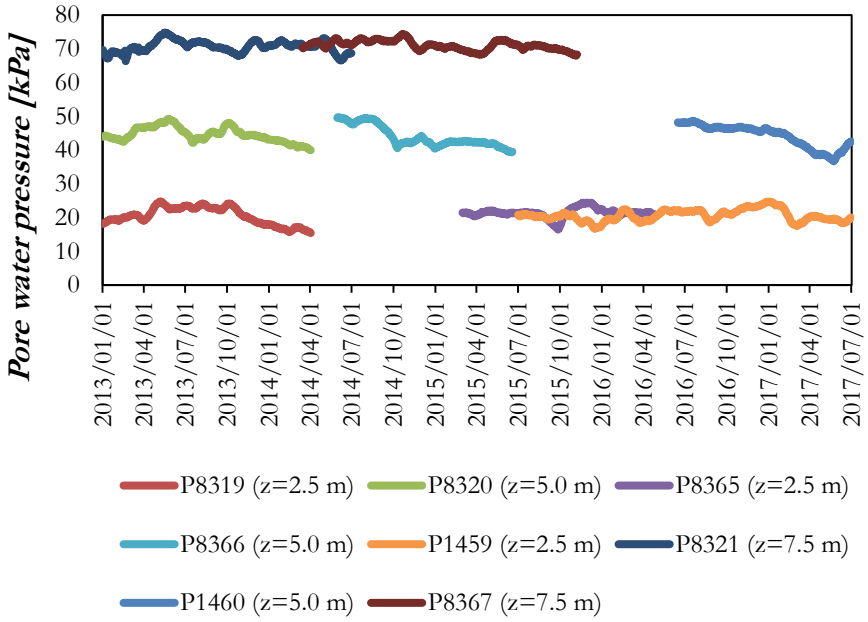

Correlation matrices:

Regional Warning Model	WL_1	WL_2	WL_3	WL_4
Landslides	0	0	2	1
No landslides	1618	13	8	0

Multi-scalar Warning Model	WL_1	WL_2	WL_3	WL_4
Landslides	0	1	1	1
No landslides	1622	10	7	0

HORVEREIDELVA basin (ID: 13913) – CW1

Main characteristics:

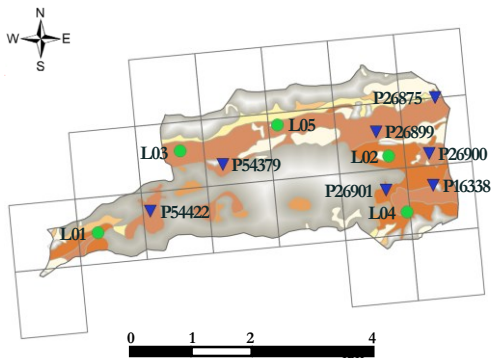

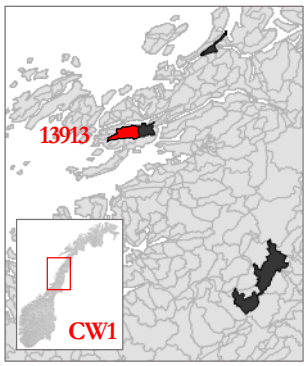

Quaternary deposits

- Moraine material, thick
- Moraine material, thin
- Terminal moraine
- Glaciofluvial deposits
- Weathered material
- Marine and fjord deposits, continuous
- Marine and fjord deposits, thin
- Marine and fjord deposits, thick
- No landslide materials
- Bare rocks

Legend

- xgeo grid
- Weather-induced landslides in soils (2013/01 – 2017/06)
- Piezometers

Shallow soil layers:

Area [km²]: ***10.58***
Loose sediments [%]: ***41***
No landslide materials [%]: ***9***
Bare rocks [%]: ***50***

Weather-induced landslides:

ID	*Date*	*Type*	*Spatial accuracy*
L01	2013/12/11	160	10 m
L02	2013/12/12	140	exact
L03	2014/12/30	140	10 m
L04	2014/12/31	144	n.r.
L05	2015/01/01	140	exact

HORVEREIDELVA basin (ID: 13913) – CW1

Pore water pressure data series:

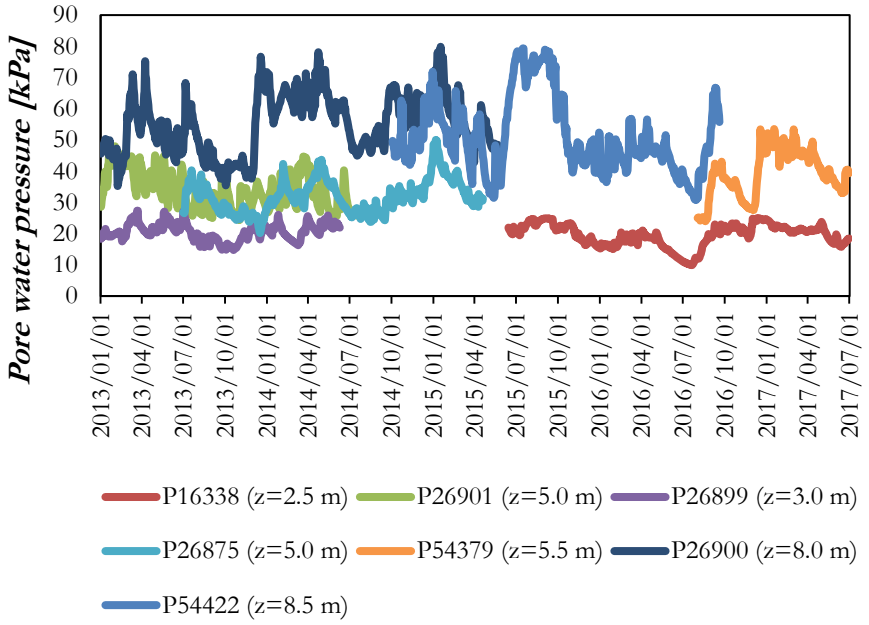

Correlation matrices:

Regional Warning Model	WL_1	WL_2	WL_3	WL_4
Landslides	0	1	4	0
No landslides	1617	18	2	0

Multi-scalar Warning Model	WL_1	WL_2	WL_3	WL_4
Landslides	0	0	1	4
No landslides	1623	13	1	0

DRAMMENSVASSDRAGET basin (ID: 14371) – SE

Main characteristics:

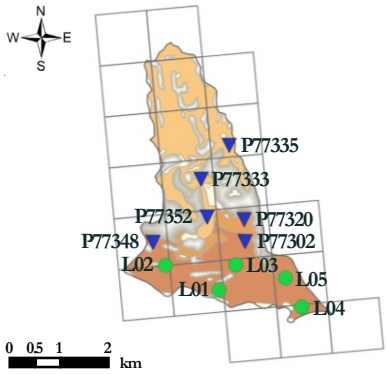

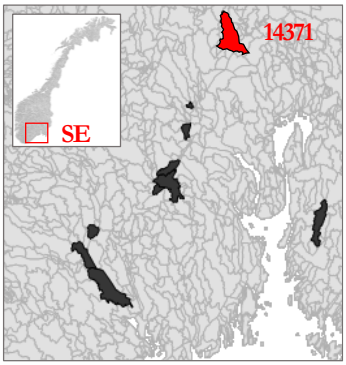

Quaternary deposits

- Moraine material, thick
- Moraine material, thin
- Terminal moraine
- Glaciofluvial deposits
- Weathered material
- Marine and fjord deposits, continuous
- Marine and fjord deposits, thin
- Marine and fjord deposits, thick
- No landslide materials
- Bare rocks

Legend

- xgeo grid
- Weather-induced landslides in soils (2013/01 – 2017/06)
- Piezometers

Shallow soil layers:

Area [km²]: ***9.43***
Loose sediments [%]: ***69***
No landslide materials [%]: ***3***
Bare rocks [%]: ***28***

Weather-induced landslides:

ID	*Date*	*Type*	*Spatial accuracy*
L01	2013/05/21	144	10 m
L02	2013/05/22	133	50 m
L03	2013/05/24	140	10 m
L04	2014/07/07	133	n.r.
L05	2016/05/22	144	1000 m

DRAMMENSVASSDRAGET basin (ID: 14371) – SE

Pore water pressure data series:

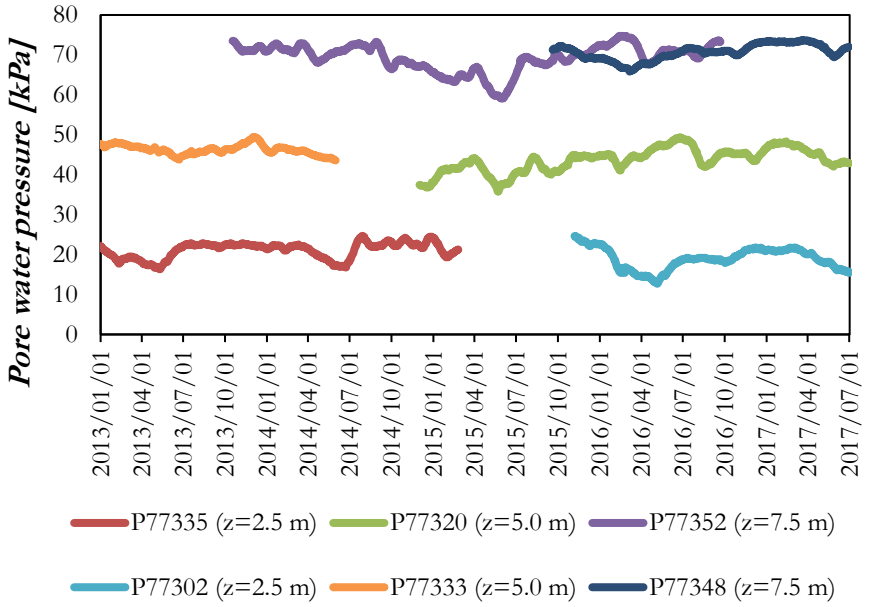

Correlation matrices:

Regional Warning Model	WL_1	WL_2	WL_3	WL_4
Landslides	0	1	2	2
No landslides	1604	29	4	0

Multi-scalar Warning Model	WL_1	WL_2	WL_3	WL_4
Landslides	0	0	2	3
No landslides	1616	14	6	1

OSELVVASSDRAGET basin (ID: 15645) – SW

Main characteristics:

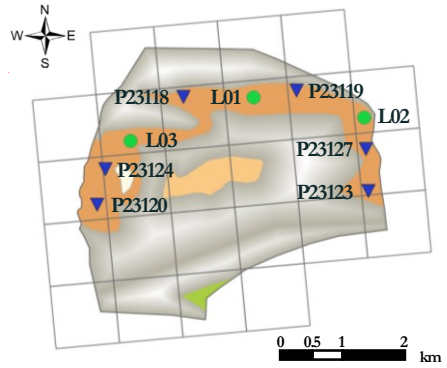

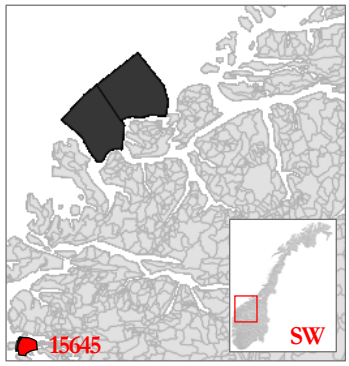

Quaternary deposits

- Moraine material, thick
- Moraine material, thin
- Terminal moraine
- Glaciofluvial deposits
- Weathered material
- Marine and fjord deposits, continuous
- Marine and fjord deposits, thin
- Marine and fjord deposits, thick
- No landslide materials
- Bare rocks

Legend

- xgeo grid
- Weather-induced landslides in soils (2013/01 – 2017/06)
- Piezometers

Shallow soil layers:

Area [km²]: ***15.25***
Loose sediments [%]: ***27***
No landslide materials [%]: ***0***
Bare rocks [%]: ***73***

Weather-induced landslides:

ID	*Date*	*Type*	*Spatial accuracy*
L01	2013/11/19	143	exact
L02	2014/10/28	133	exact
L03	2015/12/24	140	exact

OSELVVASSDRAGET basin (ID: 15645) – SW

Pore water pressure data series:

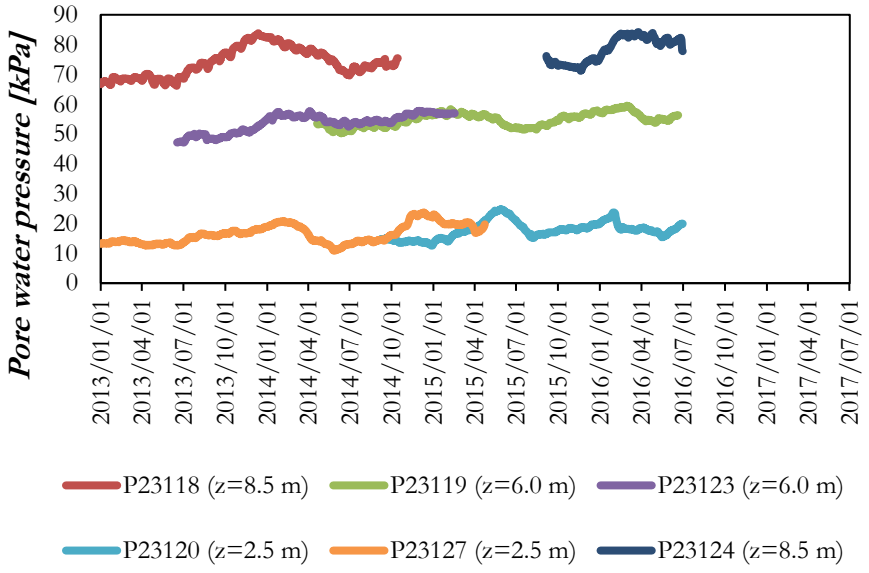

Correlation matrices:

Regional Warning Model	WL_1	WL_2	WL_3	WL_4
Landslides	1	2	0	0
No landslides	1273	1	0	0

Multi-scalar Warning Model	WL_1	WL_2	WL_3	WL_4
Landslides	1	1	1	0
No landslides	1273	1	0	0

TRONDHEIMSFJORDEN VEST basin (ID: 17074) – CW1

Main characteristics:

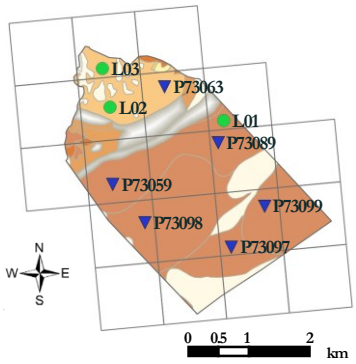

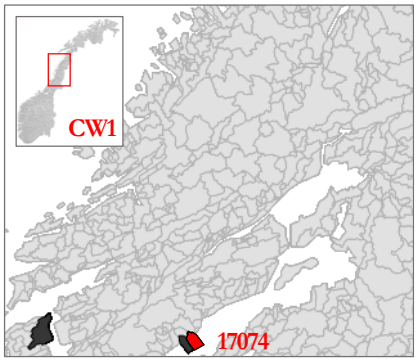

Quaternary deposits

- Moraine material, thick
- Moraine material, thin
- Terminal moraine
- Glaciofluvial deposits
- Weathered material
- Marine and fjord deposits, continuous
- Marine and fjord deposits, thin
- Marine and fjord deposits, thick
- No landslide materials
- Bare rocks

Legend

- xgeo grid
- Weather-induced landslides in soils (2013/01 – 2017/06)
- Piezometers

Shallow soil layers:

Area [km²]: ***9.83***
Loose sediments [%]: ***78***
No landslide materials [%]: ***13***
Bare rocks [%]: ***9***

Weather-induced landslides:

ID	*Date*	*Type*	*Spatial accuracy*
L01	2013/11/15	160	n.r.
L02	2015/02/08	140	exact
L03	2015/10/22	160	n.r.

TRONDHEIMSFJORDEN VEST basin (ID: 17074) – CW1

Pore water pressure data series:

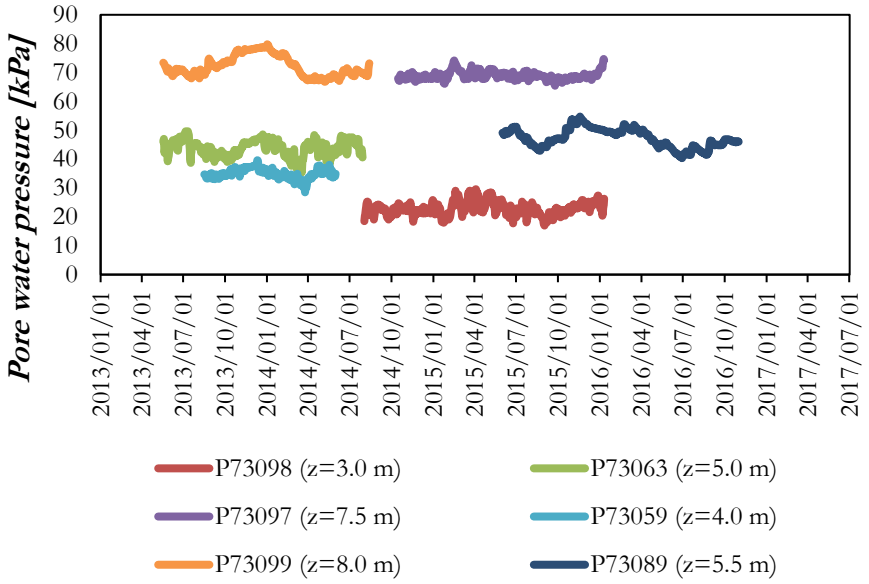

Correlation matrices:

Regional Warning Model	**WL_1**	**WL_2**	**WL_3**	**WL_4**
Landslides	2	1	0	0
No landslides	1260	0	0	0

Multi-scalar Warning Model	**WL_1**	**WL_2**	**WL_3**	**WL_4**
Landslides	2	1	0	0
No landslides	1260	0	0	0

MOSSEVASSDRAGET basin (ID: 18957) – SE

Main characteristics:

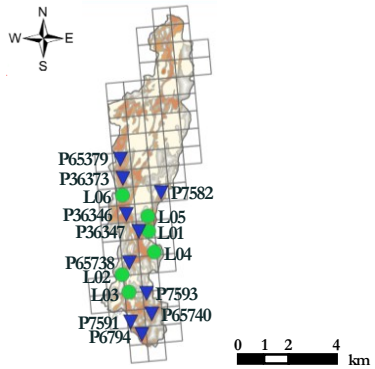

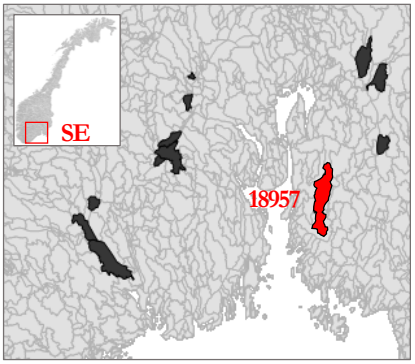

Quaternary deposits

- Moraine material, thick
- Moraine material, thin
- Terminal moraine
- Glaciofluvial deposits
- Weathered material
- Marine and fjord deposits, continuous
- Marine and fjord deposits, thin
- Marine and fjord deposits, thick
- No landslide materials
- Bare rocks

Legend

- xgeo grid
- Weather-induced landslides in soils (2013/01 – 2017/06)
- Piezometers

Shallow soil layers:

Area [km²]: ***51.39***
Loose sediments [%]: ***36***
No landslide materials [%]: ***34***
Bare rocks [%]: ***30***

Weather-induced landslides:

ID	*Date*	*Type*	*Spatial accuracy*
L01	2014/02/13	143	exact
L02	2014/02/14	143	exact
L03	2014/02/15	143	10 m
L04	2015/02/28	143	10 m
L05	2016/02/08	140	10 m
L06	2016/02/20	143	n.r.

MOSSEVASSDRAGET basin (ID: 18957) – SE

Pore water pressure data series:

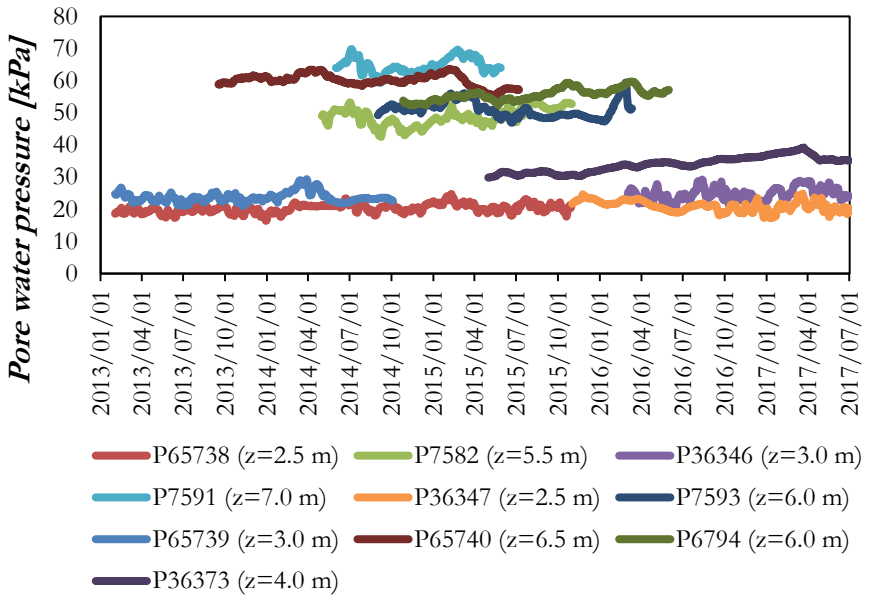

Correlation matrices:

Regional Warning Model	WL_1	WL_2	WL_3	WL_4
Landslides	0	2	4	0
No landslides	1576	24	5	0

Multi-scalar Warning Model	WL_1	WL_2	WL_3	WL_4
Landslides	0	1	2	3
No landslides	1581	19	4	1

VESTFOSSELVA basin (ID: 19897) – SE

Main characteristics:

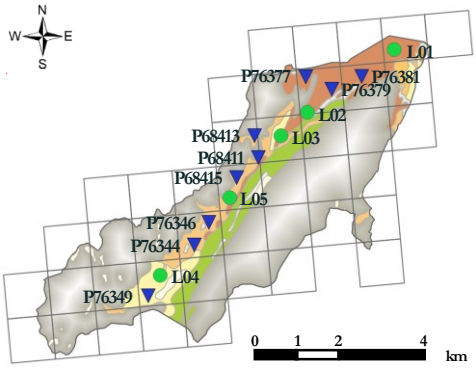

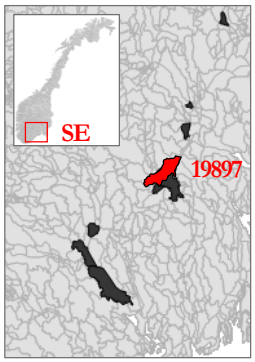

Quaternary deposits

- Moraine material, thick
- Moraine material, thin
- Terminal moraine
- Glaciofluvial deposits
- Weathered material
- Marine and fjord deposits, continuous
- Marine and fjord deposits, thin
- Marine and fjord deposits, thick
- No landslide materials
- Bare rocks

Legend

- xgeo grid
- Weather-induced landslides in soils (2013/01 – 2017/06)
- Piezometers

Shallow soil layers:

Area [km²]: ***25.08***
Loose sediments [%]: ***30***
No landslide materials [%]: ***1***
Bare rocks [%]: ***69***

Weather-induced landslides:

ID	*Date*	*Type*	*Spatial accuracy*
L01	2013/05/22	140	exact
L02	2014/01/02	143	10 m
L03	2014/01/03	144	n.r.
L04	2014/03/06	144	10 m
L05	2015/09/17	144	10 m

VESTFOSSELVA basin (ID: 19897) – SE

Pore water pressure data series:

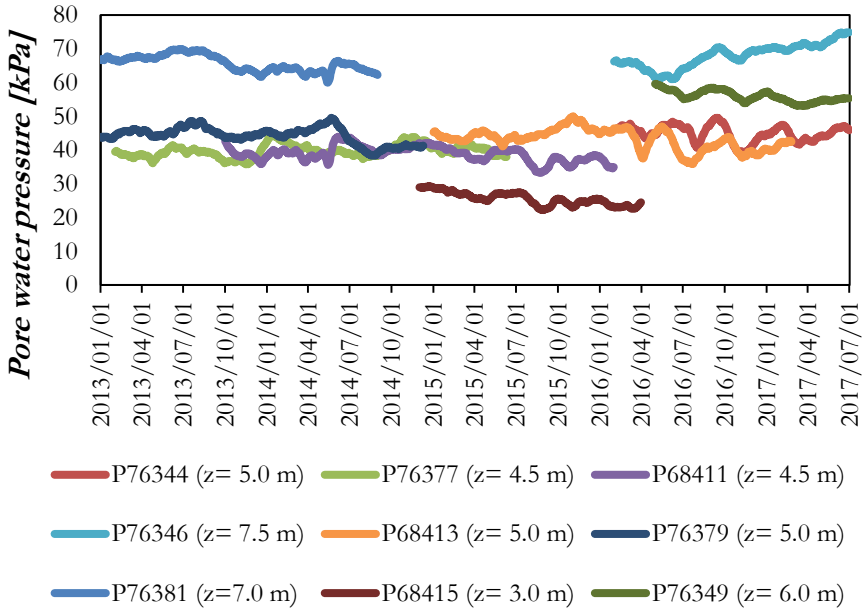

Correlation matrices:

Regional Warning Model	WL_1	WL_2	WL_3	WL_4
Landslides	0	5	0	0
No landslides	1620	17	0	0

Multi-scalar Warning Model	WL_1	WL_2	WL_3	WL_4
Landslides	0	1	3	1
No landslides	1623	13	1	0

GLOMMAVASSDRAGET basin (ID: 19903) – SE

Main characteristics:

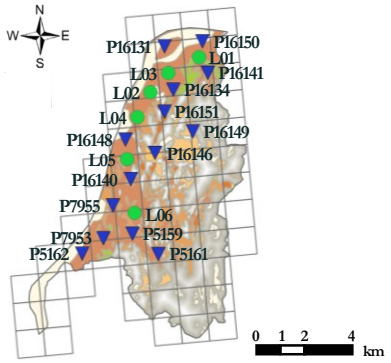

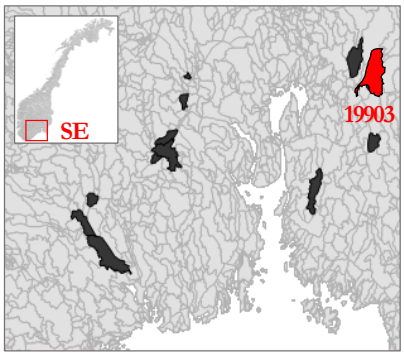

Quaternary deposits

- Moraine material, thick
- Moraine material, thin
- Terminal moraine
- Glaciofluvial deposits
- Weathered material
- Marine and fjord deposits, continuous
- Marine and fjord deposits, thin
- Marine and fjord deposits, thick
- No landslide materials
- Bare rocks

Legend

- xgeo grid
- Weather-induced landslides in soils (2013/01 – 2017/06)
- Piezometers

Shallow soil layers:

Area [km²]: ***43.46***
Loose sediments [%]: ***46***
No landslide materials [%]: ***13***
Bare rocks [%]: ***41***

Weather-induced landslides:

ID	*Date*	*Type*	*Spatial accuracy*
L01	2013/04/16	140	100 m
L02	2013/04/18	140	100 m
L03	2014/12/14	140	100 m
L04	2015/01/16	140	100 m
L05	2015/04/12	143	100 m
L06	2016/02/08	143	n.r.

GLOMMAVASSDRAGET basin (ID: 19903) – SE

Pore water pressure data series:

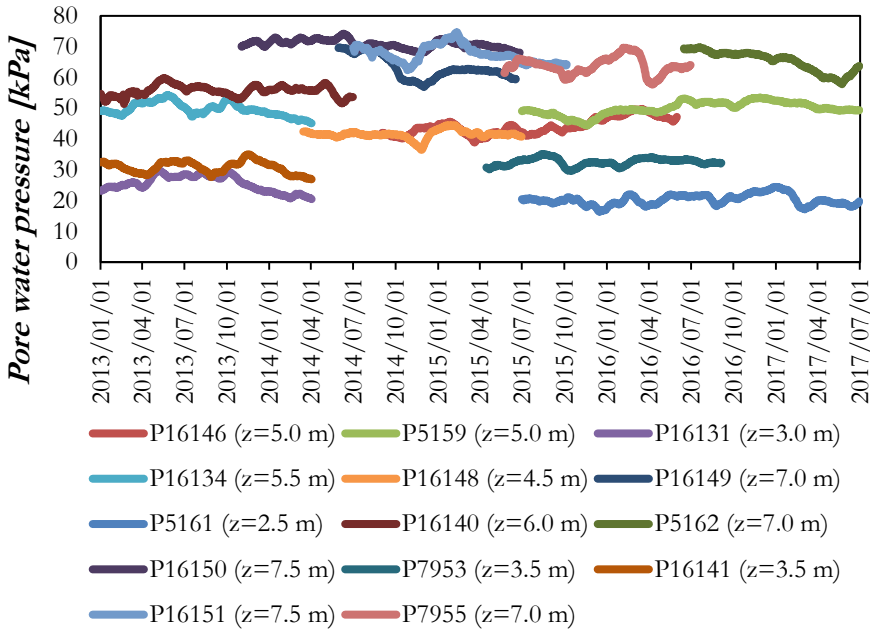

Correlation matrices:

Regional Warning Model	WL_1	WL_2	WL_3	WL_4
Landslides	0	2	4	0
No landslides	1580	39	17	0

Multi-scalar Warning Model	WL_1	WL_2	WL_3	WL_4
Landslides	0	0	4	2
No landslides	1596	32	8	0

D) MAIN VARIABLES AND ACRONYMS USED IN THE TEXT

Table A.5 Main variables and acronyms used in the text

Acronym	Description
ALE	Areal Landslide Event
C1	Very severe consequences class
C2	Severe consequences class
C3	Minor consequences class
CA	Correct Alert
D	Duration
E	Cumulated rainfall
E_R	Elements at risk
ER	Error Rate
FA	False Alert
FN	False Negative
FP	False Positive
GPM	Global Precipitation Measurement
Gre	Green class
H	Hazard
HK	Hanssen and Kuipers (1965) skill score
HR_L	Hit Rate
I_{eff}	Efficiency Index
L	Landslide event
LEWS	Landslide Early Warning System
Lo-LEWS	Local Landslide Early Warning System
LT	Lower Threshold
MA	Missed Alert
n	Time period
$N_{(D,E)}$	Rainfall events characterized by specific values of *D* and *E*
$N_{(D,E\|L)}$	Rainfall events that resulted in landslides
Ndi	Numerousness confidence descriptor
N_L	Total number of landslide events
N_R	Total number of rainfall events
OR	Odds Ratio
P(D,E)	Marginal probability
P(D,E|L)	Likelihood
P(L)	Prior probability

$P(L\|D,E)$	Posterior landslide probability
p_k	Pore water pressure recorded at day *k*
POD	Probability of detection score
POFA	Probability of false alarm score
POFD	Probability of false detection score
P_{PW}	Positive Predictive Power
P_{SM}	Probability of Serious Mistakes
R	Landslide risk
Red	Red error
R_{FA}	False Alert Rate
R_{MA}	Missed Alert Rate
ROC	Receiver Operating Characteristic
Sdi	Spatial confidence descriptor
SLE	Single Landslide Event
SMA	Simple Moving Average
Tdi	Temporal confidence descriptor
Te-LEWS	Territorial landslide early warning system
TN	True Negative
TP	True Positive
TRMM	Tropical Rainfall Measuring Mission
u_i	Simple moving average of pore water pressure data series
UT	Upper threshold
V	Vulnerability
WL	Warning Level
WZ	Warning Zone
Yel	Yellow error
δ	Euclidean distance from perfect classification in the ROC plane
Δu_i	Simple moving average difference
Δu_i^*	Normalized simple moving average difference
Δu_{imax}	Maximum simple moving average difference